Developing non-destructive techniques to predict 'Hayward' kiwifruit storability

A thesis presented in partial fulfilment of the requirements for the degree of

Doctor of Philosophy in Food Technology at Massey University,

Palmerston North, New Zealand.

Mo Li

2017

Abstract

A significant portion of New Zealand's kiwifruit production is held as stock in local coolstores for extended periods of time before being exported. Many pre-harvest factors contribute to variation in fruit quality at harvest and during coolstorage, and results in the difficulty in segregating fruit for their storage outcomes. The objective of this work was to develop non-destructive techniques utilised at harvest to predict storability of individual or batches of 'Hayward' kiwifruit based on (near) skin properties. Segregation of fruit with low storage potential at harvest could enable that fruit to be sold earlier in the season reducing total fruit loss and improving profitability later in the season.

The potential for optical coherence tomography (OCT) to detect near surface cellular structural differences in kiwifruit as a result of preharvest factors was demonstrated through quantitative image analysis of 3D OCT images of intact fruit from five commercial cultivars. Visualisation and characterisation of large parenchyma cells in the outer pericarp of kiwifruit was achieved by developing an automated image processing technique. This work established the usefulness of OCT to perform rapid analysis and differentiation of the microstructures of sub-surface cells between kiwifruit cultivars. However, the effects of preharvest conditions between batches of fruit within a cultivar were not detectable from image analysis and hence, the ability to provide segregation or prediction for fruit from the same cultivar was assumed to be limited.

Total soluble solids concentration (TSS) and flesh firmness (FF) are two important quality attributes indicating the eating quality and storability of stored kiwifruit. Prediction of TSS and FF using non-destructive techniques would allow strategic marketing of fruit. This work demonstrated that visible-near-infrared (Vis-NIR) spectroscopy could be utilised as the sole input at harvest, to provide quantitative prediction of post-storage TSS by generating blackbox regression models. However the level of accuracy achieved was not adequate for online sorting purposes. Quantitative prediction of FF remained unsuccessful. Improved ways of physical measurements for FF may help reduce the undesirable variation observed on the same fruit and increase prediction capability.

More promising results were obtained by developing blackbox classification models using Vis-NIR spectroscopy at harvest to segregate storability of individual kiwifruit based on the export FF criterion of 1 kg_f (9.8 N). Through appropriate machine learning techniques, the surface properties of fruit at harvest captured in the form of spectral data were correlated to post-storage FF via pattern recognition. The best prediction was obtained for fruit stored at 0°C for 125 days: approximately 50% of the soft fruit and 80% of the good fruit could be identified. The developed model was capable of performing classification both within (at the fruit level) and between grower lines. Model validation suggested that segregation between grower lines at harvest achieved 30% reduction in soft fruit after storage. Should the model be applied in the industry to enable sequential marketing, $11.2 million NZD/annum could be saved because of reduced fruit loss, repacking and condition checking costs.

Acknowledgement

I would like to express my deepest gratitude to my chief supervisor Assoc. Prof. Andrew East, not only for his exemplary guidance, help, encouragement and trust throughout my years of study, but also for providing remarkable opportunities for me along my preferred career path. I am grateful to both my co-supervisors, Dr. Reddy Pullanagari and Prof. Ian Yule from the Centre for Precision Agriculture at Massey University, for their invaluable contribution and support that refined the NIR work in this study.

I would like to offer special thanks to Dr. Pieter Verboven and Prof. Bart Nicolaï from Katholieke Universiteit de Leuven, Belgium, for hosting me as a visiting scholar there for two months and for their excellent input towards the OCT work. I would also like to mention Dennis Cantre from KU Leuven for providing training on OCT image analysis, and Dr. Andreas Buchsbaum from the Research Centre for Non Destructive Testing (RECENDT), Austria for his help with the OCT instrument and image capture. Many thanks should go to Dr. Alistair Mowat for his help and suggestions for the orchard manipulation trial, and Dr. Thamarath (An) Pranamornkith for setting up the light manipulation trial and collecting NIR data. In addition, both Prof. Ian Hallett and Dr. Jinquan (Ringo) Feng from Plant and Food Research, Auckland should be accredited for providing insights on topics relating to plant cell structures and NIR grading. I would also like to acknowledge Assoc. Prof. Kelvin Goh for his help and support during my Honours degree, which eventually led to a PhD opportunity for me.

I would like to thank the team of Fresh Technologists from the Centre for Postharvest and Refrigeration Research (CPRR) at Massey University. In particular, I thank Sue Nicholson and Peter Jeffery for their technical support with regards to laboratory work. I appreciate the overall guidance from Prof. Julian Heyes and his contribution to the OCT work. I am also grateful to many of my former and current colleagues, Abdul, Munazza, Matthew, Justin, Jacqueline and Celia, to name but a few, for the genuine friendships built and the intellectual discussions exchanged.

Of course I could not have completed this work without the various sponsors and organisations involved. I would like to thank Zespri® International Ltd. for providing fellowship for my PhD and providing constant support and useful feedback

for my work. I appreciate the Ministry of Primary Industries, New Zealand for the Food Structure Design Theme of the Primary Growth Partnership (PGP) research project. Many thanks should also go to the Helen E Akers PhD Scholarship from the Applied Academic Programmes at Massey University, the New Zealand Horticultural Science Advancement Trust and the Postgraduate Award from the New Zealand Institute of Agricultural and Horticultural Science, for providing funding for me to conduct research and attend international conferences.

I would like to thank my family and friends for their generous support throughout various stages of my life. I am grateful for my parents, for raising me with good values and supporting my passion in studying without doubts or conditions. Much credit should go to my dear husband Alan, for always being supportive, patient, a wonderful listener and a source of abundant joy; I really appreciate the love, hope and care we share, build and cherish in our lives. A big thank-you also goes to my friends Anynda and Isaac, for their help and supports especially during our house moving and wedding planning.

Finally, this work is dedicated to my late grandfather, Doctor Jia, who supported me financially and morally during the early days of my studying abroad in Singapore; I would not have been able to achieve any of this without your inspiration.

Table of Contents

List of Tables

List of Figures

List of Abbreviations and Symbols

2D	two dimensional
3D	three dimensional
AAO	all-at-once
ANN	artificial neuron network
AUC	area under curve
CDA	canonical discriminant analysis
CI	chilling injury
DAFB	day after full bloom
DMC	dry matter concentration
DS	decision stumps
DW	dry weight
FF	flesh firmness
FN	false negative
FP	false positive
GA	genetic algorithm
GL	grower line
GLM	general linear model
HC	high crop load
HCG	high crop load with trunk girdling
HSI	hyperspectral imaging
InGaAs	indium gallium arsenide
kg_f	kilogram-force
LC	low crop load
LCG	low crop load with trunk girdling
LDA	linear discriminant analysis
LED	light-emitting diodes
LOOCV	leave-one-out cross validation
LSD	least significant differences
MAE	mean absolute error
MLR	multivariate linear regression

MSC	multiplicative scatter correction
MSE	mean square error
MSEP	mean square error of prediction
MST	minimum taste standard
N	newton
NIPALS	non-linear iterative partial least squares
NIR	near infrared
NZD	New Zealand dollars
OAA	one-against-all
OAO	one-against-one
OCT	optical coherence tomography
PbS	lead sulfide
PC	principal component
PCA	principal component analysis
PCR	principal component regression
PLS	partial least squares
PLS-DA	partial least squares discriminant analysis
PLSR	partial least squares regression
Psa	*Pseudomonas syringae pv actinidiae*
QDA	quadratic discriminant analyses
R	correlation coefficient
R^2	coefficient of determination
RBF	radial basis function
RC	regression coefficient
RM	reflective mulch
RMSE	root mean square error
RMSEP	root mean square error of prediction
ROC	receiver operating characteristic
S.D.	standard deviation
SD-OCT	spectral-domain optical coherence tomography
SDR	division of standard deviation and RMSEP
SEC	standard error of calibration
SEP	standard error of prediction

SMO	sequential minimal optimisation
SMOTE	synthetic minority oversampling technique
SVM	support vector machines
SVMR	support vector machines regression
TN	true negative
TSS	total soluble solids
TP	true positive
TZG	taste Zespri grade
Vis-NIR	visible near infrared

1 Introduction

1.1 Research Outline

Kiwifruit (*Actinidia deliciosa* (A.Chev) C. F. Liang et A. R. Ferguson and *A. chinensis*) is an emerging horticultural crop globally. Currently the total area of kiwifruit orchards around the world is estimated to be 170,000 ha with annual production exceeding 1.8 million tonnes (Huang, 2016). The major kiwifruit producing countries include China, Italy, New Zealand and Chile, accounting for about 80% of the world production (Burdon and Lallu, 2011; Ferguson, 2011). In New Zealand, about 90% of kiwifruit production is exported (Burdon and Lallu, 2011). The sales of New Zealand-grown kiwifruit reached 117.1 million trays in the 2015/16 season, contributing to a total of 1.3 billion NZD export earnings (Anonymous, 2016a). New Zealand graded fruit were exported to over 50 countries around the world (Anonymous, 2016d).

Kiwifruit are harvested unripe and stored at cold temperatures for long periods of time (usually between 6 – 8 months) allowing for physiological development until being suitable for consumption, a process known as ripening (Beever and Hopkirk, 1990). This process enables long distance transport of kiwifruit to global markets using cost-effective shipping methods (Sale, 1990). A number of factors affect the quality of the fruit, including cultivar, climatic conditions, orchard management, maturity at harvest, storage condition, transport and handling. As a result, there is inherent variability that contributes to a wide range of storage potential.

Keeping suitable quality fruit during storage has been a challenge to the kiwifruit industry. The development of over soft or disordered fruit during storage costs the industry approximately $120 million annually (Tanner et al., 2012). As part of quality control measures, fruit are tested using destructive methods prior to shipping and again on arrival at the distant market (East et al., 2013). Removal of fruit that are unsuitable for sale, both onshore and offshore, incur costs, due to manual repacking costs and direct fruit loss. These costs contribute to a significant portion of the marginal changes in postharvest costs of per tray of kiwifruit (Fig. 1.1; Anonymous, 2012) .

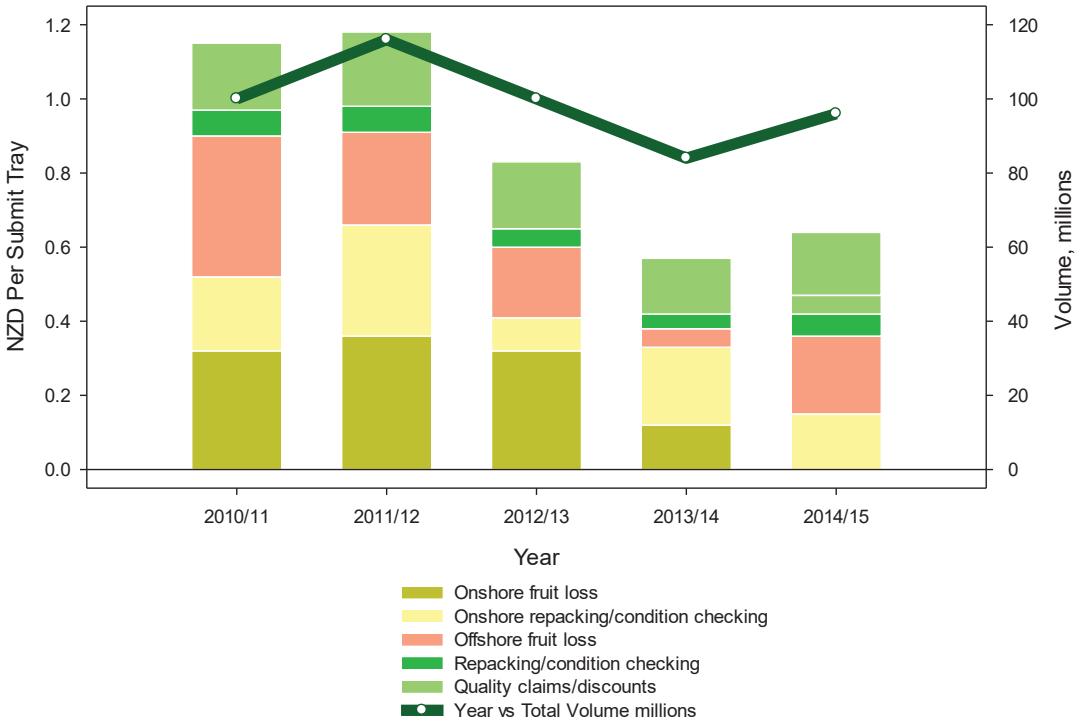

Figure 1.1 Quality costs in NZD as a function of per submit tray of exported kiwifruit and volume (million trays) of exported kiwifruit over 7 years (Anonymous, 2015b). Regenerated image.

Accurate prediction of postharvest performance of kiwifruit at harvest would help to identify individual or batches of fruit susceptible to postharvest storage disorders and hence have a shorter storage life. This would enable timely inventory decisions for sequential marketing and reduce overall fruit loss in the supply chain. Predicting the storage potential of fresh produce usually involves physical measurements at harvest such as estimates of harvest maturity (East et al., 2013). Traditionally storage potential of kiwifruit is estimated from at-harvest fruit quality data, and later assessed during storage with flesh firmness testing. This method is destructive; it requires removal of a small population of fruit from the batch for testing and only evaluates the storability of the fruit at the time of measurement. The development of real-time non-destructive testing methods is preferable because multiple attributes can be monitored over time without damaging the population.

This study aims to investigate the feasibility of using non-destructive techniques applied at harvest to predict and segregate kiwifruit for storability based on several quality predictors. Near infrared (NIR) spectroscopy and optical coherence tomography

(OCT) are investigated as potential technologies. Optical coherence tomography is used to capture three-dimensional images of the cellular structures immediately underneath the surface of kiwifruit. This information may be useful to assess the changes in cellular structure and their potential consequences for postharvest fruit storability. Near infrared spectroscopy is used to predict storage outcomes by analysing the light scattering properties of the surface of fruit and the chemical composition underneath the surface. Segregation of fruit for their storage potential based on at-harvest NIR spectra is investigated. This segregation creates two inventories: one with lower storage potential that would be shipped earlier in the season, and another with higher storage potential that would be kept for later shipment. The ultimate goal is to reduce total fruit loss in the supply chain over the season and hence improve profitability.

1.2 Thesis Outline

The majority of the experimental research was conducted at the Centre for Postharvest and Refrigeration Research, Massey University, New Zealand, while a short period of research was conducted at Katholieke Universiteit de Leuven, Belgium in order to develop an imaging analysis protocol for the OCT technique. The 'Hayward' cultivar was chosen for the purpose of this study because it is the most produced cultivar for export to the global market. The well documented studies on 'Hayward' quality and storability also enabled comparisons between the current study and the literature.

The second chapter provides a literature review on current knowledge on kiwifruit, including physiology, skin structure, important quality attributes, and the factors influencing the quality and storage potential. This chapter also introduces the principles of NIR and OCT, the instrumentation and sampling process, data analysis techniques and the applications of these methods for quality prediction in horticultural produce.

The third chapter involves an experiment conducted through manipulating preharvest growing conditions (crop load and application of trunk girdling) in order to showcase the potential relationships between growing conditions and postharvest performance of kiwifruit. This work demonstrates the inherent variability in fruit quality, and the subsequent impacts and challenges in predicting fruit storability.

The fourth chapter investigates the capability of OCT to visualise and characterise kiwifruit near-surface cellular structures non-destructively. An automated imaging analysis technique was developed in order to identify large parenchyma cells in the image data and enable quantitative analysis of these cells. The within and between-cultivar differences in cellular microstructures were examined and compared to existing knowledge. However, the capability of the technique is limited by penetration depth, resolution and equipment cost, and therefore will not be useful in monitoring or predicting future storage performance of the fruit in the near future.

The next three chapters investigate the potential for Vis-NIR spectroscopy to predict kiwifruit storability. The fifth chapter evaluates the ability of Vis-NIR spectroscopy applied at harvest time to provide quantitative prediction of postharvest storage performance of kiwifruit, using a series of datasets collected over several seasons. While the post-storage sugar content could be predicted with relatively good accuracy, the post-storage firmness which is an important influencer of storability was poorly predicted. Neither prediction was accurate enough to be suitable for online grading purposes. Results obtained in this chapter led to the decision that subsequent research should focus on qualitative prediction of fruit storage potential as an alternative approach.

The sixth chapter identifies the most suitable multivariate data analysis technique that can be applied to develop a classification model which segregates fruit based on the minimum export firmness criterion. The classification accuracy was compared using various machine learning classifiers and the best method was selected based on the highest accuracy for both calibration and validation datasets. This generated a classification model which segregates fruit for storage potential at the time of harvest.

The seventh chapter details a real-time validation trial that evaluated the robustness of the classification model developed in the sixth chapter. Fruit were scanned using NIR spectroscopy at harvest and then sorted by the model for segregation into two populations: fruit that develop post-storage firmness below the minimum export criterion and those that do not. The predicted and measured storage performance was compared. The reduction in fruit loss as a result of segregation was also assessed.

The final chapter provides overall discussions and conclusions on this research and suggests recommendations for future studies.

2 Literature review

2.1 Kiwifruit

2.1.1 Classification and general characteristics

Kiwifruit (*Actinidia* sp.) was first grown in New Zealand in 1910, by an orchardist, Alexander Allison, who received seeds from Isabel Fraser, a missionary who just returned from China. The plants producing fruit were considered the source vines of the New Zealand kiwifruit industry today (Sale, 1990). The genus *Actinidia* is comprised of 55 species (Li et al., 2007). The two economically important species of *Actinidia* are *Actinidia deliciosa* and *Actinidia chinensis* (Currie, 1997).

The green-fleshed cultivar 'Hayward' from the *A. deliciosa* species is the "original" kiwifruit, known for its brown hairy skin, large fruit size, superior flavour and long storage potential (Burdon and Lallu, 2011; Sale, 1990). Whilst 'Hayward' dominates the global kiwifruit market, many new cultivars have or are being introduced to the fruit category to cater to consumer values. In particular, efforts have been made to select *A. chinensis* cultivars with desirable characteristics for commercial purposes (Currie, 1997). The successful launch of 'Hort16A', a yellow-fleshed fruit from the species *A. chinensis* that has a 'tropical' flavour, demonstrated the potential for fruit category extension. *A. chinensis* has contributed to about a quarter of the New Zealand annual export volume nowadays (Burdon and Lallu, 2011). Additionally, in 2013, commercial volumes of 3 new cultivars were released in New Zealand, being yellow-fleshed 'G3' (Zespri® SunGold) and 'G9' (Zespri® Charm; both *A. chinensis*), and green-fleshed 'G14' (Zespri® Sweet Green), a cross of *A. deliciosa* and *A. chinensis*.

2.1.2 Important quality attributes of kiwifruit

2.1.2.1 Total soluble solids concentration

Total soluble solids (TSS) concentration is a measurement consisting of soluble sugars, as well as soluble pectins and organic, amino and ascorbic acids, often expressed as %, or °Brix (Crisosto et al., 2012b). The TSS can be readily measured with a manual or digital refractometer. The value of TSS varies between individual fruit in an orchard and also along the longitudinal axis of an individual fruit, being higher at the

blossom end than at the stem end (Hopkirk et al., 1986). Harman and Hopkirk (1982) described a standardised method of assessing the TSS of kiwifruit using an optical refractometer: fruit was sliced 1.5 cm from each end of the fruit and a few drops of juice squeezed from both end caps onto the measurement glass of the refractometer.

The TSS at harvest is used as a maturity index for kiwifruit to indicate harvest time (Beever and Hopkirk, 1990). It is also a key parameter which links closely with consumers' liking and acceptance because the flavour of kiwifruit is based largely on a sugar-acid balance (Crisosto and Crisosto, 2001). Harker et al (2009) suggested that consumers' liking grew with increased TSS. Fruit with TSS ranged from 14 to 16% are consumed with pleasure, whereas fruit with TSS below 12% is considered not acceptable (Hasey, 1994). However, a lower TSS fruit could still be acceptable if the acidity is also low (Crisosto and Crisosto, 2001).

2.1.2.2 Dry matter concentration

Dry matter refers to fruit solid contents other than water (Feng, 2003). Dry matter concentration (DMC) is defined as the ratio of dry weight to fresh weight of a test sample, expressed as a percentage (Crisosto et al., 2012b). The DMC of kiwifruit comprises both soluble sugars and insoluble solids (structural carbohydrate and starch; Burdon et al., 2004). It can be determined by cutting an equatorial kiwifruit slice of approximately 3 mm thickness and drying them at 65°C to constant weight (approx. 24 hours).

The DMC of 'Hayward' kiwifruit ranges from 12 – 20% while most fruit in New Zealand fall within the range of 14 – 17%, depending on the season, timing of harvest, orchard location and canopy management (Burdon et al., 2004). The flavour of kiwifruit and consumers' acceptance has been associated with the DMC of the fruit (Harker et al. 2009; Jordan and Seelye 2009) . Crisosto et al. (2011) proposed that a DMC of above 15.1% was required to allow a large proportion of the tested 'Hayward' kiwifruit to satisfy a high percentage of consumers. Zespri® Group Ltd. developed a Taste Zespri Grade (TZG) to meet specific market preference of sweeter fruit in Asia (Japan) and Europe; the TZG range for 'Hayward' was 15.5 – 19.5% DMC in 2015 (Anonymous, 2015a).

The DMC at harvest indicates the TSS that will develop in ripe fruit (Jordan et al., 2000; Burdon et al., 2004). It has been used as a quality prediction tool in a range of fruit including avocados (Arpaia et al., 2001), mango (Bally et al., 2000) and kiwifruit (Burdon et al., 2004). Since the DMC does not change during cool storage of kiwifruit, information on DMC provides a useful decision-making tool for marketing and distribution of kiwifruit (Harker et al., 2009). Traditionally assessment of harvest DMC is carried out by sampling a small proportion of the entire batch destructively. Non-destructive methods such as near infrared (NIR) spectroscopy have also been used to segregate future eating quality of fruit based on at-harvest DMC (Jordan et al., 2000; McGlone et al., 2002b).

2.1.2.3 Flesh firmness

Flesh firmness (FF) of kiwifruit is referred to as the maximum force required for a 7.9 mm diameter Magness-Taylor probe to penetrate into the fruit flesh after removing a 1-mm slice of skin (Feng et al., 2011). In commercial practice, kiwifruit are harvested long before they reach eating ripeness, i.e. while the fruit are relatively firm, with an FF value of 6 – 9 kg_f (~ 60 – 90 N; Beever and Hopkirk, 1990). The FF value is also an important characteristic for determining the storage potential and eating quality of kiwifruit. Over-softening of the fruit is generally considered the end of kiwifruit shelf life (Feng, 2003). Therefore, in order to ensure reasonable storage life remains to enable shipping to distant markets, a minimum standard of 1 kg_f (9.8 N) for individual fruit is required in New Zealand (Hopkirk et al., 1996). A FF value of approximately 0.6 – 0.8 kg_f (5.9 – 7.8 N) is considered an acceptable texture for consumers for 'Hayward', whereas a FF value lower than 0.4 kg_f (3.9 N) is considered too soft and therefore not acceptable for consumption (Stec et al., 1989).

Conventionally the FF is measured destructively by using a handheld (FT327, Effegi, Italy) or electric (QALink, Willowbank Electronics Ltd., Napier, New Zealand) penetrometer fitted to a 7.9 mm probe. Other devices have been developed to assess kiwifruit firmness or texture non-destructively. For instance, compression force measured by a texture analyser (TA-XT Plus, Stable Microsystems Ltd., Surrey, UK) is used as an alternative measurement of firmness. Acoustic firmness sensors (AFS, Aweta Impact & Acoustic Firmness System, Nootdorp, Netherlands) are developed based on

acoustic impulse response technology and provide measurements of acoustic firmness indices.

The FF values were found to be temperature dependent, with lower FF at elevated temperatures as a result of irreversible fruit ripening (Jeffery and Banks, 1994). Therefore, measurements immediately after removal of fruit from coolstorage (0 °C) could result in varying FF values due to rapid changes in fruit temperatures (Feng, 2003). The FF measurements also increase with increasing penetration speed (Feng et al., 2011; Li et al., 2016), regardless of cultivar, season or instrument type. Penetrometer speeds of 5 mm s^{-1} (McGlone et al., 1997; Burdon et al., 2014), 10 mm s^{-1} (Hertog et al., 2004b; Feng et al., 2006), 20 mm s^{-1} (Burdon et al., 2013) and 25 mm s^{-1} (Harker et al., 1996) have all been reported. Currently Zespri® uses a standard of 8 mm s^{-1} for evaluation of FF during onshore condition checking.

2.1.3 Kiwifruit physiology

2.1.3.1 Growth and development

Kiwifruit reach full size approximately 10 weeks after anthesis. During this period, there is an increase in both fruit volume and fruit weight. Cell division and cell enlargement occur, and the latter is found to be responsible for subsequent increase in fruit size (Beever and Hopkirk, 1990). The final fruit size is affected by cultivar, the number of seeds in the fruit, crop load and growing conditions. As the fruit reach maturity (approximately 15 – 20 weeks after anthesis), there are no obvious changes in the shape and skin colour of the fruit. However, the concentrations of chemical components vary, with the most marked change occurring in carbohydrates (Beever and Hopkirk, 1990). During early stages of development, there is a small but significant decrease in total sugar. Starch content increases and peaks at later stages of development, and may comprise up to 50% of total dry matter of the fruit at harvest (Beever and Hopkirk, 1990; Richardson et al., 1997; Burdon and Lallu, 2011). After harvest a rapid decrease in starch concentration is observed during the first 4 – 6 weeks of storage, accompanied by an increase in soluble solids (TSS) due to starch hydrolysis and a decline in FF (Snelgar and Hopkirk, 1988; Beever and Hopkirk, 1990).

2.1.3.2 Maturation and harvest

Maturation is known as the period in which the fruit develops the characteristics that are required for ripening. It occurs after completion of growth and before the fruit ripens and senesces (Burdon and Lallu, 2011). At a particular stage of maturation, the fruit may be removed from the vine and will continue to develop physiologically until it reaches eating quality. This is referred to as physiological maturity (Beever and Hopkirk, 1990). The stage of maturity at harvest influences the storage potential of the fruit, as well as its final quality for consumption (Beever and Hopkirk, 1990). In commercial practices kiwifruit are harvested at physiological maturity, when fruit are still firm and unripe. Fruit that are harvested too early, prior to physiological maturity, generally soften more rapidly and fail to develop full flavour and aroma of ripe kiwifruit during storage (Beever and Hopkirk, 1990). Fruit harvested too late may become overripe very quickly and do not have sufficient storage life (Burdon et al., 2014a). Development of a standard to indicate when to harvest is necessary. This harvest index should be based on a physiological attribute of the fruit that changes consistently during maturation and easy to measure.

During kiwifruit maturation, several physiological and biochemical changes occur, including cessation of growth, conversion of starch to sugar and softening of the fruit etc. Amongst these changes, the conversion of starch to sugar is found to have close association with fruit quality after storage (Beever and Hopkirk, 1990). The TSS of the fruit is related to sugar concentration and is readily measurable with a refractometer. Therefore it has been used as a maturity index for kiwifruit harvest. In New Zealand, the minimum TSS value before fruit can be harvested in the orchard is 6.2% (Harman, 1981). Fruit harvested with low TSS (< 6%) generally exhibited poor quality after storage. Some studies suggest that fruit harvested with a higher TSS (7 – 12%) have better storability and final eating quality. However, harvesting at very late stage is not recommended because of the increasing risk of damages from frosts (Beever and Hopkirk, 1990).

2.1.3.3 Postharvest ripening and softening

Ripening is referred to as the process of a fruit changing from physiologically mature to an optimum condition for consumption (Beever and Hopkirk, 1990).

Kiwifruit are climacteric fruit which, during ripening, undergo a rapid increase in ethylene production that is accompanied by a climacteric burst of respiration, resulting in physiological and biochemical changes such as flavour, aroma and texture (Kim, 1999). The most significant change is the decrease in flesh firmness (FF). The FF values range from 6 – 9 kg_f (≈ 60 – 90 N) at harvest to 0.5 – 0.8 kg_f (≈ 5 – 8 N) when fruit reach eating ripeness (Beever and Hopkirk, 1990). This softening is the main limiting factor for storage life of individual fruit (Feng et al., 2001). However, the time taken by individual fruit to soften varies enormously. In common practice, fruit are usually stored together within a plastic liner to ensure a more uniform rate of ripening as a result of ethylene accumulation interaction between fruit (Beever and Hopkirk, 1990).

Depending on the maturity at harvest, softening of kiwifruit occurs in two or three phases (Lallu et al., 1989; MacRae et al., 1990). Kiwifruit harvested at early maturity go through three softening stages: 1) an initial lag phase where fruit remain relatively firm and soften only slowly, 2) a rapid softening phase in which fruit soften to about 20% of their harvest FF, and 3) the final stage of softening which is marked by the start of internal ethylene production (MacRae et al., 1990; Paterson et al., 1991). For fruit that are harvested late in the season, there is no initial lag phase during softening; only the second and third phases exist (MacRae et al., 1990).

The softening of kiwifruit is due to disintegration of the cell wall, resulted from a number of activities including pectin solubilisation, cell wall swelling, degradation of pectin, reduction in molecular weight of xyloglucan, and dissolution of middle lamellae (Schröder and Atkinson, 2006). During the initial phase of softening, pectin is solid-like and water-insoluble. As the fruit starts to soften rapidly (the second phase), pectin softens to a more liquid-like state (Redgwell and Percy, 1992). This softening is not a chemical but a physical change and hence cannot be measured by chemical analysis (Schröder and Atkinson, 2006). In addition, cell wall swells as ripening proceeds and at eating ripeness will reach approximately 3 – 4 times its thickness at harvest (Hallett et al., 1992).

The conversion of starch to sugar also continues during ripening process. The TSS increases to 14 – 16% before fruit are eating-ripe (Beever and Hopkirk, 1990). However, when fruit become overripe, the TSS begin to fall slightly (Fukui et al., 1980). The internal flesh colour remains unchanged for ‘Hayward’. Upon complete ripeness,

the flavour of the fruit changes from initially acidic taste to a more pleasant delicate aroma (Beever and Hopkirk, 1990). When fruit become overripe, an 'estery' aroma may develop and it can be unacceptable to consumers (Burdon and Lallu, 2011).

2.1.4 Factors affecting kiwifruit quality and storage potential

2.1.4.1 Preharvest factors

When growing kiwifruit, many practices have been utilised to achieve improved fruit quality and maximise productivity through optimised vine performance (Patterson and Currie, 2011). These include planning block layout, ensuring good orchard shelter, spring and summer trunk girdling, "tip-squeezing" (Max and Currie, 2005), "zero-leaf" pruning (Gardiner et al., 2005) and fruit thinning (Patterson and Currie, 2011). Preharvest growing conditions and orchard management practices can affect fruit quality at the time of harvest and during subsequent storage. While several orchard and climatic factors have been suggested to influence kiwifruit storage quality, there are few published data demonstrating these effects.

2.1.4.2 Girdling

Trunk girdling, or cincturing, is a technique used to influence cropping, which involves the removal of a ring of the bark around the trunk (Sale, 1990). Fruit growth is dependent on the ability of fruit to compete with vegetative growth for a supply of carbohydrates from leaves (Seager et al., 1995). Girdling interrupts the flow of carbohydrates around the vine by redirecting them to the shoots rather than to the roots, restricting the roots from competing with the fruit to absorb carbohydrates produced by the leaves. Trunk girdling has been widely used in many horticultural products such as grapes, citrus, apple, peach and persimmon to improve fruit size and quality attributes such as DMC and TSS (Goren et al., 2003).

The implementation of girdling within the New Zealand kiwifruit industry was developed to increase orchard yield, fruit size/weight and dry matter concentration (Sale, 1990). Spring trunk girdling practices are used to increase fruit size in both 'Hayward' and 'Hort16A' whereas summer trunk girdling is applied to facilitate higher dry matter accumulation by fruit, as well as higher flowering in the spring following application (Patterson and Currie, 2011). Davison (1980) demonstrated that girdling on young

kiwifruit vines increased flower and fruit numbers. Snelgar and co-workers (Snelgar et al., 1986; Snelgar and Thorp, 1988) reported increased fruit weight with increasing leaf area on girdled vines. Girdling combined with high leaf to fruit ratios were found to improve fruit weight (Seager et al., 1995) and TSS (Seager et al., 1995; Assar et al., 2009). Boyd and Barnett (2011) suggested that extended trunk girdling increased fruit number, improved DMC and resulted in more advanced maturity at harvest. This hastening of maturation of fruit makes girdling an undesirable practice in some cases (Davison, 1990). While much research reports on the effect of girdling on at-harvest kiwifruit quality, little information is available on how girdling affects kiwifruit storage performance (Boyd, 2012). Boyd and Barnett (2011) found that trunk girdling of 'Hort16A' (*A. chinensis*) vines reduced the susceptibility of fruit to develop chilling injury (CI) during storage.

2.1.4.3 Crop load

Crop load is defined as the fresh weight obtained per canopy hectare. For 'Hayward' yields increase from approximately 7 to over 30 t/ha from 1980's to 2010's as a result of continued improvements in orchard management, with top-performing orchards producing over 50 t/ha (Thorp et al., 2011). Manipulation of crop load is achieved by light-to-moderate vegetative pruning and flower/fruit thinning. Crop load is important as it affects kiwifruit size and quality in the current season and flower induction for the following season (Sale, 1990). However, over-reduction of crop load compromises orchard yield and in turn profitability (Snelgar et al., 1986; Patterson and Currie, 2011).

Published studies on the effect of crop load on at-harvest kiwifruit quality are somewhat contradictory. While some failed to demonstrate any significant effect of manipulated crop load on fruit weight, FF, DMC and TSS (Snelgar et al., 1998; Broom et al., 2000), others reported high crop load being associated with reduced fruit weight (Patterson and Currie, 2011), higher FF (Boyd and Barnett, 2011) and reduced DMC and total titratable acidity (Famiani et al., 2012) at harvest. The effect of crop load manipulation on kiwifruit storage performance is not well established. Famiani et al. (2012) suggested that high crop load results in reduced TSS and FF after storage for 'Hayward'. Boyd and Barnett (2011) found that high crop load also increased the susceptibility of 'Hort16A' fruit to CI incidence.

2.1.4.4 Light

Light is essential for plant growth and fruit production. Vines grown under shaded areas flower poorly in the following season (Davison, 1990). Light intensity also influences photosynthesis rates of leave, growth rate of vines, water uptake and mineral accumulation in the fruit (Buwalda and Smith, 1990; Davison, 1990). Previous studies showed that insufficient light exposure resulted in smaller fruit size, reduced chlorophyll content and calcium accumulation, lower TSS and DMC, and less FF (Tombesi et al., 1993; Antognozzi, 1995; Biasi et al., 1995; Snelgar et al., 1998; Montanaro et al., 2006; Tavarini et al., 2009). In comparison, fruit grown in high light intensity had better quality and longer storability (Tombesi et al., 1993; Antognozzi, 1995).

The use of reflective mulches was discovered in an attempt to increase light availability in the canopies of apple trees (Doud and Ferree, 1980; Mika et al., 2007). Reflective mulches increase light availability by reflecting the light that passes through the canopy and reflecting the light up onto the leaves (Currie et al., 2007). More light allows for warmer air temperatures in various seasons which increase vegetative growth rate (Richardson et al., 2004). Thorp et al (2001) discovered that the use of reflective covers placed underneath 'Hayward' kiwifruit vines improved fruit weight and hence fruit yield, and increased flowering in the second year. Costa et al (2003a) confirmed the former study and pointed out a trend for higher TSS and lower FF values before harvest. A research conducted by Currie et al (2007) also suggested higher fruit weight and DMC were found in the fruit from reflective plots.

2.1.5 Skin properties of kiwifruit

2.1.5.1 Skin composition

Kiwifruit skin is composed of several surface structures such as the periderm, trichomes and lenticels, and sub-surface layers of the outer pericarp (Burdon and Lallu, 2011). The skin of *A. deliciosa* and *A. chinensis* fruit is brown, and the number and size of hairs differ among cultivars: 'Hayward' fruit have denser and more robust hairs than those of 'Hort16A' (Burdon and Lallu, 2011). Layers of dead cells on skin surface form the periderm. Development of periderm occurs after 6 to 8 weeks from fruit set, after which cell expansion from cell layers within the fruit occurs and results in small tears on the skin surface. These tears in turn develop into lenticels. Lenti-cellular structures help to improve gas transfer to and from the environment but may also promote surface spotting and pathogen infections. Underneath the periderm are two to three layers of cells forming the hypodermis region which separates the skin from the outer pericarp. This region is composed of small, closely packed cells with thick walls and a maximum diameter of approximately 0.05 mm (Burdon and Lallu, 2011).

The outer pericarp of *A. deliciosa* is composed of two types of parenchyma cells (Fig. 2.1a): small spherical cells with a diameter of up to 0.2 mm, and large elongated cells with a diameter more than 0.2 mm but most commonly more than 0.5 mm and up to 1 mm (Hallett and Sutherland, 2005; Hallett et al., 2005; Burdon and Lallu, 2011). In *A. chinensis*, sclerified cells (brachysclereides, stone cells) are found in the interface between the hypodermis and the bulk of the outer pericarp tissue (Fig. 2.1b). These stone cells are scattered amongst small parenchyma cells and have a maximum length up to 0.30 mm (Hallett and Sutherland, 2005, 2007).

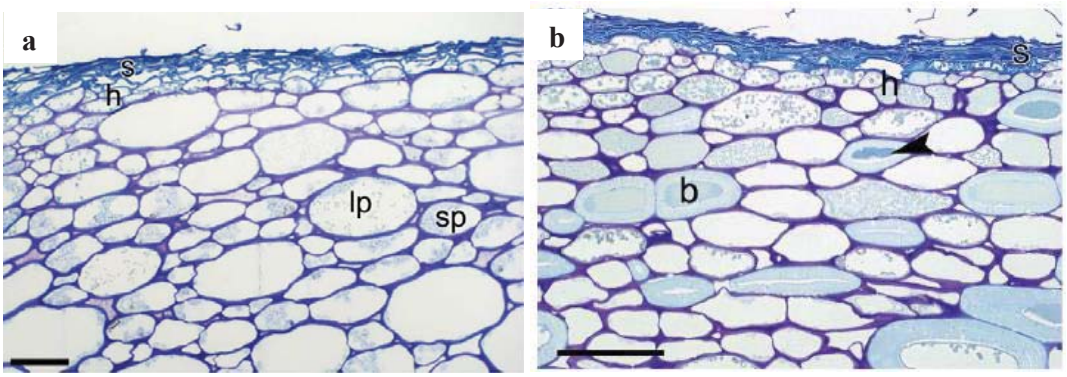

Figure 2.1 a) Cross section of skin of mature (21 weeks from petal drop) *A. deliciosa* var. *deliciosa* 'Hayward' fruit and outer flesh showing dead cell layers, hypodermis and a mixture of large and small cells in underlying flesh stained with toluidine blue. b) Cross section of skin of mature (23–24 weeks from petal drop) *A. chinensis* 'Hort16A' fruit and outer flesh, parenchyma cells are interspaced with stone cells. All images were acquired using light microscopy with underlying flesh stained with toluidine blue. s = dead cells of skin, h = hypodermis, sp and lp = small and large cells, b = stone cells, bar = 100 µm. Extracted from Hallett and Sutherland (2005). Image used with permission.

2.1.5.2 Changes in skin and near-surface cellular structures

Changes in skin and subsurface cellular structure can be resulted from environmental factors and may have potential consequences for postharvest fruit quality and storability (Nardozza et al., 2011). Celano et al. (2009) studied the changes in the structure of 'Hayward' kiwifruit skin in relation to water loss, an indicator of fruit quality during growth. As transpiration declines (decreased water loss), degradation of surface hairs, suberisation of outer cell layers and the subsequent death of the outer cells were observed. Light is another important factor influencing the skin structure of the fruit. Insufficient light exposure resulted in reduction of waxes, less hair number and more hydrated hair due to a decrease of skin temperature and an increase in relative humidity on the surface (Tombesi et al., 1993).

In 'Hayward' (*A. deliciosa*), the large cells comprise around 38 – 50% of the volume of the outer pericarp tissue (Hallett et al., 2005; Nardozza, 2008). The cell wall of these cells contributes to under 20% to the total cell wall volume of a fruit and shows resistance to softening in ripe fruit tissues (Hallett et al., 2005). The volume ratio of

small and large cells was found to affect dry matter content, an important quality factor of kiwifruit (Nardozza, 2008). While small cells are found to accumulate starch during fruit growth, larger cells do not accumulate starch to the same levels. A recent study on fruit anatomy in various *A. deliciosa* genotypes shows that small cells have a higher starch concentration than large cells (Nardozza et al., 2011). The presence of stone cells has effects on the firmness of *A. chinensis* fruit during ripening (Hallett and Sutherland, 2005). Additionally, the intercellular porosity and pore size were found to be highly variable amongst five commercial kiwifruit cultivars ('Hayward', 'Hort16A', 'G3', 'G9' and 'G14'; Cantre et al., 2014).

2.2 Non-Destructive Techniques for Assessing Kiwifruit Quality

Conventionally the quality of fruit at harvest, during storage and at consumption is assessed using simple destructive tests, such as flesh firmness by the penetrometer and total soluble solids by the refractometer. However, these tests destroy the fruit and hence only a small proportion of fruit samples can be measured. It is important in this case that a representative sample is used, as there is usually a wide variability in fruit quality within or between batches of fruit.

Development of non-destructive testing techniques enables the possibility to assess quality on a large number of fruit, to conduct multiple measurements on the same samples as well as to monitor fruit quality development over a period of time from preharvest through to the end of storage (Costa et al., 2003b). Various types of non-destructive techniques that are being used commercially, or currently under research, can be categorised based on the principles of mechanism: electromechanical (impact), electrochemical (electronic nose) and electromagnetic (e.g. near-infrared spectroscopy, nuclear magnetic resonance).

Impact technology measures the elasticity parameters of the fruit under dynamic conditions. The sensors are commonly applied to grading lines, and the progression of acceleration is recorded after fruit are gently tapped by the impact device (Chen and Tjan, 1998). This technique has been used for grading ripeness of kiwifruit (Peleg, 1999). Electronic nose (e-nose) simulates human's olfactory system and can identify the chemical composition of an odour. This technique has been used to assess kiwifruit freshness by classifying fruit based on the volatile compounds detected by the e-nose at

different storage time (Liu and Hui, 2015). Nuclear magnetic resonance (NMR) and magnetic resonance imaging (MRI) enables visualisation of internal structural changes and water mobility of a fruit sample (Costa et al., 2003b). This information can be used to identify physical and mechanical properties of the sample. Burdon et al. (2014c) utilised MRI to evaluate the water status of ripe kiwifruit and the capacity of cell wall swelling; Ward (2011) used a portable NMR system to assess textural properties of kiwifruit. The next section provides details on the use of near-infrared (NIR) spectroscopy for assessing quality of kiwifruit.

2.3 Near Infrared (NIR) Spectroscopy

2.3.1 Principle of NIR spectroscopy

Near-infrared (NIR) spectroscopy studies the spectral property of an object when irradiated with electromagnetic radiation between 780 – 2500 nm (Fig. 2.2) or 12820.5 to 4000 cm^{-1} wavenumbers (Williams and Norris, 1987; Miller, 2001; Sun, 2009). In many cases spectrometers also measure spectral properties within the visible range (400 – 750 nm; Miller, 2001). The 400 – 1000 nm range is sometimes referred to as visible-near-infrared (Vis-NIR; Williams and Norris, 2001) and the 1000 – 2500 nm range is referred to as short-wave infrared (SWIR).

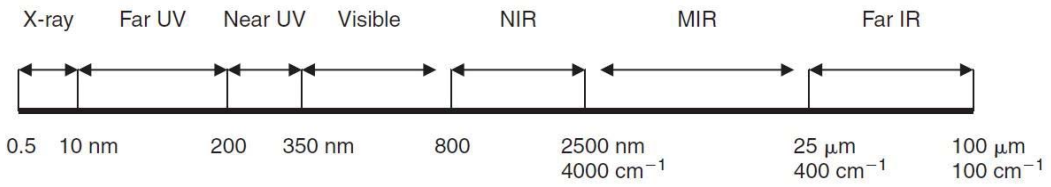

Figure 2.2 Spectral regions of interest for analytical purposes. Extracted from Sun (2009). Image used with permission.

Spectroscopy involves energy transfer between light and object. When NIR radiation reaches an object, the incident radiation may be reflected, absorbed or transmitted, depending on the physical properties and chemical composition of the sample (Nicolaï et al., 2007a). Reflection could be due to specular or diffusional reflection by glossy or rough surfaces, or scattering resulted from multiple refractions inside the object (Nicolaï et al., 2007a). Spectral absorptions are caused by the chemical and physical compositions present in the object. Chemical bonds such as the CH, NH,

OH and CO groups are subject to vibrational energy change in forms of stretching or bending when irradiated by NIR light. These anharmonic vibrations enable the occurrence of overtone transitions and combination modes, which correspond to specific absorption bands in the NIR region (Miller, 2001).

Fruit tissue contains water, carbohydrates and proteins which have large numbers of NIR-active chemical groups (Feng, 2003). For instance, strong absorption of water and carbohydrate can be found at 958 nm and 980 nm, respectively (Williams and Norris, 1987). Table 2.1 summarises several important NIR absorption bands of functional groups corresponding to various attributes of fruit tissues.

Table 2.1 Important NIR spectral regions for measuring fruit tissues.

Attributes	Functional Group	Wavelength Location	Reference
Water	O-H	744, 830-840, 938, 958, 970, 980, 1010-1030, 1458, 1442, 1932	(Williams and Norris, 1987) (Sun, 2009) (Osborne et al., 1993) (McGlone and Kawano, 1998)
Carbohydrates	C-H, O-H	830-840, 870-890, 900-930, 970-990, 1010-1030, 1053	(Williams and Norris, 1987)
Chlorophyll	C-H	680	(Mowat and Poole, 1997); (McGlone and Kawano, 1998)
Starch	C-H, O-H	901, 918, 1200, 1700, 1720, 1780	(Osborne and Fearn, 1986) (Williams and Norris, 1987)
Pectin	C-H, O-H, C-O	980	(Elvidge, 1990)
Sucrose	C-H, O-H	838, 870, 878, 888, 906, 913, 990	(Williams and Norris, 1987)
Cellulose	C-H, O-H, C-O	905, 920, 1655-1715, 2300-2360	(Williams and Norris, 1987) (Workman and Weyer, 2007)

2.3.2 Instrumentation

A generalised NIR spectroscopy system contains four main components (Fig. 2.3): 1) an NIR radiation source, 2) a wavelength selector for wavelength discrimination, 3) modes of sample measurement, and 4) a detector to convert the radiation to an electrical signal that can be sent to a signal processor and readout (usually computers).

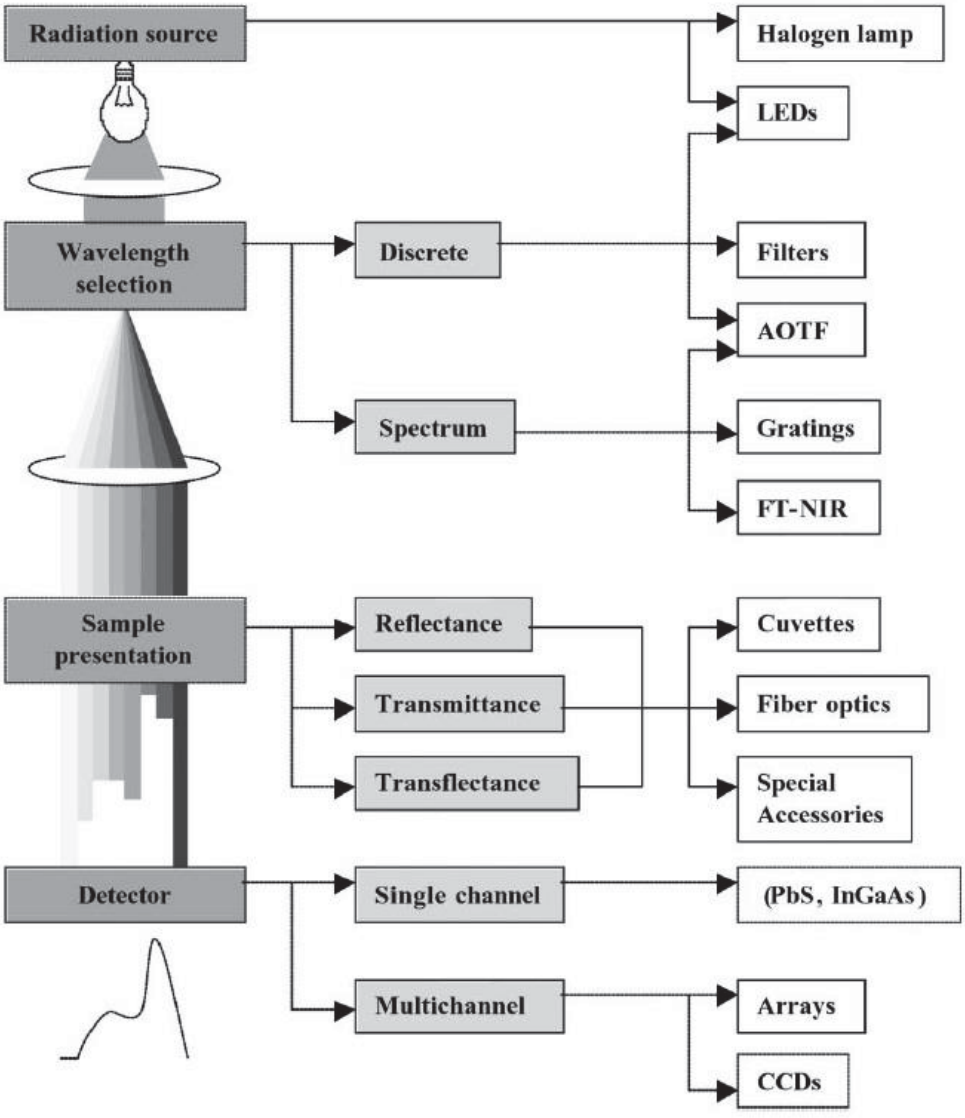

Figure 2.3 Principal features of NIR spectroscopy equipment. Extracted from Blanco and Villarroya (2002). Image used with permission.

The most common source of NIR radiation is the quartz halogen tungsten filament lamp which covers broad spectral region between 320 – 2500 nm (Osborne and Fearn, 1986). Light-emitting diodes (LED) are another source of NIR radiation (McClure et al., 2006). The LEDs release energy in the form of light of narrow wavelength bands in the process of electroluminescence (Osborne and Fearn, 1986).

Components for wavelength discrimination can be classified into two types, discrete-value and full-spectrum devices. Discrete-value spectrophotometers use filters to produce narrow wavelength bands or LEDs. As a result, they can only be used in applications with objects absorbing in specific spectral regions (Williams and Norris, 1987; McClure et al., 2006; Jha, 2010). Full-spectrum spectrophotometers usually include a diffraction grating. They are more flexible and therefore can be used in a wider variety of situations (Osborne and Fearn, 1986).

There are four modes available for the measurements using NIR spectroscopy: reflectance, transmittance, interactance and transflectance modes. Transflectance mode is designed for thin or clear samples having characteristics different from those of food and therefore is not commonly used for food samples (Williams et al., 2006). In reflectance mode (Fig. 2.4a), the object surface is illuminated by the light source and viewed by the light detector at a specific angle, e.g. 45 °C to avoid specular reflection (Schaare and Fraser, 2000; Nicolaï et al., 2007a). In transmittance mode (Fig. 2.4b), the light source is opposite to the detector. This requires very high light intensities which can cause heat damage to the object surface and alter its spectral properties (Nicolaï et al., 2007a). In interactance mode (Fig. 2.4c), the light source and detector are next to each other but separated by a light barrier which ensures that light due to specular reflection cannot directly enter the detector (Nicolaï et al., 2007a). Schaare and Fraser (2000) suggested that amongst the three measurement modes of NIR, interactance mode provide the most accurate instant estimates of TSS, density and flesh colour for measuring internal properties of kiwifruit (*A. chinensis*). However, Lammertyn et al. (2000) found little difference between interactance and reflectance configurations for the prediction of TSS of apple.

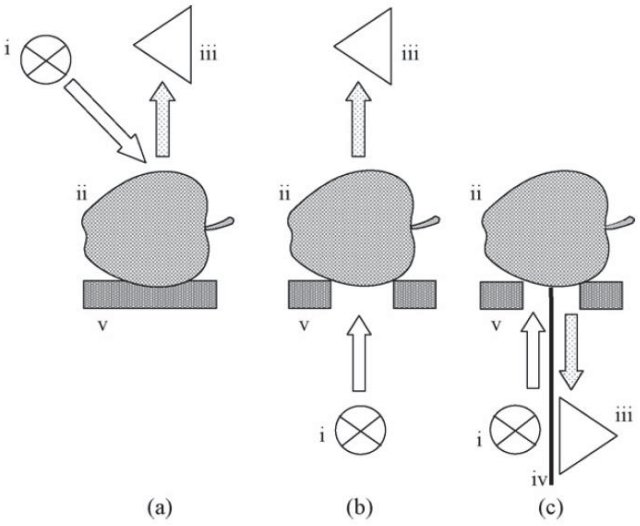

Figure 2.4 NIR measuring mode: (a) reflectance; (b) transmittance; and (c) interactance showing (i) the light source, (ii) object, (iii) detector, (iv) light barrier, and (v) support. Extracted from Nicolaï et al. (2007a). Image used with permission.

Detective devices are usually comprised of photoconductive semiconductors (PbS or InGaAs) operating in the range of 1000 – 2500 nm with a peak at 2000 nm (Blanco and Villarroya, 2002). The conduction increases with the intensity of incident radiation. Another type of detectors is photovoltaic photodiodes, which are usually formed from silicon and germanium and cover the Vis-NIR region between 400 and 1000 nm (Osborne and Fearn, 1986; Osborne et al., 1993).

The NIR technology has been adapted to devices with various configurations for specific purposes. Fig. 2.5a illustrates a commercial-scale bench-top Vis-NIR spectroscopy system (PANalytical, B.V, Boulder, Colorado, USA) suitable for both industrial and laboratory analysis. The NZ kiwifruit industry uses online multilane NIR sensors (Fig. 2.5b; Taste Tech 1, Taste Technologies Ltd., Auckland, NZ) fitted to a commercial kiwifruit grader (Compac^{TM} grading equipment, Auckland, NZ) for sorting of kiwifruit according to DMC. This system can also be used for recovering high DMC fruit from lower dry matter grower lines that do not meet the Minimum Taste Standard (MST) of DMC for 'G3' kiwifruit (McGlone and Wohlers, 2016). More recently, a breakthrough in technology (Goldring and Sharon, 2012) enabled the production of low-cost spectrometer on a "chip", leading to the development of consumer-scale NIR devices such as SCiO molecular sensor (Fig. 2.5c) (Consumer Physics Inc., Tel Aviv,

Israel), LinkSquare (Stratio Inc., Seoul, Korea) and Tellspec® Food Sensor (Tellspec Inc., Toronto, Canada), which can be integrated into smartphones and make applications of NIR accessible and affordable to a wider audience (Coates, 2014; Haughey et al., 2015).

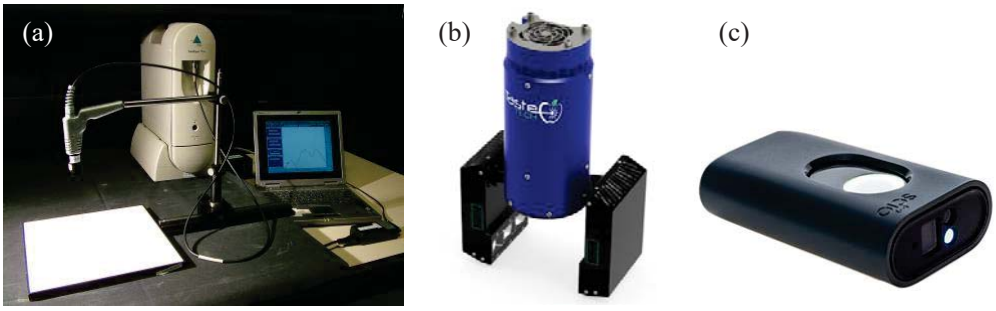

Figure 2.5 (a) A commercial ASD FieldSpec® Pro full-spectrum Vis-NIR spectroscopy system (ASD Inc., USA) coupled with a contact probe (PANalytical, B.V, Boulder, Colorado, USA); (b) an NIR sensor for online sorting of fruit (Taste Tech 1, Taste Technologies Ltd., Auckland, NZ); (c) a consumer-scale SCiO™ molecular sensor (V1.0, Consumer Physics Inc., Tel Aviv, Israel).

2.3.3 Multivariate statistical techniques

Using NIR for analysis of fruit products has several advantages, including speedy response time, simple or no sample preparation, allowing for non-destructive measurements and low cost in comparison to other spectroscopies such as mid-infrared, Raman and others (McClure, 2006). However, diffuse reflectance spectra of fruit are often non-specific because of multiple overlapping absorption features. Therefore multivariate statistical techniques (also known as chemometrics) are required to extract the information relevant to quality attributes which is hidden in the NIR spectrum (Nicolaï et al., 2007a).

2.3.3.1 Pre-processing of spectra

Data pre-processing techniques are used to remove unwanted spectral variations and baseline shifts arising from light scattering from solid samples or variations in temperature, density, and particle size of samples etc (Ozaki et al., 2006; Nicolaï et al., 2007a).

Spectroscopic measurements performed in reflectance mode are usually converted to log(1/R) (R is reflected radiation) using Beer's Law because there is a linear relationship between the concentration of an absorbing component and its contribution to the log(1/R) value at the wavelength absorbed (Williams and Norris, 1987). However, this approach does not take into account the fact that light penetration in biological tissue is complicated and also involves scattering (Nicolaï et al., 2007a).

Smoothing techniques are used to remove random noise of spectral data. During smoothing a Savizky-Golay filter (Savitzky and Golay, 1964) is usually used which functions by fitting the spectrum in a wavelength interval with a polynomial by least-squares method (Williams and Norris, 2001; Nicolaï et al., 2007a). However, smoothing sometimes also removes useful information which is not clear yet at the time of removal. Hence the usefulness of smoothing is questionable since most multivariate techniques used after pre-processing already include models for unwanted noise (Naes et al., 2004).

Baseline correction can be achieved by derivation (first or second order) or multiplicative scatter correction (MSC; Ozaki et al., 2006). Derivation is usually calculated according to the Savizky-Golay algorithm (Naes et al., 2004). The MSC is useful for correcting vertical variations and inclination of the baseline (Ozaki et al., 2006).

Normalization of spectra can be described as the changing of a set of spectra so that the new set has more features in common to suppress unwanted source of variability. Normalisation transformations are computed sample-wise. A simple example is subtracting the log(1/R) (absorbance) value at the reference wavelength from all the spectral values. This results in a set of spectra with value zero at the reference wavelength. (Williams and Norris, 1987).

Centering using the average value (also called mean centering) is often powerful in resolution enhancement. This is achieved through an adjustment to the data set to reposition the centroid of the data to the origin of the coordinate system (Ozaki et al., 2006). This shifts the focus on the differences between observations rather than their absolute value. After mean centering, all means are zero and variances are interpreted around zero.

2.3.3.2 Reduction of variables

Variable reduction or selection methods are developed to identify a small number of variables (a subset of spectral bands) from the entire range of spectra for easier data interpretation (Zou et al., 2010). Elimination of uninformative variables can improve prediction accuracy and model robustness (Cai et al., 2008). The most commonly used method is principal component analysis (PCA; Wold et al., 1987; Blanco and Villarroya, 2002). Several other methods have also been developed including correlation coefficient, interval partial least squares (iPLS), stepwise analysis and genetic algorithms (GA; Cai et al., 2008) .

Another simple way of reducing the number of variables is by taking averages over wavelengths. Commercial spectrophotometers generally have a spectral resolution of a few nanometers up to ~ 10 nm, where in most applications a 10 nm resolution is often sufficient (Nicolaï et al., 2007a). High resolution does not improve the information content of the spectra and yet increases the computational time. Nicolaï et al. (2007b) evaluated the predictive accuracy of NIR regression model using a range of spectra resolution and found that a wavelength resolution of about 5 nm provided the best results.

2.3.3.3 Model development and evaluation

For any spectroscopy technique, calibration is a process which develops the mathematical relationship, in the form of a model, between measured sample properties and the intensities or absorbance at more than one wavelength of the set of known reference samples (Zeaiter et al., 2005; Sun, 2009).

Once an NIR instrument has been calibrated against a reference method for the measurement of a particular sample property, it can be used to predict unknown samples and the prediction errors can be estimated, a process known as validation. Validation of calibration provides the basis for calculation of true measurement error by comparing NIR measurements to reference method measurements on a new set of samples (Williams and Norris, 1987). If the two are essentially the same, the model provides accurate prediction and will be useful for future predictions (Sun, 2009).

For internal validation, both *n*-fold cross-validation and internal test-set ('holdout') validation can be used to compare the predictive performance of calibration and validation. In *n*-fold cross-validation, the calibration samples are randomly divided into *n* segments. One of the segments is then removed from the dataset and the calibration model is developed from the remaining (*n* – 1) segments. The isolated segment is used to calculate the prediction errors. This process is repeated until every segment is removed from the dataset once, and the variance of all prediction residuals is estimated. For leave-one-out cross-validation (LOOCV), the process is similar except that at each time one sample, rather than one segment, is removed from the dataset. In internal test-set validation, the calibration samples are randomly divided into two populations: calibration and validation subsets. Calibration model is then developed using the calibration subset, and the prediction residuals are calculated by applying the calibration model to the validation subset. In external validation, calibration model is applied to an independent external validation data set usually obtained from a different orchard or different season (Fig. 2.6; Nicolaï et al., 2007a) .

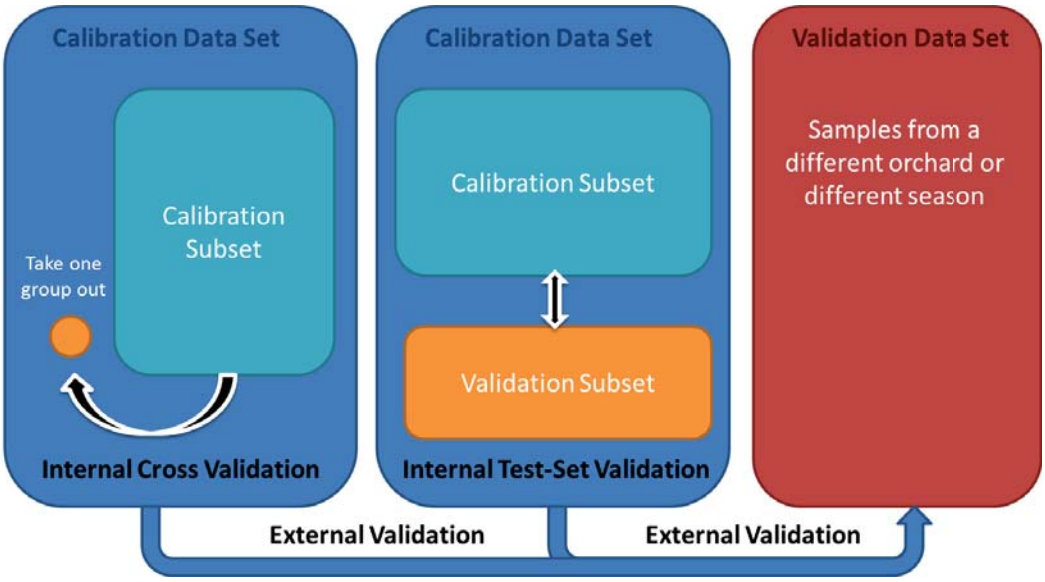

Figure 2.6 A flow chart showing the internal and external validation processes for model development.

Prediction model using NIR spectroscopy can be applied for both quantitative and qualitative analysis. In quantitative analysis, spectra of training sample set and corresponding chemical analysis are collected, and calibration model is developed using regression techniques. The accuracy for calibration is tested using a validation test set

(Westerhaus et al., 2004). In qualitative analysis, calibration involves the application of discriminant techniques to find useful relationship between spectra of training samples and their group membership instead of quantitative regressions (Kramer et al., 2004).

The efficiency of quantitative regression for a set of calibration samples can be reported as the standard error of calibration (SEC), standard error of prediction (SEP), mean square error (MSE), root mean square error (RMSE), correlation coefficient (r), and/or coefficient of determination (r^2; Williams and Norris, 2001). The selection of terms is often dependent on the software used (Westerhaus et al., 2004). When internal or external validation is used, the prediction error of a calibration model is defined as the mean square error of prediction (MSEP) or root mean square error of prediction (RMSEP; Nicolaï et al., 2007a; Sun, 2009), which can be calculated as:

$$RMSEP = \sqrt{\frac{\sum_{i=1}^{n_p}(\hat{y}_i - y_i)^2}{n_p}} \quad (2.1)$$

where n_p is the number of validated objects, and $\hat{y}_i$ and y_i are the predicted and measured value of the ith observation in the test set, respectively.

Additionally, SDR, which is the division of standard deviation (SD) and RMSEP, is also used. The SDR represents the predictive performance of a model and it usually provides more direct information rather than R^2 or RMSEP (Liu et al., 2010). The higher the SDR values the greater the power of the model to predict accurately. SDR values below 1.5 indicate that the calibration model is not useful; between 1.5 and 2 suggest that the model can discriminate low from high values of the response variable fairly well; between 2 and 2.5 indicate coarse quantitative predictions are possible, and above 2.5 correspond to good and excellent prediction accuracy (Saeys et al., 2005).

For qualitative/discriminant analysis, calculation of prediction accuracy is usually expressed as the correctly classified samples as a percentage of all samples in the designated group.

2.3.3.4 Regression and classification techniques

For linear regression, multivariate linear regression (MLR), principal component regression (PCR) and partial least squares regression (PLSR) are the three most

common techniques used in calibration of NIR spectral data (Nicolaï et al., 2007a; Zou et al., 2010). Recent development of nonlinear techniques such as artificial neuron network (ANN) and kernel functions enables the analysis of data with nonlinearilities and improves predictive performance of regression model (Nicolaï et al., 2007a). Kernel functions generate hidden units that represent the input data and map this information into a high-dimensional feature space, in which calibration is carried out (Ivanciuc, 2007). The common kernel functions include Gaussian, polynomial and radial basis. Kernel-based support vector machines (SVM) are capable of both linear and non-linear regressions but would require the tuning of parameters to achieve model robustness (Chapelle et al., 2002).

In classification, discriminant analysis of spectra can be supervised (the class to which the samples belong is known) or unsupervised (Blanco and Villarroya, 2002). Pattern recognition usually consists of three steps (Kim et al., 2000). First, the raw data is reduced by a feature extraction process; PCA is the main technique for this purpose and can work for both supervised and unsupervised cases. Second, features that are suitable for discriminating samples are selected; a number of techniques including canonical discriminant analysis (CDA) and genetic algorithms (GA) can be applied to the spectral data. The final stage involves pattern recognition based on selected features; this includes traditional methods such as linear discriminant analysis (LDA) and PLS-DA, which uses PLS to develop a model which is then used to estimate the classification of unknown samples (Kim et al., 2000; Kramer et al., 2004). More recently, machine learning techniques such as ANN and SVM have also been used in discriminant analysis and can achieve robust calibration models with good prediction outcomes.

There are many software packages available for multivariate calibration. In this research two packages were used. The Unscrambler® package (CAMO Software AS., Oslo, Norway) is user friendly and allows visual interpretation of spectral data and calibration model. The Weka (Waikato Environment for Knowledge Analysis) is open-source software (Version 3.7.12; University of Waikato, Hamilton, New Zealand; Hall et al., 2009) which provides a wide range of machine learning algorithms for solving data mining problems.

2.3.4 Applications of Vis-NIR in horticultural products

The potential of NIR spectroscopy was first discovered in the 1960s (Reh and Irudayaraj, 2008; Sun, 2009). The wide-spread application of NIR initiated in 1973 following the use of NIR spectroscopy to replace the traditional Kjeldahl measurements for the determination of protein in grain (Williams and Norris, 1987; Reh and Irudayaraj, 2008). Since then, Vis-NIR spectroscopic techniques have been used as non-destructive and rapid tools to evaluate various quality attributes of fruits and vegetable (Williams et al., 2006; Jha, 2010).

For the kiwifruit industry, NIR spectroscopy is most commonly used in quantitative analysis of quality attributes by developing regression models (Table 2.2). For instance, instant estimation of at-harvest TSS and DMC can be achieved with high regression accuracy of % RMSEP $\leq$ 5 (McGlone and Kawano, 1998; Osborne et al., 1998; Osborne et al., 1999; Schaare and Fraser, 2000; Clark et al., 2004; Moghimi et al., 2010; Lee et al., 2012). There have also been attempts to predict post-storage TSS based on at harvest NIR spectral data (McGlone et al., 2002b; McGlone et al., 2007). Prediction of at-harvest FF using NIR spectral data was not as successful (McGlone and Kawano, 1998; Costa et al., 1999).

Table 2.2 Prediction of kiwifruit quality attributes, both at harvest and after storage, using (Vis-)NIR spectral measurements acquired at harvest.

Reference	Acquisition Mode	Spectra Range (nm)	Cultivar	Storage Time* (Days)	Storage Temp.	Data Pre-treatment	Quality Attribute	Sample Size	R^2	RMSEP
Chen and Han (2012)	Reflectance	833–2500	'Qinmei'	0	-	Smoothing, derivative, multivariate scatter correction, normalisation	TSS (°Brix)	70–220	0.35–0.94	0.66–0.89
Lee et al. (2012)	Reflectance	408–2492	*A.deliciosa* 'Hayward'	0	-	Standard normal variate, detrend, derivative	FF (N) TSS (°Brix) Acidity (%)	180 180 180	0.88 0.98 0.91	3.32 (SEP) 0.49 (SEP) 0.28 (SEP)
Moghimi et al. (2010)	Tansmittance	400–1000	*A.deliciosa* 'Hayward'	0	-	Smoothing, derivative, multivariate scatter correction, standard normal variate	TSS (°Brix) pH	100 100	0.86 0.89	0.26 0.08
McGlone et al. (2007)	Interactance	300–1140	*A.chinensis* 'Hort16A'	84	0°C	Log transformation, smoothing, standard normal variate	DMC (%) TSS (%) Hue (°)	123 123 123	0.92 0.89 0.83	0.39 0.38 1.19
Clark et al. (2004)	Interactance	300–1140	*A.chinensis* 'Hort16A'	0	-	Log transformation, smoothing, scaling, normalisation	DMC (%) TSS (%) Hue (°)	864–2642 886–2678 868–2663	0.90–0.93 0.69–0.94 0.63–0.86	0.44–0.54 0.76–1.43 0.85–1.37
McGlone et al. (2002b)	Interactance	300–1140	*A.deliciosa* 'Hayward'	0	-	Log transformation, smoothing, scaling, normalisation	DMC (%) TSS (%)	180 180	0.86 0.87	0.46 0.52

				2–7	20°C		DMC (%) TSS (%)	179 179	0.91 0.92	0.39 0.39
Schaare and Fraser (2000)	Reflectance Interactance Transmittance	300–1100	*A.chinensis* 'Hort16A'	0	-	Smoothing, log transformation, multivariate scatter correction, standard normal variate, derivative, normalisation	TSS (°Brix)	50	0.86 0.93 0.89	1.18 (SEP) 0.80 (SEP) 1.01 (SEP)
							Density (kg m^{-3})	50	0.59 0.74 0.55	4.5 (SEP) 3.6 (SEP) 4.8 (SEP)
							Hue (°)	50	0.76 0.82 0.74	1.88 (SEP) 1.63 (SEP) 1.95 (SEP)
Costa et al. (1999)	Reflectance	650–1200	*A.deliciosa* 'Hayward'	0	-	Log transformation, smoothing, derivative	FF (kg·cm^{-2}) TSS (°Brix)	80 80	0.42 0.65	0.65 (SEC) 0.36 (SEC)
Osborne et al. (1999)	Interactance	330–1140	Not Stated	0	-	Smoothing	DMC (%) TSS (°Brix)	192–322 192–322	- -	0.32–0.68 0.27–0.47
McGlone and Kawano (1998)	Interactance	400–1100	*A.deliciosa* 'Hayward'	0	-	Derivative	FF (N) DMC (%) TSS (°Brix)	41–318 41–318 41–318	0.42–0.76 0.85–0.92 0.76–0.92	4.5–11.8 0.36–0.96 0.42–0.69
Osborne et al. (1998)	Interactance	306–1139	Not Stated	0	-	Smoothing, multivariate scatter correction	DMC (%) TSS (°Brix)	97 97	- -	0.41 0.45

*Storage time refers to the delay in time (days) between NIR spectral measurements and fruit quality measurements

However, use of NIR spectroscopy to perform qualitative analysis in kiwifruit is not well established. In particular, little research was carried out to discriminate kiwifruit storage potential based on export firmness criterion (FF < 1 kg_f or 9.8 N) using classification models. Feng (2003) used at-harvest NIR spectral data to classify 'Hayward' grower lines based on softening rate and incidence of physiological disorders (e.g. soft patch, low temperature breakdown). Clark et al. (2004) categorised 'Hort16A' kiwifruit into two groups ('disordered' and 'good') based on at-harvest NIR spectral data and after storage firmness values. In other crops, Zude et al. (2006) classified apples by different 'quality levels' using NIR spectra data and firmness measured before and after storage. In addition, Feng et al. (2013) segregated apricots for storage potential using at-harvest Vis-NIR spectral data by developing an exponential model.

2.4 Optical Coherence Tomography (OCT)

2.4.1 Principle of OCT

The OCT technique is a purely optical, non-destructive, non-invasive, and contactless high resolution imaging method applicable to semi-transparent and turbid media (Drexler and Fujimoto, 2008). It allows for the acquisition of three-dimensional (3D) depth resolved image data of (sub)surface regions in situ and in real-time with resolution as good as one micrometre.

This technique detects the discontinuities in refractive index corresponding to the boundaries between different types of tissues (Landahl et al., 2012). To capture an OCT image, the sample is irradiated with near-infrared light and the light beam is back-scattered from different layers of sub-surface tissue structures such as pores and cells. A depth scan is obtained by comparing the arrival times of the light path scattered from the sample with the light path reflected from a reference mirror. Cross-sectional images are obtained by scanning the light laterally across the surface of the sample and a 3D volume is generated by several depth scans at adjacent lateral positions (Verboven et al., 2013). OCT provides excellent axial resolution with an accuracy of a few micrometers. The penetration depth however depends on the scattering and absorption properties of the tissue. In fruit media the penetration depth is up to 2 mm with 5 – 20 μm resolution (Meglinski et al., 2010; Verboven et al., 2013).

2.4.2 Image acquisition

Depth scans can be obtained either by moving the reference mirror (time-domain OCT, TD-OCT) or, by spectral analysis of the interference signal with the reference mirror kept fixed and subsequent fast Fourier transformation (spectral-domain OCT, SD-OCT; Fercher et al., 1995) .

In SD-OCT, a dispersive element such as a grating is used for spectral analysis and depth scans are acquired quasi-instantaneously by a line scan camera within a few milliseconds. This technique allows for high acquisition rates as required in real-time measurements. However, for two-dimensional (2D) images the light beam needs to be scanned laterally in one dimension. Single depth scans and cross-sections are classified as A- and B-scans, respectively. The 3D measurements require 2D scanning across both lateral directions. The scanning process can be performed by different means, such as by one (2D image) or two galvanometer mirrors (3D data). Single (2D) images acquired by SD-OCT are always cross-section images. A schematic diagram of a SD-OCT system is depicted in Fig. 2.7.

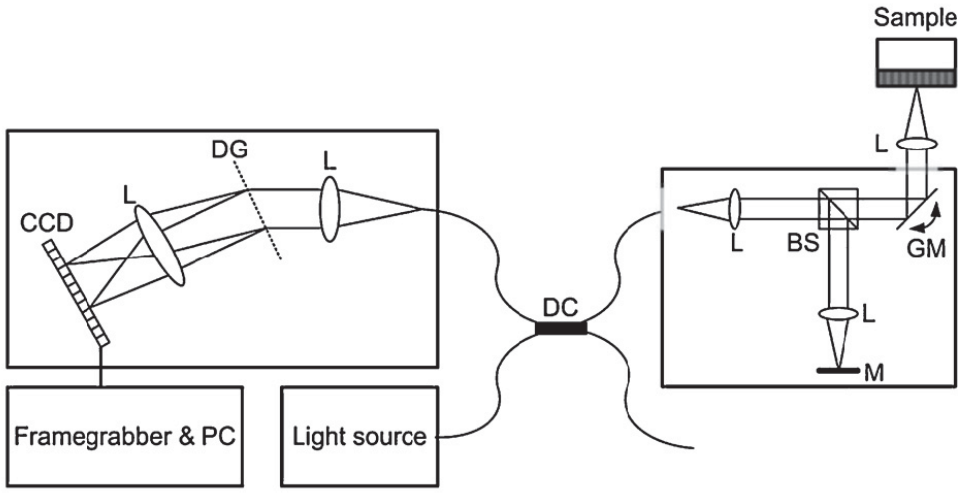

Figure 2.7 Schematic diagram of a spectral-domain OCT (SD-OCT) system. The boxes represent portable and independent modules. DC: directional coupler; BS: beam-splitter; GM: Galvanometer mirror; L: lens; DG: diffraction grating; CCD: charged coupled device (Podoleanu, 2012; Verboven et al., 2013). Image used with permission.

Figure 2.8 illustrates the image capture of a kiwifruit sample using the commercial TELESTO™ SD-OCT imaging system (Thorlabs, Lübeck, Germany). Real-time visualisation of the sample in 2D and 3D is available from the software accompanying this system. However, for high level image processing, sophisticated image processing software such as Matlab® (MathWorks, Inc., Natick, USA). and Avizo® (Visualization Sciences Group, France) are usually required, in order to allow display, modification and quantification of the images.

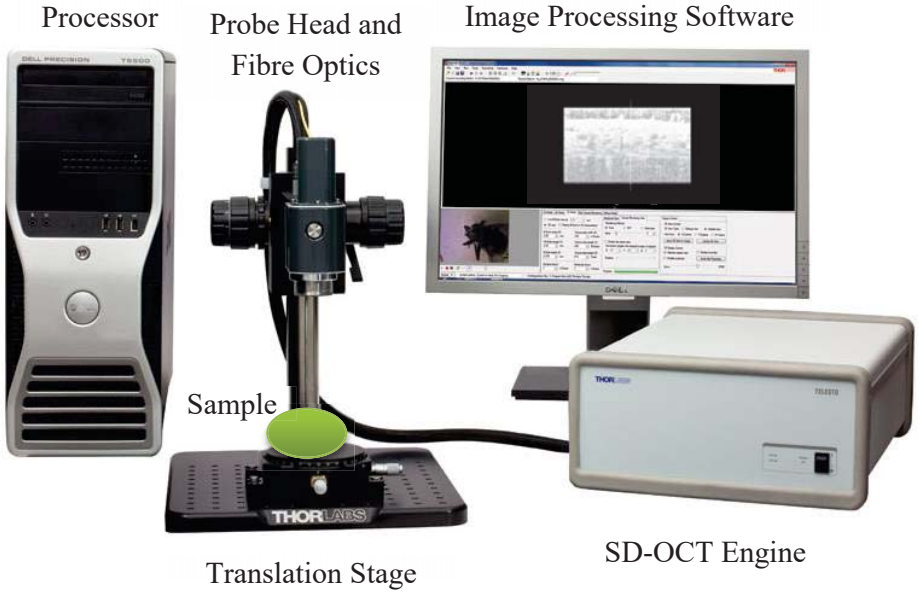

Figure 2.8 Schematic diagram of a commercial SD-OCT system: Variable-Rate TELESTO™ OCT Imaging System operating at 1325nm (Thorlabs, Lübeck, Germany). Axial resolution: 7.5 µm. Lateral resolution: 15 µm. Operating rates: 5.5 kHz, 28 kHz, and 91 kHz.

2.4.3 Applications of OCT in horticultural products

The OCT has the advantages of minimal sample preparation in comparison to conventional optical methods and it enables the potential for repeated measurements on the same sample matured over a period of time. Although OCT has already been widely applied in biomedical areas such as dermatology and ophthalmology, this technique has also found an increasing number of applications in assessment of horticultural products.

Clements et al. (2004) used OCT to compare hull layer thickness of four genotypes of lupin seeds, and were able to distinguish between different species of

lupins and also identify thin-hulled seeds from normal seeds. Meglinski et al. (2010), Ford et al. (2012) and Landahl et al. (2012) demonstrated the use of OCT to detect defects, rots and diseases in onions based on visualisation and quantification of 2D OCT images. Loeb and Barton (2003) produced OCT images of kiwifruit showing some thin-walled parenchyma cells in the outer pericarp (Fig. 2.9a). However, the images were not obtained from intact kiwifruit samples but from a radial transverse section removed from the equator of the fruit. Magwaza et al. (2013) investigated the feasibility of using OCT in the visualization of histological and microstructural features in intact rind tissues of mandarins. Image processing enabled the development of 3D models of oil glands, which is associated with progressive rind breakdown in mandarins (Fig. 2.9b). Rizzolo et al. (2013) reported the differences in mechanical and acoustic characteristics between two types of air-dried apple rings were due to different subsurface structure as found with OCT analysis (Fig. 2.9c). Verboven et al. (2013) used OCT to visualise peel structural differences between apples and measured structural changes that occur during storage (Fig. 2.9d).

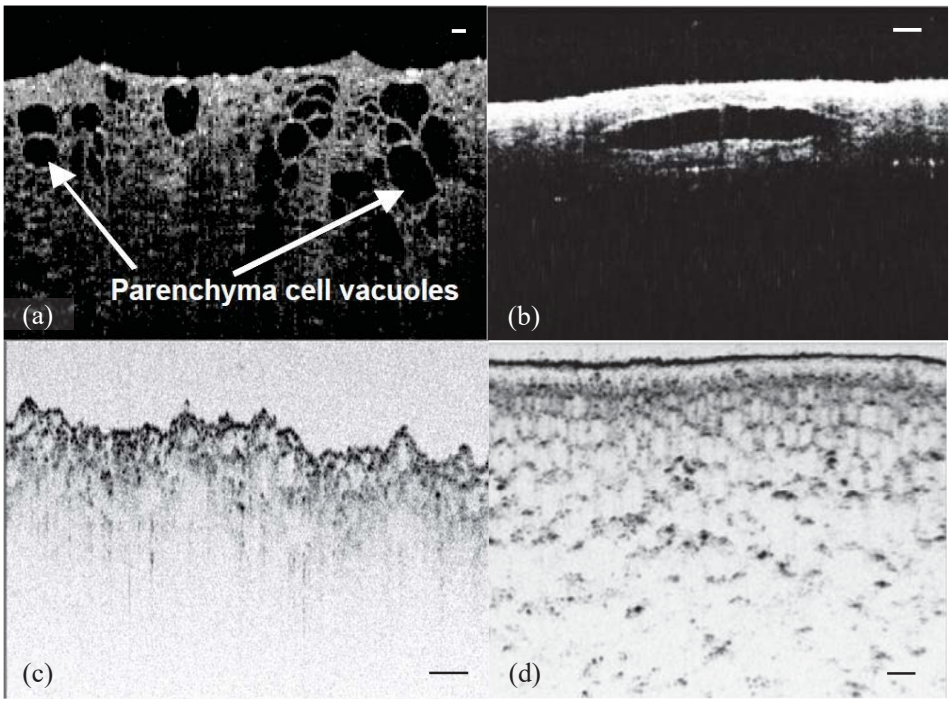

Figure 2.9 OCT images of (a) sectioned kiwifruit (Loeb and Barton, 2003); (b) mandarin with moderate degree of RBD (Magwaza et al., 2013); (c) untreated air-dried apple ring (Rizzolo et al., 2013); and (d) 'Royal Gala' apple (Verboven et al., 2013). Images used with permission. Scale bars = 0.1 mm

2.5 Conclusion and Opportunity for Research

The green-fleshed 'Hayward' kiwifruit is the most dominating cultivar globally and is the major export cultivar in New Zealand. At commercial harvest there is often huge inherent variability in fruit quality as a result of preharvest conditions and orchard manipulation techniques. This leads to a wide range of storage potential when fruit are stored locally prior to export. The development of oversoft fruit during storage not only renders the affected fruit unsaleable, but also produces an ethylene environment which softens fruit that are otherwise long-storing, leading to significant financial losses. The ability to predict the potential of fruit to develop rapid softening is essential for making inventory decisions and reducing total loss.

The effects of preharvest conditions on at harvest kiwifruit quality have been well established. The main driving force has been improving production yield and sugar content in order to meet consumers' preferences. Knowledge of how preharvest conditions influence postharvest performance is also important. The first part of this thesis will look at the effects of two most common commercial practices on postharvest quality and storability of kiwifruit.

The development of new technologies such as OCT and NIR spectroscopy allows rapid and non-destructive measurements of fruit. The application of OCT in horticultural products is not well studied. This research explores the type of information that can be captured by OCT using kiwifruit samples, and investigates the potential for OCT to provide useful information on harvest and postharvest fruit quality.

The application of NIR technology in horticultural products has been well established. Whilst strong correlation can be found between spectral data and the chemical properties of the fruit by developing regression methods, there is little success in predicting physical attributes such as FF quantitatively. Additionally, in most cases evaluation of NIR focuses on instant estimation of fruit properties; research on the ability of NIR to predict future quality is scarce. In this thesis an attempt will be made to investigate the potential of NIR to indicate future FF and storage potential using qualitative analysis.

3 Effects of preharvest orchard management practices on at-harvest and post-storage kiwifruit quality

3.1 Introduction

Kiwifruit quality is defined by many factors including fruit size, shape, flavour, texture and length of storage time (Ferguson and Seal, 2008). The internal quality attributes of the fruit are more important in determining (re)purchase decisions by consumers (Buxton, 2005). Flavour of kiwifruit has been associated with fruit DMC at harvest (Harker et al., 2009; Jordan and Seelye, 2009) and TSS that will develop in ripe fruit (Jordan et al., 2000; Burdon et al., 2004). Additionally, fruit FF is an important attribute for determining the postharvest storability of kiwifruit.

Preharvest factors such as growing conditions and orchard management practices can affect fruit quality at the time of harvest and during subsequent storage. Good orchard management practices aim to achieve optimal flowering and fruit yield for the current season, help to obtain desirable fruit quality and reduce chances of poor yield in the following season (Sale, 1990). However, preharvest factors also contribute to large inherent variation in fruit quality within and between kiwifruit orchards at the time of harvest (Woodward, 2007). Such variability contributes to the difficulty for the industry to accurately predict quality changes during postharvest storage and distribution (Shewfelt, 1999). While several orchard and climatic factors have been suggested to influence kiwifruit storage quality, few published data demonstrated these effects. It is important to understand how at-harvest characteristics such as size, appearance, taste and texture etc. are imposed (or not) from previous growing conditions and environmental factors, and what kinds of consequences are likely to occur during storage.

This chapter aims to elucidate the effects of preharvest orchard practices on at-harvest and postharvest storage quality of 'Hayward' kiwifruit, through the manipulation of crop load and the application of girdling during cropping. The individual and the combined effects of both practices will be observed in order to investigate if these practices can be utilised to affect or improve postharvest fruit quality and storability for distribution.

3.2 Materials and Methods

3.2.1 Experimental design

In a commercial orchard located in Te Puna, Bay of Plenty, an experiment was established in the form of a 2 × 2 matrix of treatments, consisting of 56 'Hayward' kiwifruit female vines with manipulated crop load (industrial average, 36 t/ha and ultrahigh, 43 t/ha) and the application (or not) of girdling. There were 16 vines each for low crop load treatment with and without girdling, and 12 vines each for high crop load treatment with and without girdling. The vines were about 35 years old and grown on a pergola using opposing females. Hydrogen cyanamide was used at commercial rates to treat the vines to improve budbreak and reduce the incidence of side flowers.

Crop thinning occurred on 4 – 5 January 2013 (42 – 43 day after full bloom; DAFB) and trunk girdling occurred on 10 December 2012 (17 DAFB) and 2 February 2013 (71 DAFB). The fruit thinning in this experiment was designed to simulate conventional fruit thinning practices, in which the smallest fruit and poorly shaped or 'Hayward' marked (a shallow sunken line running down the side of the fruit, sometimes ending in a hook or protuberance caused by a stamen sticking to the fruit and the hook by an anther sticking) were removed first, and the remaining fruit removed to reach the final crop load by taking into consideration the local leaf to fruit loading relative to shoot length. Prior to pollination the vines were flower-thinned to remove any side flowers. Fruit were then thinned to the final crop load 6 weeks after the last pollination.

Selected vines for each treatment were arranged according to a four-by-four Latin square (Fig. 3.1) with each treatment represented on each row and column of the trial as plots, which accounted for in-orchard location effects but avoided unusual plants caused by e.g. regrafting. Commercial harvest occurred on 15 May 2013, with all treatments being harvested on the same day. At harvest, 24 trays of 30 mixed-sized fruit per tray were sampled from each of the four plots for each treatment representing replicates. The samples were collected by dividing each vine quarter into 9 quadrants and then randomly sampling a fruit from each quadrant. Fruit were delivered from the orchards in Te Puke and cured at ambient temperature for two days during transport. Fruit trays arrived at Massey University on 17 May 2013, and were wrapped in polyliner films and stored at 20 °C overnight before the commencement of measurements (day 0).

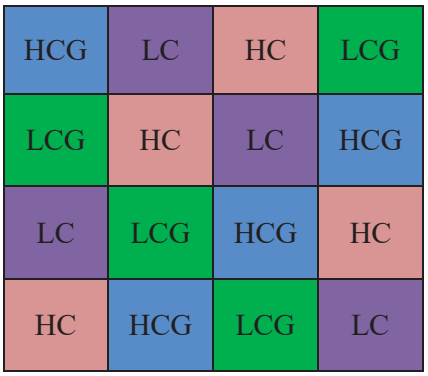

Figure 3.1 Design of orchard layout to minimise in-orchard location effects. HCG: High crop load with girdling. LCG: Low crop load with girdling. HC: High crop load. LC: Low crop load. Letters represent different rows whereas numbers represent different columns. Each square represents a single plot.

3.2.2 Fruit quality attributes

The at-harvest (prior to transportation) fruit weight, DMC and TSS of kiwifruit were randomly collected from 90 fruit of each treatment at the packhouse. The TSS and FF were also monitored upon arrival at the laboratory (day 0) and during storage (14 – 175 days). Single trays (30 fruit) from each of the 16 plots were assessed destructively for FF and TSS at 0, 14, 28 and 50 days. Four trays (120 fruit) from each of the 16 plots were measured at 25-day intervals from 75 to 175 days. During storage, ethylene concentration in the cool room was monitored using ethylene analysing equipment (photoacoustic ETD-300, Sense B.V., Nijmegen) and maintained below 5 nL L^{-1}. Fruit were equilibrated to ambient temperature (20 ºC) over a period of 15 hours prior to fruit quality measurement.

Fruit weight (g) was measured by using a digital balance (Mettler PG-503S, Toledo, Switzerland) with 0.001 g accuracy. The DMC (%) was determined using an oven drying technique by dehydrating a known mass of 2-3 mm thick equatorial fruit slice at 60-65°C for 24 hours. Data were expressed as percentage of the wet mass. The FF (N) was measured using an electronic QALink Penetrometer (Willowbank Electronics Ltd., Napier, New Zealand) fitted with the standard 7.9 mm Magness-Taylor probe. Two measurements of peak penetrating force were made at two locations (90° apart) around the equator of the fruit after removal of a thin layer (1 mm) of the fruit skin. The penetration speed was 20 mm s^{-1} and the puncture depth was 8 mm. The TSS

(ºBrix) was measured using a digital pocket refractometer (PAL-1, Atago, Japan) using the juice taken from both end caps of the fruit. The proportion of soft fruit during storage was calculated as the percentage of fruit with FF values below 9.8 N.

3.2.3 Data analysis

The effects of preharvest factors on fruit quality both at harvest (before transportation), at day 0 (after arrival at laboratory) and during storage were investigated. In addition to the measured quality attributes, fruit dry weight (DW), which is a combination of solid materials (excluding water) within the fruit, was calculated as fresh weight × DMC. The ratio of at-harvest TSS to DMC (TSS/DMC) indicates the proportion of solubilised sugar relative to total carbohydrate storage, and hence can be used as an alternative measure to represent maturity at harvest. This was also calculated for this study.

Data analysis for comparison of factors and calculation of least significant differences (LSD) was carried out at the plot level using the general linear model (GLM) in Minitab® (Version 16.1.0, Minitab Inc., Pennsylvania, USA). Factors considered included crop load, trunk girdling and the interaction between the two. In addition, comparisons of incidence of soft fruit (FF < 9.8 N) amongst treatments were carried out using a Chi-square test in Minitab®.

3.3 Results and Discussion

3.3.1 Effects on at-harvest fruit weight, DMC, DW and TSS/DMC

Low crop load increased fruit weight and DMC at harvest (Table 3.1). This agrees with the previous findings for ‘Hayward’ (Famiani et al., 2012) and ‘Hort16A’. (Boyd and Barnett, 2011; Patterson and Currie, 2011). Low crop load also increased at-harvest DW and TSS/DMC (Table 3.1). Woodward (2007) found similar results for ‘Hayward’ kiwifruit: DW accumulation was negatively correlated with crop load, i.e. low crop load increased DW. Table 3.1 suggests that low crop load and use of girdling both resulted in higher ratio of TSS/DMC, i.e. more advanced maturity of ‘Hayward’ kiwifruit. This is in accordance with the study on ‘Hort16A’ kiwifruit (Boyd and Barnett, 2011).

While extended trunk girdling was previously found to improve at-harvest kiwifruit DMC for 'Hort16A' vines (Boyd and Barnett, 2011), in this study trunk girdling alone did not have any significant impact on at-harvest DMC and fruit weight (Table 3.1). However, girdling in combination with low crop load increased at-harvest fruit weight (116.9 g; Table 3.1). The effect of low crop load on improving at-harvest fruit weight seemed to be more pronounced without girdling (8.5 g vs. 6.9 g increase). In addition, trunk girdling increased DW at harvest, suggesting higher total solid materials within the fruit, despite that the total weight of the fruit seemed to be unaffected by girdling treatment (Table 3.1).

Table 3.1 Effects of pre-harvest manipulation of crop load (36 or 43 t/ha) and the application (or not) of girdling on at-harvest fruit weights (g), dry weight (g/fruit), dry matter concentration (%) and at-harvest soluble solids as a proportion of at-harvest dry matter. N.S. means there is no significant difference between populations.

		Fruit weight at harvest (g)	Dry weight at harvest (g/fruit)	Dry matter conc. at harvest (%)	TSS / Dry matter at harvest
Crop load	High	106.0^{b}	19.6^{b}	18.47^{b}	0.43^{b}
	Low	113.7^{a}	21.7^{a}	19.04^{a}	0.46^{a}
	p-Value	0.04	0.02	0.01	0.00
	$LSD_{0.05}$	5.2	1.6	0.42	0.01
	n	8	8	8	8
Girdling	Positive	N.S.	21.4^{a}	N.S.	0.47^{a}
	Negative		19.8^{b}		0.43^{b}
	p-Value	0.05	0.04	0.16	0.00
	$LSD_{0.05}$	N.S.	1.6	N.S.	0.01
	n	8	8	8	8
Crop load × girdling	High × girdling	110.0^{ab}	20.3^{ab}	N.S.	0.45^{b}
	High	101.9^{b}	18.8^{b}		0.41^{c}
	Low × girdling	116.9^{a}	22.6^{a}		0.48^{a}
	Low	110.4^{ab}	20.7^{ab}		0.44^{b}
	p-Value	0.80	0.83	0.23	0.70
	$LSD_{0.05}$	14.9	3.1	N.S.	0.02
	n	4	4	4	4

3.3.2 Effects on TSS at harvest and during storage

In general, low crop load treatment advanced TSS at day 0 and improved TSS after storage, with exceptions at 14, 50 and 125 days (Fig. 3.2; Table 3.2). This increase in TSS somewhat agrees with Famiani et al. (2012) where higher TSS was found in fruit from low crop load vines after 5 months (approx. 150 days) of storage. The application of girdling increased TSS at day 0, which corresponds to the advanced fruit maturity (TSS/DMC) at harvest (Table 3.1). Increase in TSS was also observed later when fruit were stored for 50, 100, 150 and 175 days once starch to sugar conversion had completed (Fig. 3.2; Table 3.2). The combined effect of girdling and crop load resulted in significant differences amongst treatments at day 0, as well as at 100, 150 and 175 days after storage with the low crop load × girdling treatment resulting in the highest TSS values at those times (Table 3.2).

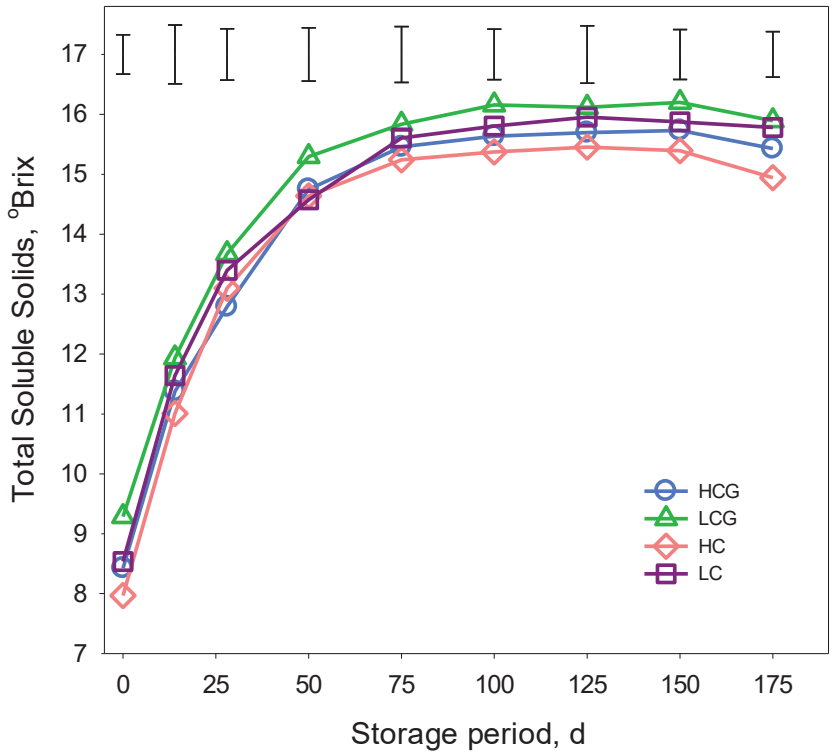

Figure 3.2 Average TSS (°Brix) during storage (days) as a result of preharvest manipulation of crop load and girdling. HCG: High crop load with girdling. LCG: Low crop load with girdling. HC: High crop load. LC: Low crop load. Bars represent the least significant difference (LSD).

Table 3.2 Effects of pre-harvest manipulation of crop load (36 or 43 t/ha) and the application (or not) of girdling on total soluble solids concentration (°Brix) at day 0 and during storage (14 – 175 days). N.S. means there is no significant difference between populations.

Storage time (days)		0	14	28	50	75	100	125	150	175
Crop load	High	8.20^{b}	N.S.	12.94^{b}	N.S.	15.35^{b}	15.51^{b}	N.S.	15.56^{b}	15.19^{b}
	Low	8.91^{a}		13.54^{a}		15.72^{a}	15.98^{a}		16.04^{a}	15.84^{a}
	$LSD_{0.05}$	0.23	N.S.	0.54	N.S.	0.36	0.30	N.S.	0.32	0.28
	n	8	8	8	8	8	8	8	8	8
Girdling	Positive	8.86^{a}	N.S.	N.S.	15.02^{a}	N.S.	15.90^{a}	N.S.	15.97^{a}	15.66^{a}
	Negative	8.25^{b}			14.61^{b}		15.59^{b}		15.63^{b}	15.36^{b}
	$LSD_{0.05}$	0.23	N.S.	N.S.	0.41	N.S.	0.30	N.S.	0.32	0.28
	n	8	8	8	8	8	8	8	8	8
Crop load × girdling	High × girdling	8.43^{bc}	N.S.	N.S.	N.S.	N.S.	15.64^{ab}	N.S.	15.73^{ab}	15.43^{ab}
	High	7.97^{c}					15.37^{b}		15.39^{b}	14.94^{b}
	Low × girdling	9.28^{a}					16.16^{a}		16.20^{a}	15.89^{a}
	Low	8.54^{b}					15.80^{ab}		15.88^{ab}	15.78^{a}
	$LSD_{0.05}$	0.46	N.S.	N.S.	N.S.	N.S.	0.60	N.S.	0.64	0.55
	n	4	4	4	4	4	4	4	4	4

3.3.3 Effects on FF at harvest and during storage

The average FF at day 0 was 70.1 N with no significant difference found between treatments. For post-storage FF, the effect of crop load on firmness was insignificant with one exception at 100 days where the FF for high crop load fruit was lower (Fig. 3.3; Table 3.3). On the contrary, the application of girdling resulted in reduced kiwifruit FF at 50, 125, 150 and 175 days after storage (Fig. 3.3; Table 3.3). In particular kiwifruit from girdled vines softened more rapidly especially after 125 days, and reached the minimum firmness criterion (9.8 N) sooner (Fig. 3.3). This result agrees with the study by Boyd and Barnett (2011) where 'Hort16A' fruit from girdled vines were softer during storage. The combined effect of girdling and crop load was mostly insignificant except for at 175 days after storage where the application of girdling resulted in lower FF of fruit (Table 3.3).

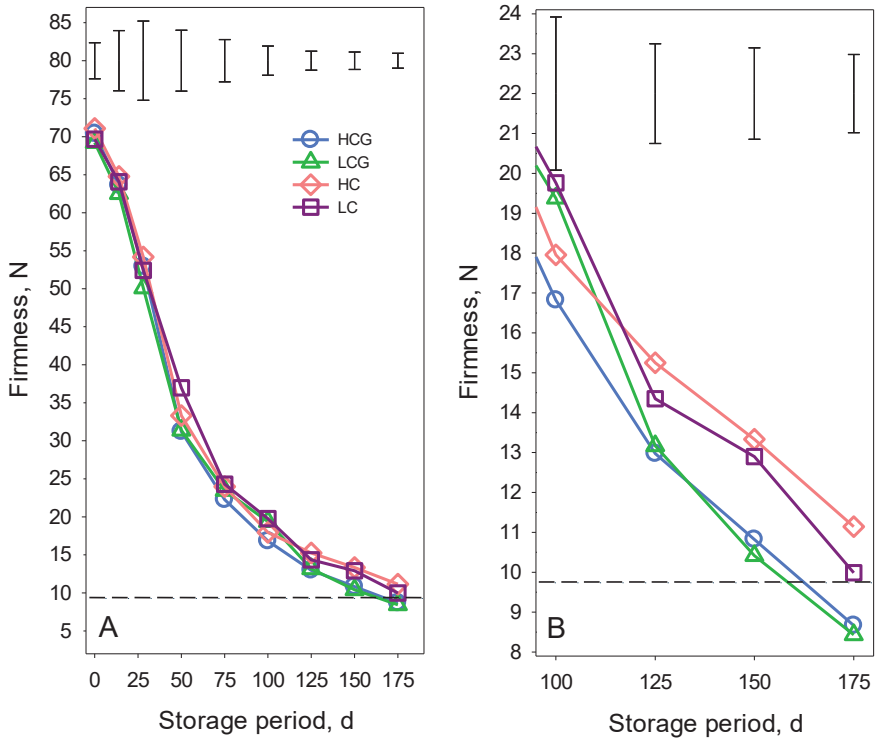

Figure 3.3 Average FF (N) as a result of preharvest manipulation of crop load and girdling (A) during the entire storage (days) period and (B) after 100 days of storage. HCG: High crop load with girdling. LCG: Low crop load with girdling. HC: High crop load. LC: Low crop load. Dashed lines represent the minimum standard of FF for exporting purposes. Bars represent the least significant difference (LSD).

Table 3.3 Effects of pre-harvest manipulation of crop load (36 or 43 t/ha) and the application (or not) of girdling on flesh firmness (N) at day 0 and during storage (14 – 175 days). N.S. means there is no significant difference between populations.

Storage time (days)		0	14	28	50	75	100	125	150	175
Crop load	High	N.S.	N.S.	N.S.	N.S.	N.S.	17.4[b]	N.S	N.S.	N.S.
	Low						19.6[a]			
	$LSD_{0.05}$	N.S.	N.S.	N.S.	N.S.	N.S.	2.0	N.S.	N.S.	N.S.
	n	8	8	8	8	8	8	8	8	8
Girdling	Positive	N.S.	N.S.	N.S.	31.3[b]	N.S.	N.S.	13.0[b]	10.6[b]	8.53[b]
	Negative				35.1[a]			14.8[a]	13.1[a]	10.59[a]
	$LSD_{0.05}$	N.S.	N.S.	N.S.	3.1	N.S.	N.S.	1.6	1.5	0.88
	n	8	8	8	8	8	8	8	8	8
Crop load × girdling	High × girdling	N.S.	N.S.	N.S.	N.S.	N.S.	N.S.	N.S.	N.S.	8.7[b]
	High									11.2[a]
	Low × girdling									8.4[b]
	Low									10.0[ab]
	$LSD_{0.05}$	N.S.	N.S.	N.S.	N.S.	N.S.	N.S.	N.S.	N.S.	1.8
	n	4	4	4	4	4	4	4	4	4

The proportion of soft fruit (FF < 9.8 N) in each population was recorded throughout the storage period (Fig. 3.4; Table 3.4). Chi-square tests suggest the proportion of soft fruit varied as a result of trunk girdling and crop load manipulation throughout storage (Fig. 3.4). The difference in % soft fruit became more prominent with increasing storage time. At 75 days after storage, the percent of soft fruit in girdled and non-girdled vines was 2.0% and 2.2%, respectively (Table 3.4; χ^2 = 0.102; p = 0.749). After 175 days of storage, the percent of soft fruit from girdled vines was 70%, much higher than 44.4% found for non-girdled vines (Table 3.4; χ^2 = 128.735; p < 0.001). The effect of crop load on firmness during storage was inconsistent. When girdling was not applied, the proportion of soft fruit was higher when accompanied by low crop load; when girdling was applied, the proportion of soft fruit was very similar irrespective of crop load (Fig. 3.4; Table 3.4).

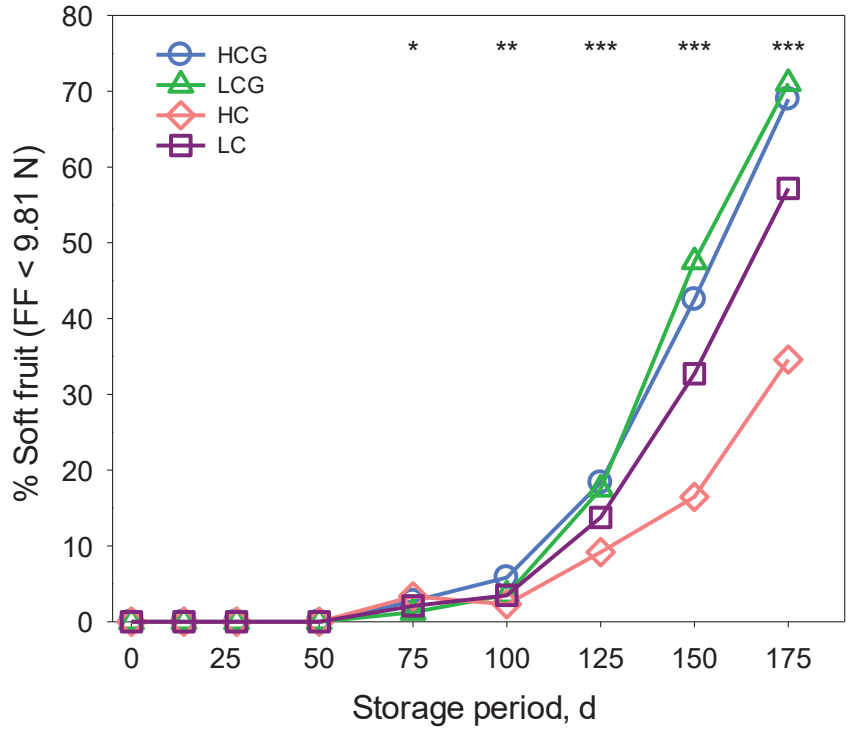

Figure 3.4 Percentage of soft fruit (flesh firmness < 9.8 N) during storage (days) as a result of manipulated crop load (36 or 43 t/ha) and the application (or not) of girdling. HCG: High crop load with girdling. LCG: Low crop load with girdling. HC: High crop load. LC: Low crop load. Asterisks indicate the degree of significant differences amongst treatments (*, **, or * being p < 0.05, 0.01 or 0.001) as indicated by Chi-square tests.**

Table 3.4 Proportion of soft fruit (%) during storage (up to 175 days) as a result of preharvest manipulation of crop load and girdling.

Storage Time (Days)		n	0	14	28	50	75	100	125	150	175
Crop Load	High	960	0	0	0	0	3.02	4.06	13.75	29.48	51.77
	Low		0	0	0	0	1.15	2.92	13.75	35.94	62.60
Girdling	Positive	960	0	0	0	0	1.98	4.69	17.92	45.00	70.00
	Negative		0	0	0	0	2.19	2.29	9.58	20.42	44.38
Crop Load × Girdling	High × Girdling	480	0	0	0	0	2.71	5.83	18.33	42.50	68.96
	High		0	0	0	0	3.33	2.29	9.17	16.46	34.58
	Low × Girdling		0	0	0	0	1.25	3.54	17.50	47.50	71.04
	Low		0	0	0	0	1.04	2.29	10.00	24.38	54.17
Total		1920	0	0	0	0	2.08	3.49	13.75	32.71	57.19

3.3.4 Further discussions

In this study girdling was applied at two time points: late spring (17 DAFB) when cell division was at peak (0 – 30 DAFB; Hopping, 1976) , and late summer (71 DAFB) during starch accumulation (> 50 DAFB; Beever and Hopkirk, 1990) and the second stage of rapid cell expansion (58 – 76 DAFB; Hopping, 1976) . Girdling during late spring has been shown to increase fruit weight by an average of 7 g in 'Hort16A' kiwifruit (Patterson and Currie, 2011). In the current study, although a comparable increase in fruit weight (7.3 g) was obtained for 'Hayward' kiwifruit with girdling application (113.5 g with girdling vs. 106.2 g without) this increase was not statistically significant at the block level (Table 3.1).

Trunk girdling applied during late summer has been found to achieve increases in fruit DMC of 0.8 – 1.0% for high-yielding 'Hort16A' vines (Patterson and Currie, 2011). In the current study, albeit not statistically different, the average DMC of fruit with girdling treatment (18.9%) was 0.3% higher compared to control (18.6%) in DMC for 'Hayward'. A possible explanation could be an inhibitory effect of girdling when applied during cell division: Currie (1997) observed smaller fruit weight, dry weight and DMC with cane girdling applied 14 DAFB (similar to the first girdle in this study) compared to girdling applied at other dates (7, 28, 42 and 56 DAFB). The same study also found no increase in DMC compared to control when girdling was applied earlier than 28 DAFB. It was proposed that the period during cell division or seed formation (0 – 30 DAFB) might be a crucial period in kiwifruit growth and girdling during this period could limit fruit growth potential due to increased vegetative growth which emits an inhibitory growth signal. This inhibitory effect might have interfered with the positive impact of the second girdle on fruit weight and DMC, as observed in the present study (Table 3.1).

The effect of crop load on fruit DMC, DW and TSS (Tables 3.1 and 3.2) may have resulted from combined effects of additional sugar accumulation and enhanced fruit expansion. The summer period of December and January is considered the peak period for fruit growth (Sale, 1990). Hence, orchard practices applied at this time are critical in controlling fruit growth. In this experiment fruit thinning was carried out in January, when fruit expansion occurs via expansion of parenchyma cell (Ezura and Hiwasa-Tanase, 2010). The magnitude of cell enlargement could be influenced by water

retention properties of the cell (Coombe, 1976). Ezura and Hiwasa-Tanase (2010) suggested that accumulation of sugar in parenchyma cells leads to an increase in water flow due to osmotic pressure, thereby resulting in overall fruit expansion. Hence fruit grown on low crop load vines were able to assimilate more carbohydrate and water due to reduced competition with other fruit on the same vine, assisting in cell enlargement and resulting in larger fruit size (Table 3.1). While low crop load improved assimilate accumulation in the fruit, it should be considered that the increase in DMC, DW and fruit weight should be sufficient to justify the lower crop load, as the reduction of total fruit number will potentially compromise orchard profitability because of reduced yield (Patterson and Currie, 2011).

Famiani et al. (2012) reported that high crop load reduced FF of kiwifruit after approx. 150 days of storage when fruit were harvested (at different dates) based on a standard minimum TSS maturity. This suggests that high crop load could lead to a higher rate of softening in storage, given the same initial maturity. In the current study, however, all fruit were harvested on the same day; the initial physiological maturity of fruit varied, with fruit from high crop load having less advanced maturity (lower at-harvest TSS and TSS/DMC; Table 3.1 and 3.2). It is possible that the effect of high crop load accelerating softening during storage, as demonstrated in Famiani et al. (2012), could have been masked by this heterogeneity in maturity stages. However, an important finding based on the current study is that, the effect of crop load on kiwifruit quality may be very different when observations were made at different storage points. This somewhat explains the discrepancy in previous findings where experiments were often conducted at a single storage point and this point varied between studies.

3.4 Conclusions

This chapter demonstrates that preharvest orchard management practices altered the growing conditions of kiwifruit vines and had considerable effects on at-harvest and postharvest quality and storability of ‘Hayward’ kiwifruit. While low crop load increased fruit weight, DMC and DW, and resulted in advanced maturation of fruit at harvest, the use of girdling did not seem to have any impact on at-harvest fruit weight and DMC. Both low crop load and trunk girdling improved TSS at day 0 and during storage. No significant crop load effect was observed on fruit softening or FF. Trunk girdling was found to hasten fruit softening and resulted in lower FF and a higher

proportion of undesirable soft fruit during later stages of coolstorage. Hence careful consideration should take place when applying trunk girdling to improve fruit DMC and/or TSS as this technique may compromise the storage potential of the fruit. When low crop load is selected to improve fruit weight, DMC and/or TSS, it should be justified that the improvement is sufficient to compensate the reduction in fruit yield. The effects of growing conditions during fruit development in the orchard can be captured by assessing fruit physiology at the time of harvest, and will serve as important information for prediction of future fruit quality and storability.

4 Characterising kiwifruit near skin cellular structures using optical coherence tomography

Acknowledgement:

Material from this chapter is included in the following papers:

Li, M., Verboven, P., Buchsbaum, A., Cantre, D., Nicolaï, B., Heyes, J., Mowat, A., East, A., 2015. Characterising kiwifruit (*Actinidia* sp.) near skin cellular structures using optical coherence tomography. Postharvest Biology and Technology 110, 247-256.

Li, M., East, A.R., Heyes, J.A., Verboven, P., Nicolaï, B., Buchsbaum, A., 2016. Development of an optical coherence tomography image analysis method to characterise cellular structure of kiwifruit. Acta Horticulturae, 1119, 127-134.

4.1 Introduction

Preharvest factors such as growing conditions and orchard management practices can affect macrostructural fruit quality at the time of harvest and during storage (Chapter 3). The effects of preharvest factors have also been related to changes in microstructural cellular properties of fruit. Currie (1997) found that shoot-girdling with high leaf:fruit ratios increased cell expansion in the outer pericarp tissue of kiwifruit and hence increased fruit weight at harvest. The same authors also suggested that crop load could affect fruit via cell division; low crop load increased the diameter of both small and large cells in the near surface tissue of the outer pericarp. Changes in cellular structure have potential consequences for postharvest fruit quality and storability (Nardozza et al., 2011).

The OCT imaging is a novel technique capable of 3D characterisation of subsurface cellular structures of an object (Section 2.3.1). Previous applications of OCT on other horticultural products (Section 2.3.3) demonstrated the potential for this technology to also provide useful information for intact kiwifruit samples. Therefore, the objective of this work was to visualise and characterise the sub-surface cellular structures of five commercial kiwifruit cultivars non-destructively, and determine if differences which may be influenced by cultivar or growing conditions are detectable. The OCT technique was used to produce 3D images of the layers of structures

immediately underlying kiwifruit skin, allowing subsequent analysis on the microstructures of these structures. The combined results investigate if OCT shows promise as a non-destructive assessment tool for kiwifruit and evaluate the potential applications of this technique to measure kiwifruit quality.

4.2 Materials and Methods

4.2.1 Plant material and treatment manipulation

A total of 90 kiwifruit from five commercial cultivars were sourced: yellow-fleshed cultivars (all *A. chinensis*) 'G3' (Zespri® Sun Gold), 'G9' (Zespri® Charm) and 'Hort16A' (Zespri® Gold), and green-fleshed cultivars 'G14' (*A. deliciosa* × *chinensis*, Zespri® Sweet Green) and 'Hayward' (*A. deliciosa*). These included 10 fruit each of 'G9', 'Hort16A' and 'G14', 20 fruit of 'G3' (10 fruit plus 5 fruit each of two additional grower lines) and 40 fruit of 'Hayward' (10 fruit each of four treatments from the growing condition manipulation trial; Chapter 3). All of the 90 samples were obtained in New Zealand and delivered via airfreight to RECENDT, Linz, Austria, in June 2013 prior to OCT image capture and fruit quality measurement.

4.2.2 Fruit quality measurement

Fruit flesh firmness (FF) and total soluble solids (TSS) content were assessed using the methodologies described in Section 3.2.2. Means were obtained from 5 fruit of each cultivar for 'G9', 'G14' and 'Hort16A', and 5 of each grower line/treatment for 'G3' and 'Hayward' respectively. At the time of measurement all fruit could be considered firm and ripe given that high TSS development had been achieved and FF was within 10 – 20 N (Table 4.1).

Table 4.1 Condition of kiwifruit from five commercial cultivars at time of OCT measurement. Values represent mean and standard deviation (in brackets). Means were averaged from 5 fruit per cultivar for 'G9', 'G14' and 'Hort16A', 15 for 'G3' and 20 for 'Hayward. Means denoted with different letters are different with statistical significance (α = 0.05).

Fruit Quality	Kiwifruit Cultivar				
	G3	G9	Hort16A	G14	Hayward
Total Soluble Solids, %	18.49[a] (1.53)	18.56[a] (2.26)	19.36[a] (1.15)	17.64[a] (1.45)	14.69[b] (0.66)
Firmness, N	10.29[c] (2.55)	10.49[c] (2.74)	12.15[bc] (2.06)	16.46[ab] (1.76)	19.50[a] (2.74)

4.2.3 OCT instrumentation and image capture

The OCT instrument was a commercially-available spectral domain OCT (SD-OCT) system (Telesto, Thorlabs, Lübeck, Germany) operating at 1325 nm (Fig. 2.8). A wavelength of 1325 nm was chosen by the need to balance against the transparency and scattering properties of the kiwifruit skin. OCT systems operating at lower wavelength (e.g. 800 nm) do offer higher axial resolution in many cases; however, the light at 800 nm does not penetrate under the kiwifruit skin. OCT systems operating at higher wavelength are available but do not have sufficient axial resolution. Therefore using 1325 nm is a compromise between penetration depth and axial resolution.

For the OCT measurements of the kiwifruit no prior sample preparation was required. To capture an image, the basic steps include: focusing the laser onto the surface of the fruit; choosing a relatively flat surface on the fruit skin and then capturing the raw image. Single 3D images (3 mm (L) × 3 mm (W) × 1.498 mm (D)) were obtained for each fruit. After raw image capture, the depths of images were corrected with Avizo® (Version 7.1, Visualization Sciences Group, France) to reflect the sample refractive index. The choice of refractive index affects the depth scale of the final estimated values (i.e. volume and size) and a single value is applied across an entire data image. For this work, the refractive index was estimated from the average measured TSS of the fruit. This is because the error from applying an average across the

entire data set was small given that the difference in depths estimated was approximately 0.006 mm between a medium containing 14% soluble solids (similar to 'Hayward'; Table 4.1) and one containing 20% soluble solids (similar to 'Hort16A'; Table 4.1). Therefore, a refractive index of 1.36 (Anonymous, 2013) corresponding to the average total soluble solids (17.75%) for all five cultivars was applied.

4.2.4 Image processing

Raw OCT images displayed surface and sub-surface structures of the skin of fruit but some image artefacts were also observed (Fig. 4.1 and 4.2). The affected volumes were estimated by manual selection of the shadows cast by lenticels and trichomes on the top and bottom slice, followed by interpolation across all slices in the vertical direction (Fig. 4.3). The aim was to identify and select only large parenchyma cells from the background tissue in order to enable further analysis of these objects. Image processing using both automated and manual methods was carried out using Avizo® (Version 7.1, Visualization Sciences Group, France; Fig. 4.4).

The raw image was first treated with a smoothing filter to reduce effects of artefacts (Fig. 4.4a). Box-filtering was carried out by averaging 27 voxels in the enclosing 3 × 3 × 3 box of volume (Table 4.2), without altering the information contained in the region.

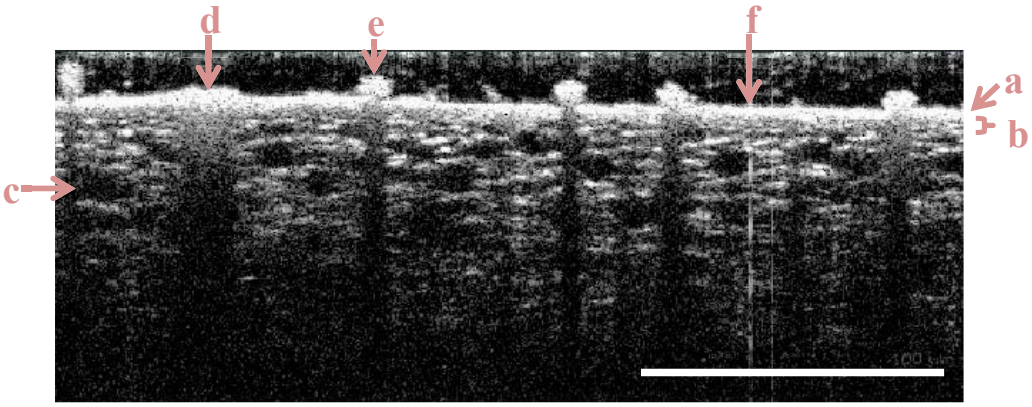

Figure 4.1 Example of a 2D OCT raw image for 'G14' kiwifruit: (a) the periderm layer; (b) a layer of homogeneous small cells; (c) large cells (black voids); (d) shadowing effects caused by lenticels; (e) shadowing effect caused by trichomes; (f) direct reflection of light back into the sensor from the surface. Bar = 1 mm.

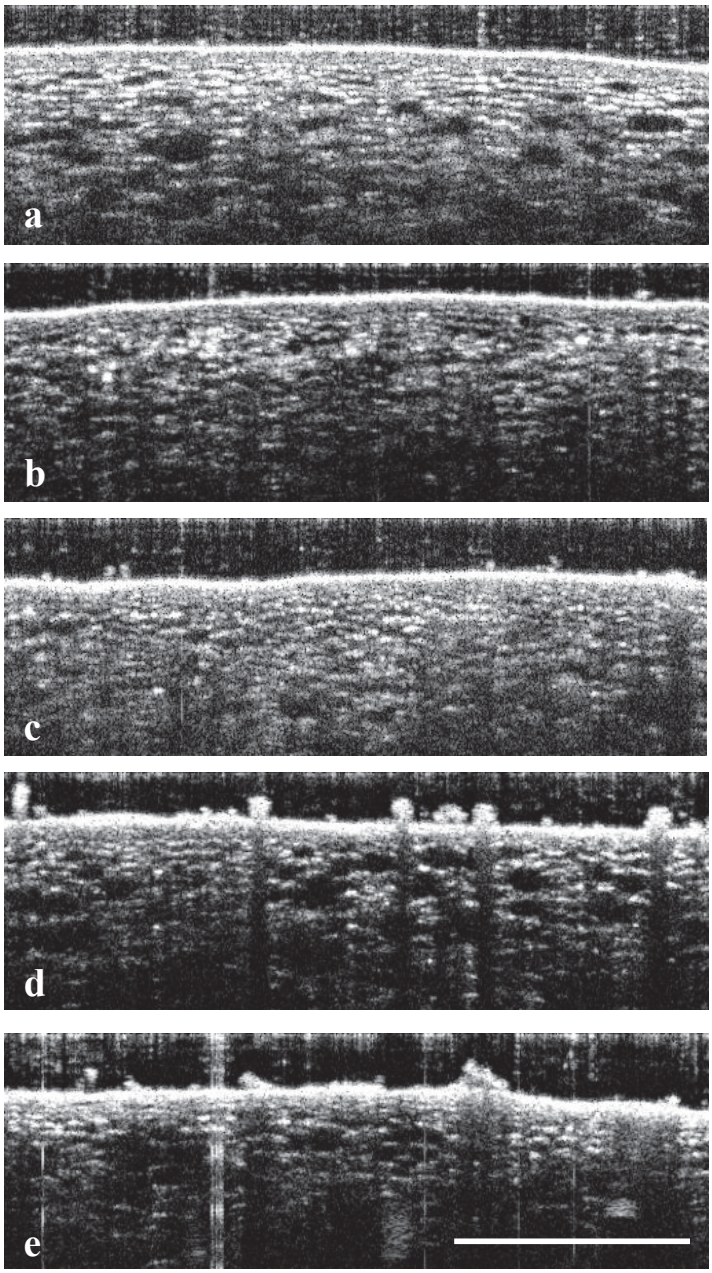

Figure 4.2 Example of 2D OCT images showing cultivar differences: (a) 'G3', (b) 'G9', (c) 'Hort16A', (d) 'G14' and (e) 'Hayward'. Bar = 1 mm.

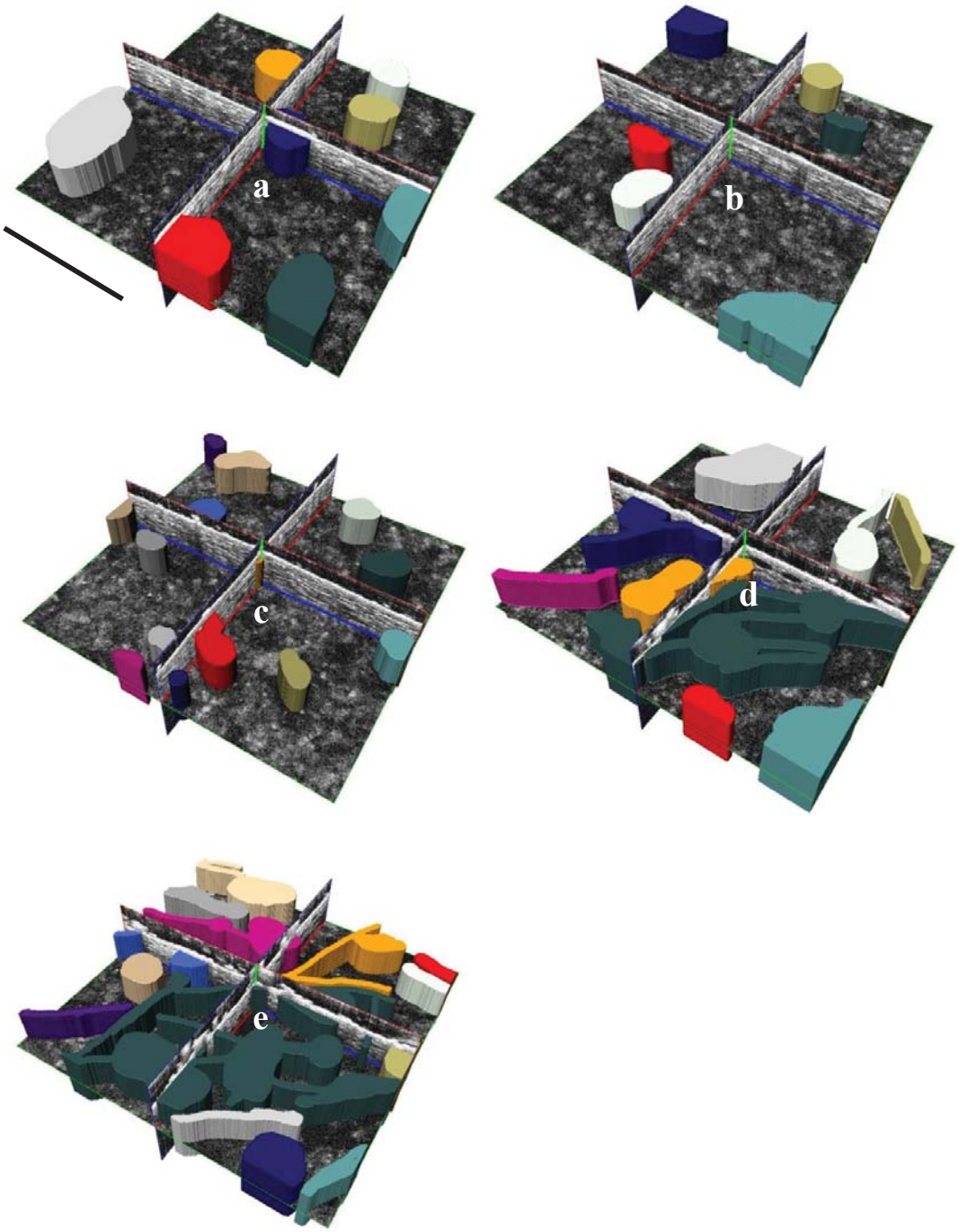

Figure 4.3 Visualisation of shadowing effects caused by lenticels and trichomes throughout the tissue underneath the surface layer in an example of: a) 'G3', b) 'G9', c) 'Hort16A', d) 'G14' and e) 'Hayward' kiwifruit. Bar = 1 mm.

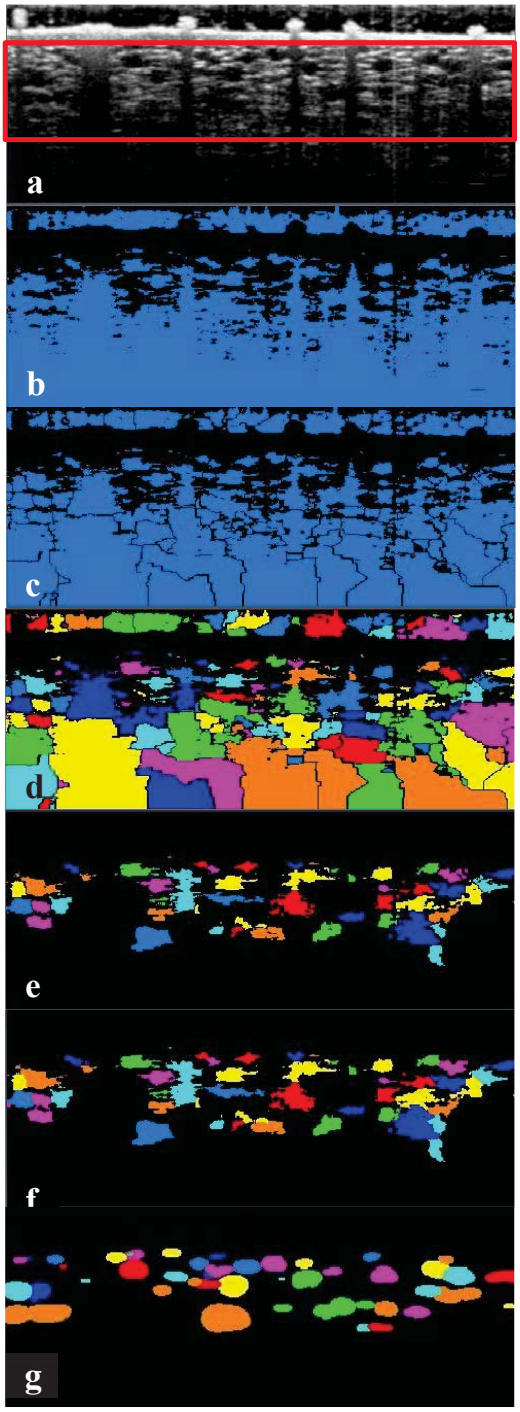

Figure 4.4 OCT image processing techniques presented in 2D cross-sectional images, for the identification of large parenchyma cells of kiwifruit skin using Avizo® in an example ('G14'): (a) smoothing; (b) interactive threshold binarisation; (c) watershed separation; (d) labelling; (e) filtering; (f) closing and (g) manually selected large cells. The red rectangle in (a) indicates the region of interest.

To select the large parenchyma cells, both automated image segmentation and manual selection methods were developed. For the automated segmentation method, firstly an interactive threshold binarisation was used (Fig. 4.4b). In this technique, the 8-bit greyscale raw image was transformed into a binary image, which is a 16-bit label image with only interior and exterior materials, enabling the segmentation of objects of interest from the background. The lower threshold was set as the lowest grey level value of the image, and the upper threshold was set at a value where there was the best contrast between dark cells and the lighter background tissue. Objects with an initial grey level value between these two thresholds were selected.

Table 4.2 Procedures and settings for automated OCT image processing of kiwifruit using Avizo® (Version 7.1, Visualization Sciences Group, France).

Procedure	Parameter	Setting
Smoothing	Volume of average	3 × 3× 3 voxels
Threshold Binarisation	Greyscale	55 - 75
Separation	Contrast factor	1
Filtering	Vertical depth	0.43 – 0.98 mm
	Maximum length	≥ 0.20 mm
	Equivalent diameter	≤ 0.25 mm
Closing	Kernel size of dilation	2 voxels added to 6 neighbouring voxels

After segmentation, many of the boundaries between selected cells were merged and not clear. To separate them, a watershed algorithm was applied to detect cell boundaries (Fig. 4.4c). This algorithm simulates 'flooding' using different coloured water (labels) from a series of marker regions in a 3D image. The efficiency of separation was maximised by adjusting the contrast factor, which determines the size of the seed areas for flooding (Table 4.2). Separated cells were then displayed using a 16-colour cyclic colour-map so that the cells in close proximity were labelled in a different hue (Fig. 4.4d).

Comparing the labelled objects to the black voids in the raw image, it is clear that unwanted objects which had the same grey level values as the large cells were also selected. Therefore, filtering of mislabelled objects was conducted (Fig. 4.4e). This included the screening of three different types of undesirable objects using different image processing techniques (Table 4.2). Firstly, the vertical distance of the object from the surface of the skin was restricted to 0.13 – 0.68 mm deep (0.43 – 0.98 mm from the top of the images as the image depth covers a region above the skin surface) for all the images. Secondly, a threshold for the minimum value for maximum cell length was chosen. In *A. deliciosa* large cells start to appear beneath the hypodermis (approx. 0.10 mm from the skin) with a maximum length more than 0.20 mm and become more prevalent at 0.30 – 0.40 mm from the skin with maximum length of 0.25 – 0.30 mm (Hallett and Sutherland, 2005); in *A. chinensis* large cells start to appear 0.25 mm from the skin and further extend to the bulk of the outer pericarp, with a mix of up to and more than 0.50 mm maximum diameter (Hallett and Sutherland, 2005). Since the maximum length of small cells within the same region was 0.12 mm for *A. deliciosa* and 0.10 mm for *A. chinensis*, a minimum length of 0.20 mm was selected for large cells. Finally a maximum equivalent diameter (D_e) was set as 0.25 mm, based on the results of manual segmentation method (Section 4.3.2). These ensured that most of the under- or over-sized objects other than the large parenchyma cell were removed (Fig. 4.4e).

The final step of the protocol was to apply a 'closing' of the assessed region (Fig. 4.4f). This technique performs a dilation of the selected cells, followed by an erosion. This helped to fill up small holes inside the cells and ensure the cell boundaries are smoother. The kernel size of dilation was set as 2 voxels (Table 4.2) so that separated cells were not reconnected and additional volume was not added to the large cells.

Quantitative analysis was conducted on the processed images of all fruit samples using the automated method to evaluate the number and describe the characteristics of the large cells (Table 4.3). The image processing time using the automated segmentation method was 5 – 10 minutes for each image and the number of cells that could be identified was unconstrained. The volume fraction calculation of large cells was conducted on the basis of the volume of the sample that could be analysed after removal of image artefacts (Fig. 4.3). The effect of cultivar was analysed using the GLM in Minitab® to examine the differences amongst the means. A two-way ANOVA was

conducted within 'Hayward' samples using Minitab®, in order to study the effects of crop load and girdling on the cellular structure of the fruit.

Table 4.3 Microstructural parameters of large parenchyma cells of kiwifruit and description used to quantify these parameters.

Microstructural parameters	Unit	Description
Total volume	mm^3	Total volume of all the objects
Average volume	mm^3	Volume of an individual object
Total surface area	mm^2	Total surface area of all the objects
Average surface area	mm^2	Surface area of an individual object
Maximum length	mm	The feret diameter which measures the distance between two outermost tangential lines of the object projected to a plane
Equivalent diameter, D_e	mm	The diameter of a spherical object of equivalent volume as the irregularly-shaped object
No. of cells	-	The number of objects within the assessed region
Density	mm^{-3}	The number of objects within 1 mm^3 of assessed volume
Sphericity	-	The ratio of the surface area of a sphere of the same volume to the surface area of the object

The manual segmentation (Fig. 4.4g) method identified individual cell cross-sections in three orthogonal planes, yielding a 'skeleton' of the structure of the cell. A 'wrapping' method was followed which enfolds the selected pixels into a 3D volume based on scattered data interpolation with a radial basis (Wevers et al., 2012). This method was carried out on one kiwifruit sample ('G14'), as it was used as a reference to validate the automated method. The quantitative analysis results from the manual method were compared to the automated method for the same fruit sample.

4.3 Results and Discussion

4.3.1 Features of raw image

The complete data set is a 3D image (Fig. 4.5) consisting of 512 two-dimensional (2D) vertical slices at 5.9 μm spacing. However, for the purpose of ease of demonstration, 2D slices of the data set are presented in this chapter. Several layers of sub-surface structures were observed in the raw images (Fig. 4.1 and 4.2). These structures include: (a) the suberised periderm layer (the 'skin'), (b) a layer of homogeneous small cells, intermingling with (c) elongated black voids (large cells) located in the sub-surface region. In addition, some image artefacts are present as a result of: (d) shadowing effect caused by lenticels observed as grey spaces throughout the tissue underneath without detailed texture boundaries, (e) shadowing effects caused by trichomes observed as "black streaks" underneath the hair throughout the tissue, and (f) direct reflection of light back into the sensor from the surface observed as "white streaks" in the vertical direction (Fig. 4.1). Lenticels were a common issue for all the cultivars, whereas trichomes were a significant issue for the hairy green-fleshed 'G14' (Fig. 4.2d) and 'Hayward' (Fig. 4.2e). This can be more clearly observed in Fig. 4.3 where shadows of lenticels and trichomes were manually selected on cross-sectional slices and then visualised in 3D images. Details of any cellular structures within the shadowed volumes were unable to be observed or extracted. The fraction of volume being affected by these artefacts of the assessed image region varied between cultivars, with 9-13% losses for all three yellow cultivars ('G3', 'G9' and 'Hort16A'; Fig. 4.3a-c) and 25-29% for the hairy green cultivars ('G14' and 'Hayward'; Fig. 4.3d-e).

Visualisation of the cellular structures immediately underneath the skin (Fig. 4.2) showed that the large cells were observed to be less prevalent and smaller in volume in 'G9' (Fig. 4.2b) and 'Hort16A' (Fig. 4.2c) but more prevalent and larger in volume in 'G3' (Fig. 4.2a), 'G14' (Fig. 4.2d) and 'Hayward' (Fig. 4.2e). In yellow-fleshed cultivars ('G3', G9' and 'Hort16A') the large cells were commonly observed to be flat and elongated and further away from the skin surface, whereas in green-fleshed cultivars ('G14' and 'Hayward') they were observed to be more spherical and closer to the periderm layer.

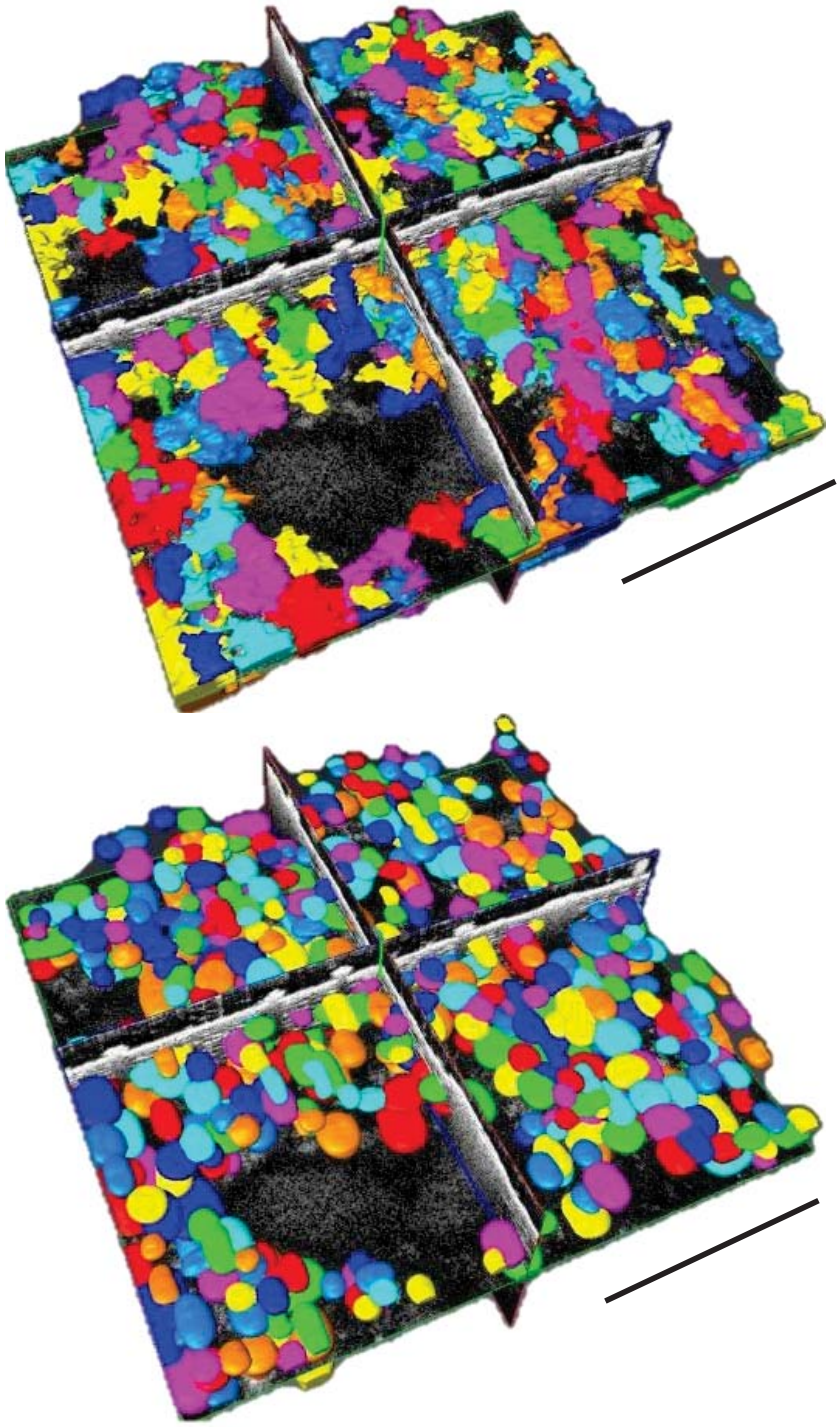

Figure 4.5 Surface view of large cells presented in 3D image in an example ('G14') using a) automated method and b) manual method. The grey regions in the image represent the image artefacts as a result of lenticels and trichomes which were removed from analysis as part of image processing. Bar = 1 mm.

4.3.2 Comparison of image segmentation methods

Both manual and automated segmentation methods identified large cells from the background tissue and enabled further analysis of these cells. For manual method, there was found to be approximately 25 large cells per mm^2 cross-sectional (perpendicular to the skin surface) area and 60 large cells per mm^3 volume of tissue, with these cells occupying around 22.4% of the total outer pericarp tissue (Table 4.4). For the automated method, large cell density was estimated at 38 per mm^2 cross-sectional area and 114 per mm^3, with a 28.9% volume fraction of cells in the outer pericarp tissue (Table 4.4). Cell equivalent diameter (D_e) ranged from 0.10 mm to 0.25 mm and 0.05 mm to 0.35 using the manual and automated methods respectively (Fig. 4.6), with both methods finding cells with D_e between 0.10 – 0.15 mm being most prevalent.

The observed difference in cross-sectional density is most likely because there is a maximum threshold of the number of objects being selected using manual method; for an 8-bit greyscale image, this number equals to 255 ($2^8 – 1$), although more than 400 cells could be observed. There is no such limitation when using the automated method since the maximum threshold is large enough for a 16-bit image after binarisation ($2^{16} – 1$). Apart from this observed difference, other microstructural characteristics were similar between the two methods, therefore further quantitative analysis and comparisons of cultivars were carried out using the automated method for the ease of computation.

Table 4.4 Microstructural properties of large cells in the outer pericarp of 'G14' kiwifruit obtained using automated and manual methods for the same sample (n = 1), and using automated method for all samples of 'G14' (n = 10).

Imaging Method	Volume Fraction (%)	Maximum Length (mm)	D_e (mm)	Density (no. /mm^2)
Manual	22.4	0.35	0.17	25
Automated	28.9	0.32	0.14	38
Automated (n = 10)	24.8 – 33.8	0.31 – 0.33	0.14 – 0.15	35 – 40

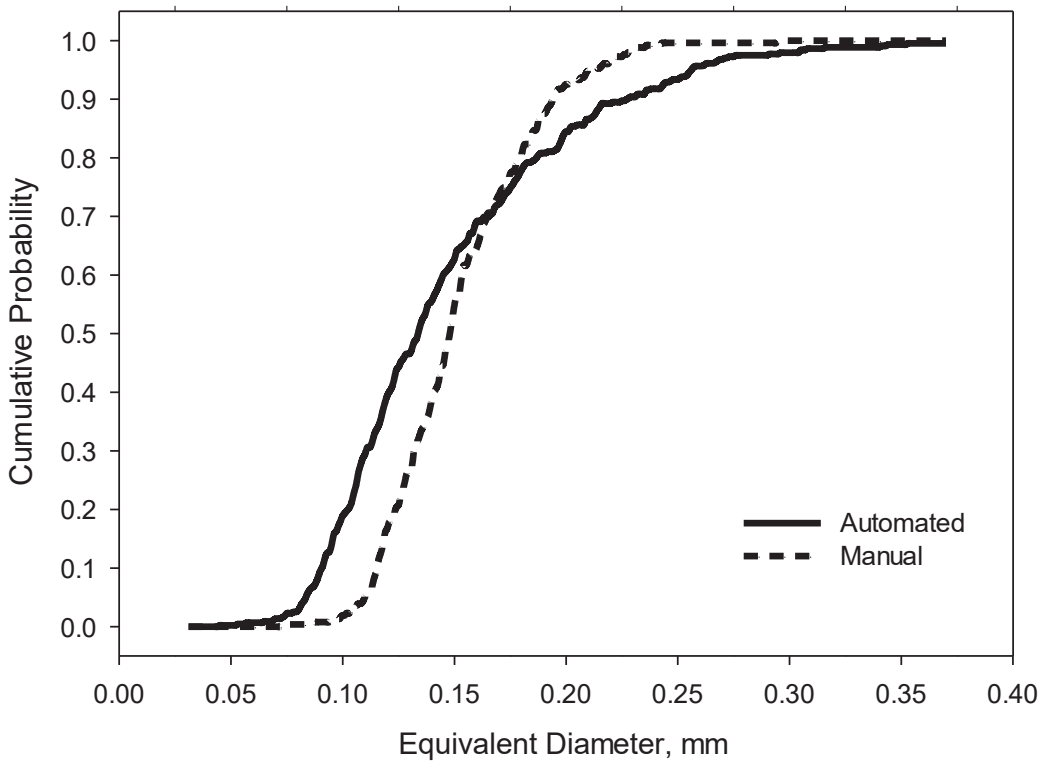

Figure 4.6 Size distribution of large cells expressed as cumulative probability of number of cells as a function of equivalent diameter. Values were obtained from the same fruit evaluated by both manual and automated segmentation methods.

4.3.3 Charaterisation of large cells

Processing of the OCT images enabled quantification of the number, size and shape of the large cells observed. The average maximum cell length (maximum feret diameter, Table 4.3) for 'Hayward' ranged between 0.31 – 0.34 mm. The large cells found using the automated method were irregular shaped (Fig. 4.5a) and this is a result of image processing and could have contributed to the differences found between manual and automated methods. Ellipsoids could be fitted to the cells to be more realistic (Mebatsion et al., 2009). However, for the purpose of this work to compare between cultivars, this tedious step was not taken. The large cell density for 'Hayward' ranged between 54 – 126 cells per mm^3 volume of tissue, with these cells occupying 17 – 35% of the analysed near skin tissue, disregarding the proportion of tissue affected by image artefacts.

4.3.4 Differences between cultivars

Automated analysis of OCT images was able to differentiate the microstructures amongst five kiwifruit cultivars with statistical significance (Table 4.5). Overall, 'G14' had the highest total large cell volume and total surface area of large cells compared to the other cultivars. 'G3' and 'Hayward' had higher total volume of large cells than 'G9' and 'Hort16A'. For each individual large cell, 'G3', 'G14' and 'Hayward' had higher average large cell volume and equivalent diameter than that of 'G9' and 'Hort16A'. For those cultivars with larger individual cells, 'G3' had higher maximum large cell length in comparison to 'G14' and 'Hayward', suggesting that the large cells of 'G3' are more elongated as observed in Fig. 4.2a. This is also evidenced by a higher average large cell surface area in 'G3' than that of other cultivars. 'G14' and 'G9' had higher total large cell number compared to other cultivars but 'G14' had much higher total large cell surface areas than 'G9' because the individual cells of 'G14' are larger. In contrast, 'Hort16A' had the lowest total large cell volume and number, and the smallest individual maximum large cell length and average large cell surface area. The volume fraction of large cells was found to be lower for yellow-fleshed cultivars, 'G9' and 'Hort16A' than green-fleshed cultivars, 'G14' and 'Hayward'. The yellow-fleshed 'G3' had lower fraction of large cells than 'G14' but not 'Hayward' (Table 4.5).

The cell size distribution curves for the five commercial cultivars demonstrate that the equivalent diameter (D_e; Table 4.3) of large cells ranged between 0.05 – 0.30 mm (Fig. 4.7). For 'Hort16A' all the large cells had a D_e smaller than 0.25 mm. For the other cultivars, a small proportion of large cells were found to have a D_e larger than 0.25 mm. For 'G9' and 'Hort16A', the large cells with D_e between 0.05 – 0.20 mm contributed to almost 90% of the total volume of large cells (Fig. 4.7a); and those with D_e more than 0.20 mm contributed to only less than 10% of the total volume. For 'G3', 'G14' and 'Hayward', the large cells with D_e between 0.05 – 0.20 mm contributed to about 60% of the total volume of large cells and those with D_e more than 0.20 mm contributed to up to 40% of the total volume (Fig. 4.7a). Consequently, the significant difference observed in cumulative large cell volumes (Fig. 4.7b) was a result of the added volumes from the large cells sized with D_e between 0.20 – 0.30 mm.). The difference in total volume of large cells between 'G9' and 'G14' was a result of the lack of large cells above 0.2 mm in 'G9' (Fig. 4.7b).

Table 4.5 Microstructure description of large parenchyma cells and statistics of the cell size distribution at eating ripe condition. Mean values are presented with their 95% confidence interval. Values were averaged from 10 fruit per cultivar for 'G9', 'G14' and 'Hort16A', 20 for 'G3' and 40 for 'Hayward' after removing volumes affected by image artefacts. Means denoted with different letters are different with statistical significance (α = 0.05).

Microstructural parameter	Unit	Kiwifruit Cultivar				
		G3	G9	Hort16A	G14	Hayward
No. of cells	-	380 ± 10^{b}	480 ± 24^{a}	298 ± 16^{c}	460 ± 12^{a}	367 ± 11^{b}
Total volume	mm^3	0.84 ± 0.02^{ab}	0.66 ± 0.04^{c}	0.39 ± 0.03^{d}	0.95 ± 0.03^{a}	0.78 ± 0.02^{b}
Total surface area	mm^2	50 ± 1^{b}	50 ± 2^{ab}	33 ± 2^{c}	57 ± 1^{a}	45 ± 1^{b}
Density	mm^{-3}	95 ± 3^{c}	116 ± 6^{ab}	75 ± 4^{d}	134 ± 4^{a}	113 ± 3^{b}
Volume Fraction	%	20.9 ± 0.6^{c}	15.8 ± 0.8^{d}	9.8 ± 0.5^{e}	27.6 ± 0.8^{a}	23.9 ± 0.6^{b}
Average volume	mm^3	0.0022 ± 0.0000^{a}	0.0014 ± 0.0001^{b}	0.0013 ± 0.0001^{b}	0.0021 ± 0.0000^{a}	0.0021 ± 0.0000^{a}
Average surface area	mm^2	0.13 ± 0.00^{a}	0.11 ± 0.00^{c}	0.11 ± 0.00^{c}	0.12 ± 0.00^{b}	0.12 ± 0.00^{b}
Maximum length	mm	0.34 ± 0.00^{a}	0.31 ± 0.00^{c}	0.30 ± 0.00^{d}	0.32 ± 0.00^{b}	0.32 ± 0.00^{b}
Equivalent diameter	mm	0.15 ± 0.00^{a}	0.13 ± 0.00^{b}	0.13 ± 0.00^{b}	0.15 ± 0.00^{a}	0.15 ± 0.00^{a}
Sphericity	-	0.62	0.57	0.53	0.63	0.65

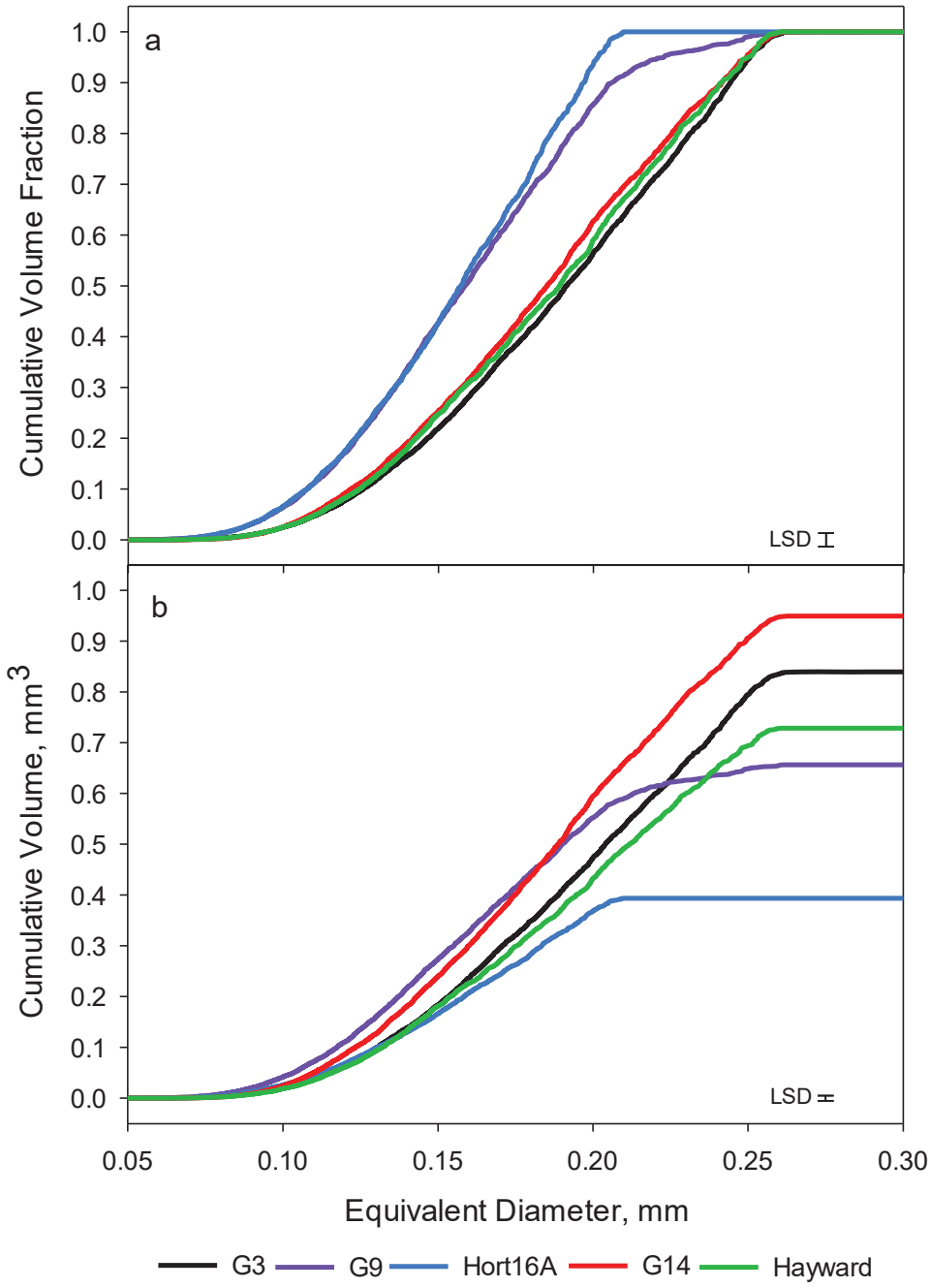

Figure 4.7 Size distribution of large cells expressed as a) cumulative volume fraction of large cells; and b) cumulative volume of large cells, as a function of cell equivalent diameter. Sample volumes analysed were immediately underlying the skin (0.13 – 0.68 mm from the surface of the skin) of commercial kiwifruit cultivars. Values were averaged from 10 fruit per cultivar for 'G9', 'G14' and 'Hort16A', 20 for 'G3' and 40 for 'Hayward'.

4.3.5 Differences within 'Hayward' cultivar

Both girdling and crop load significantly affected fruit quality at the time of harvest (Table 3.1). Despite the macro-scale effects of these treatments observed, the internal cellular structures of fruit from the subsamples showed minimal difference (Table 4.6). Neither girdling nor the interaction between girdling and crop load was found to affect microstructural changes of large cells in 'Hayward', despite that the latter increased fruit weight at harvest (Table 3.1), and that previous results showed girdling with high leaf:fruit ratios increased large cell size (Currie, 1997). It is possible that, due to the limitation that the assessed images only represented the cellular layers near to the surface and had a limited resolution, any significant changes to the bulk of the outer pericarp were not reflected or only reflected to a limited extent.

Crop load was found to have a significant effect on maximum large cell length (Table 4.6). Kiwifruit harvested from low crop load vines had larger maximum length for large cells (0.33 mm), in comparison to kiwifruit from high crop load vines (0.32 mm). This agrees with Currie (1997) where low crop load resulted in increased large cell diameter. It has been suggested that accumulation of sugar in parenchyma cells leads to an increase in water flow due to osmotic pressure, thereby resulting in cell and overall fruit expansion (Ezura and Hiwasa-Tanase, 2010).

Table 4.6 Significance table showing p-values ($\alpha = 0.05$) for the effects of crop load and girdling on the microstructure description of 'Hayward' kiwifruit outer pericarp large cells at eating ripe condition.

Microstructures	Unit	p-value		
		Crop Load	Girdling	Crop Load × Girdling
Total volume	mm^3	0.07	0.82	0.39
Average volume	mm^3	0.67	0.81	0.70
Total surface area	mm^2	0.06	0.73	0.29
Average surface area	mm^2	0.60	0.86	0.96
Maximum length	mm	**0.03**	0.49	0.42
Equivalent diameter	mm	0.84	0.78	0.54
No. of cells	-	0.14	0.67	0.33

4.3.6 Differences between batches of 'G3' kiwifruit

Between three grower lines of 'G3', there were no detectable differences observed in the microstructure of the large cells (data not shown), indicating that either the cellular structural differences between growers were minimal, or the analysis based on OCT images was not sensitive enough to pick up any differences caused by orchard location (i.e. grower lines in this case).

4.3.7 Further discussions

In general, the manual segmentation method was less affected by image artefacts as only ovoid smooth-surfaced cells were selected (Fig. 4.5b). Hence it provided a good reference for understanding the general microstructural features of the large cells (e.g. maximum length and D_e). However, this method is highly labour-intensive with 5 – 6 hours of processing time per image, and the maximum number of objects was limited to 255 (Section 4.3.2). As a result subsequent analysis based on these cells is compromised if these cells were not representative of the whole population. The density and volume of cells within the image region could also have been underestimated.

The automated segmentation method was able to identify cells more efficiently with 5 – 10 minutes of processing time per image; and it was not constrained to the number of cells that could be identified. The size distribution and total volume of large cells found was comparable to the results obtained using manual method (Table 4.4). Despite the fact that some undesirable objects remained selected due to the 'bleeding' of cell surface boundaries as a result of image artefacts, the automated method has benefits of rapid processing and computation of large sets of images, and the minimisation of human error and bias during selection of large cells.

A primary limitation of the images captured is that the depth of penetration of the data was estimated to be approximately 1 mm underneath the skin even though the outer pericarp of kiwifruit could be a 10 mm thick region. There is no published evidence as to whether the distribution of small and large cells in the analysed region is the same as the majority of the outer pericarp. Therefore the data probably represents only the sub-surface layers of the outer pericarp of the fruit and the regions observable in the images may not necessarily represent the outer pericarp as a whole. Despite these limitations there is still potential for this technology to provide potentially useful

information on near surface cell size and structure non-destructively. For this reason this chapter continues to discuss the differences observed between cultivars and to compare with known data for the pericarp due to the lack of other quantitative sub-surface data, despite that these may not be directly comparable due to the limitation in image depth.

For *A. chinensis* cultivars stone cells have been previously reported to be scattered amongst small parenchyma cells in the region approximately 0.10 – 0.25 mm (for 'Hort16A'; Hallett and Sutherland, 2005) from the skin slightly above the bulk of the outer pericarp where large cells start to show prevalence, and may further extend to deeper region (0.60 – 0.70 mm from the skin) for some cultivars. The images, however, showed no obvious differentiation between the observed large voids and the stone cells approximately in the assessed image region. This could be another weakness of the technique as it is possible that some of the near-surface layers of large cells observed in yellow-fleshed cultivars, especially 'G3', could have been stone cells. While acknowledging that the technique is unable to potentially differentiate between large cells and stone cells, discussions in this chapter will be under the assumption that all large objects observed are large cells.

The penetration and the resolution of the images were compared with previous studies on other horticultural products. When operating at the same wavelength (1325 nm), the depth resolution (5.9 μm) and the penetration depth (0.68 mm), to which cellular discrimination was possible, were comparable to those in apples (5 μm and 0.5 mm, respectively; Verboven et al., 2013) but the resolution was lower compared to those in onions (1 μm and 0.5 mm, respectively; Meglinski et al., 2010) . The penetration depth was lower but the depth resolution was better than those in mandarins (7 μm and 1.1 mm, respectively; Magwaza et al., 2013) where a shorter wavelength (930 nm) was used. The common problems identified across the studies included the choice between good penetration depth and high resolution, and the compromise in data processing speed when manual selection was used instead of automated method for better accuracy or vice versa.

The shape and total volume of large cells may affect relative porosity of the tissue. In this study, the total volume of large parenchyma cells was estimated to be high in 'G3' and low in 'Hort16A' and 'G9' (Table 4.5). Cantre et al. (2014) found that the relative porosity was low in 'G3' and high in 'G9' and 'Hort16A' for fruit obtained

from the same growers sampled at the same time as the current study. However, 'G14' and 'Hayward' were found to have higher total volume of large cells and also a high porosity. In these two cultivars the observed large cells were most likely to be actual large cells and therefore they were more spherical (smaller maximum large cell length, Table 4.5), whilst in 'G3' the observed large cells were possibly a mixture of more flattened stone cells and some of the actual large cells. More spherical cells may cause more intercellular spaces as cellular packing may be less dense in comparison to flat cells (Mebatsion et al., 2009). It might be the case that the large cells were stacked less densely against one another, resulting in a more porous near skin tissue compared to 'G3'. This could also be evidenced from the results that 'G14' and 'Hayward' had higher pore connectivity and lower pore fragmentation in comparison to 'G3' (Cantre et al., 2014). However, the packing of small cells around the larger cells may also influence porosity. Large number of small cells occupying the spaces around the large cells could in fact reduce porosity. This might explain why 'Hayward' had lower porosity in comparison to 'G9' and 'Hort16A'(Cantre et al., 2014), despite that 'Hayward' had more spherical large cells (Table 4.5). There seems to be no relationship between the porosity of fruit tissue and the total number of large cells. For instance, 'G9' was found to have higher total number of large cells but also higher relative porosity than 'G3', due to 'G9' having smaller individual large cells and thus smaller total volume of large cells.

The use of OCT as a tool is still in its infancy and there are required improvements of the methods for it to become a ubiquitous tool for assessing horticultural produce. For instance, increased signal-to-noise ratio and improved resolution are necessary to allow applicability to a wider range of horticultural produce for quantification purposes. Better depth penetration will be required to provide more information for understanding microstructural or cultivar differences. Nonetheless, the information obtained in this study still suggests that OCT has potential as a non-destructive tool to provide information on the near-surface cellular structures of horticultural products with thin cuticles, especially to detect the differences at the cell level between crop varieties and cultivars. The technology may be used to monitor the 3D cellular changes in a crop during plant development, at the time of harvest and during storage. Such information would be useful in understanding the physiology of the crop in relation to internal quality changes and the variability in storage potential.

With improved speed of data capture and analysis it can be used as a fast screening tool during plant breeding, should the nature of the large cells be associated with an important attribute.

4.4 Conclusions

OCT has potential as a non-destructive technique to characterise microstructure of large parenchyma cells immediately underlying kiwifruit skin. The details of the skin surface, the periderm layer, and the presence of large cells and their structures in the near skin tissue can be observed from raw images but there was no clear differentiation between large cells and stone cells. The data acquired were limited to a penetration depth of up to 1 mm underneath the skin and might not represent the outer pericarp as a whole. The developed image processing techniques enabled identification and characterisation of large parenchyma cells in the near skin tissue of five commercial kiwifruit cultivars in an efficient manner. Green-fleshed 'G14' and 'Hayward' were found to have higher volume fraction of large cells than yellow-fleshed 'G3', 'G9' and 'Hort16A'. The size and density of large cells were greater in 'G3', 'G14' and 'Hayward' than those of 'G9' and 'Hort16A'. Girdling did not affect the microstructure of large cells whereas low crop load increased maximum cell length. The ability to describe large cell structures non-destructively may be useful for cultivar or batch selection. However, improvement in the penetration depth is required to provide more comprehensive information and better understanding on the observed differences.

5 Quantitative prediction of post storage 'Hayward' kiwifruit attributes using at harvest Vis-NIR spectroscopy

Acknowledgement:

Material from this chapter is included in the following paper:

Li, M., Pullanagari, R.R., Pranamornkith, T., Yule, I.J., East, A.R., 2017. Quantitative prediction of post storage 'Hayward' kiwifruit attributes using at harvest Vis-NIR spectroscopy. Journal of Food Engineering, 202, 46-55.

5.1 Introduction

During ripening kiwifruit undergo two major changes: the decrease of flesh firmness (FF) and the conversion of starch to sugar (as indicated by TSS). The TSS at ripening is strongly associated with sweetness, eating quality, consumer acceptance and repeat purchases of kiwifruit (Crisosto et al., 2012a). The FF is an important ripening index for indicating the postharvest storability of kiwifruit (Beever and Hopkirk, 1990). In New Zealand, a minimum standard of 9.8 N for FF is required to ensure reasonable storage life remains to enable shipping to market (Hopkirk et al., 1996). Traditionally, the assessment of TSS and FF is destructive and hence unable to be used for monitoring large volumes of fruit. Development of a non-destructive technique may allow prediction of fruit quality and enable strategic marketing of fruit.

Vis-NIR spectroscopic techniques have been used as non-destructive and rapid tools to evaluate various quality attributes of fruits and vegetable (Williams et al., 2006; Jha, 2010). Previous attempts of using NIR spectroscopy to provide instant estimation of at-harvest TSS have been moderately successful. Good predictions have been achieved by McGlone and Kawano (1998), Osborne et al. (1998), Osborne et al. (1999), Schaare and Fraser (2000), Moghimi et al. (2010), Lee et al. (2012) and Chen and Han (2012). For post-storage TSS, prediction was usually based on estimates of at-harvest attributes generated using predictive models calibrated with that quality data measured. For instance, McGlone et al. (2002b) predicted post-storage TSS of 'Hayward' kiwifruit based on a predictive model calibrated with at-harvest fruit density. Similarly, McGlone et al. (2007) predicted post-storage TSS of 'Hort16A' kiwifruit based on estimated at-

harvest DMC data. Both approaches required testing of specific attributes at harvest and if this testing method is destructive, validation of the uncertainty in sample selection is essential. Ignat et al. (2014) used an approach similar to the philosophy of this study and predicted post-storage TSS of apples using at-harvest spectral data with good accuracy (R^2 = 0.76 – 0.94, RMSEP = 0.68 – 1.02 ºBrix, SDR = 2.1 – 3.1).

Prediction of at-harvest firmness using NIR spectral data was not as successful. Poor predictions were found in 'Hayward' kiwifruit (McGlone and Kawano, 1998; Costa et al., 1999; Lee et al., 2012), apples (Lu et al., 2000) and peaches (Fu et al., 2008). Prediction of post-storage firmness has also been studied by McGlone et al. (2002a) on 'Royal Gala' apples and Feng et al. (2013) on apricots but not as yet on 'Hayward' kiwifruit. In both studies the initial FF values were measured in order to develop a calibration model which was then applied for prediction. Similar to prediction of at-harvest firmness, no strong correlation was found between spectral data and post-storage firmness; prediction errors were relatively high. For kiwifruit, the initial firmness at harvest has no direct relationship with post-storage firmness (Ghasemnezhad et al., 2013; Burdon et al., 2014a). The softening rate in storage is dependent on the stage in softening achieved at the time of harvest (Burdon and Lallu, 2011), and fruit harvested at late maturity were found to maintain firmness better compared to early harvested fruit (Gordon Mitchell et al., 1992). Hence, the final firmness is influenced by a range of fruit characteristics at harvest which affect both maturity stage and rate of softening at harvest.

This paper investigates the ability of Vis-NIR spectroscopy utilised at harvest as the sole input variable, to quantitatively predict both TSS and firmness after cool storage. Because no additional at-harvest information is required, the objective is to apply Vis-NIR spectroscopy to capture the (near) skin properties of fruit which may be representative of various pre-harvest conditions resulting in a wide range of variability within the population, and perform prediction for future quality attributes using a blackbox model. The aim is to investigate whether information on skin properties extracted from spectral data can be indicative of physical/chemical properties of the fruit which in turn affects quality attributes after storage. The performance of regression methods used to develop quantitative model will be evaluated. Comparisons of prediction error to the literature will be drawn. Successful prediction of future quality

attributes would allow industry to identify batches that have higher quality potential and enable better inventory decisions.

5.2 Materials and Methods

A total of four Vis-NIR spectral and fruit quality data sets were collected over two fruit seasons from 2012 to 2013 (Table 5.1). The first two sets of Vis-NIR spectral data and quality after storage were available as a resource generated by two postdoctoral students in 2012 (Sections 5.2.1 and 5.2.2). In 2013, two more sets of Vis-NIR spectral data and fruit quality data were obtained from the trial with manipulation of crop load and girdling (Chapter 3) and the trial with manipulation of light. Both firmness (FF) and total soluble solids (TSS) data were collected for all the data sets except for the first set which only contained firmness measurements.

Table 5.1 Summary of NIR data sets collected in 2012 – 2014 available for analysis. Numbers represent the number of fruit measured. RM: Reflective mulch. HCG: High crop load with girdling. LCG: Low crop load with girdling. HC: High crop load. LC: Low crop load.

Data Sets	Treatment	Firmness					Total Soluble Solids				
		Storage time (day)				**Total**	Storage time (day)				**Total**
		75	100	125	150		75	100	125	150	
51 grower lines (2012)	Grower Lines	255	255	255	0	**765**	0	0	0	0	**0**
Manipulation of light (2012)	RM Control	40	40	40	40	**160**	40	40	40	40	**160**
Manipulation of light (2013)	RM Control	40	240	40	240	**560**	40	80	40	80	**240**
Manipulation of crop load and girdling (2013)	HC LC HCG LCG	0	320	0	320	**640**	0	320	0	320	**640**
Total		**335**	**855**	**335**	**600**	2125	**80**	**440**	**80**	**440**	1040

These data sets were later used to assess if Vis-NIR collected at harvest can assist in predicting kiwifruit quality attributes after storage. Since the data were collected from multiple orchards, multiple seasons and various types of trials with manipulation treatments, a vast variety of data was used to generate the model. This data variety increases the likelihood of a robust model being developed because, instead of tuning on a specific set of data, this study tries to capture the large variability that is observed within the industry.

5.2.1 Experiment 1: 51 grower lines

This experiment was part of a larger trial that investigated the potential to segregate 'Hayward' kiwifruit for storage potential using an accelerated fruit library rapid test methodology (Jabbar, 2014). Commercial 'Hayward' kiwifruit from 51 grower lines located in the Bay of Plenty, New Zealand were sourced during the 2012 season. Fruit were delivered in temperature controlled transport. The first grower line arrived on 10th May 2012 and the last on 14th June 2012. Each grower line consisted of 150 (5 trays of count 30) Class 1 export grade fruit. Only fifteen selected fruit (3 fruit per tray) from each grower line were subjected to initial Vis-NIR spectral measurements at day 0 (on arrival at the lab), resulting in a total of 765 fruit for corresponding post-storage firmness measurement. All the fruit were then placed into a cold room at 0°C. Each tray was randomly labelled for removal from the cold room for firmness measurement at 75, 100 and 125 days of storage, respectively.

5.2.2 Experiment 2: manipulation of light (season 2012)

This trial was part of a larger experiment that investigated the effects of light manipulation in the orchard on growth and storability of 'Hayward' kiwifruit (Pranamornkith, unpublished work). The experiment was conducted on a T-bar trained block at the Plant Growth Unit (PGU) at Massey University, Palmerston North and consisted of a control and a manipulated treatment using reflective mulch (RM) to enhance light exposure of kiwifruit. The selected reflective film was Ultramat white UV woven reflective ground cover (Cosio Industries, Auckland, New Zealand). The film was laid down on 20th December 2011, and maintained in position, with frequent cleaning and removal of trash, until harvest. The film was placed under both sides of 6 kiwifruit vines and the width of the film from the central leader was 4.15 m. Two blocks of film-treated vines were established. Control kiwifruit vines were selected no less than

2 m from the end of the reflective film. At harvest (11th May 2012), each treatment contained 240 mixed-sized fruit (8 trays of 30 fruit). Only 10 fruit out of the 30 fruit per tray were measured for initial Vis-NIR spectral data and subsequent post storage firmness, resulting in a total of 160 fruit for two treatments. All fruit were then placed into a cold room at 0 °C and firmness and TSS measurement was conducted for 20 fruit of each treatment at 75, 100, 125 and 150 days of storage, respectively.

5.2.3 Experiment 3: manipulation of light (season 2013)

For the 2013 harvest season, a light manipulation experiment was carried out on the Massey University PGU T-bar trained vines using the same Ultramat white UV woven reflective mulch described in Section 5.2.2. The film was laid down on 21st November 2012, under eastern side of 9 kiwifruit vines and both eastern and western sides of 4 vines. All fruit were harvested on 31st May 2013. At harvest, each of the treated and control fruit generated 2 replicates of 300 mixed-sized fruit (10 trays of 30 fruit), resulting in a total of 1200 fruit. Fruit were cured in the laboratory for two days at 20 °C, 60% R.H. Five fruit each from two trays of each replicate (20 fruit per treatment) were measured for Vis-NIR spectral data at day 0 (2nd June), and both firmness and TSS data after 75 and 125 days of cool storage at 0 °C. Another two full trays (30 fruit) from each replicate (120 fruit per treatment) were measured for spectral and firmness data after 100 and 150 days of storage, respectively. Additionally, ten fruit each from two trays of each replicate (40 fruit per treatment) were measured for spectral data and post-storage TSS after 100 and 150 days of storage, respectively.

5.2.4 Experiment 4: manipulation of crop load and girdling

The experimental setup for this experiment is in accordance with that described in Section 3.2.1. For the purpose of this study, at harvest, each of the four treatments contained 4 replicates consisting of 8 trays of 30 mixed-sized fruit per tray. The resulting total number of fruit was 3840. Only 5 selected fruit each of 2 trays per replicate of each treatment were measured for Vis-NIR spectral data at harvest, resulting in a total of 640 fruit for all four treatments. The post-storage TSS and FF data of corresponding fruit were measured after 100 and 150 days of storage at 0 °C.

5.2.5 Vis-NIR spectral data measurements

A commercial full-range Vis-NIR spectroscopy system (FieldSpec® Pro, ASD Inc., USA) was used in this study (Fig. 2.5a). Within the instrument, three types of detectors are installed to cover both the visible and the NIR range of the spectrum including: a silicon detector (350 – 1000 nm); an InGaAs detector that measures shortwave infrared (1000 – 1800 nm); and a second InGaAs detector (1800 – 2500 nm). The optical fibre of the instrument was coupled with a contact probe (Hi-Brite, PANalytical B.V., Boulder, USA) for contact measurements with a spot size of 10 mm in diameter. The contact probe was fitted with a high intensity halogen lamp to produce consistent illumination in a broad electromagnetic spectrum. The probe was fixed to a burette stand in a nadir position and connected to the instrument through an optical fibre cable. A diffuse reflectance material (Spectralon®, Labsphere Inc., North Sutton, USA) panel was used as a reflectance standard and to convert raw spectra to reflectance.

At the time of scanning each fruit were measured at two locations (90° apart) around the equator of the fruit. The sampling interval was 1.4 nm (350 – 1000 nm) and 2 nm (1000 – 2500 nm). The spectral resolution was 3 nm (at 700 nm), 10 nm (at 1400 nm) and 12 nm (at 2100 nm).

5.2.6 Fruit quality measurements

During storage, ethylene concentration in the cool room was monitored and maintained below 5 nL L^{-1}. Fruit flesh firmness (FF) and total soluble solids (TSS) content were assessed using the methodologies described in Section 3.2.2.

5.3 Near-Infrared Spectra Data Analysis

5.3.1 Pre-processing of spectral data

The raw spectral data were pre-processed using The Unscrambler® (Version X10.3; CAMO Software AS., Oslo, Norway). Spectral data from all experiments were first truncated to 400 – 2450 nm (Fig. 5.1a) so that fluctuations and noises at both ends were eliminated. Reflectance was then converted to absorbance by a Log transformation (Fig. 5.1b) which can be related to concentration by Beer's law:

$$A_\lambda = -\log_{10}(R) \tag{5.1}$$

where A_λ is the absorbance at a wavelength λ. R is the reflectance detected.

First order derivation using a Savitzky-Golay smoothing algorithm (Fig. 5.1c) was then applied. The purpose was to reveal the hidden information in the spectra as well as to reduce the noise in the data without reducing the number of variables. Derivation was the differentiation of the fitted polynomial at each point:

$$S'_n = S_{n+g} - S_{n-g} \tag{5.2}$$

where n is the degree of the fitting polynomial; S'_n is the first derivative at point n for evenly spaced wavelength λ_n; g is an integer called the gap or derivative size. The Savitzky-Golay smoothing algorithm (Savitzky and Golay, 1964) was used to estimate the polynomial approximation of the curve segment.:

$$\sum_{i=-m}^{m} i^r y_i = \sum_{k=0}^{n} (b_{nk} \sum_{i=-m}^{m} i^{r+k}) \tag{5.3}$$

where r = 0, 1, …, n; m is the number of points on either side of the central point (2 m + 1 is the total number of points to fit); λ_i is the wavelength at which the smoothed value is desired; y_i is the absorbance value at wavelength λ_{y+i}; b_{nk} is the coefficient of the kth term of the nth degree polynomial; b_{n0} is the smoothed value at λ_i.

Spectra were then normalised sample-wise (Fig. 5.1d) so that the resulting spectra were on the same scale and had more features in common, and unwanted sources of variability were suppressed.

$$\widehat{X}_\iota = \frac{X_i}{\sqrt{\sum_j X_{ij}^2}} \tag{5.4}$$

where X_i is the observation at a specific variable for one sample; X_i and X_{ij} are an element of the jth spectrum and of a data matrix X, respectively.

Lastly, mean centering was applied (Fig. 5.1e) by subtraction of an average value from each variable so that the final data was interpreted in terms of variation around the mean rather than the absolute values of the observations. For a data set of n samples each of j wavelengths, the mean centered jth wavelength of the nth sample is defined by:

$$X_{n,j\ cent} = X_{n,j} - \left(\frac{1}{n}\sum_{j=1}^{j} X_{n,j}\right) \tag{5.5}$$

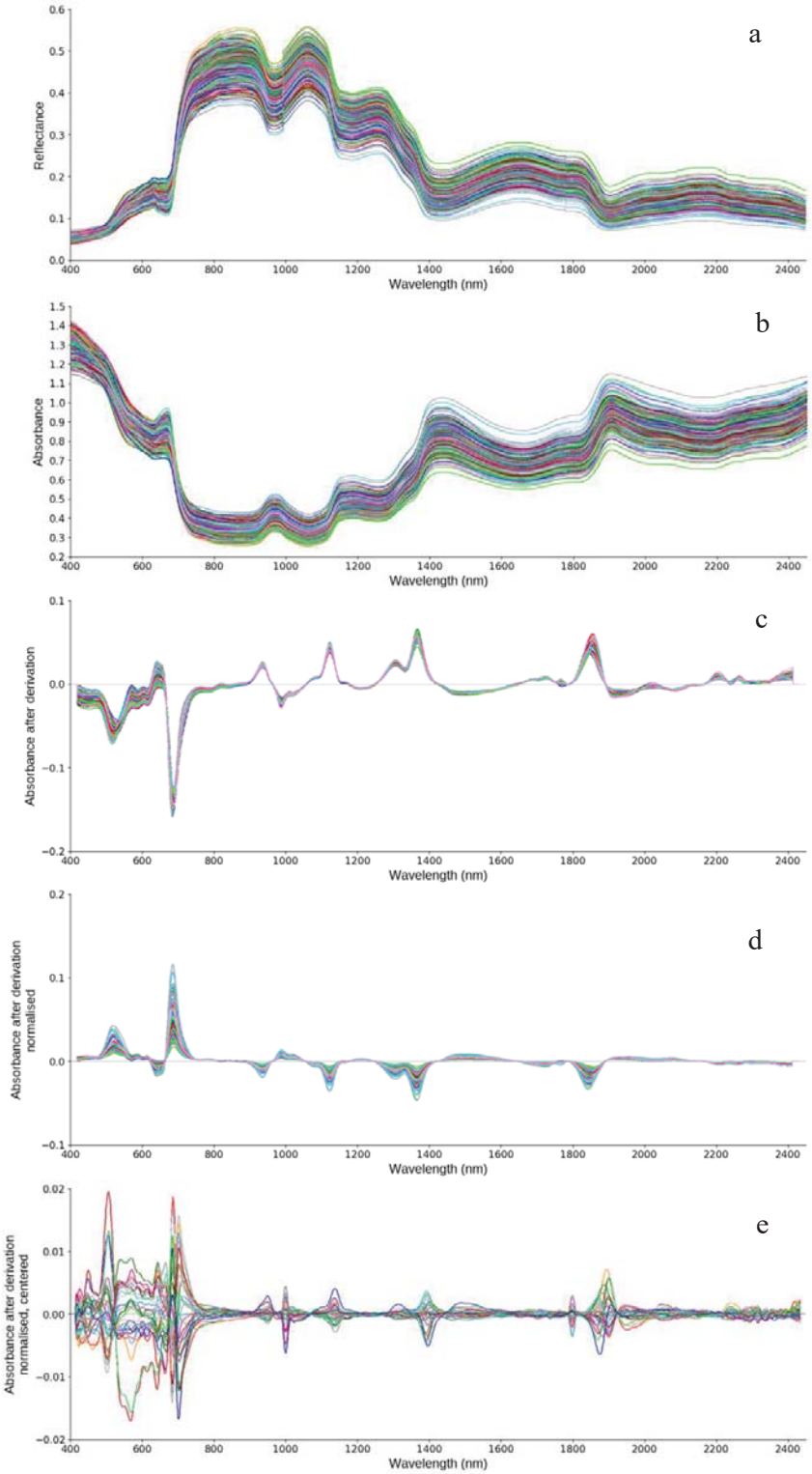

Figure 5.1 Pre-processing of Vis-NIR spectral data after: a) removal of noise regions; b) log transformation; c) first order derivation; d) normalization and e) mean centering in the 400 – 2450 nm range.

5.3.2 Algorithm for regression models

5.3.2.1 Partial least squares regression

Partial least squares (PLS) was introduced by Wold (1975) in algorithmic form as a modification of the non-linear iterative partial least squares (NIPALS) algorithm (Wold, 1966) to overcome disadvantages found in principal component regression. PLS projects the input data onto a small number of latent variables (LVs) which maximise the covariance between X-variables (spectral data) and Y-variables (TSS and FF) by developing a linear multivariate model. Including too many LVs in the PLS model may lead to over fitting, whereas too few LVs may result in under fitting (Gowen et al., 2011). Therefore, full cross validation (LOOCV) was used in this study to determine the optimal number of LVs.

The underlying model of multivariate PLS is shown in Eq. 5.6 and 5.7:

$$X = TP^T + E \tag{5.6}$$

$$Y = UQ^T + F \tag{5.7}$$

where X is a matrix of predictors, Y is a matrix of responses; T and U are matrices that are projections of X and Y respectively.; P and Q are orthogonal loading matrices; and E and F are the error terms. The decompositions of X and Y are made so as to maximise the covariance between T and U (Kalivas and Gemperline, 2006).

5.3.2.2 Support vector machine regression

Support vector machines regression (SVM-R) was first proposed by Vapnik (1995). In ideal cases the SVM-R identifies a function, where, for all training patterns x has a maximum of ε (ε > 0) deviation from the actual response y, and at the same time is as flat (simple) as possible (Smola and Schölkopf, 2004). However, for most real-world cases, the regression model is presented as a threshold tube with radius ε fitted to the data (Fig. 5.2; Ivanciuc, 2007). Any error situated inside the threshold tube is considered as zero and ignored by the loss function, whereas patterns situated outside the threshold tube have an error that increases with the distance to the tube margin (Ivanciuc, 2007). This is also known as the soft margin SVM-R using slack variables.

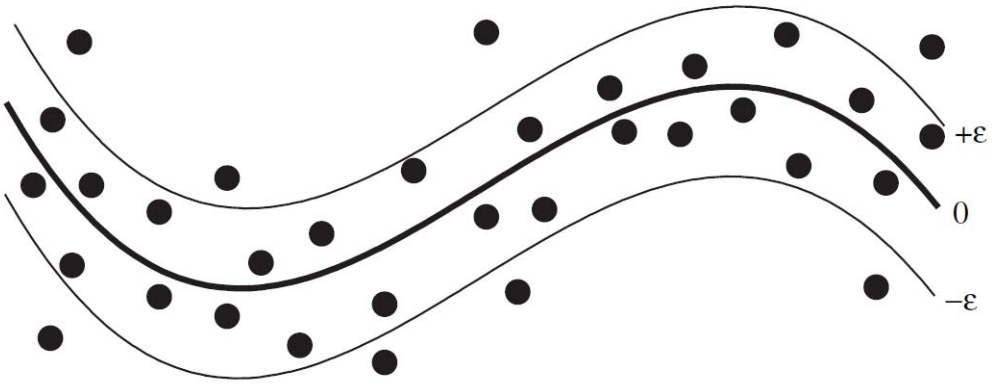

Figure 5.2 Support vector machines regression determines a tube with radius ε fitted to the data (Ivanciuc, 2007). Image used with permission.

The formulation of soft margin SVMR is stated in Eq. 5.8 and 5.9:

$$\text{minimise } \frac{1}{2}\|w\|^2 + C\sum_{i=1}^{l}(\xi_i + \xi_i^*) \tag{5.8}$$

$$\text{subject to } \begin{cases} y_i - \langle w, x_i\rangle - b \le \varepsilon + \xi_i \\ \langle w, x_i\rangle + b - y_i \le \varepsilon + \xi_i^* \\ \xi_i, \xi_i^* \ge 0 \end{cases} \tag{5.9}$$

where w is a weight vector and b is a bias; $y_i = \langle w, x_i\rangle - b - \varepsilon$ and $y_i = \langle w, x_i\rangle + b + \varepsilon$ indicate the hyperplanes forming borders of the regression tube; and ξ_i and ξ_i^* represent the slack variables associated with an underestimate and overestimate of the calculated response respectively, for the input vector, x_i (Vapnik, 1995). The constant C $(C > 0)$determines the trade-off between model complexity (flatness), and the degree to which deviations larger than ε are tolerated in optimisation formulation (Smola and Schölkopf, 2004).

For linear SVM-R models the threshold tube is a cylinder. For non-linear cases, the coordinates of the input objects are mapped into a high-dimensional feature space using a kernel function. The support vectors are those points that do not fall strictly within the threshold tube. All the other points are considered unimportant and can be removed from the training data without changing the outcome of the learning process (Witten et al., 2011). The radial basis function (RBF) kernel was used in this study to build non-linear regression model because this method is simple and capable of modelling complex data sets.

5.3.3 Model development and evaluation

Data sets at different storage times were randomly divided into two subsets: calibration (66.7%) and validation (33.3%). The statistics for quality measurements of the calibration and validation datasets are shown in Table 5.2. Calibration models were developed on The Unscrambler® using both PLS-R and SVM-R. In PLS regression, leave-one-out cross validation (LOOCV) was applied to avoid over-fitting. In this method one sample is removed from the data set and a calibration model is developed based on the remaining samples. The model is then used to predict the sample left out, and the prediction error is estimated. The process is repeated until every sample has been left out once, and the average prediction error is estimated. In SVM regression, internal L-fold (L = 20) cross validation was used. This method is similar to LOOCV except that samples are divided into L segments. At each time a segment of samples is left out rather than one sample. Predictions were compared with reference values and the R^2 and the RMSEP values were estimated.

Table 5.2 Summary statistics of quality measurements for kiwifruit after coolstorage of 75, 100, 125 and 150 days, respectively. S.D. stands for standard deviation.

	Storage time (d)	Flesh firmness (N)				Total soluble solids (°Brix)			
		n	Mean	S.D.	Range	n	Mean	S.D.	Range
Calibration data set	75	221	15.9	6.0	32.9	54	13.2	1.1	4.9
	100	564	17.4	6.6	38.9	294	15.0	1.6	8.2
	125	221	11.4	4.2	30.3	54	13.1	1.4	6.9
	150	396	13.7	5.2	25.2	294	15.2	1.5	7.5
		n	Mean	S.D.	Range	n	Mean	S.D.	Range
Validation data set	75	114	15.9	6.2	33.6	26	13.0	1.4	5.3
	100	291	17.3	6.6	35.6	146	15.1	1.7	8.5
	125	114	12.2	3.9	19.2	26	13.0	1.5	5.7
	150	204	14.2	5.3	27.1	146	15.1	1.6	8.0

The stability of the SVM algorithm was enhanced by finding the appropriate values of constant C (cost) and kernel parameter γ (Gamma) using Matlab (Version R2012a, MathWorks, Inc., Natick, USA), which are usually on a logarithmic scale. The values were determined through a grid search and applying a 10-fold cross validation to reduce the chance of under and over-fitting. The search window was set between 10^{-6} and 10 for γ, and between 10^{-3} and 100 for C with a step size of 1. The optimal parameters (Table 5.3) corresponding to the lowest RMSEs were used in the final model.

Table 5.3 Appropriate values of constant C (cost) and kernel parameter γ (Gamma) used for developing quantitative models which corresponded to lowest RMSE values.

Storage time (day)	FF		TSS	
	Cost	Gamma	Cost	Gamma
75	1	0.00032	100	0.0000032
100	31.62	0.000032	31.62	0.000032
125	100	0.000010	100	0.000031
150	10	0.00010	100	0.000010

5.3.4 Selection of important waveband

Several variable selection techniques were also applied to the pre-processed spectra data to eliminate unimportant variables so as to reduce computation cost and improve prediction accuracy (Zou et al., 2010). Principal component analysis (PCA) was carried out to find linear combinations of variables that contribute most to making the samples different from each other. The first PC is one that carries most information; the second PC carries the maximum share of the residual information, and so on. Genetic algorithm (GA) selected important variables using genetic algorithm which simulates the process of natural selection based on fitness (indicated by R^2 and RMSE). In addition, the sampling intervals were increased from 1 nm to 5 or 10 nm by taking mean of every 5 or 10 data points respectively (Fig. 5.3). This helped to reduce localised fluctuations in the spectra. Determination of the best variable selection technique was done by comparing regression outcomes using full spectrum.

Amongst the selected techniques, increasing sample intervals was found to perform best for overall regression accuracy (Tables A.1 – A.4). This technique has several advantages: broader sampling intervals (5 – 10 nm) yield better results while reducing computational cost (Kemper and Sommer, 2002; Shepherd and Walsh, 2002); the resultant sampling intervals also match more closely to the spectral resolution of the instrument used (3 – 12 nm). The improved accuracy is probably because variable loadings with localised fluctuations were smoothed without losing important information (e.g. Fig. 5.2d). Nicolaï et al. (2007b) found that the accuracy of PLS model was increased by removing redundant high resolution information by means of wavelet compression and the best results corresponded to a wavelength resolution of about 5 nm. In this study increasing sampling intervals to 5 and 10 nm was found to provide the best accuracy for firmness and TSS respectively, and hence were used for subsequent regression models.

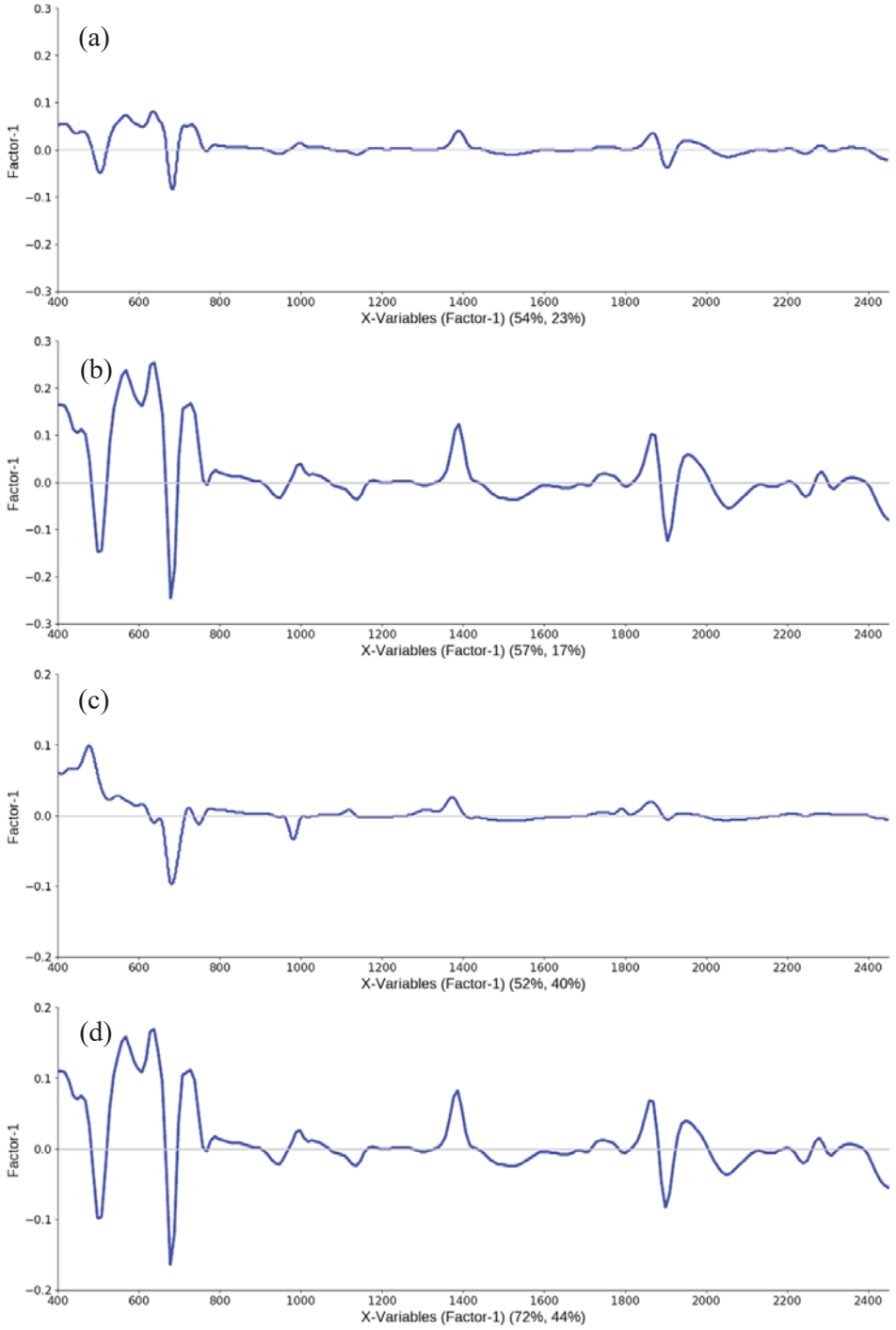

Figure 5.3 X-loadings for TSS PLS regression model (75 days) using (a) original spectra and (b) pre-processed spectra by taking averages of every 10 nm in the 400 – 2450 nm range; and x-loadings for firmness regression model (75 days) using (c) original spectra and (d) pre-processed spectra by taking averages of every 5 nm in the 400 – 2450 nm range.

5.4 Results and Discussion

5.4.1 Prediction of total soluble solids during storage

The reflectance spectra comprised of several overlapping absorptions corresponding to overtones and combinational chemical bonds present in different organic compounds (Osborne, 2000). The regression coefficient plot for TSS (Fig. 5.4a) shows a few peaks with high RC values at 780, 880, 970, 1200–1210, 1400–1450, 1700, 1820 nm and 1940 nm, suggesting important contribution to the regression model from these wavebands. These absorption bands correspond to the water spectrum with overtone bands of OH-bonds at 760, 970, 1450 (Nicolaï et al., 2007a), 1200, 1820 and 1940 nm (Workman and Weyer, 2007). The absorptions around 880 and 970 are caused by second overtone of C−H stretching (McGlone and Kawano, 1998).

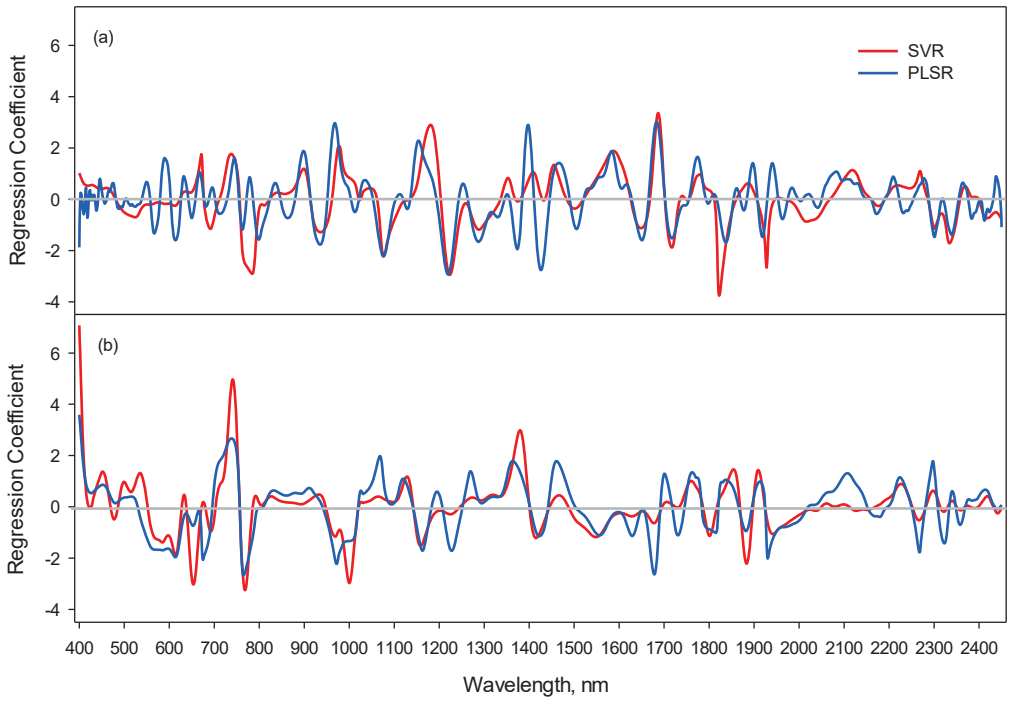

Figure 5.4 Regression coefficient curves for the prediction of (a) total soluble solids and (b) flesh firmness of 'Hayward' kiwifruit using support vector machines (red) and partial least squares (blue) regression.

In general the predictive performance for TSS was good (Table 5.4), suggesting good correlation between at-harvest Vis-NIR spectral data and post-storage TSS data. Regression models built with SVM-R method produced better results compared to those

with PLS-R. Specifically, considerably lower RMSE and higher SDR values (SDR > 2) were obtained using SVM-R for predictions at 100, 125 and 150 days (Table 5.4). This is probably because SVM-R models with kernel functions could handle non-linear complex multivariate data correlation which might exist between post-storage TSS values and at-harvest NIR spectral data, whilst PLS-R models were merely based on linear projection.

The prediction results for validation from SVM-R model (R^2 = 0.68 – 0.83) were not as good as those reported by McGlone et al. (0.89; 2007) in which prediction was based on estimated at-harvest DMC of 'Hort16A' kiwifruit, and Ignat et al. (0.76 – 0.94; 2014) which performed prediction for apples using at-harvest spectral data directly. However results were comparable to those found by McGlone et al. (0.70; 2002a) which used estimated at-harvest density for 'Royal Gala' apples. The RMSE values (0.66 – 0.86 °Brix) were higher compared to those found by McGlone et al. (0.38 °Brix; 2007) and McGlone et al. (0.50 °Brix; 2002a) but were lower than those found in Ignat et al (0.68 – 1.02 ºBrix; 2014). The SDR values (1.6–2.3) were comparable to that obtained by McGlone et al. (1.8; 2002a).

The SDR values obtained in this study, however, suggest that a good regression model can be developed by finding correlations between at-harvest Vis-NIR spectral data and post-storage TSS values. Hence, quantitative prediction of TSS using the developed model may be promising, especially for storage times of 100, 125 and 150 days. However, a significant regression model does not necessarily guarantee viable industrial applications such as online sorting of kiwifruit. McGlone and Kawano (1998) recommend that an SDR value of 3 should be considered as the minimum value for sorting/grading purposes of kiwifruit. In this study the highest SDR value obtained was 2.3. This indicates that it would still be challenging to apply the predictive models for on-line TSS sorting purposes without further improvement of the models. One would argue that the selection of thresholds of SDR values can vary since there is no statistical basis used to determine the thresholds (Bellon-Maurel et al., 2010). Therefore, an online testing at existing packhouses, combined with storage studies on the same fruit/batch, may be helpful to determine whether the developed model is sufficiently robust to be used for online prediction of future TSS.

Table 5.4 Prediction of post-storage total soluble solids (TSS) of kiwifruit based on at-harvest Vis-NIR spectral data using partial least square (PLS) and support vector machines (SVM) regression. The results obtained in calibration are cross-validated.

Storage Time (d)	Predictive Performance									
	PLS-R					SVM-R				
	Calibration		Validation			Calibration		Validation		
	R^2_{CV}	RMSECV (°Brix)	R^2	RMSEP (°Brix)	SDR	R^2_{CV}	RMSECV (°Brix)	R^2	RMSEP (°Brix)	SDR
75	0.73	0.70	0.70	0.84	**1.7**	0.67	0.78	0.68	0.86	**1.6**
100	0.71	0.89	0.66	0.96	**1.7**	0.80	0.75	0.80	0.74	**2.2**
125	0.58	1.13	0.58	0.93	**1.8**	0.70	0.95	0.74	0.74	**2.2**
150	0.58	0.95	0.60	1.02	**1.5**	0.80	0.67	0.83	0.66	**2.3**

5.4.2 Prediction of flesh firmness during storage

The regression coefficient plot for FF (Fig. 5.4b) shows two major peaks at 740 and 1395 nm, and several secondary peaks at 650, 770, 1680 and 1890 nm, indicating important roles of these wavebands to the regression model. These could be related to a combination of water absorption bands at 740, 770 and 1400 nm (Workman and Weyer, 2007), and the pectin absorption bands at around 1670 nm which was responsible for measuring textural properties of fruit (Kojima et al., 2004). However, several other known pectin absorption bands (e.g. 1590, 1730 and 2400 nm; Kojima et al., 2004) did not seem to have a significant contribution to the regression model.

The predictive performance for firmness (Table 5.5) was not as good as that for TSS. In general model validation showed poor to moderate predictability with low R^2 (0.24–0.60) and SDR values around 1.5. Comparing the two regression algorithms, SVM-R had better prediction because of lower RMSE and higher SDR values than PLS-R, suggesting a possible non-linear correlation between post-storage FF values and at-harvest Vis-NIR spectral data.

Comparing results to the literature (using SVM-R), the R^2 values (0.38 – 0.60) were comparable to those found by McGlone et al. (0.59; 2002a) and Ignat et al. (0.18 – 0.73; 2014) for 'Royal Gala' apples, and Feng et al. (0.50; 2013) for 'Clutha Gold'. The achieved RMSE values (3.53 – 4.12 N) were considerably lower than those obtained in McGlone and Kawano (7.8 N; 1998) for 'Hayward' kiwifruit, Feng et al. (8.8 N; 2013) for 'Clutha Gold' apricot, McGlone et al. (7.5 N; McGlone et al., 2002a) for 'Royal Gala' apples, and Ignat et al. (4.6 – 6.5 N; 2014) for various apple cultivars, respectively. This suggests that FF is possibly affected by various quality attributes within the fruit and hence, prediction based on an overall status may be a better approach rather than only looking at initial FF value of the fruit. The SDR values (1.5 – 1.7) obtained in this study (using SVM-R) were comparable to those found in McGlone et al., (1.6; 2002a) but slightly lower than those reported in Ignat et al. (1.1 – 2.5; 2014).

Table 5.5 Prediction of post-storage flesh firmness (FF) of kiwifruit based on at-harvest Vis-NIR spectral data using partial least square (PLS) and support vector machines (SVM) regression. The results obtained in calibration are cross-validated.

Storage Time (d)	Predictive Performance									
	PLS-R					SVM-R				
	Calibration		Validation			Calibration		Validation		
	R^2_{CV}	RMSECV (N)	R^2	RMSEP (N)	SDR	R^2_{CV}	RMSECV (N)	R^2	RMSEP (N)	SDR
75	0.60	3.95	0.30	4.32	**1.4**	0.56	4.17	0.38	4.12	**1.5**
100	0.53	4.62	0.50	4.41	**1.5**	0.60	4.26	0.60	3.92	**1.7**
125	0.43	3.31	0.24	3.04	**1.4**	0.43	3.31	0.46	2.65	**1.6**
150	0.48	3.87	0.42	3.83	**1.4**	0.58	3.46	0.51	3.53	**1.5**

The small RMSE values obtained in this study indicate better model fitting and lower error achieved as compared to previous studies. However, low overall SDR values suggest that spectral information of individual fruit obtained at harvest may not be indicative to post-storage firmness, and accurate quantitative predictions using the developed model would be difficult. Based on the minimum threshold recommended by McGlone and Kawano (1998), the developed regression models were not suitable for online sorting purposes.

The prediction of firmness is related to loss of cell wall structures such as pectin, cellulose and hemicellulose as they contribute to the mechanical strength of the wall and to the adhesion between cells. The ripening process which is observed as fruit softening is associated with significant changes in the structures of the pectic substances (Lodge and Roberston, 1990). Cho et al. (1992) found changes in pectin and water absorbance bands of NIR at around 1900 nm, and suggested that a successful firmness model works through reliance on water state changes in the softening fruit; pectin breakdown products bind some of the free water that existed when the fruit was firmer. Since the total amount of pectic substances in kiwifruit is very low (< 1% by fruit weight; Beever and Hopkirk, 1990) , McGlone and Kawano (1998) propose that pectin structural changes (hence, changes in firmness) are possibly more difficult to detect than changes in more abundant constituents such as TSS.

Additionally, Paz et al. (2008) suggests that the lower predictive capacity of firmness prediction models as opposed to those of TSS, was to be expected since firmness is a physical parameter whose measurement using the reference method is already prone to considerable error. In fact a closer look at the difference between the two firmness measurements carried out on the same fruit showed that there was large variation in firmness readings between the two locations on the same fruit, with this variation decreasing as the average firmness of the population decreased, i.e. storage time increased (Fig. 5.5). It is possible that this variation contributed as a source of error, to affect final model accuracy. At 95% confidence level, the error caused by variation in physical measurements using penetrometer were found to be ± 3.8 N, ± 3.1 N, ± 2.3 N and ± 2.3 N for 75, 100, 125 and 150 days respectively (Fig. 5.5). This means that up to 80% of the observed RMSE in regression models could have been originated from variations in physical measurements of firmness (Table 5.5). This suggests that the key

to improving predictive accuracy of FF does not only rely on model robustness but also require a more precise way of conducting physical measurements of firmness.

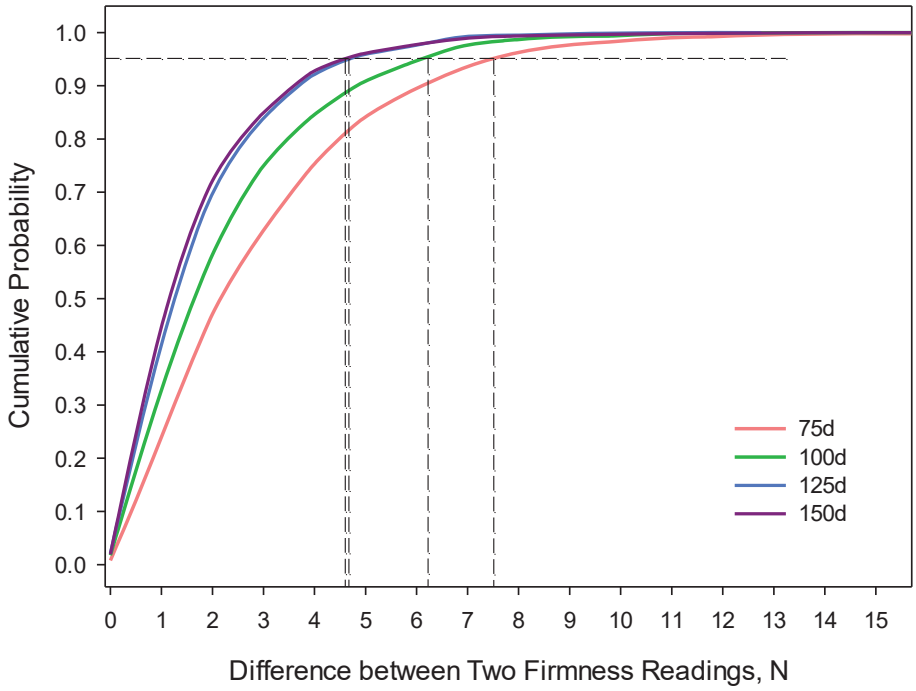

Figure 5.5 Cumulative probability of the difference found between two firmness readings (N) using an electronic QALink Penetrometer fitted with the standard 7.9 mm Magness-Taylor probe, for measurement at 75, 100, 125 and 150 days respectively. Horizontal dash line represents 95% confidence level (cumulative probability = 0.95).

Although quantitative prediction of future FF has been shown to be challenging, there is still potential to investigate qualitative prediction of future FF using classification methods. One major concern of NIR technique for fruit and vegetables is that model performance and robustness is largely affected by the 'richness' of variation in the calibration sample (Nicolaï et al., 2007a). Model error can drastically increase when the calibration model is applied to a new dataset from a different batch or season, or have been subjected to changes in physical condition, temperature or replacement of instrument. In this case the calibration model loses its validity and a new model or recalibration is needed (Swierenga et al., 2000). This would be time-consuming and labour-intensive. Qualitative prediction would reduce chances of error resulted from re-calibration, and would enable the possibility of focusing on relative correlation, rather

than absolute correlation, between spectral data and firmness retention properties of kiwifruit. Therefore, the next two chapters will explore this potential application of Vis-NIR spectroscopy.

5.5 Conclusion

In this chapter, the potential of using at-harvest Vis-NIR spectra as the sole predictor to forecast post-storage quality attributes of kiwifruit was investigated. Four sets of at-harvest spectral data and post-storage firmness and TSS data were collected. Both PLS and SVM were used to develop regression models, with SVM-R generating better predictions than PLS. Predictive accuracy of TSS ($R^2 = 0.58 – 0.83$; RMSE = 0.66 – 1.02 °Brix) was comparable to previous studies that used both NIR spectral and initial fruit quality data for prediction. Although the developed model shows potential to be utilised as a predictive tool, the SDR values (1.5 – 2.3) suggest that models are not as yet useful for online sorting purposes. Prediction of firmness was poor to moderate ($R^2 = 0.30 – 0.60$; RMSE = 2.65 – 4.32 N) but results were comparable to the literature. The RMSE values were lower compared to previous studies, suggesting better model fitting. The firmness prediction model was not useful for online grading purposes due to low SDR values (1.4 –1.7). A significant source of variation was observed during physical measurement of firmness, contributing to final RMSEs. Confirming and reducing this variation would be recommended for future development of regression models of FF, as this may reduce RMSE considerably and potentially improve the accuracy for quantitative prediction of firmness. Alternatively, classification models can be developed using at-harvest spectral data, in order to investigate the potential of qualitative prediction of post-storage kiwifruit firmness.

6 Segregation of 'Hayward' kiwifruit for storage potential using Vis-NIR spectroscopy – development of an appropriate multivariate data analysing method

6.1 Introduction

The work in Chapter 5 concluded that although quantitative prediction of post-storage total soluble solids content could be achieved with some success, it was not possible to obtain accurate prediction of fruit firmness, a quality indicator that is important for storage potential prediction. It was recommended that, qualitative prediction may be an alternative approach and may have better potential applications. This is particularly useful for segregation/sorting of fruit/grower lines for export purposes. There is huge financial benefit if fruit or grower lines can be segregated at harvest for potential storability and shipped sequentially based on the prediction.

Despite the many previous attempts carried out to utilise NIR spectroscopy for quantitative prediction of kiwifruit quality attributes, little research has been conducted to evaluate the ability of NIR to perform qualitative prediction using classification models.

Feng (2003) used NIR spectral and fruit quality data collected at harvest to classify individual 'Hayward' kiwifruit for storage potential using canonical discriminant analysis (CDA). At-harvest NIR spectra were calibrated with various at-harvest fruit attributes, and the calibrated model was then used for the prediction of post-storage firmness, allowing for segregation of disordered fruit from healthy ones. Poor prediction of post-storage firmness was obtained. The classification accuracy was 67%, 35% and 46% for healthy fruit, fruit with soft patch and fruit that developed CI respectively.

Feng et al. (2014) also attempted to segregate storage potential of individual kiwifruit based on at-harvest NIR spectra using models calibrated with various at-harvest attributes (skin and flesh colour, FF, TSS and DMC) and in-storage acoustic firmness measurements. Fruit that developed rots or became overly soft after coolstorage and seven days simulated shelf life were classified as rejected fruit.

Amongst many multivariate analysis techniques logit-boost decision stumps was found to generate the best segregation performance. Results suggested that the false positive rate (good fruit classified wrongly) was 30% and 40% respectively for 'Hayward' and 'SunGold' ('G3') for a targeted 75% true positive rate (rejected fruit accurately classified).

In addition, Clark et al. (2004) categorised 'Hort16A' kiwifruit based on Vis-NIR reflectance intensities at 227 selected wavelengths at harvest using the unsupervised pattern recognition CDA classification. In this study fruit from two maturity stages were used for developing classification models that segregate the fruit into two groups: 'good' and 'disorder' (with rots and chilling injuries after storage). The classification accuracy was 66% and 52% for disordered fruit and 80% and 89% for good fruit, respectively for fruit from two harvest stages. This would indicate a reduction in disorder incidence from 33.9 to 17.9% and 14.7 to 8.5% for both harvests. However external validation was not conducted hence the robustness of the model to perform prediction on an independent data set was not determined. Similarly, Burdon et al. (2014b) used at-harvest NIR spectral data calibrated with at-harvest attributes to predict the incidence of CI of stored 'Hort16A' kiwifruit, and concluded that such a generally applicable approach was not useful in this case due to a large orchard factor which contributed to considerable variation in the minimum or maximum threshold for the development of CI.

In other crops, prediction of the storability of apricots was carried out by fitting an exponential model to describe the relationship between FF_0, the at-harvest FF estimated by Vis-NIR spectral data, and FF_{Final}, post-storage firmness predicted based on FF_0 (Feng et al., 2013). Segregation of storage potential was based on the projected FF_{Final} in comparison to the minimum standard for sale at retail (10 N). This segregation provided theoretical limits for initial firmness of apricot for the two cultivars studied but validation of the segregation model was not conducted. In addition, Zude et al. (2006) discriminated post-storage quality levels of apple as a result of storage condition treatments using non-destructively estimated TSS (Vis-NIR) and FF (acoustic impulse resonance frequency) values measured after storage, and obtained 77% and 84% overall accuracy respectively. The authors suggested that the superior results obtained using non-destructive methods were possibly due to the fact that more representative data of

the heterogeneous fruit material could be obtained, compared to destructive methods which only provided localised data.

To date most relevant studies required calibration of the model with at-harvest attributes in addition to spectral data in order to perform prediction or segregation of future storability. In-storage quality measurements were sometimes required (e.g. Feng et al., 2014). However this approach involves destructive measurements of fruit and the accuracy for prediction is affected by sample selection for the calibration process. Additionally data collection during storage would be challenging for packhouses as this would require extra labour reshuffling pallets of fruit in order to obtain a representative sample. An alternative approach would be to perform prediction/classification prior to storage using NIR spectra data as the only input. In this case a black-box model is developed using supervised machine learning algorithms for classification. The spectral data capture an overall initial state of the fruit whilst the post-storage firmness values provide training for pattern recognition (Fig. 6.1).

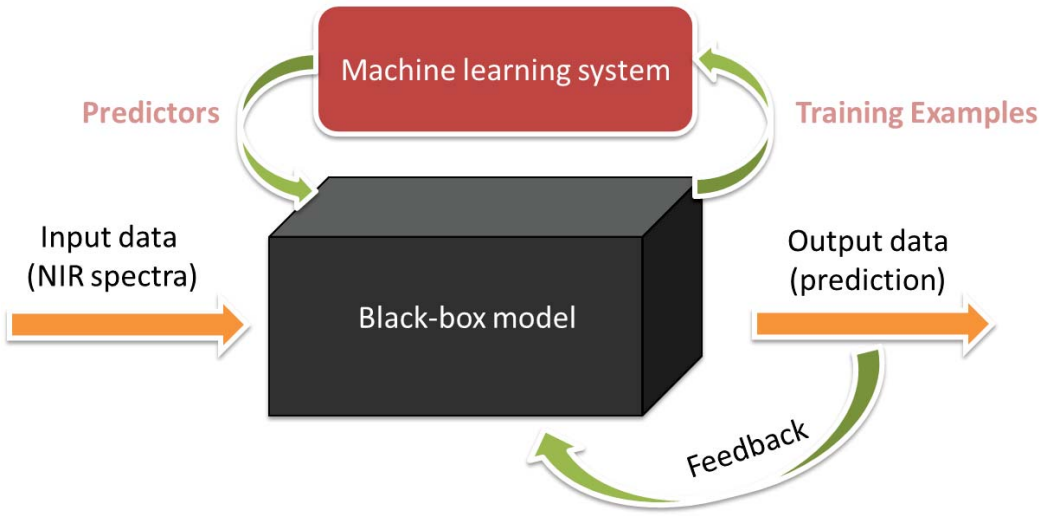

Figure 6.1 Conceptual diagram of a black-box model using NIR spectral data as the sole input to predict storability of kiwifruit.

In this chapter, an attempt was made to utilise NIR spectra data as the sole input at harvest, to perform qualitative prediction of kiwifruit firmness retention properties after coolstorage using the blackbox model proposed as above. Various pattern recognition algorithms were selected to develop a suitable classification model which aims to segregate individual kiwifruit into two groups based on the export firmness criterion (FF $\geq$ 9.8 N). The predictive performance of each of the algorithms was evaluated, and the classifier that resulted in the model with the most satisfactory accuracy and robustness was identified. The resulting final classification model will be tested in the next chapter (Chapter 7) using a new data set. Segregation of fruit by storage potential may allow rapid identification of fruit unsuitable for export and in turn reduce fruit and financial losses.

6.2 Materials and Methods

6.2.1 Data sets

The same four data sets discussed in Chapter 5 (Section 5.2, Table 5.1) were also used in this chapter for the purpose of building classification models using at-harvest spectral and post-storage firmness data. Additionally, in 2014, another set of data was collected from a larger trial that studied the relationship between storage temperature and the development of chilling injury (Zhao, 2017). The fruit measured for this study were from 9 grower lines of the 'control' samples meaning that fruit were stored at 0°C. Fruit were sourced in the Bay of Plenty, New Zealand at three maturity stages with delivery dates sequenced by 1-week intervals commencing 8 May 2014. Each maturity stage consisted of 6 trays of count 33 fruit from three grower lines (2 trays per GL), resulting in a total of 594 fruit for three maturities. At day 0 (on delivery day), Vis-NIR spectral data of individual fruit were collected prior to subsequent storage at 0°C for extended periods of time. Single trays from each maturity stage were assessed for firmness at 75 and 100 days after storage, and two trays assessed at 125 and 150 days after storage. For model development, the four data sets (n = 2125) from 2012 – 2013 were used for calibration whereas the data set collected in 2014 (n = 594) was used for external validation (Table 6.1).

Table 6.1 Summary of Vis-NIR spectral and post-storage firmness data sets collected in 2012 – 2014 for developing and validating classification models. Numerical values represent the number of fruit measured at each time of storage. Soft and good means flesh firmness of the fruit is < 9.8 N and ≥ 9.8 N respectively.

Storage time (day)	Calibration						Validation		
	Season				Total		Season	Total	
	2012	2012	2013	2013	Soft	Good	2014	Soft	Good
75	255	40	40	0	**35**	**300**	99	**6**	**93**
100	255	40	240	320	**87**	**768**	99	**2**	**97**
125	255	40	40	0	**121**	**214**	198	**53**	**145**
150	0	40	240	320	**133**	**467**	198	**68**	**130**

6.2.2 Data collection and spectral pre-processing

The experimental procedures for spectral data collection and firmness measurements were in accordance with those described in Sections 5.2.5 and 3.2.2 respectively. The raw spectral data were pre-processed using the steps described in Chapter 5 (Section 5.3.1) except that mean centering was not applied for the purpose of this chapter, as this technique is mostly useful in simplifying spectral data for regression models (Boysworth and Booksh, 2007). Since the objective of this chapter was to develop classification models, this technique was not used to pre-process the spectral data.

6.2.3 Machine learning algorithms for classification models

In order to identify the most suitable pattern recognition algorithm for classification of samples, several machine learning techniques were explored using two data mining software: Weka (Version 3.7.12; University of Waikato, Hamilton, New Zealand; Hall et al., 2009) and The Unscrambler® (Version X10.3; CAMO Software AS., Oslo, Norway). Each of these techniques will be discussed in the following sections.

6.2.3.1 Naïve Bayes

The Naïve Bayes classifier is one of the simplest probabilistic classifiers based on the "Bayes' Theorem". It assumes that all variables of the samples are independent of each other given the context of the class. This is also known as the "Naïve Bayes assumption". The assumption is based on the fact that classification is only a function of the sign (or the class); function approximation can still be poor while classification accuracy remains high (McCallum and Nigam, 1998). This method uses a collection of labelled training samples to estimate the parameters of the generative model. Classification on new samples is performed by selecting the class that is most likely to have generated the sample (McCallum and Nigam, 1998). By Bayes Theorem, the posterior probability of *Y* given *X* is:

$$P\,(Y = k|X = x) = \frac{P\,(X = x|Y = k)P(Y=k)}{\sum_{i=1}^{K} P\,(X = x|Y = i)P(Y=i)} \quad (6.1)$$

where $X_1, \ldots, X_j$ are the J predictors considered in the model. The Naïve Bayes model assumes that $X_1, \ldots, X_J$ are conditionally independent given the target, that is:

$$P\,(X = x|Y = k) = \prod_{j=1}^{J} P\left(X_j = x_j \middle| Y = k\right) \quad (6.2)$$

where *P* values are the probabilities estimated from the training data set; *X* is the categorical predictor vector; *j* is the number of predictors considered; *Y* is the categorical target variable; *k* is the number of categories of *Y*.

6.2.3.2 Quadratic discriminant analysis

Linear and quadratic discriminant analyses are orthogonal classifiers. The linear discriminant analysis (LDA) assumes that data is normally distributed and that the covariance matrices of the two classes are equal (Sun, 2009). As such the variability within each group has the same structure. The only difference between classes is that they have different centres. In this case linear separation of groups is possible (Witten et al., 2011). If the covariance matrices are not identical and the curve separating groups is not linear, quadratic discriminant analysis (QDA) should be used. This method performs better when the training data sets used are large. The quadratic discriminant function can be expressed as:

$$g_i(X) = -\frac{1}{2}(X-\mu_i)^T \sum_i^{-1}(X-\mu_i) - \frac{1}{2}\log(|\sum_i|) + \log(\pi_i) \quad (6.3)$$

where $g_i(X)$ is a simple max gate function used as a classification rule; X is the vector of feature variables, which is multivariate normally distributed in the group with the mean vector μ_i; π_i is the prior probability of class i; $\sum_i$ is the group specific covariance matrix for QDA; and T is a transpose operator.

6.2.3.3 Random forests

A decision tree finds features in the input variables and identifies the threshold for the features that best splits the data into separate classes (Quinlan, 1986). Each feature attribute is presented as a node in the tree, with each possible threshold of each attribute as a branch and a class label as each leaf. However, this method is prone to over-fitting and has high variance. Random Forests are an ensemble of decision trees. In this method each model (tree) is trained independently using a random small subset of features for the split. As a result the predictions from the sub-trees are uncorrelated or weakly correlated, resulting in lower variance (Nguyen et al., 2006). The generalisation error for forests converges to a limit as the number of trees in the forest becomes large. Prediction is made by aggregating majority vote for the predictions of the ensemble (Anne-Michelle and Mousumi, 2007). The algorithm of RF was developed by Breiman (2001):

$$\{T_1(X), \ldots, T_J(X)\} \quad (6.4)$$

where $X = \{x_1, \ldots, x_p\}$ is a p-dimensional vector of a sample or properties associated with a sample. The ensemble produces J outputs $\{\hat{Y}_1 = T_1(X), \ldots, \hat{Y}_J = T_j(X)\}$ where $\hat{Y}_j$, j = 1, …, J, is the prediction for a sample by the jth tree. Outputs of all trees are aggregated to produce one final prediction, $\hat{Y}$. For classification problems, $\hat{Y}$ is the class predicted by the majority of the trees (Svetnik et al., 2003).

6.2.3.4 Support vector machine classification

The concept of SVM regression was introduced in Section 5.3.2.2. In this chapter, SVM with sequential minimal optimisation (SMO; Platt, 1999) was used for classifying the spectral data. For any set of two-class objects, the SVM finds the unique hyperplane having the maximum margin for optimal discrimination. The hyperplane

defines the borders for each class with specific objects within the class, and these objects are referred to as support vectors (Ivanciuc, 2007). The support vectors are used to classify the samples. For non-linear classification, the coordinates of the input objects are mapped into a high-dimensional feature space using different kernel functions. The kernels can be computed in the same space as the input objects allowing linear algorithms to work with higher dimensional feature space. Classification is accomplished by a weighted sum of kernels evaluated by the support vectors (Ivanciuc, 2007). The SMO algorithm was used to speed up the training of SVMs by reducing a large quadratic programing optimisation problem into a series of small optimisations (Mohri et al., 2012). Suppose there are N data points in the training dataset,

$$\{(x_1, y_1), (x_2, y_2), \dots, (x_N, y_N)\} \tag{6.5}$$

where $x_i \in \mathbb{R}_N$and $y_i \in (+1, -1)$.

Consider a hyperplane defined by (w, b), where w is a weight vector and b is a bias. A new object *x* can be classified with:

$$f(x) = sign\,(wx + b) = sign\,(\sum_i^N a_i y_i(x_i x_j) + b) \tag{6.6}$$

where (x_i, x_j) is a set of training data points and a_i is the Lagrange multipliers which is minimised with respect to w and b and maximised with respect to $a_i \geq 0$ (Gunn, 1998; Pachghare and Kulkarni, 2011).

For real-world data, the common approach is to solve the classification using a soft margin, meaning that the hyperplane separates most but not all of the data points. In this case the soft slack variable, ξ_i and the capacity constant, C will be required:

$$\text{minimise } \frac{1}{2}\|w\|^2 + C\sum_i \xi_i \tag{6.7}$$

$$\text{subject to } \begin{cases} y_i f(x_i) \geq 1 - \xi_i \\ \xi_i \geq 0 \end{cases} \tag{6.8}$$

In this study the RBF kernel was used. This function generates hidden units that represent the coordinates of the objects in the input space (NIR spectral data and FF values). The output of an object for a given instance (the class that the sample belongs to) depends on the distance between the object and its instance. This distance is

converted into a non-linear measure. The hidden units are referred to as RBFs and the hyperplane is formed when a given hidden unit for the objects in the instance space produces the same outputs (Witten et al., 2011). The algorithm for RBF kernels is:

$$\text{Kernel}\left(x_i, x_j\right) = exp\left(-\gamma \parallel x_i - x_j \parallel^2\right) \quad (6.9)$$

where γ is the variable parameter (Gunn, 1998).

The robustness of the calibration model could be optimised by finding the optimal constant C and kernel parameter γ. However due to the limitation of the software Weka and time constraints, a grid search of the least RMSEs was not conducted. The default values (C = 1 and γ = 0.01) were used for developing all the models.

6.2.3.5 Boosted decision stumps

Decision stumps (DS) are one level decision trees with two terminal nodes (Friedman et al., 2000). In this method, each node in a DS represents a feature in a sample, and each branch represents a threshold value that the node can take. Samples are classified starting at the root node and sorting them based on their feature values (Kotsiantis et al., 2006). Stumps are weak leaners and usually have low variance but high bias (Friedman et al., 2000).

Boosting algorithms were first introduced by Freund and Schapire (1996) to provide a way of combining performance of many weak classifiers to produce a powerful committee. It uses a sequential algorithm in which each new weak learner is built based on the performance of the previously generated predictors (Jung, 2009).

AdaBoost algorithm (Freund and Schapire, 1996) assigns equal weight to all samples in the training data. When a classifier is formed by the learning algorithm, the algorithm reweights each sample according to the prediction output. The weight of correctly classified samples is decreased and that of misclassified samples is increased. A new classifier is then built for the reweighted data and focuses on predicting the previously misclassified samples correctly. Once again the algorithm reweights the samples according to the new classifier. The weights after iteration reflect how often the samples have been misclassified. Whenever error on the weighted training data exceeds

or equals 0.5, or equals 0, the boosting procedure deletes the current classifier and does not perform any more iteration. To predict a new sample, the output of a series of classifiers generated by the boosting method is combined using a weighted vote, where:

$$weight = -\log\frac{e}{1-e} \text{ (Witten et al., 2011)} \quad (6.10)$$

where e denotes the classifier's error on the weighted data and is a fraction between 0 and 1 (Witten et al., 2011).

LogitBoost was first introduced by Friedman et al. (2000) for fitting additive logistic regression models by maximum probability. It computes 'response variable' that encodes the error of the currently fit model on the training examples in terms of probability estimates (Landwehr et al., 2004). LogitBoost decision stumps use the logit transform to translate the probability estimation problem into a regression problem, and solve the regression task using DS (Witten et al., 2011). The probability of a sample being class A is a number between 0 and 1. If the number is more than 0.5 the algorithm will categorise the sample as class A, and vice versa. The probability for each instance can be calculated as:

$$\mathrm{p}\left(\frac{1}{\mathbf{a}}\right) = \frac{1}{1+e^{-\Sigma f_{j(\mathbf{a})}}} \quad (6.11)$$

where f_j is the jth regression model and $f_{j(\mathbf{a})}$ is its prediction for sample **a** (Witten et al., 2011).

6.2.4 Model calibration and validation

The pre-processed spectral data from the four different experimental trials in 2012 – 2013 and the corresponding fruit firmness values for the same fruit (n = 2125) were used to develop the calibration model. The data set obtained in 2014 (n = 594) was used for external validation (Table 6.1). For classification, fruit were categorised into two groups based on their firmness values after coolstorage: soft (FF < 9.8 N) and good (FF ≥ 9.8 N). The predictive relationship between at-harvest spectral data and post-storage fruit grouping was investigated at four storage times (75, 100, 125 and 150 days) by developing four corresponding models.

A ten-fold cross-validation method was used for internal validation. In this method the samples were randomly divided into 10 segments. One of the segments was then removed from the dataset and then the calibration model was developed from the remaining 9 segments. The isolated segment was then used to assess classification performance. This process was repeated until every segment was removed from the dataset once and their predictive performance averaged. Once this was completed, the calibration models developed at specific storage times were used to predict fruit grouping for the validation data set.

6.2.5 Model assessment

6.2.5.1 Comparison of data sets

Comparisons between the calibration and validation data sets were carried out by generating respective cumulative distribution graphs of FF measurements and conducting the non-parametric Kolmogorov-Smirnov test using Matlab® (Version R2012a, MathWorks, Inc., Natick, USA). In this test, the hypothesis, H, was tested based on the maximum difference between the empirical distribution functions of calibration and validation data set, D:

$$D_{mn} = \sup_x |F_m(x) - G_n(x)| \tag{6.12}$$

where $F_m(x)$ is the distribution of a first population $X_1,\ldots, X_m$ of size m, and $G_n(x)$ is the distribution of a second population $X_1,\ldots, X_n$ of size n; H = 0 if $D_{mn} \leq 1.36\,(\frac{mn}{m+n})^{\frac{1}{2}}$, i.e. $F = G$ (p-value > 0.05) and H = 1 if $D_{mn} > 1.36\,(\frac{mn}{m+n})^{\frac{1}{2}}$, i.e. $F \neq G$ (p-value $\leq$ 0.05).

Additionally, PCA plots of spectral data for both calibration and validation data sets were obtained and compared using Scikit-learn (Version 0.18.1, BSD License, USA).

6.2.5.2 Classification performance

The ability of Vis-NIR spectroscopy to assist in predicting kiwifruit storability on an individual fruit basis was evaluated. To assess the model performance, the percentage of accurate classification was calculated for each group. In addition, Table

6.2 illustrates the performance metrics used to evaluate the classifiers. True positive (TP) is referred to as correctly classified soft fruit (< 9.8 N). True negative (TN) is the correctly classified good fruit (≥ 9.8 N). False positive (FP) is the number of classified soft fruit which are actually good. False negative (FN) is the number of classified good fruit which are in fact soft. For the purpose of this study, the proportion of actual soft fruit in the segregated soft population as well as in the predicted good group, i.e. the TP and FN rates, were used to assess model robustness. This is because the TP rate represents the true correct classification of soft fruit and the FN rate indicates the potential fruit loss in the segregated good fruit population which is very important for justification of industrial applications.

Table 6.2 A typical confusion matrix used to evaluate performance of classification models.

		Predicted	
		Soft	Good
Actual	Soft	TP	FN
	Good	FP	TN

6.2.5.3 Classification algorithm comparison

In order to compare the predictive performance amongst various classifiers, several parameters including overall accuracy, kappa values, mean absolute error, FN rates, recall and precision and computation time were estimated.

Overall accuracy (OA) is the percentage of correct predictions in the entire population, i.e. (TP + TN) / *n*, where *n* is the total number of samples.

Kappa is a value that ranges between 0 and 1 which indicates the reliability of a classifier on a specific dataset. The closer the value is to 1, the more reliable the classifying algorithm is. The kappa statistic can be calculated using the equation:

$$\text{Kappa} = \frac{\text{Observed accuracy - expected accuracy}}{\text{1 - expected accuracy}} \tag{6.13}$$

where observed accuracy is the total number of instances that were classified correctly throughout the entire confusion matrix; expected accuracy is defined as the

accuracy that any random classifier would be expected to achieve based on the confusion matrix and can be calculated as:

$$\text{Expected accuracy} = \frac{\frac{(TP+FN)\times(TP+FP)}{n} + \frac{(TN+FP)\times(TN+FN)}{n}}{n} \quad (6.14)$$

where *n* represent the number of total observations

Mean absolute error (MAE) is the mean of overall error made by the classifier.

$$MAE = \frac{1}{n}\sum_{i=1}^{n}\left|\hat{\theta}_i - \theta_i\right| \quad (6.15)$$

where $\hat{\theta}_i$ is the predicted value and θ_i is the observed value.

Recall is the proportion of samples belonging to the positive class (i.e. Soft) that are correctly predicted, i.e. Recall = TP / (TP + FN).

Precision is the proportion of actual positive samples in the predicted positive class, i.e. Precision = TP / (TP + FP).

Training time is the time in seconds consumed to compute the model.

In addition, the performance of the models using different classifiers was evaluated using the receiver operating characteristic (ROC) curves. The ROC curve is used to characterise the trade-off between hit rate (signal) and false-alarm rate (noise) over a noisy channel (Gorunescu, 2011; Witten et al., 2011). As a result the ROC curves can be used to visualise, organise and select classifiers, based on their performance (Gorunescu, 2011). Often the ROC curves are plotted using the TP rates ('benefits') against the FP rates ('costs'). However for this study, the FN rates are more important as they are the true costs of a poor segregation (number of soft fruit in the predicted good batch). Therefore the ROC curves were obtained by plotting the TN values against the FN values. The samples were sorted in descending probability order according to the predicted probability of a true response. The ROC curve started from the origin, and each point corresponded to drawing a line at a certain position on the ranked list, counting the True's and/or False's above it, and plotting them vertically and/or horizontally, respectively (Witten et al., 2011).

In ideal situations the curves should be as close to the upper left corner (vertical axis) as possible (Witten et al., 2011) because high TN rate results in consecutive vertical lines which will bring the curve to coordinates with low FN rate. The point (0, 1) represents perfect classification (i.e., no FNs), whereas a completely random guess would form a diagonal line (no discrimination) from the left bottom to the upper right corner (Gorunescu, 2011).

A simple way of evaluating ROC curves is to estimate the area under curve (AUC). A higher AUC value suggests better classification performance. Hence the AUC values were also used for algorithm comparison. In general an AUC value between 0.8 – 1.0 indicates good to excellent classification accuracy, whereas 0.7 – 0.8 is considered fair accuracy. However, cautions should be taken when using AUC to evaluate model performances, because over-simplifying ROC curves into a single AUC number may lose information about the pattern of trade-offs of a particular classifier (Gorunescu, 2011).

Final ranking of classifiers was carried out using the Garrett's Ranking Technique (Garrett, 2002). It was calculated as percentage score using the equation:

$$\text{Percentage score} = \frac{100\ (R_{ij} - 0.5)}{N_j} \tag{6.16}$$

where R_{ij} is the rank given for the i^{th} item j^{th} individual; N_j is the number of items ranked by j^{th} individual.

6.2.5.4 Further improvement through data balancing

In the calibration data set the distribution of the incidence of soft and good fruit were highly imbalanced especially at 75 and 100 days (Table 6.1) where the vast majority of the fruit were firm. This class imbalance problem is common to many real world data mining problems. The minority class is often the one that has the highest interest and usually implies a great cost when it is not well classified (Elkan, 2001).

The solutions to deal with this can be categorised into three major groups: 1) data resampling including under or oversampling, 2) algorithmic modification and 3) cost-sensitive learning (Barandela et al., 2003; López et al., 2013). Amongst these, data resampling is the most popular due to its simplicity. In this chapter the Synthetic

Minority Oversampling Technique (SMOTE) filter was employed as a resampling technique, in order to improve the performance of imbalanced data set. This was carried out using only the top two ranked classifiers after algorithm comparison (Section 6.3.3).

The SMOTE technique, proposed by Chawla et al. (2002), is a supervised filter that alters the distribution of classes by oversampling the minority class. This is achieved by creating synthetic samples using a *k*-nearest-neighbour approach (Witten et al., 2011). This causes the decision boundaries for the minority to spread further into the majority class space (Batista et al., 2004).

For the purpose of this chapter, the percentage of oversampling was determined by aiming for a final ratio of about 2:1 for good : soft fruit (Table 6.3). To achieve this, 300% of the original number of soft fruit was simulated by the SMOTE filter, resulting in a total of 400% of the original number of soft samples for storage times at 75 and 100 days. Similarly, 100% of the original number of soft fruit was synthesised for storage time at 150 days, contributing to a total of 200% of the original number of soft. The number of soft fruit after data balancing is obtained by multiplying the original number with the percentage of fruit simulation.

Table 6.3 Number and ratio of good and soft fruit before and after data balancing using the SMOTE filter.

Storage time (day)	Soft (original)	Good : Soft (original)	% of Soft simulated	Soft (after data balancing)	Good : Soft (after balancing)
75	35	8.6 : 1	300	140	2.1 : 1
100	87	8.8 : 1	300	348	2.2 : 1
125	121	1.8 : 1	-	121	1.8 : 1
150	133	3.5 : 1	100	266	1.8 : 1

The performance of the models developed using the original and balanced data sets was evaluated using the ROC curves. Comparisons of AUC values were carried out using the GLM in Minitab®.

6.2.5.5 Multiclass classification

Data noise generated by variation in physical measurements of firmness using the penetrometer was also considered. Fig. 6.2a shows the differences observed between the two firmness readings measured on the same fruit. As the measured average firmness values increase so does the potential difference between the two measured values determining the average. Given that only two values were used to determine each average firmness value, either of these values could be considered as the true fruit firmness.

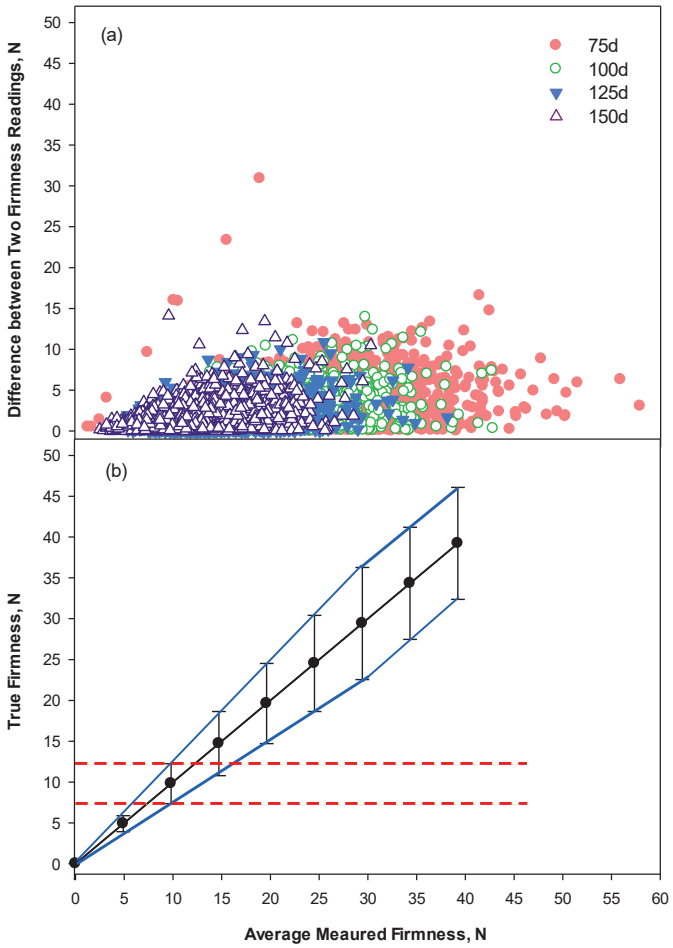

Figure 6.2 (a) Difference between two measured firmness readings as a function of average measured firmness; (b) True firmness as a function of average measured firmness. Dots represent average values where blue lines represent potential error margins and red dotted lines indicate the range of actual firmness when the measured firmness is 9.8 N.

Following this thought, data on Fig. 6.2a were converted to Fig. 6.2b which represents the relationship between the measured average and potential true firmness of a kiwifruit. A fruit with an average firmness of 9.8 N (1 kg_f) may have a true firmness ranging from 7.4 N to 12.3 N. A fruit is only considered really soft if the measured firmness value is below 7.4 N, and a fruit is truly exportable if the measured firmness is greater than 12.3 N. Fruit with measured firmness values falling in between these two boundaries could either be soft or good and therefore is considered as unsure.

Based on this observation, attempts were also made to develop classification models to segregate fruit into three classes, Real Soft ($FF_{Average} \leq 7.4$ N), Unsure ($7.4 < FF_{Average} < 12.3$ N), and Real Good ($FF_{Average} \geq 12.3$ N). Again this was carried out only using the top two ranked classifiers after algorithm comparison (Section 6.3.3).

Within multiclass classification there are two popular methods of simplifying the decisions made: one-against-all (OAA) and one-against-one (OAO). These methods achieve classification by reducing a multiclass problem to a binary one and hence simplifying predictions. The OAA builds a classifier for each class in a multiclass dataset. As a result it builds n models for a dataset with n classes. The OAO approach builds classifiers by taking any two classes as a pair and ignoring the remaining one. As a result n (n – 1) / 2 classifiers are needed to be built for a dataset with n classes (Eichelberger and Sheng, 2013b).

An alternative approach is known as all-at-once (AAO) which applies multiclass algorithms directly. It classifies a test example into anyone of the multiple classes using one decision function only (Eichelberger and Sheng, 2013b). Eichelberger and Sheng (2013a) compared the performance of these three methods and concluded that OAA and OAO should not be used for algorithms that can perform multiclass classifications directly, i.e. AAO. Similarly, Mathur and Foody (2008) also suggested that one-shot multiclass classification (AAO) was better than the OAA approach. Therefore, for this study, we only applied algorithms directly for multiclass classifications.

6.3 Results and Discussion

6.3.1 Comparison of data sets

The storage performance data appeared to be highly imbalanced, with the soft fruit class under-represented relative to the good fruit class in all data sets (Table 6.1). As the storage time increased the number/proportion of soft fruit increased and hence the data became relatively more balanced. The distributions of firmness were found to be different between calibration and validation data sets at 75, 100 and 125 days ($p < 0.05$; Fig. 6.3a, b, d) but were comparable at 125 days ($p > 0.05$; Fig. 6.3c). This is probably because external factors such as orchard, season and other growing conditions result in different physiological properties of fruit when using an independent data set.

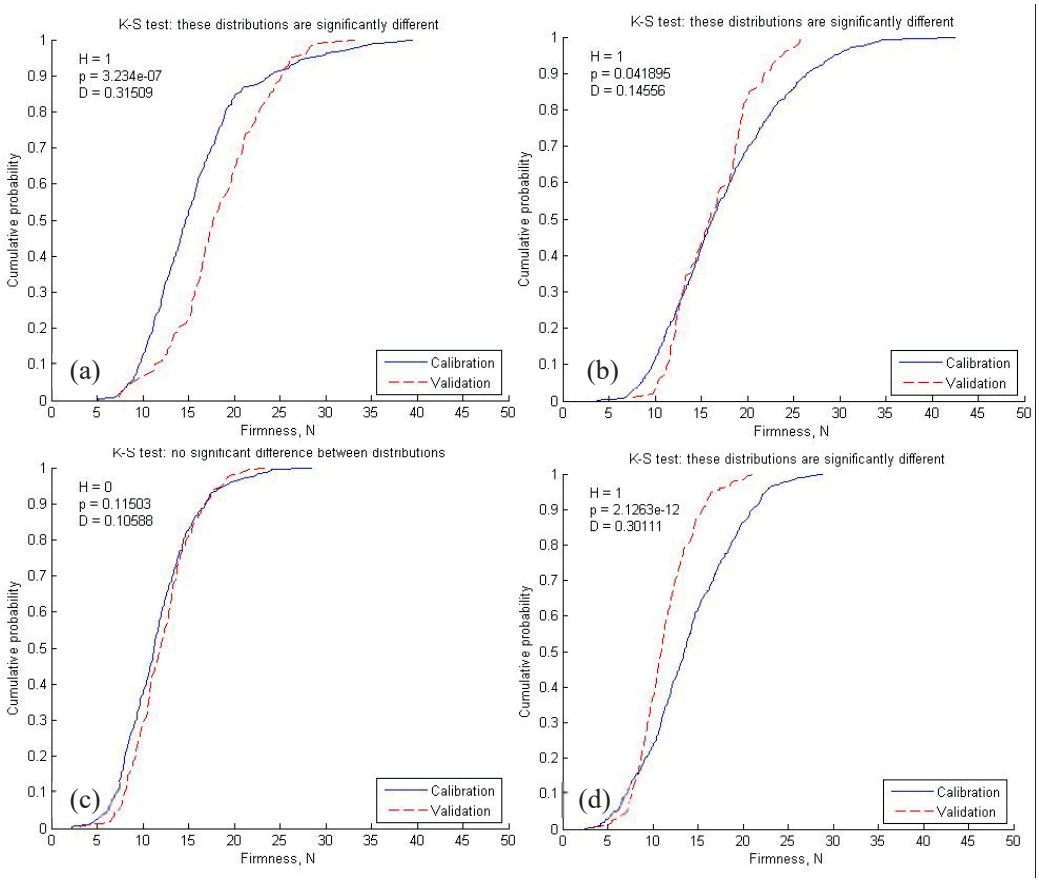

Figure 6.3 Kolmogorov-Smirnov test comparing cumulative distributions of flesh firmness (N) for calibration and validation data sets at (a) 75, (b) 100, (c) 125 and (d) 150 days after storage.

In addition, PCA test was conducted at each time point, to visualise the differences in spectral properties of fruit skin between the calibration and validation data set (Fig. 6.4). In model calibration, a wide range of fruit variability was captured in order to increase the likelihood for future validation data to exhibit similar spectral properties as what was observed in the calibration data set. This was true for fruit stored for 100 and 150 days as the calibration and validation data sets overlap with each other, suggesting similar spectral characteristics of fruit. However the validation samples for 75 and 125 days exhibited different spectral properties and hence were separate from the calibration samples (Fig. 6.4).

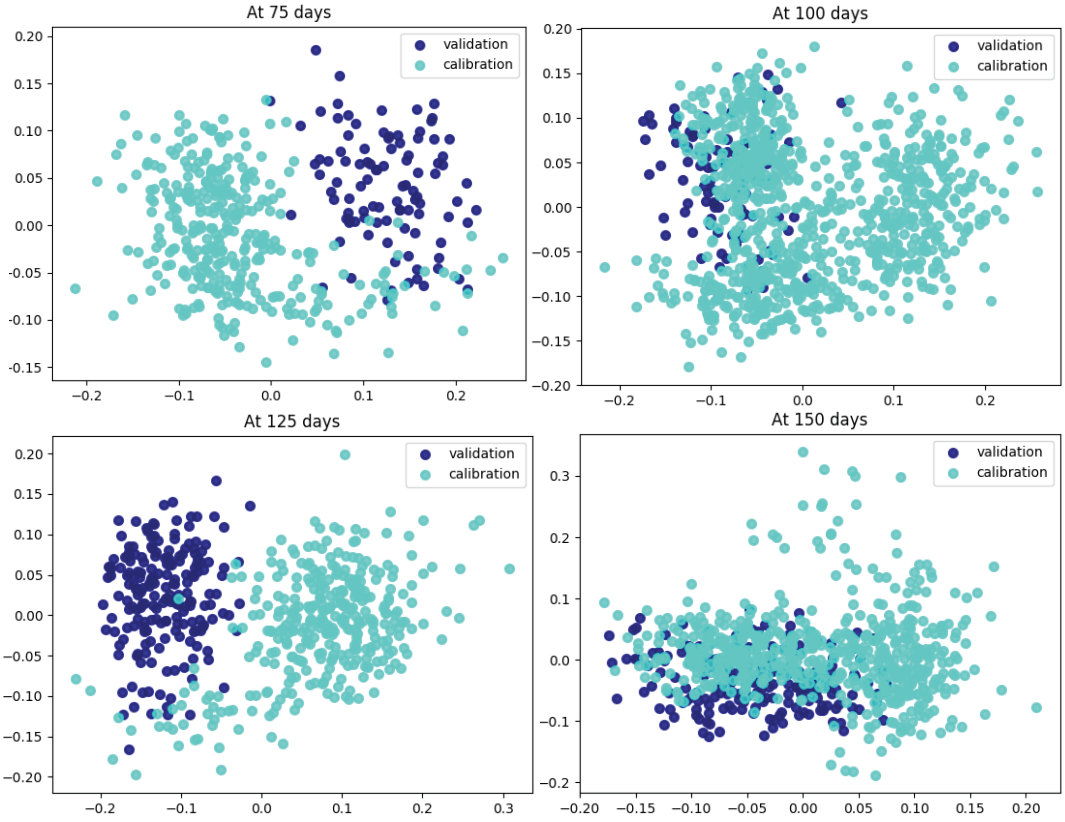

Figure 6.4 Visualisation of spectral differences between calibration and validation data sets using principal component analysis (PCA). Data points represent individual fruit samples present in the data sets. x- and y-axes represent PCs 1 and 2 correspond to an individual PCA test for each storage time.

The differences observed between calibration and external validation samples are not uncommon for real-world model prediction problems. Various external parameters such as temperature, moisture, wavelength shifts and crop season can vary

largely in industrial conditions and alter the spectral properties of validation samples (Roger et al., 2003). As such, corrections to reduce the effect of external parameters are required in order to improve model performance. One approach is to optimise the calibration sample which includes collection of a comprehensive data set that covers all the variations including those caused by external parameters so that the model would be insensitive to these parameters (Roger et al., 2003). This approach was used during the development of the calibration model for this study but seasonal differences were still observed (Fig. 6.4). Alternatively, spectral preprocessing techniques such as external parameter orthogonalisaiton and orthogonal signal correction can be applied to eliminate the effects of external parameters.

6.3.2 Classification performance

The predictive outcomes of various classifiers using 10-fold cross validation are summarised in Table 6.4. Samples size seems to have affected predictive performance of the classification models, with better prediction accuracy observed for the good group (> 78%) than the soft group (< 54%) for all classifiers except for Naïve Bayes and QDA. In general prediction of soft fruit was better at 125 and 150 days (~ 40 – 50%) compared to that at 75 and 100 days (~ 20 – 40%). This could also be related to the higher number of soft fruit (hence, more balanced data sets) found at those storage times. Results obtained for 125 and 150 days were comparable to the results found by Feng (2003) for the classification of healthy and soft-patched fruit (67% and 35% respectively), and those reported by Clark et al. (2004) for segregation between good and disordered fruit (~85% and ~59% respectively).

In external validation (Table 6.5), the models were unable to segregate soft fruit at 75 and 100 days regardless of the classifiers used; all (or most) of the fruit were identified as good fruit. Better TP rates (accurately classified soft fruit) were found at 125 and 150 days using SVM and LogitBoost DS. For QDA, Naïve Bayes, Random Forest and AdaBoost DS, segregation of soft fruit was only possible at 150 days however with relatively low TN rates (accurately classified good fruit). In general as storage time increased the TP rates improved but the TN rates decreased.

The poor validation performance was likely attributed to the extremely low levels of soft fruit found in the validation data set, in particular for storage times at 75

and 100 days (6 and 2 soft fruit respectively), compared to that found in the calibration data set (35 and 87 respectively; Table 6.1). Hair et al. (2006) recommended at least 20 samples per group for discriminant analysis design in order to improve the chance of classification. The number of soft fruit in the validation data set was below 20 at both 75 and 100 days. As a result the calibration models were less likely to identify soft fruit from the population, hence the poor classification accuracy. At 125 days, the number of soft fruit in the validation data set was more than 20 and the proportion increased to 27%. In this case, classification accuracy of soft fruit improved using SVM and Logit-Boost DS (11% and 40% respectively) but not for the other classifiers (0%). At 150 days, 34% soft fruit were found in the validation data set. Prediction accuracy improved significantly for soft fruit (44 – 99%) for all classifiers but became less successful for good fruit (< 53%; Table 6.5) compared to that at other storage times. This further suggests that classification accuracy was affected by group size.

In addition, the spectral differences observed in Fig. 6.4 also contributed to the discrepancy in classification performance between classification and validation. This explains the poor validation prediction at 75 and 125 days, where the validation data set had patterns and trends different from those of the calibration data set (Fig. 6.4a, c). In comparison, classification accuracy at 150 days was higher since the spectral properties between the two data sets were much more similar (Fig. 6.4d).

Table 6.4 Calibration of classification models to predict kiwifruit storage potential based on at-harvest Vis-NIR spectra data (original data) using 10-fold cross validation. Data represents classification of 2125 fruit from 4 trials in 2012 – 2013 at different storage times.

Storage time (day)	Classification Accuracy (%)											
	Naïve Bayes		Quadratic Discriminant Analysis		Random Forest		Support Vector Machine		AdaBoost Decision Stumps		LogitBoost Decision Stumps	
	Soft	Good	Soft	Good	Soft	Good	Soft	Good	Soft	Good	Soft	Good
75	66	69	80	60	3	99	46	91	17	96	17	97
100	77	72	82	76	2	99	41	96	20	98	26	96
125	77	34	63	50	34	86	50	79	50	78	54	79
150	59	78	33	87	38	94	51	91	47	91	41	96

Table 6.5 External validation of cross-validated classification models to predict kiwifruit storage potential based on at-harvest Vis-NIR spectra data (original data). Data represents classification of 594 fruit from 2014 trial independent to that used for model calibration.

Storage time (day)	Classification Accuracy (%)											
	Naïve Bayes		Quadratic Discriminant Analysis		Random Forest		Support Vector Machine		AdaBoost Decision Stumps		LogitBoost Decision Stumps	
	Soft	Good	Soft	Good	Soft	Good	Soft	Good	Soft	Good	Soft	Good
75	0	100	0	100	0	100	0	100	0	100	0	100
100	0	100	0	97	0	100	0	99	0	100	0	100
125	0	100	0	100	0	100	11	91	0	99	40	81
150	93	7	99	2	44	53	79	30	72	37	49	52

6.3.3 Classification algorithm comparison

Tables 6.6 – 6.9 summarise the statistics for model evaluation and Garrett's ranking of model performance amongst classifiers. Considering a total of eight performance metrics, the best two performing classifiers were SVM and LogitBoost DS regardless of storage time, with LogitBoost DS performing better at 125 and 150 days whereas SVM performing better at 75 and 100 days. Amongst the remaining classifiers AdaBoost DS and Random Forest showed better performance whereas QDA and Naïve Bayes performed poorly.

The Overall Accuracy (OA) showed the combined predictive performance of both classes but did not indicate the accuracy of predictions for each group. For instance, SVM and LogitBoost had similar OA but SVM had higher Recall at 75, 100 and 150 days whereas LogitBoost DS had lower FN rates at all times (Tables 6.6 – 6.9). In this case low FN rates are preferable because the proportion of soft fruit in the predicted good class should be as low as possible in order to ensure exportability and long storability of the predicted good batch. Similarly, QDA and Naïve Bayes had high Recall rates most of the time but the FN rates were also high and hence were considered undesirable. Amongst all classifiers, SVM had the highest precision at 75 and 100 days but was outperformed by LogitBoost DS at 125 and 150 days (Tables 6.6 – 6.9). AdaBoost DS seemed to have lower MAE (error) values compared to the top-two classifiers (SVM and LogitBoost DS) despite lower overall ranking (Tables 6.6 – 6.8). Naïve Bayes consistently had the highest MAE at all storage times. The SVM had the highest Kappa values except for at 125 days, indicating better reliability.

The AUC ranged from 0.70 – 0.80 for most classifiers with one exception of Naïve Bayes at 125 days (AUC = 0.56), indicating fair accuracy. The SVM had the highest AUC values at 75 and 100 days, indicating better classification performance. However, at 125 and 150 days LogitBoost DS was found to be superior given the higher AUC values at those storage times (Tables 6.6 – 6.9). The computational cost was highest for AdaBoost DS as it consumed the longest time to build models. The costs of Random Forest, Naïve Bayes and QDA were noticeably less than those of SVM, LogitBoost and AdaBoost DS but their performance was poor (Tables 6.6 – 6.9). Amongst the top performing classifiers, SVM and LogitBoost were more cost effective as compared to AdaBoost.

Table 6.6 Ranking of classifier performance in predicting storability of kiwifruit at 75 days after coolstorage using 10-fold cross-validation.

Rank	Name of Classifier	Evaluation Parameter (Range)							
		Overall Accuracy (0 – 100%)	ROC AUC (0 – 1)	Kappa (0 – 1)	Mean Absolute Error (> 0)	False Negative (0 – 1)	Recall (0 – 1)	Precision (0 – 1)	Training Time (s)
1	Support Vector Machine	86.567	0.830	0.3404	0.1459	0.087	0.457	0.381	2.56
2	LogitBoost Decision Stumps	88.358	0.778	0.1816	0.1243	0.033	0.171	0.375	10.87
3	AdaBoost Decision Stumps	88.060	0.800	0.1744	0.1258	0.037	0.171	0.353	19.17
4	Random Forest	88.955	0.781	0.0305	0.1714	0.010	0.029	0.250	0.48
5	Naïve Bayes	68.358	0.738	0.1690	0.3158	0.313	0.657	0.197	0.13
6	Quadratic Discriminant Analysis	61.446	-	-	-	0.397	0.800	0.114	0.89

Table 6.7 Ranking of classifier performance in predicting storability of kiwifruit at 100 days after coolstorage using 10-fold cross-validation.

Rank	Name of Classifier	Evaluation Parameter (Range)							
		Overall Accuracy (0 – 100%)	ROC AUC (0 – 1)	Kappa (0 – 1)	Mean Absolute Error (> 0)	False Negative (0 – 1)	Recall (0 – 1)	Precision (0 – 1)	Training Time (s)
1	Support Vector Machine	90.292	0.856	0.4120	0.1213	0.042	0.414	0.529	18.22
2	LogitBoost Decision Stumps	89.240	0.814	0.2791	0.1236	0.036	0.264	0.451	31.65
3	AdaBoost Decision Stumps	89.708	0.815	0.2340	0.1195	0.023	0.195	0.486	52.74
4	Random Forest	89.591	0.857	0.0303	0.1534	0.005	0.023	0.333	1.23
5	Naïve Bayes	72.515	0.766	0.2459	0.2749	0.280	0.770	0.238	0.33
6	Quadratic Discriminant Analysis	76.018	-	-	-	0.243	0.818	0.150	3.56

Table 6.8 Ranking of classifier performance in predicting storability of kiwifruit at 125 days after coolstorage using 10-fold cross-validation.

Rank	Name of Classifier	Evaluation Parameter (Range)							
		Overall Accuracy (0 – 100%)	ROC AUC (0 – 1)	Kappa (0 – 1)	Mean Absolute Error (> 0)	False Negative (0 – 1)	Recall (0 – 1)	Precision (0 – 1)	Training Time (s)
1	LogitBoost Decision Stumps	70.149	0.733	0.3389	0.3290	0.206	0.537	0.596	10.94
2	Support Vector Machine	69.697	0.720	0.2966	0.3561	0.215	0.504	0.570	6.29
3	AdaBoost Decision Stumps	67.463	0.727	0.2781	0.3385	0.224	0.496	0.556	19.16
4	Random Forest	66.866	0.702	0.2127	0.4010	0.145	0.339	0.569	0.92
5	Quadratic Discriminant Analysis	52.439	-	-	-	0.154	0.625	0.233	5.20
6	Naïve Bayes	49.254	0.562	0.0872	0.5056	0.664	0.769	0.396	0.13

Table 6.9 Ranking of classifier performance in predicting storability of kiwifruit at 150 days after coolstorage using 10-fold cross-validation.

Rank	Name of Classifier	Evaluation Parameter (Range)							
		Overall Accuracy (0 – 100%)	ROC AUC (0 – 1)	Kappa (0 – 1)	Mean Absolute Error (> 0)	False Negative (0 – 1)	Recall (0 – 1)	Precision (0 – 1)	Training Time (s)
1	LogitBoost Decision Stumps	83.833	0.859	0.4431	0.2268	0.041	0.414	0.743	21.01
2	Support Vector Machine	82.500	0.840	0.4563	0.1940	0.086	0.511	0.630	11.01
3	Random Forest	81.833	0.858	0.3822	0.2469	0.058	0.383	0.654	1.07
4	AdaBoost Decision Stumps	81.200	0.840	0.4151	0.2019	0.086	0.466	0.608	37.07
5	Naïve Bayes	73.833	0.794	0.2609	0.5099	0.221	0.594	0.434	0.24
6	Quadratic Discriminant Analysis	70.946	-	-	-	0.242	0.326	0.500	5.20

Previous findings on the comparison of machine learning techniques in classification models showed contradictory results. For instance, the study of Zhang and Fang (2007) found that when tested on an (external) independent data set, LogitBoost using Decision Tree as a base learner performed similarly with SVM for discrimination of proteins according to their primary structures. Cai et al. (2006) however, suggested LogitBoost DS outperformed SVM in predicting the structural classes of protein. Contradictory results have also been found between the two boosting algorithms. While Dehzangi et al. (2011) found that AdaBoost performed better than LogitBoost, McDonald et al. (2003) and Ridgeway (1999) indicated that the difference in performance between the two was limited. Yet Krishnaraj and Reddy (2008) showed that better results were obtained using LogitBoost for the prediction of protein fold recognition using decision stumps as a weak learner on Weka. In addition, the performance of different classifiers varies with experimental conditions. Khorshid et al. (2015) demonstrated that the performance of SVM as opposed to the other classifiers (such as AdaBoost, LogitBoost, Naïve Bayes and Random Forest) varied across three experiments.

The No Free Lunch Theorem (Wolpert and Macready, 1997) suggests that "any two optimisation algorithms are equivalent when their performance is averaged across all possible problems". This was also true for this study. There is no single classifier that had the best performance under all circumstances. Predictive performance amongst the classifiers varied at different storage times, and was depended on the parameters selected for evaluation (Tables 6.6 – 6.9). For instance, LogitBoost and SVM performed poorly in some cases (low recalls at 75 and 100 days) but classifiers with low overall performances predicted well in a few occasions (e.g. QDA and Naïve Bayes had higher recalls at 75 and 100 days; Tables 6.6 – 6.7). Therefore it is more sensible to say that there is no absolute best learning algorithm. The choice of the most suitable classifier is dependent on the nature of the data set and the criteria for discriminant analysis. In this case LogitBoost and SVM were the better classifiers because they performed well in cases that are more critical for the purposes of this study.

Nonetheless, the observed differences in performances amongst classifiers have been addressed and explained in many previous studies. Dettling and Bühlmann (2003) suggested that the lower error rates obtained with LogitBoost were because, unlike

AdaBoost which uses an exponential function, LogitBoost uses the binomial log likelihood, which increases linearly rather than exponentially for strong negative margins. As such LogitBoost usually performs better on noisy data or mislabelled samples. This is important for the current study as the variation in firmness measurements by penetrometer could result in a large margin of error for sample grouping and hence, resulting in misclassification of fruit (Fig. 6.2). Caruana and Niculescu-Mizil (2006) suggested that SVM had high error because the measurement of error interprets predictions as posterior probabilities but SVM is not designed to predict probabilities; the output of an SVM are just normalised distances to the decision boundary. Similarly, Naïve Bayes had much higher error than the others because NB models predict calibrated probabilities poorly due to the unrealistic independence assumption ("Naïve Bayes assumption"). In addition, Wu et al. (2010) suggested that LogitBoost DS was more capable of handling mixed data because, unlike SVM which relies on the Euclidean distance between two data points, the decision split at each stump branch does not rely on any particular distance measure between any pair of data points. Hence it should be more robust to outliers in both input and feature spaces.

Amongst all the classifiers, only SVM and LogitBoost DS were capable of prediction of soft fruit at both 125 and 150 days in external validation (Table 6.5), with LogitBosot performing slightly better at 125 and 150 days. Identifying long storing fruit is important for making inventory decisions because firmness decreases rapidly for all the fruit from ~80 N to 15 N during the first 70 days of storage (Beever and Hopkirk, 1990). During this period the proportion of soft fruit is very low and majority of the fruit would have already been shipped. Afterwards fruit continue to soften slowly during 100 – 175 days of storage and the average firmness will be approaching and eventually go below 9.8 N or 1 kg_f (Beever and Hopkirk, 1990; Jabbar, 2014), causing soft fruit to become prominent and problematic. As a result the proportion of soft fruit in the remaining batch would be significantly consequential. The ability to predict and segregate fruit with storability beyond 100 days would not only enable the reduction of direct fruit loss resulted from short-storing fruit becoming unacceptable for export, but also enable the separation of long-storing fruit from an ethylene environment produced by short-storing fruit during softening (Samarakoon, 2013), preventing secondary fruit loss (Jabbar and East, 2016). In addition, LogitBoost DS was considered superior to SVM because of the lower FN rates at all storage times (Tables 6.6 – 6.9), i.e. less soft

fruit were classified as good fruit and hence, less fruit loss in storage should the predicted good fruit population be kept for later shipment in the season. As such LogitBoost DS would be more suitable to be used to segregate potential soft fruit from the entire batch.

Computational cost is also an important consideration. AdaBoost was found to have a substantial speed advantage as compared to SVM as reported in Bartlett et al. (2004) where LOOCV was used. Krishnaraj and Reddy (2008) also suggested that AdaBoost and LogitBoost DS with 100 iterations were less expensive than SVM (with SMO) when 10-fold cross-validation was used. However our study showed contradictory results. With 100 iterations boosted algorithms were not as fast compared to SVM using sequential minimal optimisation (Tables 6.6 – 6.9). In many of the previous studies the parameters for SVM prediction (e.g. C and γ values) were optimised and this might have increased its computational cost. Only default values for the parameters of SVM were used in the present study. This might explain why SVM was more cost effective compared to boosting algorithms.

The ranking of the classifiers carried information specific for the data set used in this study. However, it is important to note that when Garrett's Ranking Technique was applied, equal importance was assigned to all the performance metrics. The best classifier(s) were chosen based on the assumption that all the metrics considered for evaluation contributed equally for final model performance. It is important to bear in mind that the rankings could be modified by assigning different weightings to the selected metrics, should such requirements be needed for a particular case.

6.3.4 Further improvement through data balancing

Data balancing using the SMOTE filter seemed to improve classification accuracy during model calibration, especially for soft fruit (Table 6.10). Predictive accuracy of good fruit was similar to that using the original data (Table 6.4). The improvement in performance was more prominent at 75 and 100 days as compared to at 150 days (where original data was more balanced; Tables 6.4 and 6.10). The overall outcomes predicted by LogitBoost DS were slightly better (higher TP and TN rates) in comparison to those by SVM (Table 6.10). The ROC curves shifted to the upper left direction for both SVM and LogitBoost DS (Fig. 6.5 – 6.6), with higher AUC values

obtained using the balanced data (p = 0.023). There were no difference in AUC values between the two classifiers (p = 0.347). Before data balancing the FN rate was approximately 20 – 40% for a targeted 75% TN rate. After data balancing the FP rates reduced to less than 20% for achieving the same level of TP rates.

Despite the promising results from model calibration, it is quite obvious that data balancing using SMOTE filter also led to over fitting, as evidenced by the poor accuracy obtained in external validation (Table 6.10). Segregation of soft fruit was not improved at 75 and 100 days (0%). Predictive accuracy of soft fruit at 150 days was improved with SVM but was reduced for LogitBoost DS compared to those using original data (Table 6.5 and 6.10). Predictive accuracy of good fruit reduced considerably with SVM but improved slightly with LogitBoost DS (Table 6.10). Overall the performance in predicting independent sample was similar between the original and balanced data.

Table 6.10 Calibration and validation of classification models to predict kiwifruit storage potential based on balanced Vis-NIR spectra data using Support Vector Machines and LogitBoost decision stumps (data balancing was not applied at 125 days).

Storage time (day)	n	Calibration Accuracy (%)				Validation Accuracy (%)			
		Support Vector Machine		LogitBoost Decision Stumps		Support Vector Machine		LogitBoost Decision Stumps	
		Soft	Good	Soft	Good	Soft	Good	Soft	Good
75	440	88	91	95	92	0	100	0	100
100	1116	73	88	78	89	0	100	0	100
150	733	71	86	66	89	91	9	41	67

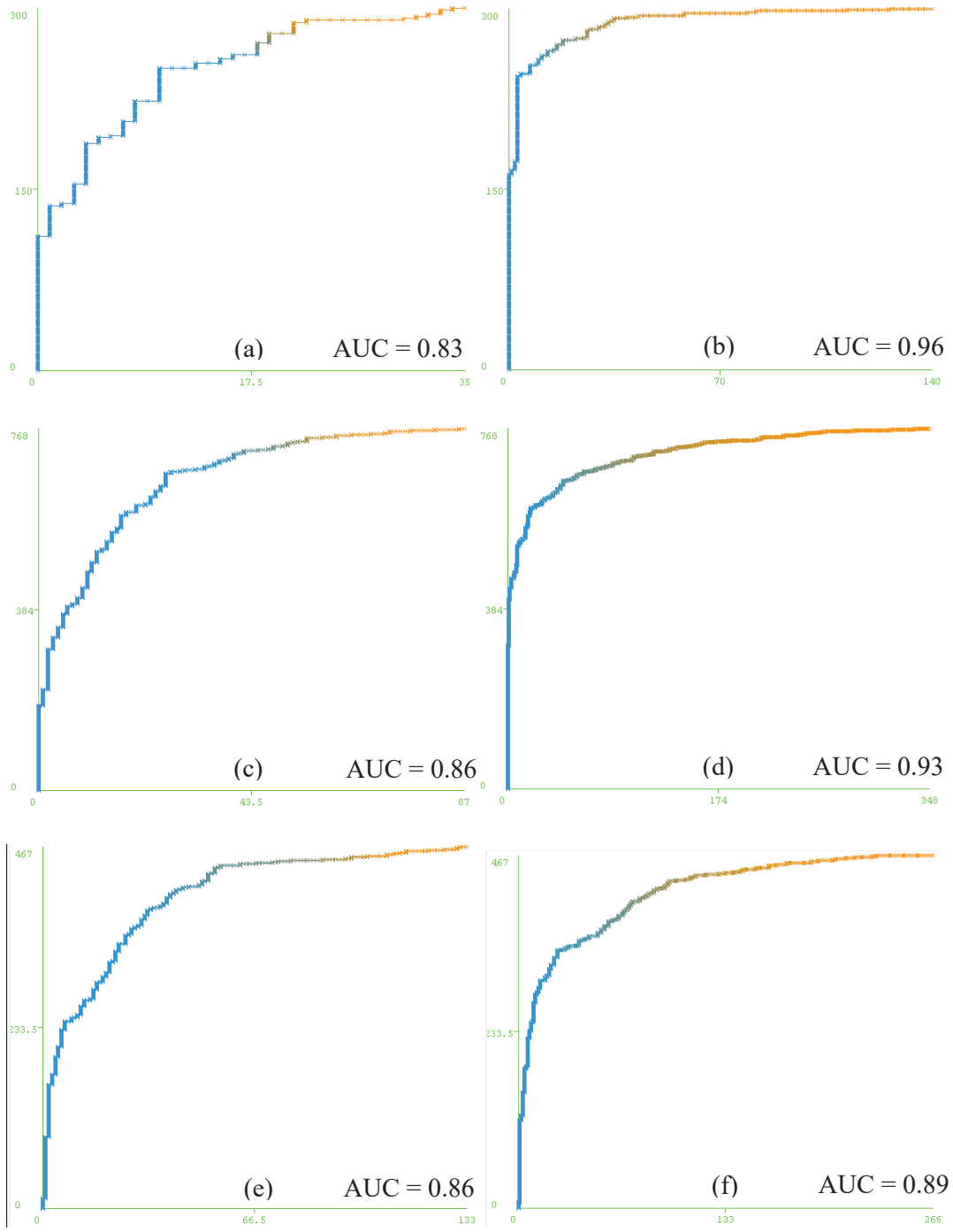

Figure 6.5 ROC curves of models developed at 75 (a – b), 100 (c – d) and 150 days (e – f) using SVM classification based on original (a, c, e) and balanced (b, d, f) data.

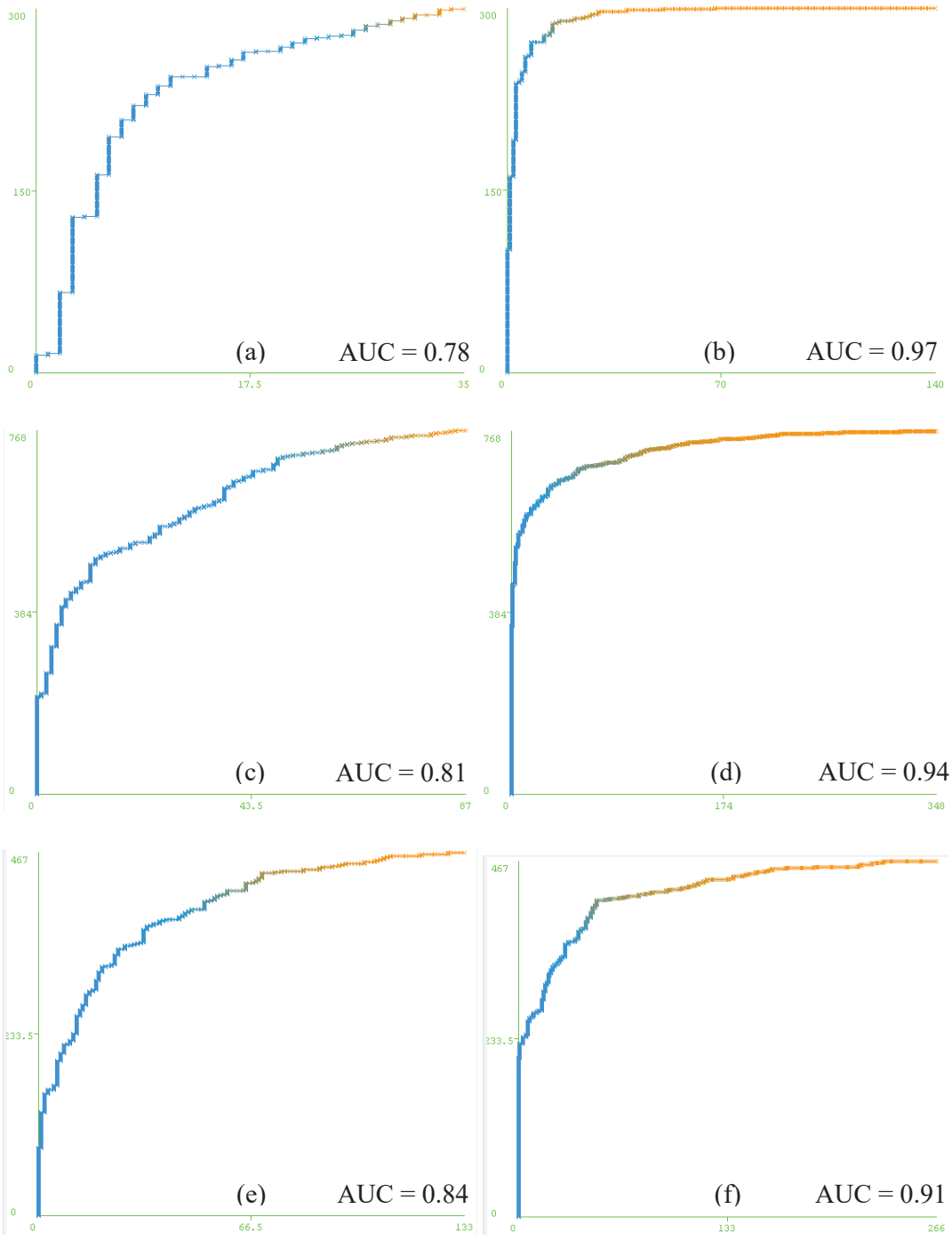

Figure 6.6 ROC curves of models developed at 75 (a – b), 100 (c – d) and 150 days (e – f) using LogitBoost DS classification based on original (a, c, e) and balanced (b, d, f) data.

Yen and Lee (2009) suggested that the SMOTE algorithm had disadvantages such as over generalisation of the minority class since it did not concern the majority class when generating the synthetic examples for the minority class. As a consequence this increases the occurrence of overlapping between classes (López et al., 2013) and results in difficulty for discrimination. Elrahman and Abraham (2013) also suggested that the SMOTE filter stopped functioning well when the number of samples in the minority class was not adequate for estimating the accurate probability distribution for the actual data. This is likely to be the case for this study (only 6% and 2% soft fruit at 75 and 100 days, respectively in validation; Table 6.1).

For the purpose of this study, the use of this filter was not justified since it did not contribute to any improvement in performance during model validation while additional computational cost was introduced as there were more samples to process. Some studies recommended under-sampling using data cleaning techniques as an alternative method. For instance, Wilson (1972) used edited nearest neighbour rule to remove samples that differ from two of its three nearest neighbours. An SVM method could also be used to discard redundant or irrelevant majority class samples (López et al., 2013). However, under-sampling also has a great disadvantage: some of the important information might be lost from the majority class (Dubey et al., 2014). Hence it may not be suitable for the current study as a wide range of variability is required to represent characteristics of fruit from various sources, and removing some of the samples could potentially remove some of the desirable variation. Ramentol et al. (2012) recommended a hybrid method which uses both under- and over-sampling by eliminating some of the minority class samples expanded by the oversampling method to reduce over-fitting. Since this method does not eliminate samples from the majority class, it could be considered for future improvement of the models.

6.3.5 Multiclass classification

In multiclass classification, the calibration model suggests that the segregation of Real Soft fruit (≤ 7.4 N) from the entire population was possible at 75 and 100 days with SVM but was unsuccessful with LogitBoost DS (Table 6.11). The overall predictive accuracy of SVM was considered better than that of LogitBoost because of the better prediction of Real Soft fruit. Predictions of Real Good fruit (≥ 12.3 N) were acceptable (~ 80%) at 75, 100 and 150 days but were poor (< 50%) at 125 days for both

classifiers. Predictions of Unsure fruit (7.4 – 12.3 N) were better at 125 days (71%) but were relatively poor (< 52%) at other storage times. Compared to binary-class models (Table 6.4), for SVM the predictive performance of (real) soft fruit was better at 75 and 125 days but was poorer at 100 and 150 days; prediction of (real) good fruit was not as good at all times. For LogitBoost DS the predictive accuracy of (real) soft and (real) good fruit was not as good at all storage times.

Table 6.11 Calibration of multiple-class classification models to predict kiwifruit storage potential based on at-harvest Vis-NIR spectra data (original) using Support Vector Machines and LogitBoost decision stumps

Storage time (day)	Classification Accuracy (%)					
	Support Vector Machine			LogitBoost Decision Stumps		
	Real Soft	Unsure	Real Good	Real Soft	Unsure	Real Good
75	50	46	81	0	39	83
100	17	43	87	0	52	84
125	75	71	46	25	71	48
150	33	40	79	26	47	78

In external validation (Table 6.12), predictive accuracy at 75 and 100 days was good for prediction of Real Good fruit but was poor for Unsure fruit. There was no Real Soft fruit in the validation data set at 75 or 100 days (i.e. FF > 7.4 N for all fruit). This suggests that the fruit that were previously grouped as 'soft' could have actually been good (as illustrated in Fig.6.2b). This most probably contributed to the difficulties in classification of (real) soft fruit in binary-classification and further explained the poor performance of validation observed in Table 6.5. For this reason segregation of soft fruit at storage times less than 100 days might be more challenging compared to that at 125 and 150 days. At 125 days for both classifiers predictive accuracy was good for Real Good fruit and was poor for Unsure fruit; SVM achieved good prediction for Real Soft class whereas LogitBoost DS was unable to segregate Real Soft fruit. At 150 days both classifiers performed similarly; prediction accuracy was good for Real Soft fruit but was poor for Unsure and Real Good fruit.

Table 6.12 Validation of multiple-class classification models to predict kiwifruit storage potential based on at-harvest Vis-NIR spectra data (original) using SVM and LogitBoost DS.

Storage time (day)	Accuracy of Classification (%)					
	Support Vector Machine			LogitBoost Decision Stumps		
	Real Soft	Unsure	Real Good	Real Soft	Unsure	Real Good
75	-	0	90	-	0	100
100	-	0	100	-	5	93
125	73	0	63	0	4	98
150	60	39	9	60	42	8

Compared to binary-class models (Table 6.5), for SVM the predictive performance of (real) soft fruit was better at 125 days but not as good at 150 days; prediction of (real) good was not as good. For LogitBoost DS the predictive performance of (real) soft fruit was not as good compared to binary-class models; prediction of (real) good fruit was better at 125 days but poorer at 150 days.

Previous studies found contrary results on the performance of SVM and LogitBoost directly applied for multiclass classification. Kim et al. (2015) compared the performance of four-class classification models to predict places of origin of animal-related food products using k-nearest-neighbour, LogitBoost and SVM with SMO, and found that LogitBoost gave better predictive accuracy than the other classifiers in most situations. Aires et al. (2004) on the other hand, found that SVM with SMO achieved better results than the others including LogitBoost for classification of web texts according to users' need. In our study SVM seemed to have outperformed LogitBoost during both calibration and validation, especially for the prediction of Real Soft fruit (Table 6.11 – 6.12). The result suggests that SVM may be more suitable for multiclass segregation of real soft fruit using the data set generated for the current study. However significant improvement of predictive performance of Unsure and Real Good fruit is required in order to justify the proposed multiclass approach.

6.4 Final Model

Considering the predictive performance in both calibration and external validation, it seems that the best approach for developing a suitable classification model for this study is to use original spectral data to segregate fruit into two groups based on the export firmness criterion using boosted decision stumps.

The final model adapts the LogitBoost ensemble algorithm in which the base learner, single decision tree with one root node (a decision stump), is boosted through an adjustment process which involves weighting and re-sampling in order to develop a strong final learner. The assumption is that although the model developed by a weak learner such as single layer decision stump may be prone to high bias and prediction error, this error can be reduced through iterations of a series of such models (decision stumps) and the assembled accuracy will be greater than a single classifier.

Figure 6.7 illustrates the process to develop the final model. The input variables x are a set of fruit spectral data which are defined over a range of attributes, i.e. reflectance over a range of wavelengths. The outcomes are labelled class signs y (+ or – for soft or good) for the input variables. Before the training begins, each input sample x_i is assigned an equal weight w_0 and the initial probability p_0 of y = +1 (i.e. soft) is 0.5. $F(x)$ and $f_m(x)$ are both predictor functions of the input variables whereas$[F(x)]$ is the class sign. The initial function $F_0(x)$ is 0. At each iteration m, the decision stump evaluates all possible splitting thresholds for each attribute of a sample, selects the one attribute a_m with the maximum information gain, and then generates an output y_i^* based on the threshold value. After the first iteration the weights w_i are estimated using $p(x)$ in the previous iteration. A dummy output response z_i, which reflects the error from the previous iteration, is also computed. A new model is trained in the next iteration by fitting the function $f_m(x)$ with a weighted least-square regression of z_i and w_i. The new probability $p(x)$ is obtained from $F(x)$ through a logistic link function, and is maximised by minimising the squared error in the regression model $f_m(x)$. The output response $[F(x)]$ is updated after each iteration and the final $[F(x)]$ for each sample after M iteration is determined based on a majority voting scheme, i.e. the class with the most votes is selected (Fig. 6.7).

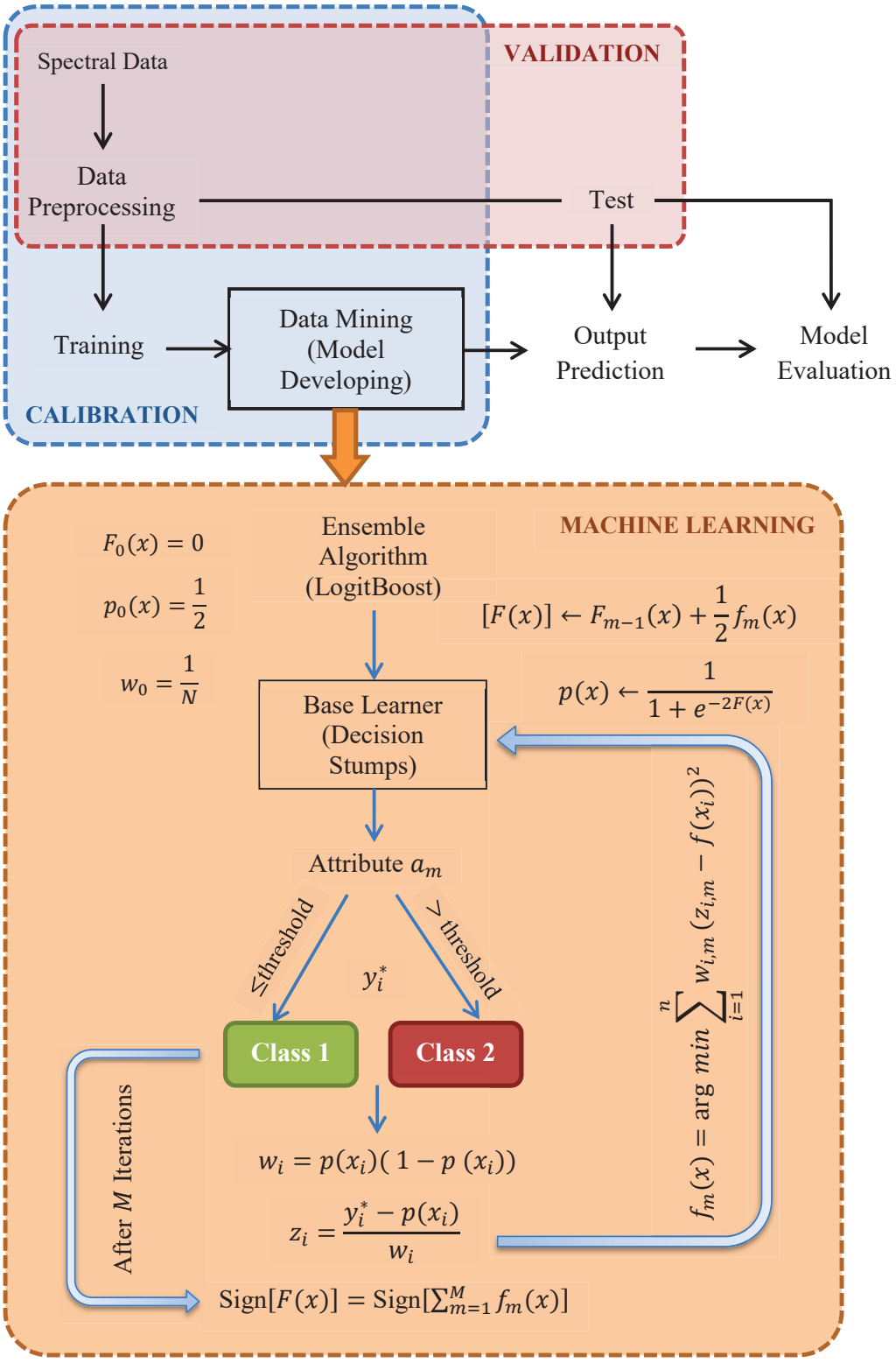

Figure 6.7 A schematic diagram showing the process of final model development, calibration and validation.

Once the model is developed the prediction outcome is presented in a confusion matrix showing true positive, true negative, false positive and false negative rates, and the predictive performance is evaluated using analytical tools such as recall, precision and ROC curves. Once model calibration is completed it can then be applied to an independent data set for validation (Fig. 6.7).

6.5 Conclusion

Segregation of kiwifruit storability based on the export firmness criterion could be achieved using Vis-NIR spectral data collected at harvest by developing a blackbox model using machine learning algorithms. In general the prediction of good fruit was better than that of soft fruit possibly due to data imbalance. Amongst the six classifiers studied, Support Vector Machines and LogitBoost Decision Stumps performed better than the other classifiers in calibration models. In external validation segregation of soft fruit was possible at 125 days and 150 days for SVM and LogitBoost DS but was only possible at 150 days for the other classifiers. The poor validation performance was likely due to a combination of low soft fruit count in the validation data set and different spectral characteristics of validation samples, which can be corrected by applying pre-processing algorithms to remove effects of external parameters.

Data balancing by oversampling using the SMOTE filter improved performance of calibration models but did not make any changes during external validation. An alternative technique which combines both under- and over-sampling may be considered for further work. Multiclass classification using directly applied algorithms to account for variations generated by physical measurements of firmness was possible using SVM and LogitBoost DS. However the overall predictive performance was not as good compared to original calibration models. Because of its better predictive power at 125 and 150 days, LogitBoost DS was selected as the most suitable classifier for final model development.

7 Segregation of 'Hayward' kiwifruit for storage potential using Vis-NIR spectroscopy – validation of classification model

7.1 Introduction

For kiwifruit growers, it is important that orchard gate returns are maximised and costs are minimised (Tanner et al., 2012). Due to packhouse rejection penalties, there are limited options for growers to save on-orchard costs. However, there is potential for segregation technology to improve orchard gate returns by improving the efficiency of packing operations and reducing postharvest cost through fruit loss (Tanner et al., 2012). The variability in fruit at the point of harvest contributes to a wide range of storage potential. Screening out kiwifruit with shorter storage life potential from the entire population could enable fruit or batches of fruit to be sold earlier in the season without affecting the remaining batch. This is important because although a large percent of the fruit would store well through the season, it is the poorest-storing fruit in a line that influences the storability of the line (Tanner et al., 2012). It would be beneficial to utilise the variability in the population and segregate fruit with different intended storability in the supply chain. There are two potential segregation systems: within grower line and between grower line. Fig. 7.1 illustrates the two systems conceptually.

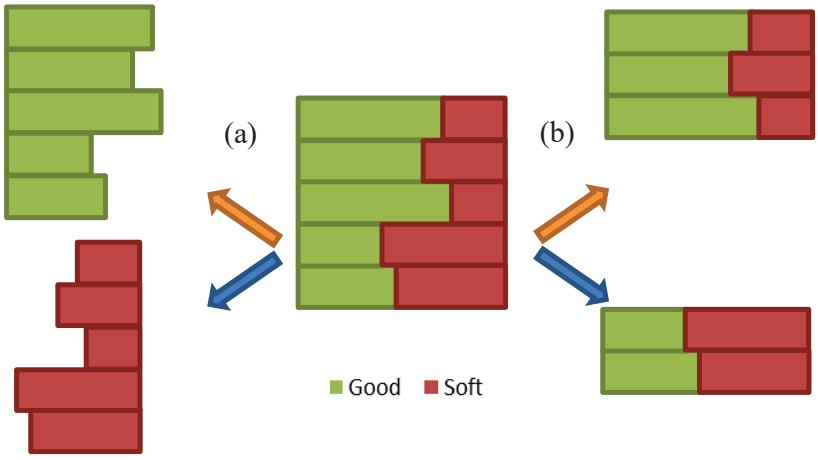

Figure 7.1 Conceptual diagram of segregation of five batches of kiwifruit (a) within grower line and (b) between grower line. Orange arrow indicates good-storing fruit/lines whereas blue arrow indicates poor-storing fruit/lines.

Within grower line segregation (Fig. 7.1a) identifies individual short-storing fruit and aims to separate these fruit from long-storing ones within the same batch. The outcome of this segregation would be two lines of fruit for each grower line with the poor-storing fruit from each line being separated and shipped earlier in the season. For between grower line segregation (Fig. 7.1b), poor-storing lines are identified as they contain a larger number of potentially short-storing fruit and hence have, on average, lower storability. Segregation would result in these grower lines being separated from the population for earlier sale. Both systems would be useful to assist with inventory decisions for sequential marketing, but would require different implementation and have different outcomes on postharvest performance and grower orchard gate return.

In 2012 and 2013, several sets of at-harvest Vis-NIR spectral and post-storage firmness data were collected from various 'Hayward' kiwifruit sources to develop a qualitative classification model which could be applied to segregate kiwifruit for their storability. An external validation showed that using LogitBoost Decision Stumps, the developed model successfully predicted storability of 40% of soft fruit (FF < 9.8 N) and 81% of good fruit (FF ≥ 9.8 N) after storage at 0ºC for 125 days (Table 6.5, Chapter 6). This result suggests there is potential for the developed model to be useful as a segregating tool when applied prior to storage. However, more work is needed to investigate the repeatability of the model in real-world cases and whether commercial applicability can be justified should the technique be applied on an industrial scale. As such a new experiment was conducted in 2015. This trial was designed to assess whether the model would be helpful in segregating, both within and between batches of fruit, by ranking storage potential prior to coolstorage. At-harvest Vis-NIR spectra was utilised together with the calibrated classification model (Chapter 6). The aim was to assess whether segregation of fruit identified as poor storing at an early stage would benefit storability of the remaining batch and hence assist with marketing and inventory management decisions and ultimately reduce fruit loss later in the season.

7.2 Materials and Methods

7.2.1 Experimental philosophy

Kiwifruit softening is known to be highly sensitive to ethylene, even in coolstorage conditions (Jabbar and East, 2016), with ethylene production of kiwifruit dramatically increasing as fruit soften (Samarakoon, 2013). Consequently, as short-storing fruit become soft, they have the potential to produce within pack an ethylene environment that softens otherwise long-storing fruit during storage, reducing overall firmness in the same tray. This 'cross-contamination' effect can be greatly reduced if short-storing fruit can be identified and separated from long-storing fruit prior to storage. This is because short-storing fruit would be closely kept next to one another. During softening, they would go through rapid softening and produce a large amount of ethylene within the same tray. Stored separately, long-storing fruit would go through normal softening in a relatively uncontaminated cooling environment with minimal interferences from soft fruit within the tray. As a result, the after storage average firmness within the tray is expected to be higher for long-storing fruit and lower for short-storing fruit as shown in Fig. 7.2. The number of soft fruit in the short-storing trays should also be higher than that in the long-storing trays.

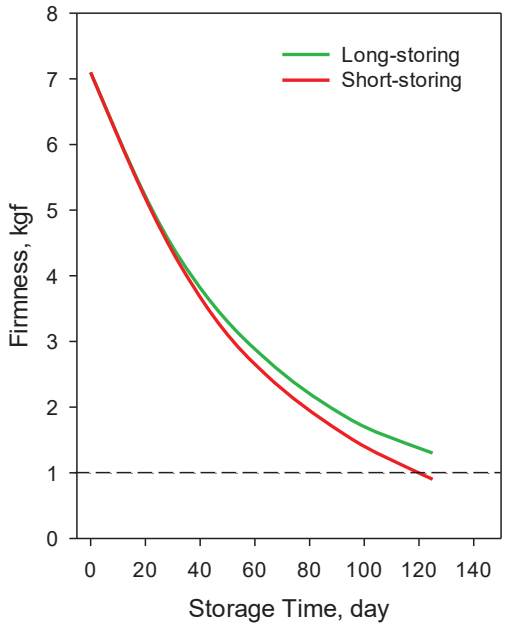

Figure 7.2 Expected softening curve of kiwifruit with segregation within batches prior to storage. Data is theoretical curves and not observed experimental results.

As a result the experiment was designed in which physical separation of fruit was performed in order to facilitate the potential benefits of the pre-softening segregation (Fig. 7.3). At-harvest Vis-NIR data was captured and analysed with the existing model (Chapter 6), and then individual fruit ranked on prediction of storability and resorted into trays based on this ranking, within each grower line. This process results in trays of fruit which are sorted by their storage potential as predicted from the Vis-NIR data, which were then stored in a coolroom, with firmness measured after long term storage. At the same time the Vis-NIR data and resulting predictions from the data enable a prediction of the between grower line storability. The remaining methodological sections provide the details of how each of these processes was achieved.

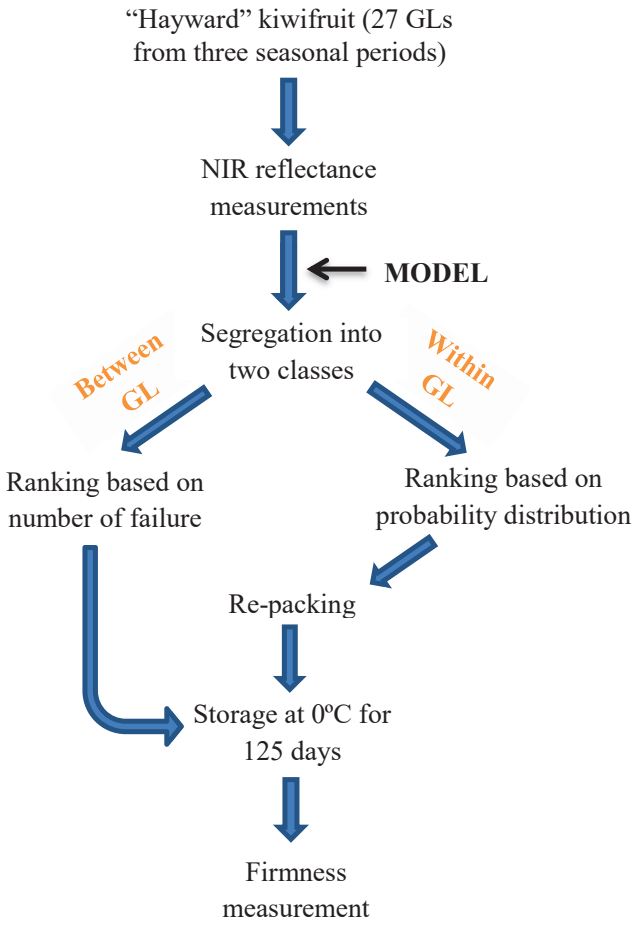

Figure 7.3 A systematic diagram of validation trial: two types of ranking was achieved based on segregation by the model: within grower line using probability distribution and between grow line using predicted number of failed fruit.

7.2.2 Pre-storage Vis-NIR measurements

'Hayward' kiwifruit form a total of 27 commercial grower lines were harvested at early, mid and late periods of the season. Fruit from each seasonal period were delivered to Massey University at two-week intervals with the first batch commencing 7 May, 2015 and the last batch arriving on 5 June, 2015. Each seasonal period consisted of nine growers arriving as 3 grower lines on three different days during the same week. Each selected grower line contained 3 trays of fruit (count 30), resulting in a total of 2430 fruit for all 27 growers. At each delivery, fruit were scanned using the ASD FieldSpec® Pro spectroradiometer in the reflectance mode (Section 5.2.5).

7.2.3 Segregation of fruit based on Vis-NIR measurements

The captured Vis-NIR spectral data was processed with each fruit being assigned a class label ('Soft' or 'Good') by the developed classification model (Chapter 6) based on their measured Vis-NIR reflectance.

For within grower line segregation, the probability of each fruit belonging to the 'Soft' class (a value between 0 and 1) was estimated in order to assist with classification and subsequent fruit organisation. If the probability of a fruit belonging to the 'Soft' class is greater than 0.5, fruit will be classified as 'Soft'; if the probability is less than 0.5, fruit will be classified as 'Good'. The probability values assigned to each fruit were then used to rank fruit in a specific order so that the fruit from the same group are more likely to be sorted next to each other, while being separated from those from the other class. An example of ranking based on probability distribution is shown in Fig. 7.4. Ninety fruit from the same batch with random probability arrived in three trays (30 fruit per tray) and were initially numbered (Fig. 7.4a). Subsequently, fruit were ranked based on their at-harvest Vis-NIR reflectance data by the model on their probability to turn soft after 125 days of storage at 0ºC. This resulted in segregation into a new set of trays where fruit were ordered according to their ranking (Fig. 7.4b). In the example provided the first 21 fruit (fruit 69 to fruit 36) in the first tray would be segregated as soft (probability > 0.5) and the last 69 fruit identified as long-storing (fruit 64 to fruit 73; probability < 0.5, Fig. 7.4b). However, the repacking method resulted in creating 3 batches of 30 fruit per tray, with the ranking by probability resulting in separation of the most likely short-storing fruit from the most likely long-storing fruit.

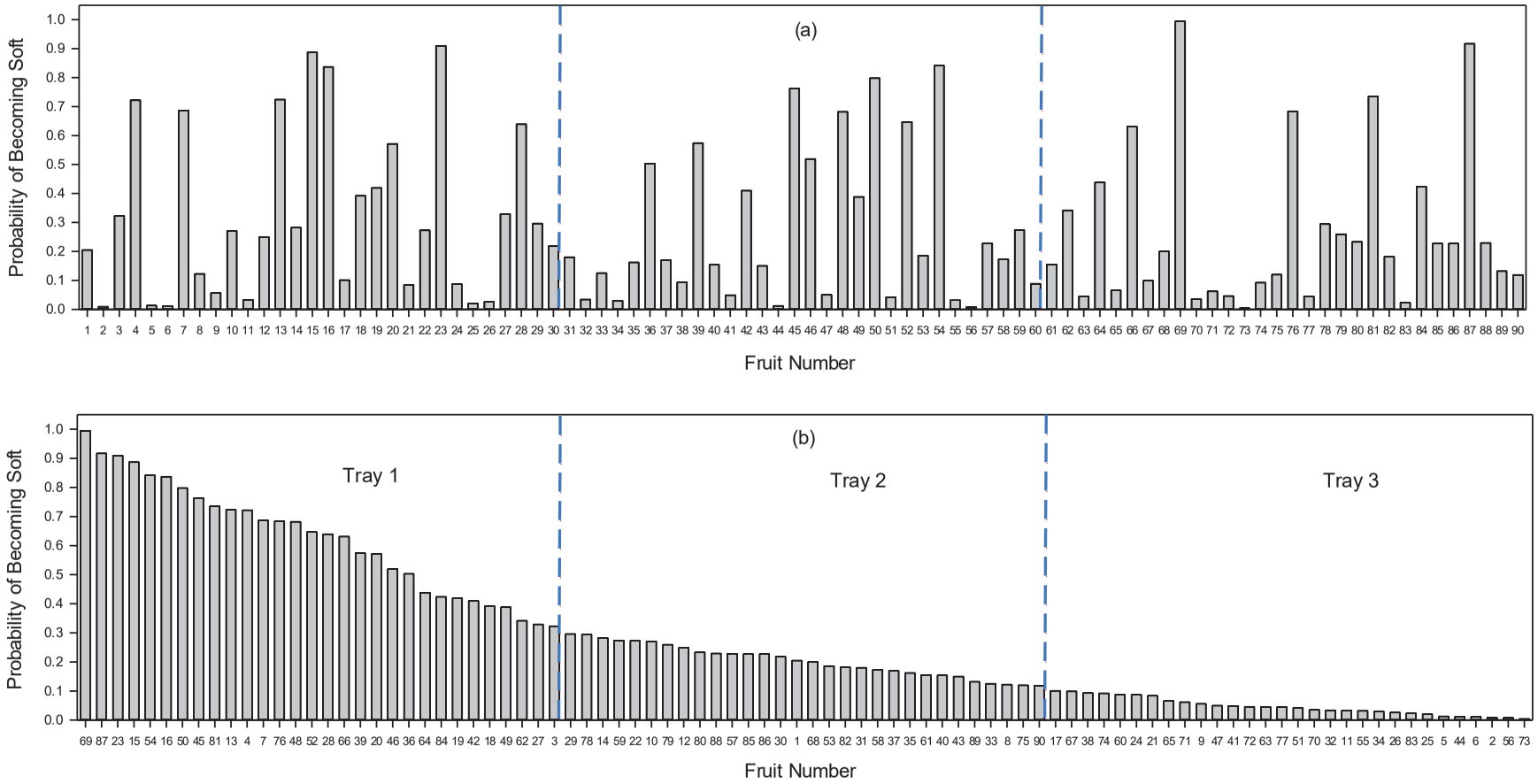

Figure 7.4 Segregation within grower line: probability of becoming soft (FF < 9.8 N) after 125 days of storage for kiwifruit packed in a set of three trays (30 fruit per tray): a) before ranking and b) after ranking.

The applied experimental method ensured an equal and maximum number of fruit in each tray. An alternative experimental method would have been to segregate fruit by the prediction of short- and long-storing fruit. However this would have resulted in creating unbalanced trays (i.e. 21 predicted soft fruit for the provided example in a 30 fruit tray). This method was avoided due to the introduced risk of influencing firmness by changing the water loss dynamics within the polylined tray that would occur with changes in product mass inside the tray. For every set of three trays the Vis-NIR measurement, ranking and repacking time was about three hours.

For between grower line segregation, the proportion of failed fruit for each grower line was predicted by the model (Fig. 7.5a). The 27 lines were then ranked based on this prediction in ascending order with the top 9 lines being the longest storing fruit (≤ 10% failure) and the remaining being 9 lines each of medium (≤ 30% failure) and short storing fruit (> 30% failure), respectively (Fig. 7.5b). However, no re-packing was required for this sorting because individual grower lines were separated by default, as a result of storing fruit in units of three trays per grower line.

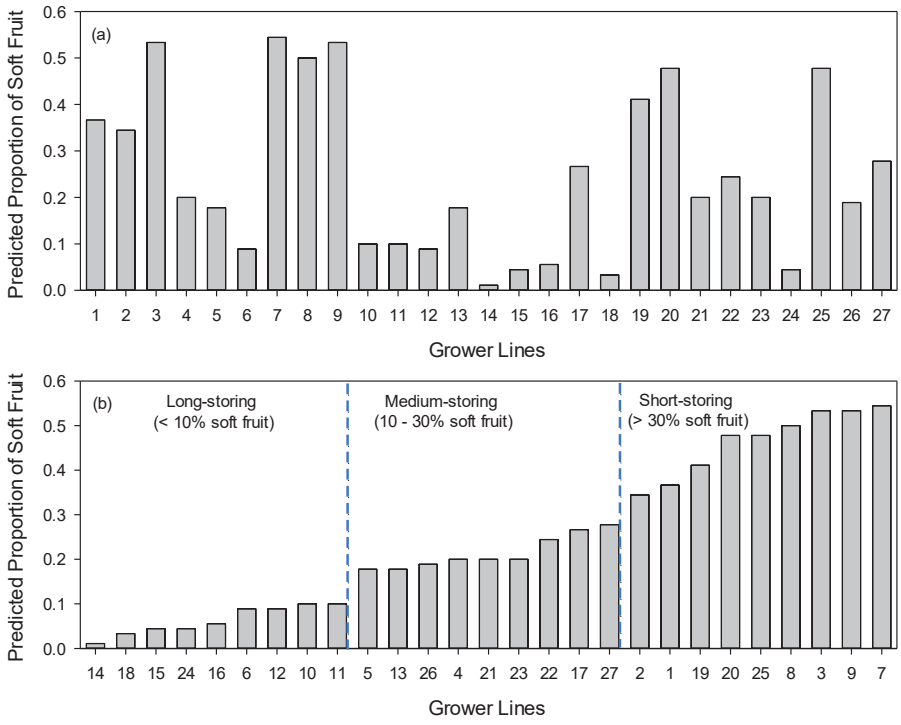

Figure 7.5 Segregation between grower line: predicted proportion of failed fruit (FF < 9.8 N) after 125 days of storage for 27 kiwifruit grower lines: a) before ranking and b) after ranking.

7.2.4 Cool storage and destructive firmness measurements

After segregation and repacking, fruit were immediately stored in a controlled cool room at 0 ºC. During storage, ethylene concentration in the cool room was monitored and maintained below 5 nL L^{-1}. After 125 days of storage, firmness measurements were performed on individual fruit using the methods described in Section 3.2.2, except that in this experiment the penetration speed for FF measurements using the electric penetrometer was changed to 8 $mm \cdot s^{-1}$ due to a change in standard industrial procedure.

7.2.5 Data analysis

The potential for within batch segregation was assessed by determining if differences in firmness were obtained between the different trays of fruit within the same grower line as a result of the sorting applied. The effect of segregation on average firmness within grower lines was analysed using the GLM in Minitab®. The number of failed fruit in different trays within grower line was also analysed using a Chi-square test in Minitab® to indicate evidence of potential benefit.

The performance of between grower line segregation was assessed by comparing the predicted and actual storage performance of different lines. The percentage of accurate prediction was estimated for each of the short, medium and long storage lines. The correlation between predicted proportion of soft fruit and measured data was established using Fitted Line Plot regression in Minitab®. Additionally, the proportions of soft fruit found in the segregated populations were compared using a Chi-square test in Minitab®.

In addition, the percentage of fruit loss with and without segregation was calculated to indicate whether segregation prior to storage has potential to reduce costs and improve profitability. For within grower line segregation, reduction was estimated on the basis that fruit stored in the short- and medium-storing trays were to be shipped earlier whereas fruit in the long-storing trays would be kept for later in the season. For between grower line segregation, reduction was based on the assumption that predicted short- and medium-storing lines were to be distributed earlier whereas long-storing lines would be shipped later in the season.

7.3 Results and Discussion

7.3.1 Within grower lines segregation

Table 7.1 shows that the average firmness amongst the three trays within the same grower line differed as a result of segregation before storage. Fruit from the first trays (highest probability of becoming soft at the end of storage) had lowest average firmness (12.56 N), whereas those from the third trays (lowest probability of becoming soft at the end of storage) had highest average firmness (14.03 N). The total number of soft fruit was highest in the first trays (30.7%), followed by the second (23.3%) and the third trays (21.2%). Chi-square analysis confirmed that the proportion of soft fruit was significantly different amongst the three trays ($p < 0.001$) as a result of ranking prior to storage. In addition, Table 7.1 shows that the effect of segregation within grower line seemed to be more pronounced in the fruit harvested during early seasonal period (especially in G1 – G6) than those in late seasonal fruit (e.g. G22 – G27). The effect also seemed to be more pronounced within growers with lower proportion of firmness failure (e.g. G1 – G6, G11, G21) but there were a few exceptions (e.g. G17).

The initial water content of the fruit is inversely proportional to the at-harvest DMC of the fruit. Famiani et al. (2012) found that higher initial DMC (hence lower water content) was associated with better firmness retention during storage. Tombesi et al. (1993) found that the higher initial water content in shaded kiwifruit resulted in high transpiration during storage, which consequentially reduced cell turgor and FF during storage. This suggests that fruit that soften more quickly during storage are more likely to have higher water content at harvest (lower initial DMC). For fruit with higher water content, the at-harvest NIR reflectance signal would be attenuated due to stronger absorption in water absorption bands, masking any significant peaks over absorption bands by other chemicals such as pectin. As a result, it is possible that some information was lost during NIR data capture which would in turn affect model prediction. This may explain the poor prediction of grower lines with higher proportion of failure, which may have higher initial water content compared to those with lower proportion of failure. However, the DMC range in the mentioned previous studies was between 13 – 16%, lower than the likely range of DMC for the fruit used in this study (usually ≈ 18% for 'Hayward'). Hence, it is also possible that the finding in these studies may not be directly relevant to the current study.

Table 7.1 Average flesh firmness (N) and number of soft fruit amongst the three trays (T1 – T3) within a grower line after storage at 0°C for 125 days as a result of pre-storage within grower line segregation.

Grower	Average firmness (N)			No. of soft fruit		
	FF T1	FF T2	FF T3	n T1	n T2	n T3
G1	13.44^{b}	14.52^{b}	17.07^{a}	4	3	0
G2	12.65^{b}	14.32^{b}	18.44^{a}	7	3	2
G3	14.32^{b}	17.66^{a}	19.72^{a}	2	0	0
G4	14.52^{b}	16.97^{ab}	19.03^{a}	1	0	1
G5	15.60^{b}	17.85^{ab}	19.52^{a}	3	0	1
G6	14.52^{b}	17.56^{a}	18.64^{a}	1	0	1
G7	13.34^{a}	13.93^{a}	14.13^{a}	9	5	6
G8	8.24^{a}	9.81^{a}	8.83^{a}	22	19	17
G9	14.81^{a}	13.83^{a}	15.50^{a}	2	4	3
G10	11.87^{a}	11.97^{a}	12.75^{a}	6	5	6
G11	15.70^{b}	17.27^{ab}	18.15^{a}	2	0	0
G12	12.95^{a}	14.42^{a}	15.50^{a}	8	3	6
G13	12.75^{a}	13.15^{a}	14.03^{a}	5	1	3
G14	18.44^{a}	19.91^{a}	18.74^{a}	2	0	0
G15	10.59^{a}	10.79^{a}	10.20^{a}	13	10	11
G16	15.50^{a}	17.46^{a}	17.56^{a}	3	0	0
G17	10.20^{b}	10.69^{b}	14.42^{a}	14	12	4
G18	11.18^{a}	12.26^{a}	10.99^{a}	10	8	12
G19	9.61^{a}	10.59^{a}	10.01^{a}	15	13	14
G20	9.22^{a}	9.81^{a}	9.81^{a}	17	14	13
G21	12.46^{ab}	11.38^{b}	13.15^{a}	2	6	2
G22	10.69^{a}	10.40^{a}	11.28^{a}	10	8	5
G23	9.03^{a}	9.52^{a}	9.71^{a}	25	17	18
G24	9.81^{a}	10.40^{a}	10.79^{a}	14	11	9
G25	9.81^{a}	10.10^{a}	10.40^{a}	17	13	10
G26	10.30^{a}	11.48^{a}	11.28^{a}	12	8	6
G27	7.06^{a}	6.77^{a}	8.14^{a}	23	26	22
Total	12.56^{c}	13.15^{b}	14.03^{a}	249	189	172

Softening of kiwifruit occurs in two or three phases depending on the maturity at harvest (Section. 2.1.3.3). Kiwifruit that are harvested late in the season only go through the second and third stages; there is no lag phase during softening. In addition, Redgwell and Percy (1992) found that little pectin solubilisation was observed during the softening of kiwifruit from about 81 N to 56 N (during the lag phase), whereas pectin became more soluble as fruit continued to soften below 56 N (the second and third phases). It is possible that the near skin characteristics exhibited in kiwifruit, specifically, the amount of pectin that is solubilised during the lag phase played a more important role or provided more comprehensive information for model prediction. As a result, segregation within grower line was more successful in those lines harvested during early seasonal period.

Statistically significant differences amongst trays suggest that prediction based on segregation was not simply a result of random variability. The model was able to identify a proportion of the actual short-storing fruit from the population. Repacking ensured that short-storing fruit were separated from the better storing ones and hence the production of ethylene as fruit soften would have minimal effect on long-storing fruit. As a result, these long-storing fruit go through natural softening without interference of soft fruit.

7.3.2 Between grower line segregation

The model predicted that the majority of the grower lines harvested during early seasonal period (G1 – G9) would have medium or short storability; these lines would likely to have 17.8 – 54.4% (16 – 49 fruit) of the population turning soft. However, G6 was predicted to be an exception: only 8.9% (8 fruit) would be turning soft at the end of storage (Table 7.2; Fig. 7.6). The late harvested fruit (G19 – G27) were predicted to perform similar to those harvested during early seasonal period, with most lines having medium or short storability (18.9 – 47.8% failure; 17 – 43 soft fruit) except for G24 being long-storing (4.4% failure; 4 soft fruit). For grower lines harvested during mid seasonal period (G10 – G18), the model predicted that most lines were to have long storage with 3.3 – 10% failure (3 – 9 fruit). The remaining lines (G13 and G17) were predicted to have medium storage with 17.8% (16 fruit) and 26.7% (24 fruit) failures, respectively (Table 7.2; Fig. 7.6). The predicted number of soft fruit was lowest for mid seasonal fruit but was higher in both early and late seasonal fruit (Table 7.2).

Table 7.2 Proportion of soft fruit and ranking between grower lines as predicted by classification model and measured after storage at 0°C for 125 days.

Grower	Predicted Soft	Predicted Soft Proportion	Measured Soft	Measured Soft Proportion	Rank Predicted	Rank Measured
1	33	36.7%	7	7.8%	20	8
2	31	34.4%	12	13.3%	19	12
3	48	53.3%	2	2.2%	25	1
4	18	20.0%	2	2.2%	13	1
5	16	17.8%	4	4.4%	10	7
6	8	8.9%	2	2.2%	6	1
7	49	54.4%	20	22.2%	27	15
8	45	50.0%	58	64.4%	24	25
9	48	53.3%	9	10.0%	25	9
10	9	10.0%	17	18.9%	8	13
11	9	10.0%	2	2.2%	8	1
12	8	8.9%	17	18.9%	6	13
13	16	17.8%	9	10.0%	10	9
14	1	1.1%	2	2.2%	1	1
15	4	4.4%	34	37.8%	3	20
16	5	5.6%	3	3.3%	5	6
17	24	26.7%	30	33.3%	17	18
18	3	3.3%	30	33.3%	2	18
19	37	41.1%	42	46.7%	21	23
20	43	47.8%	44	48.9%	22	24
21	18	20.0%	10	11.1%	13	11
22	22	24.4%	23	25.6%	16	16
23	18	20.0%	60	66.7%	13	26
24	4	4.4%	34	37.8%	3	20
25	43	47.8%	40	44.4%	22	22
26	17	18.9%	26	28.9%	12	17
27	25	27.8%	71	78.9%	18	27
Total	602		610			

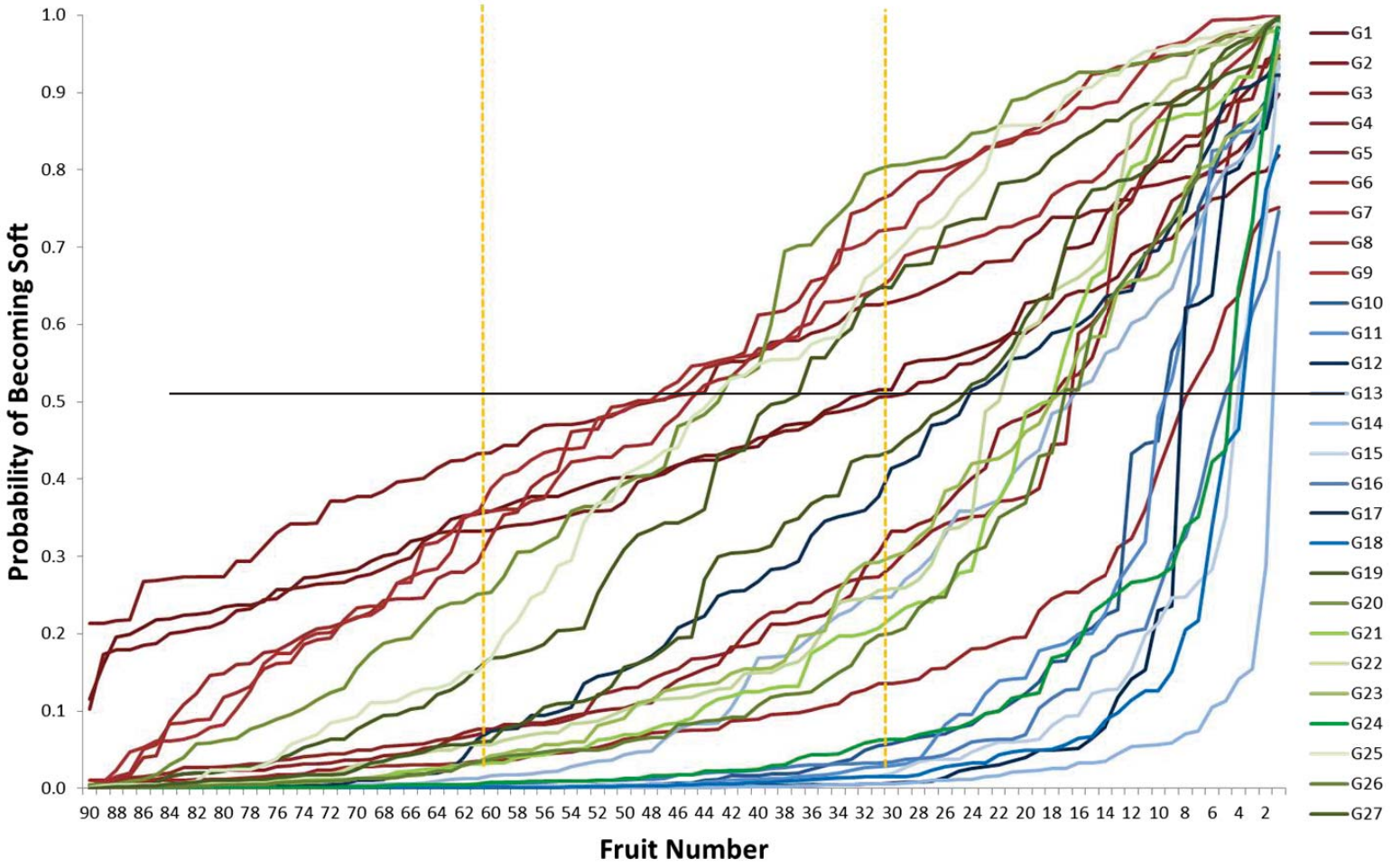

Figure 7.6 Probability distribution of kiwifruit predicted by the classification model developed using Vis-NIR spectral data collected at harvest and flesh firmness data measured after storage.

Post-storage firmness measurements showed that there was a large variation in storage potential between grower lines (Table 7.1). In general, fruit harvested during early and mid-seasonal periods (G1 – G18) had lower proportion of soft fruit and higher average firmness after 125 days of storage compared to those harvested during late seasonal period (G19 – G27). The number of actual soft fruit also generally increased from early to late seasonal periods (Tables 7.1 and 7.2). Most early harvested lines had long to medium storability (2.2 – 22.2% failure; 2 – 20 soft fruit) except for G8 which had 58 soft fruit (64.4% failure). Similarly, most of the mid harvested lines had long to medium storability (2.2 – 18.9% failure; 2 – 17 soft fruit) except for G15, G17 and G18 (37.8%, 33.3% and 33.3% soft fruit, respectively). Although the predicted and the measured number of soft fruit was somewhat similar (602 and 610, respectively), the model overestimated the number of soft fruit in early harvested lines, but underestimated the proportion of failure in the mid harvested lines.

Table 7.3 displays the classification accuracy for segregation between grower lines for storability. For each of the short, medium and long storage group, 4 out of 9 lines were classified accurately, whilst the remaining 5 lines were classified incorrectly. The percentage of actual short, medium and long storage lines in the predicted short, medium and long storage lines was 44.4% each, compared to 37.0%, 29.6% and 33.3% respectively by chance (Table 7.3). The overall accuracy (44.4%) is not as good compared to the 52.8% accuracy achieved by Feng (2003) for the segregation of 36 grower lines using CDA based on several at-harvest attributes including solublised DMC, harvest date, fruit lightness and mineral content. This is probably because in Feng's study, results were obtained from internal validation data set and hence were not subjected to errors as a result of unknown variability from an independent new data set.

The prediction in this study seemed to have equal performance for each of the three designated classes, in contrast to the poorer prediction of medium storage lines (33.3 – 46.7%) than the short or long storage lines (60.0 – 80.0%) as observed by Feng (2003). The average FF for the predicted long, medium and short storage groups was 14.29 N, 12.27 N and 12.74 N respectively, compared to 16.65 N, 12.85 N and 9.79 N respectively for the actual groups (Table 7.3). Both predicted and actual long-storing groups had the highest average FF. However, the lowest FF was found in the medium-storing group based on prediction.

Table 7.3 Classification accuracy based on segregation into three groups: short (≥ 30% soft fruit), medium (10 – 30% soft fruit) and long (< 10% soft fruit) storability between 27 grower lines.

Actual number	Predicted number (percentage) of grower line				Average FF (N)
	Short	Medium	Long	Total	
Short	**4 (44.4%)**	3 (33.3%)	3 (33.3%)	10 (37.0%)	9.79
Medium	2 (22.2%)	**4 (44.4%)**	2 (22.2%)	8 (29.6%)	12.86
Long	3 (33.3%)	2 (22.2%)	**4 (44.4%)**	9 (33.3%)	16.65
Total	9	9	9	27	-
Average FF (N)	12.74	12.27	14.29	-	

A fitted regression line showed that the proportion of soft fruit increased from 0 – 40% with increasing predicted proportion of soft fruit (0 – 55%; Fig. 7.7a). However, there was no significant linear correlation ($p = 0.237$) between measured and predicted proportion of soft fruit. This could be due to the poor predictions of a few grower lines resulting in outliers. Removing the three lines with > 50% predicted proportion of soft fruit (G3, G7 and G9; Table 7.2) significantly improved this correlation ($p = 0.021$).

Similarly, there was no significant linear correlation between measured average FF values and predicted soft fruit proportion ($p = 0.298$). The average post-storage firmness for each grower line reduced from 14 N to 12 N when the proportion of predicted soft fruit increased from 0 to 55% (Fig. 7.7b). The fitted linear line was improved ($p = 0.026$) after removing G3, G7 and G9 (with > 50% predicted soft fruit). However, the range of measured firmness for a specific predicted proportion of soft fruit could be as high as 9 N (Fig. 7.7b). This suggests that segregation between grower line was rather qualitative and incapable of quantitative prediction of post-storage firmness measurements.

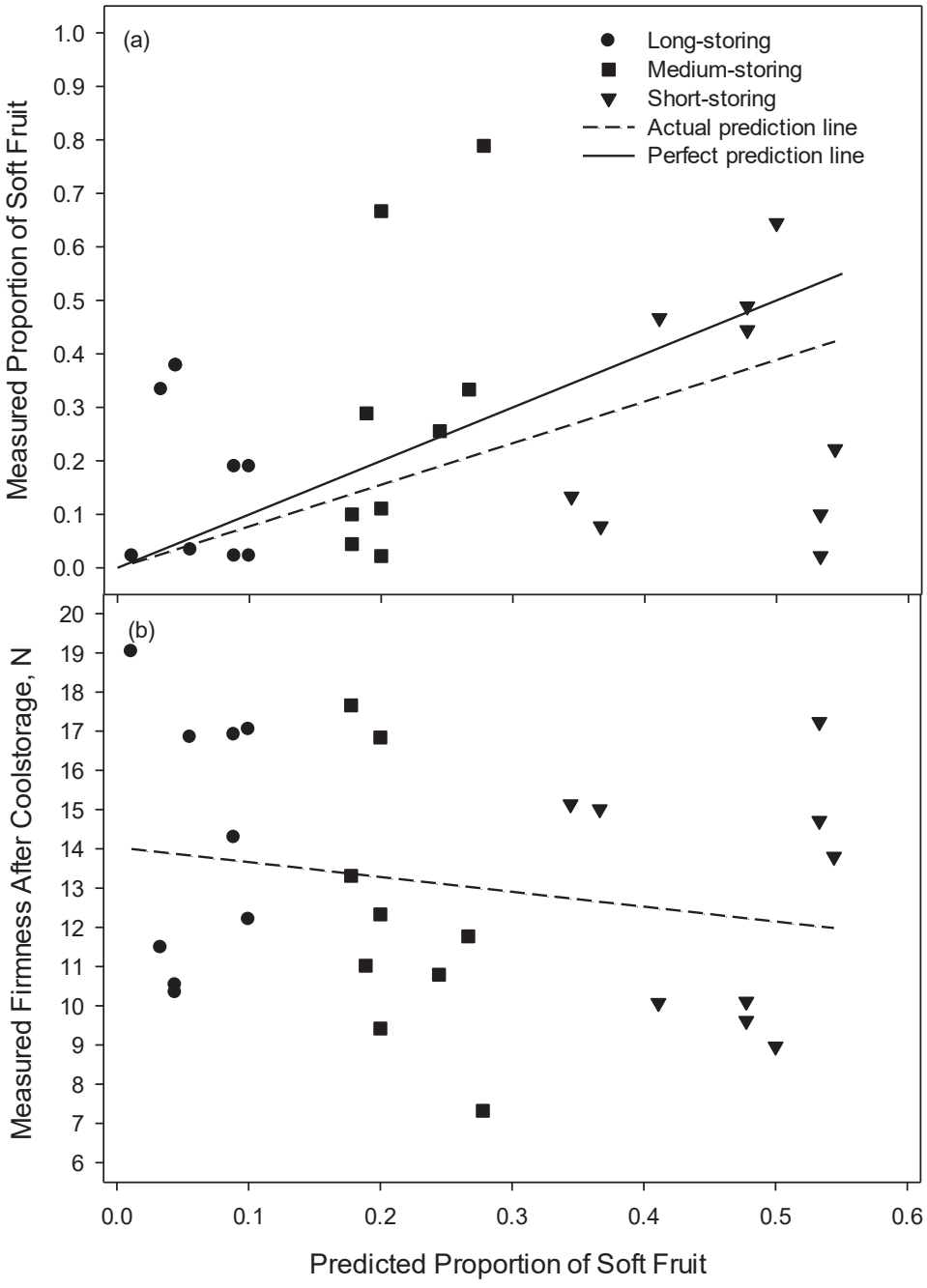

Figure 7.7 Relationship of predicted proportion of soft fruit to (a) measured proportion of soft fruit and (b) post-storage firmness measurements for 27 grower lines. Circle, square and triangle shapes represent grower lines with predicted long (9), medium (9) and short (9) storability, respectively. Solid lines are fitted linear regression lines based on all data points.

7.3.3 Soft fruit reduction

In the test data set, 25.1% (610 fruit) of the total population were soft after 125 days of coolstorage at 0°C (Table 7.4, Fig. 7.8a and Fig. 7.9a). At the time of harvest the model accurately predicted 196 out of 610 soft fruit and 1418 out of 1820 good fruit (Table 7.4). The TP and TN rates were 32.1% and 77.9% respectively, compared to 24.6% and 75.4% respectively by chance. The FN rate was 22.6% (414 out of 1832) which indicate the actual fruit loss in the predicted good batch.

Table 7.4 Confusion matrix for 2015 validation trial using developed classification model.

	Predicted		
Actual	Soft	Good	Total
Soft	196 (32.1%)	**414 (67.9%)**	610 (25.1%)
Good	402 (22.1%)	1418 (77.9%)	1820 (74.9%)
Total	598 (24.6%)	1832 (75.4%)	2430

The predictive accuracy for 'Soft' (32.1%) and 'Good' (77.9%) was slightly lower than the 40% and 81% obtained in the calibration model for 'Soft' and 'Good', respectively (Table 6.5; Chapter 6). The true positive rate (32.1%) was comparable to the 17 – 47% for kiwifruit that developed soft patches found by Feng (2003) but was lower compared to the 46 – 63% for kiwifruit that developed disorders found by Clark et al. (2004). The false positive rate (22%; 402 fruit out of 1820) was lower than the 33 – 86% for healthy fruit found by Feng (2003), but was higher than those obtained in Clark et al. (2004) for good fruit (8 – 18%).

According to Hair et al. (2006), the classification accuracy should be at least one-fourth (25%) greater than that achieved by chance, in order to justify the significance of improvement using a discriminant model. In this study, the classification accuracy for soft fruit was 32.1%. This is more than 25% greater than that achieved by chance (30.8% = 24.6% × 1.25). However, the classification accuracy for good fruit was

77.9 %, less than the 94.3% (75.4% × 1.25) required to justify a significant segregation. This suggests that in general, classification for soft fruit resulted in more significant improvement compared to that for good fruit, despite a lower % classification accuracy.

For segregation within grower lines, it was intended that segregation followed by ranking and repacking of fruit would reduce final soft fruit proportion by allowing earlier shipping of fruit stored in the first and second trays while keeping those in the third trays for later in the season. Post-storage firmness results showed that 438 out of 1620 (27.0%) early-shipment fruit (first and second trays) were soft (Fig. 7.8b), whereas 638 out of 810 (78.8%) late-shipment fruit (fruit stored in the third trays) were sound (Fig. 7.8c). Segregation resulted in two populations: early shipment with a slightly higher proportion of short-storing fruit than the whole population and late shipment with a higher proportion of long-storing fruit. The proportion of soft fruit reduced from 25.1% (shipment without segregation) to 21.2% (shipment based on segregation). Chi-square test suggests that the proportion of soft fruit was significantly different between the two segregated populations ($\chi^2 = 9.670$; $p = 0.002$).

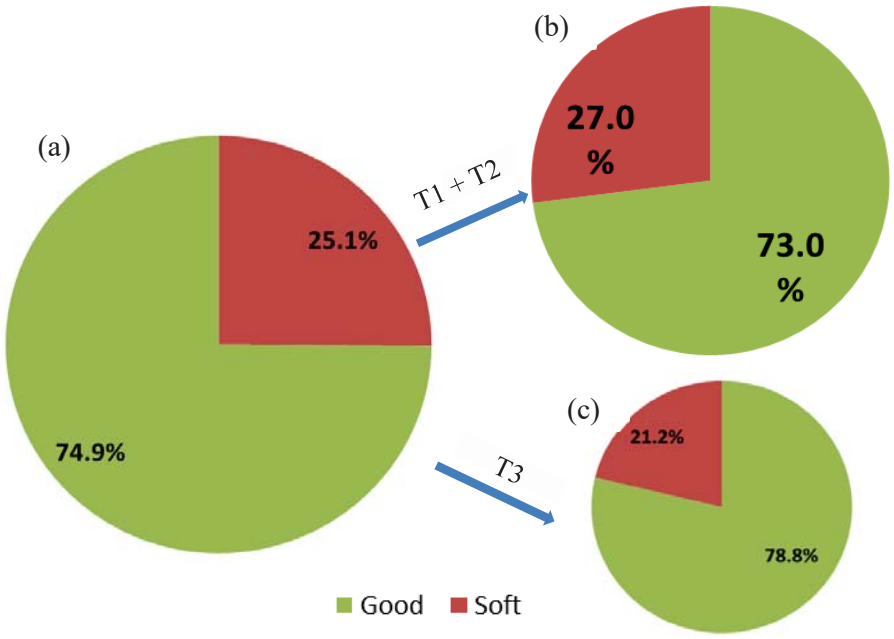

Figure 7.8 Distribution of actual soft (FF < 9.8 N) and good (FF ≥ 9.8 N) fruit in (a) whole validation population, (b) fruit stored in the first and second trays, and (c) fruit stored in the third trays. The size of each population is indicated by area of the corresponding pie chart.

For segregation between grower lines, it was intended that the predicted short- and medium-storing grower lines (lines with more than 10% predicted proportion of soft fruit) would be shipped earlier in the season while the predicted long-storing lines would be kept for later sales. Nine of the grower lines (one-third of the population) were identified as long-storing by the model: G6, G10 – G12, G14 – G16, G18 and G24 (Table 7.2). Post-storage firmness results showed that 469 out of 1620 (29.0%) fruit in the early shipment lines were soft (Fig. 7.9b), whereas 669 out of 810 (82.6%) fruit in the late shipment were sound (Fig. 7.9c). The proportion of soft fruit reduced from 25.1% (shipment without segregation) to 17.4% (shipment based on grower line segregation). Chi-square test suggests that the proportion of soft fruit in the two segregated populations was significantly different ($\chi^2 = 38.270$; $p < 0.001$).

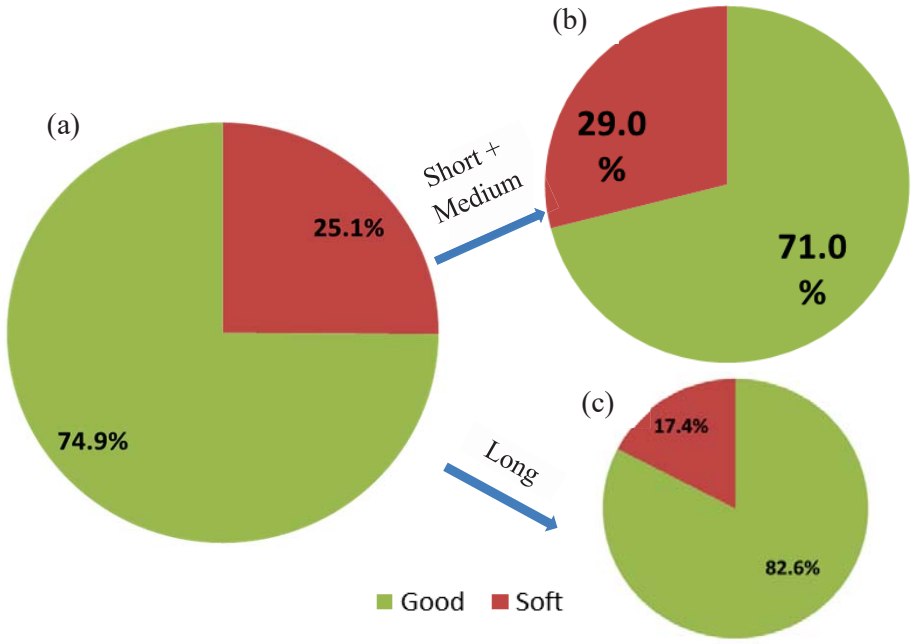

Figure 7.9 Distribution of actual soft (FF < 9.8 N) and good (FF ≥ 9.8 N) fruit in (a) whole validation population, (b) short- and medium-storing grower lines, and (c) long-storing grower lines. The size of each population is indicated by area of the corresponding pie chart.

The significance of soft fruit reduction as a result of segregation was also assessed based on the minimum criterion as defined by Hair et al. (2006). For segregation within grower line, the proportion of soft fruit (21.2%; Fig. 7.8c) in the

segregated long-storing population was less than 25% reduction from that achieved by chance (20.1% = 25.1% ÷ 1.25), indicating that the reduction of soft fruit was not significant. However, for segregation between grower line, the proportion of soft fruit in the segregated long-storing group (17.4%; Fig. 7.9c) was more than 25% less than that achieved by chance (20.1%), suggesting a significant reduction in soft fruit. Significant reduction in fruit loss may justify industrial application of the developed segregation system on current packing lines.

7.3.4 Validation performance evaluation

The performance of the model in this validation trial was comparable to that during model calibration (Section 7.3.3), suggesting good repeatability of the model. This is possibly attributed to the large number of training samples in the calibration data set with a wide variety of factors including growth conditions, maturity, grower lines and seasonal variation. The slight reduction in ability to predict between model calibration and validation is to be expected. The purpose of validation is to ensure that results obtained in the calibration model are not specific to only the calibration sample, but could also be generalised to an independent population (Hair et al., 2006). However, multivariate models in food processes can take years to build and/or improve up to a desirable level. The lack of selectivity in the multivariate NIR signal and the time span required for model building can be problematic when unwanted sources of variation are present in the data (Sileoni et al., 2011). This is especially true for natural products such as food raw materials (in this case, freshly harvested fruit) in open biological processes where the composition cannot be exactly predetermined. In this study, the predictive accuracy could have been improved by recalibration of the model by adding a set of NIR spectral and fruit storage data obtained from the validation trial. However this is impractical because prediction needs to take place prior to cool storage and hence it would not be possible to collect fruit storage data at the time of model prediction.

For between grower line segregation, the fact that the model overestimated the proportion of failure for grower lines harvested during early seasonal period suggests the lack of reliability to rank grower lines according to their harvesting time. It is recommended that, for future improvement, harvesting time (e.g. ISO days) or harvesting seasonal periods (e.g. early, mid or late) should be included in the calibration model as an input variable, so as to improve the prediction accuracy of the model.

7.4 Conclusions

The robustness of the developed classification model (Chapter 6) was tested using a validation trial conducted in 2015. At harvest fruit were ranked by the model both within and between grower lines, based on the probability of individual fruit to become soft after cool storage. Fruit were then repacked and stored in separate trays so as to segregate long-storing fruit from the remaining population. Fruit flesh firmness was measured after 125 days of storage at 0ºC. For within grower line segregation, the average storability of fruit was significantly different amongst trays, with lowest FF and highest number of soft fruit found in short-storing trays, suggesting that the model was capable of segregating individual kiwifruit within population. For segregation between grower lines, the developed model accurately classified 44.4% of the grower lines, with long-storing lines having the highest average FF values. This demonstrates the ability for the developed model to segregate storability of grower lines of kiwifruit. Should the model be applied at harvest and the fruit/grower lines be shipped sequentially, the proportion of soft fruit would be reduced from 25.1% by chance, to 21.2% and 17.4% (15% and 30% fruit loss reduction) for segregation within and between grower line respectively. Applying a segregation system to sort grower lines may have industrial viability through direct fruit loss reduction and more importantly reduction of associated postharvest costs.

8 General Discussions

8.1 Introduction

In New Zealand, kiwifruit are often harvested unripe and stored in cool temperature for long periods of time before being exported to the global market. During coolstorage, a significant proportion of fruit soften and this contributes to fruit and financial losses. It was demonstrated that pre-harvest manipulation of crop load and girdling had significant influence on at-harvest kiwifruit attributes and postharvest fruit storability (Chapter 3). As such, it is important to be able to capture this inherent information at harvest while keeping the fruit intact, so that future fruit quality can be forecasted prior to coolstorage. The main purpose of this thesis was to develop an appropriate non-destructive technique applied at harvest to predict 'Hayward' kiwifruit storability. The aim was to assist with inventory management decisions for export and help to reduce fruit loss in the supply chain. Even a small percentage of reduction could potentially contribute to a significant improvement, because of the current size of the industry and the associated labour costs being reduced. A positive result would compound as the volume of the New Zealand kiwifruit increases.

Several batches of 'Hayward' kiwifruit were sourced commercially from multiple orchards, different seasons, various harvesting periods and several growing condition treatments. Two non-destructive techniques were investigated: optical coherence tomography (Chapter 4) and near infrared spectroscopy (Chapters 5, 6 and 7). Experiments were carried out to determine the correlation between at-harvest data captured by the proposed techniques and fruit quality and storability prior to as well as after coolstorage. Figure 8.1 is a schematic illustration of the work carried out in this thesis. The key findings and the implications of the studied technologies will be discussed in this chapter.

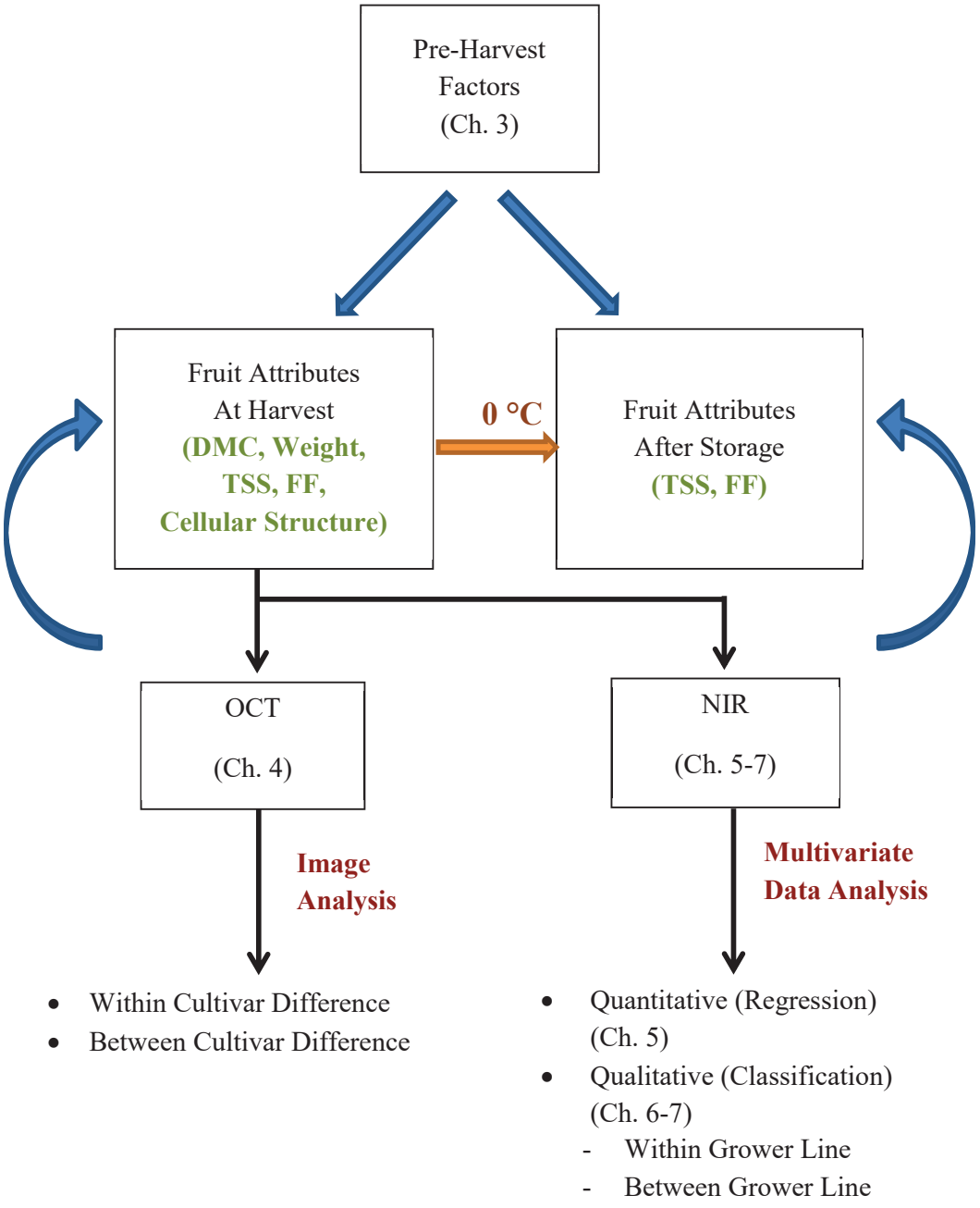

Figure 8.1 A diagrammatic representation of how pre-harvest factors could affect kiwifruit attributes both at harvest and after coolstorage at 0 °C (Chapter 3). The application of non-destructive techniques including OCT and NIR at the time of harvest would help to assess at-harvest fruit attributes (Chapter 4) and predict post-storage fruit quality and storability (Chapters 5, 6 and 7).

8.2 Effects of Pre-Harvest Factors on Fruit Quality

The quality of a horticultural product is determined in the field prior to harvest. Postharvest technologies help to maintain but not improve quality (Hewett, 2006). Preharvest factors can interact to affect plant growth and fruit development, and ultimately lead to the inevitable variability in fruit quality within the population at the time of harvest as well as during storage. While the main objective of this thesis is to utilise non-destructive techniques to predict and segregate storage outcomes of kiwifruit based on at harvest attributes, it is important to understand how at-harvest quality attributes such as size, appearance, taste and texture etc. are imposed (or not) from previous growing conditions and environmental factors, and how these attributes affect the rate of postharvest deterioration in storage and consumers' decision to purchase the product.

The current study found that trunk girdling improved sugar content at harvest and during storage but led to lower FF of fruit during storage (at 50, 100, 150 and 175 days after storage) and fruit reached the minimum export standard (FF = 9.8 N) sooner (Sections 3.3.2 and 3.3.3). Previous studies also reported that girdling led to advanced maturity and more rapid softening in 'Hort16A' (Boyd and Barnett, 2011) and 'Gold3' kiwifruit (Snelgar and Blattmann, 2012), apples (Autio and Greene, 1994), peaches (Crisosto and Costa, 2008), nectarines (Agusti et al., 1998), and persimmon (Juan et al., 2009). Boyd (2012) and Scarrow (2014) suggested that if the right timeframe for harvesting was chosen, fruit treated with trunk girdling could exhibit the same softening behaviour as a non-girdled population. To minimise the adverse effect of girdling on fruit storability, future studies should further investigate the relationship between girdling, at-harvest maturity and softening curves of fruit, in order to identify the optimal harvest time for maintaining storability.

High crop load reduced fruit eating quality because of reduced TSS during storage but did not seem to affect storability (i.e. post-storage FF) of the fruit (Sections 3.3.2 and 3.4.3). High crop load could enable economic advantages if an increased yield can be achieved without adverse impacts on kiwifruit harvest and postharvest quality. The limits to 'Hayward' kiwifruit productivity are yet to be reached (Thorp et al., 2011). Advances in management with higher cropping systems such as selection of lower vigour wood (improving DMC) and closer cane spacing (improving sunlight and

maximising DMC) are evolving to reduce the risk of adverse impacts on fruit quality. If the adverse impacts on at harvest DMC, fruit weight and postharvest TSS (Sections 3.3.1 and 3.3.2) can be alleviated through such cropping systems, high crop load would have the potential to improve productivity without affecting storability. However, this would require detailed studies on storage performance of the treated fruit and sensory tests conducted to ensure consumers' acceptability regarding taste profile of the product.

Postharvest cooling-induced disorders such as chilling injuries (also known as low temperature breakdown and storage breakdown disorder) can also be affected by preharvest environmental conditions and orchard practices (Ferguson et al., 1999). For kiwifruit, the susceptibility to CI can be affected by seasons (Arpaia et al., 1985), orchard location (Lallu, 1997), preharvest chilling treatment (Sfakiotakis et al., 2005), harvest maturity (Burdon et al., 2007), curing temperature and time (Doleh, unpublished work), cooling rate and storage temperature (Lallu, 1997; Zhao, 2017). Boyd and Barnett (2011) also found that extended trunk girdling reduced the CI susceptibility of 'Hort16A' kiwifruit. In the current study the effect of crop load and trunk girdling on CI development in 'Hayward' kiwifruit was not evaluated. Trunk girdling and low crop load resulted in more advanced maturity at harvest and during storage (Section 3.3.2), and hence are likely to reduce the incidence of CI in the treated fruit. However, Burdon et al. (2014b) also pointed out that the quality of fruit that developed CI differed considerably and as such using a threshold based on maturity was not sensible. Therefore, future studies should be carried out to elucidate how CI susceptibility of 'Hayward' is affected by crop load and girdling.

Knowledge of how preharvest factors affect fruit quality may help to manipulate biological variability of fruit at harvest. For instance, Peirs et al. (2003) found that more than half of the variability in NIR spectral data collected on apple samples could be attributed to seasonal and orchard variations as a result of different growing conditions. The robustness of models for external validation was found to improve with more variability in the calibration data set for quality prediction of apple (Peirs et al., 2003; Bobelyn et al., 2010) and avocado (Wedding et al., 2013). Hence, manipulation of preharvest conditions (e.g. including samples from various seasons and multiple orchards) may help to ensure a wide range of relevant variability in fruit quality for the data set and improve robustness of predictive models.

On the other hand, large biological variability between and within batches of fruit induced by growing conditions may contribute to unwanted variations in postharvest quality and storability and result in losses due to storage disorder. This calls for the need to decrease this variability prior to storage, by means of sorting or grading in order to reduce losses and assist with inventory management (Tijskens et al., 2003). Previous studies attempted to describe the effects of preharvest factors on the observed variability using mathematical languages. Specifically, abstract model mechanisms including prediction of DMC during fruit growth to indicate harvest fruit quality and incidence of CI as a function of antioxidants assimilation during development can be found in Tijkens et al. (2003). Pérez-Marín et al. (2011) used NIR spectroscopy to segregate postharvest storability of nectarines as a result of preharvest irrigation strategies. The ability to capture, model and predict the sources and effects of variability helps to integrate with existing knowledge and provide segregation solutions for optimisation of product quality. For instance, the effects of preharvest factors on biological variability of batches of kiwifruit at harvest can be integrated with the study of Jabbar (2014), which modelled and segregated the variability in softening rates during storage, to provide a better overview of fruit behaviour from orchards through to the supply chain.

Rivera et al. (2017) proposed that the postharvest ripening behaviour of avocado was affected by multiple preharvest factors including seasonal temperature, humidity, plant nutrition and irrigation management and hence, prediction of postharvest quality using a single pre- or at-harvest variable could be misleading. However, in practice extensive data collection requires intensive labour and data analysis and thus may not be pragmatic. In the current study, non-destructive methods were used to capture the (near) skin properties of fruit at harvest. Given that fruit skin is the first point of contact with growing environment, it is assumed that this information may be representative of various pre-harvest conditions and therefore, can be indicative of physical/chemical properties of the fruit at harvest, which in turn affect quality attributes after storage.

8.3 Assessment of Near-Surface Cellular Structures using OCT

Prior to this work, there is no existing knowledge on the type of information that can be extracted from OCT images of intact kiwifruit. Loeb and Barton (2003) investigated the application of OCT on cut kiwifruit along the outer pericarp (parallel to skin). In this thesis, OCT imaging enabled non-destructive identification of large cells in near skin kiwifruit tissue, with subsequent automated segmentation and analysis identifying and describing large cells efficiently (Chapter 4). The automated OCT data analysis method developed in this chapter has benefits of rapid processing (approx. 10 mins) and computation of large 3D data sets of images, and the minimisation of human error and bias during selection of large cells (Section 4.2.4). This study conducted a number of preliminary comparisons amongst cultivars and growing systems to investigate what the resulting information on large cells may be useful for.

Cellular structure and composition have also been associated with quality attributes of kiwifruit. For instance, White et al. (2016) studied the impact of cell membrane integrity on taste perception in both soft and firm fruit. In soft fruit the large cells tended to maintain membrane integrity during mastication while the small cells lost membrane integrity, whereas in firm fruit both the large cells and small cells tended to lose membrane integrity during mastication resulting in high juiciness. High cell membrane integrity would lead to mealiness. A potential application of OCT would be to look at whether the membrane integrity of large cells for soft and firm fruit can be differentiated by OCT imaging.

Additionally, Nardozza (2008) suggested that the ratio of small to large cells affects dry matter content and fruit size. Small cells made a much higher contribution to the total fruit starch concentration than large cells because starch granules were mainly found in small cells whereas large cells usually appeared empty. Assuming the remaining outer pericarp tissue is comprised of small cells and intercellular spaces, the yellow-fleshed cultivars, ‘G3’, ‘G9’ and ‘Hort16A’ may have larger volume fraction of small cells in comparison to the green-fleshed ones, ‘G14’ and ‘Hayward’, since the volume fraction of large cells in the outer pericarp tissue was lower for yellow-fleshed cultivars than green-fleshed cultivars (Chapter 4). This agrees with the existing knowledge that ‘Hort16’ fruit have a higher dry matter content at harvest and are much sweeter tasting than ‘Hayward’ fruit when ripe (Lowe et al, 1999).

The cell wall of large cells contributes to a significant portion of the total cell wall volume in the fruit and plays an important part in delaying softening in ripe fruit (Hallett et al., 2005). This suggests that at harvest, fruit with larger volume fraction of large cells (hence, larger volume fraction of cell walls) potentially have better resistance to softening. It was also observed that at harvest 'G14' and 'Hayward' had significantly higher firmness values than 'G3', 'G9' and 'Hort16A' (Table 4.1). It may be helpful to examine the storage performance of fruit for future studies, in order to fully explore the relationship between volume fraction of large cells and fruit quality during storage.

In addition, OCT has the capability of enabling continuous monitoring of cellular changes over a period of time. It may provide useful information on cellular structural changes during kiwifruit ripening and softening without damaging the fruit. Hallett et al. (1992) used microscopy to study the structural changes of kiwifruit cells during ripening on separate fruit tissues, and found that as fruit tissues softened, the cellular profiles became more rounded, i.e., packing of more spherical bodies. The intercellular spaces also increased in the outer pericarp (increased percent volume of intercellular spaces and increase in the percentage of the tissue occupied by free gas). However, different fruit samples were used at each ripening/softening stage; hence the results were based on the assumption that cellular structures are identical for fruit with similar firmness measurements. Applying OCT would allow the same fruit to be measured at different stages. This could be useful to study the differences in cellular structural changes during softening between commercial cultivars or batches of kiwifruit.

OCT also has the potential to provide information for cultivar or batch selection, since cellular structural properties can affect physiological features of the breed. For instance, cell density and diversity of sizes and shapes of the cells making up a fruit tissue may contribute to differences in water mobility in the same tissue. Kenouche et al. (2014) found that various cell density and structures in cherry tomato tissue resulted in different magnetic resonance imaging (MRI) T1 values, which are relaxation times indicative for the mobility of water within the fruit tissue. The T1 values for yellow-fleshed kiwifruit cultivars have been previously reported by Burdon et al. (2014c), with T1 values in 'G9' being lower than in 'G3' and 'Hort16A', suggesting lower water mobility and limited potential for mass water transfer within the 'G9' fruit. This, in

combination with fruit softening, may have resulted in shrivel development in 'G9' fruit during storage, which is a known problem for the industry (Burdon et al., 2014c). In Chapter 4, the large cells were found to be relatively small but in higher density in 'G9' as compared to 'G3' and 'Hort16A', and this could be a possible contributor for the reduction in water mobility in 'G9' fruit tissue since cell density plays a role in affecting T1 values of the fruit. However, more research may be needed to investigate the relationship between large cell density and water mobility in the tissue.

In addition, chilling injury is observed in cool-stored kiwifruit which leads to extreme softening of the fruit. Fruit that develop CI may contribute to a large proportion of soft fruit (Bauchot et al., 1999). Symptoms of CI include a ring of granular and water-soaked soft tissue in the outer pericarp, and a dark scald-like appearance in the skin (Lallu, 1997). Bauchot et al. (1999) also observed large airspaces within cells affecting both small and large cells. Given that OCT is capable of detecting the boundary of tissues having different refractive indices, it is possible that water-soaked regions in the sub-surface structures and the presence of air bubbles may be identifiable. This would be helpful for non-destructive detection of early development of CI symptoms in kiwifruit.

Although OCT was capable of segregation between cultivars, it failed to detect any differences within cultivars resulting from pre-harvest manipulation of growing conditions, except that low crop load was found to increase maximum cell length (Chapter 4). In addition, there seems to be a trade-off between penetration depth and the clarity of information that can be extracted vertically from the images. At low penetration depth (e.g. 0.68 mm under the skin as used in Chapter 4), near-surface cellular structures were observed with relatively high axial resolution, enabling image processing and quantitative analysis. However, the data captured by the images would only be relevant to the layers of tissue immediately underneath the skin surface and may not be representative to the entire outer pericarp which could be up to 10 mm thick. Further work should be carried out to investigate the distribution and microstructural properties of small and large parenchyma cells across the outer pericarp. Improvement of penetration depth would also improve applicability of this technique and help to provide more convincing and comprehensive data for the assessment of internal quality or quality changes of the crop examined.

8.4 Prediction of Post-Storage Kiwifruit Quality using Vis-NIR Spectroscopy

8.4.1 Blackbox modelling

The present study provides an attempt to predict post-storage quality of 'Hayward' kiwifruit using at-harvest spectral measurement. Due to the multicollinear nature (a large number of absorption bands that overlap heavily with each other) of the NIR spectral data, advanced 'black-box' multivariate data processing models were used to perform quantitative and qualitative predictions. Prediction is based on pattern recognition using machine learning algorithms and the actual correlation between input data and prediction outcome is highly empirical. Therefore, although specific information such as absorption peaks and regression coefficients for a specific waveband could be obtained, the underlying relationship between the input spectral data and model predictions was not clearly defined. Fundamentally there is a physical relationship between input spectral data and the output attribute. However, when working under complex environmental conditions, light interacts with many other physique-chemical properties including sensor artefacts, sensor offsets and multiple confounding chemical properties. As a result, the physique-chemical relationship between input and output data becomes complex and obscure. Black box models effectively extract the hidden complex information.

Black-box models are not uncommon for predictions using NIR spectroscopy (Zerbini, 2006). For instance Lammertyn et al. (1997) found that although a physique-chemical background could be established for quantitative prediction of TSS of apples, for the other analysed parameters such as pH and FF it was difficult to interpret the spectral data to assign a specific vibration to a wavelength, resulting in most models being black-box. Contrary to explanatory models which generally contain a series of sub-models describing biochemical processes at the cellular level, black-box models do not require comprehensive understanding of the system to be predicted. As such they are more efficient for industrial applications and can be used for predictions and analyses at the crop level. In addition, an increasing number of open-source data mining software and machine learning libraries are becoming available, enabling the ability to continuously improve the performance of the model.

However, while black-box models are usually more accurate for predicting nonlinear correlations, there is often a trade-off between interpretability and model accuracy due to the fundamental complex nature of the algorithms used (Feelders et al., 2000). For instance, the algorithms discussed in Chapter 6 (SVM and boosted decision stumps) typically generated pure black-box models which cannot be easily interpreted (Friedman, 2006) or re-performed manually. If the purpose is simply to develop an effective automated prediction system then this is sufficient. However, the ability to understand what happens inside the black box can help rationalise model predictions and provide ideas for future improvements. The recently-developed local interpretable model-agnostic explanation (LIME) approach (Ribeiro et al., 2016) can be utilised in the future to provide more meaningful interpretation of machine learning predictions.

8.4.2 Quantitative prediction of post-storage TSS

Quantitative prediction of postharvest TSS using at-harvest NIR spectral data was somewhat successful: approximate predictions were achieved (Section 5.6.1). Lower errors were obtained in the current study, compared to Ignat et al. (2014) who also used at-harvest NIR data directly to predict post-storage TSS of apples.

The assessed storage time did not seem to largely affect predictive performance of the regression models. Predictions at 100, 125 and 150 days were similar and slightly better compared to that at 75 days (Section 5.6.1). Ignat et al. (2014) also found no significant changes in RMSEP for TSS of apples in relation to time of storage (after 2, 4 and 6 months). This is probably because during kiwifruit ripening, the conversion of starch into soluble sugar would have already been completed after 50 days of postharvest coolstorage (MacRae et al., 1992; Ritenour et al., 1999; Jabbar, 2014; Zhao, 2017). Therefore there is little change in TSS content during the storage times investigated in this study. This suggests that the at-harvest spectral data can be used as a good indicator of post-storage TSS when fully developed. This supports the good predictive performance of DMC (which is an indicator of post-storage TSS once fully developed) in many previous studies using NIR spectral data collected at harvest (Osborne et al., 1998; McGlone et al., 2002b; Clark et al., 2004; McGlone et al., 2007).

Williams and Norris (2001) proposed that sampling error could be a major component contributing to differences between reference and predicted values. In the

current study, sampling error can be caused by the lack of homogeneity in the material being sampled. Similar to OCT, the low penetration depth of NIR (~ 2 – 3 mm in fruit media) could result in biased sampling because the fruit sample has an outer pericarp as deep as 10 mm but only a near skin portion of the sample is being measured. In addition, the TSS of kiwifruit is higher in the core compared to that in the outer and inner pericarp (Martinsen and Schaare, 1998). Given the small penetration depth, spectral measurements fail to take into consideration the role of the kiwifruit core, contrary to the destructive methods. Hu et al. (2017) demonstrated the potential to use hyperspectral imaging to visualise and quantify the distribution of soluble sugars within the fruit by taking scans of sectioned slices. This method could be used to describe the changes of TSS in different tissue zones and hence, provide corrections for model predictions affected by heterogeneity of fruit sweetness.

Sugar levels vary within kiwifruit, being higher at the blossom-end and lower at the stem-end. However, this distribution is not linear along the longitudinal axis. According to Hopkirk et al. (1986), the TSS of kiwifruit at the equatorial position was not the middle point between the stem and the blossom ends; the increase of TSS from stem end to the equator appeared to be higher than that from the equator to the blossom end. In this thesis, TSS measurements were carried out by combining the juice from both stem and blossom ends of the fruit, in order to obtain an average TSS value across the fruit. However, NIR measurements were conducted at the equatorial position of the fruit. Hence in the current study the equatorial scans which indicate mid-point TSS were used to predict the average TSS measured from both ends of the fruit.

Measurement location has been found to affect the robustness of NIR models for prediction of TSS in apples (Fan et al., 2016). To determine if this difference in location plays a role in adding error to the prediction, a simple test can be carried out by collecting and averaging the spectral data around locations a few centimeters from both ends to find out if improvement in model prediction can be achieved. Fan et al. (2016) also suggested that the development of a global position model improved the robustness of NIR models for prediction of TSS of apples at any surface locations of the fruit. Therefore, future studies could also investigate whether the development of a global position model would improve the prediction of TSS in kiwifruit. Alternatively, NIR sensors with spatial imaging capabilities such as hyperspectral imaging (HSI)

technologies can be utilised to account for the variation in sugar content as a result of spatial distribution, as demonstrated in Martinsen and Schaare (1998).

8.4.3 Quantitative prediction of post-storage FF

Prediction of post-storage FF using at-harvest spectral data has been studied on other crops such as apples and apricots but not for 'Hayward' kiwifruit. Although lower RMSEs were obtained in comparison to previous findings on other crops/cultivars (McGlone and Kawano, 1998; McGlone et al., 2002a; Ignat et al., 2014), quantitative prediction of post-storage FF was still unsuccessful (Section 5.6.2).

Kiwifruit firmness is a physical measurement that is influenced by internal cellular structures which can manifest as a change of surface spectral or scattering properties, a change in pectin structure as a result of pectin solublisation and changes in degree of cell turgor. Compared to soluble sugar concentration which tends to form a linear correlation with spectral absorbance, it is more challenging for NIR to estimate a physical structural change. Whole fruit turgor is dependent on water content and rate of water loss in both outer and inner pericarp (Li et al., 2016). However, there is a limitation for NIR light to penetrate any tissues more than 2 mm below the skin. In addition, the NIR spectra of fruit are dominated by the water spectrum and hence any structural changes of constituents with low concentration (such as pectin solubilisation in kiwifruit) might be barely detectable because of this dominance of water (Pojić et al., 2015). As such, quantitative prediction of FF is more difficult compared to that of TSS, as shown by many previous studies (McGlone and Kawano, 1998; McGlone et al., 2002a; Ignat et al., 2014) and the current study. The ability of NIR technology to provide accurate quantification of firmness remains questionable, at best.

For crops such as apples and cherries, the correlation between NIR spectral data and at-harvest or post-storage FF measurements is more likely to be attributed to a change in skin or background colour during maturation and ripening which influences the absorbance of certain colour pigments. For instance, apple peel chlorophyll content was found to be strongly correlated with fruit firmness (Kuckenberg et al., 2008). Given that chlorophyll has peak absorbance bands at around 670 – 680 nm, any change in chlorophyll content coinciding with firmness would be detectable by Vis-NIR spectroscopy in the visible range. Similarly, the firmness of sweet cherries was found to

be correlated with skin colour (*h*°; Muskovics et al., 2006) with Lu (2001) finding "relatively good predictions" of the firmness of sweet cherries (SEP = 0.44 – 0.55 N). However, for 'Hayward' kiwifruit there is no colour change during physiological development. Hence, it is not possible to develop such a secondary correlation based on changes in colour absorption.

The number of NIR scans collected per fruit can also influence the accuracy of the model. For spectra data collection, most previous NIR work and the current study used two measurements corresponding to the two locations used for firmness measurements. This is mainly due to time constraints and the limitation of speed of lab-scale NIR sensors especially when a large sample size is required. However firmness can be position dependent; hence it is possible that the two spots used for measurements may not represent the overall firmness of the fruit. McGlone and Kawano (1998) used 50 scans per fruit for instant estimation of FF (no storage) of 'Hayward' kiwifruit and obtained better results compared to Feng (2003), in which only two scans per fruit were used. Increasing the number of spectral measurements should be considered for future research. However, the number of measurements should also be small enough to allow industrial applicability. The industrial NIR sensors are capable of approximately 20 scans per fruit on a packing line (Feng, 2003). For future experimental designs this number should be considered. Alternatively hyperspectral imaging which can provide a global measure of firmness can also help to reduce the variation caused by spatial location.

8.4.4 Qualitative prediction of kiwifruit storability

Segregation of 'Hayward' kiwifruit for storage potential was carried out at individual fruit level using at-harvest Vis-NIR spectral data as the sole input data for fruit stored at various periods of storage (Chapter 6). This enabled classification both within (at fruit level) and between grower lines based on the export firmness criterion of 1 kg_f (9.8 N). The external validation trial (Chapter 7) showed that the model performed better in segregation between grower lines and achieved significant reduction in soft fruit (Section 7.3.3).

The penetration speed of the electric penetrometer influences the value of firmness obtained. Feng et al. (2011) demonstrated that the measured FF values

increased with increasing penetration speeds varying from 4 $mm \cdot s^{-1}$ to 40 $mm \cdot s^{-1}$. Similarly, Li et al. (2016) found that increasing the penetrometer measurement speed from 5 $mm \cdot s^{-1}$ to 20 $mm \cdot s^{-1}$ increased the firmness values obtained. For 'Hayward' kiwifruit, this difference only became apparent when fruit FF were below 40 N. The difference in firmness could be up to ~ 10 N particularly in samples stored for 8 – 16 weeks (56 – 112 days). Both studies suggest the influence of change in penetration speed on FF values was high in stored 'Hayward' fruit with low FF values (< 20 N). In the present study, there were multiple data sets collected over four seasons during 2012 – 2015. Due to a change in standard measurement procedures, the penetration speed of firmness measurements using the electric penetrometer was changed from 20 $mm \cdot s^{-1}$ for model calibration (2012 – 2014), to 8 $mm \cdot s^{-1}$ for the validation trial (2015). This change in penetration speed could have resulted in slightly different firmness values for fruit, hence affecting the decision of the model to determine whether a fruit is commercially acceptable (FF > 9.8 N).

Using the firmness-speed model provided in Feng et al. (2011), a plot showing the ratio between a FF value measured at a specific penetration speed and that measured at 10 $mm \cdot s^{-1}$ on the same fruit can be obtained (Fig. 8.2). From this plot, a quick calculation suggests that a fruit read 9.8 N at 20 $mm \cdot s^{-1}$ penetration speed (which would have been grouped as a good fruit) would obtain a firmness value of ≈ 7.6 N at 8 $mm \cdot s^{-1}$ penetration speed. This would mean that the soft fruit found in the validation trial, which had firmness readings between 7.6 – 9.8 N, would likely to be classified as good fruit using the calibration model. In order to evaluate the effect of penetration speed on classification accuracy, the FF data used in the validation trial were corrected using the mentioned firmness-speed model with the segregation performance re-assessed (Tables 8.1 and 8.2).

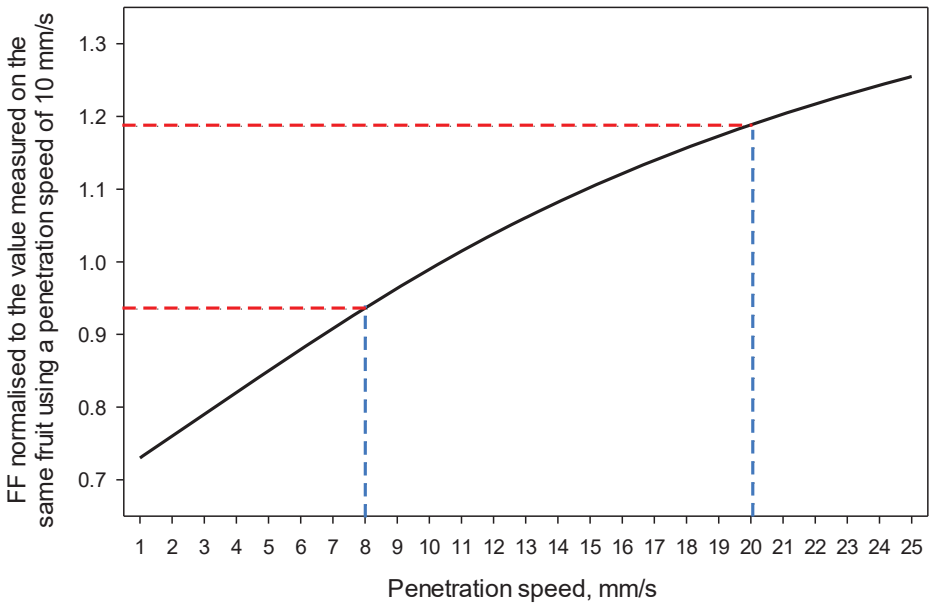

Figure 8.2 Firmness-speed model proposed by Feng et al. (2011) displaying the relationship between penetration speed (mm·s^{-1}) and FF normalised to the value on the same fruit using a reference penetration speed of 10 mm·s^{-1}.

Overall the segregation performance improved after correction of FF values using the firmness-speed model. In this case the proportion of soft fruit in the entire batch was reduced to 13.6% by chance. Approximately 33.8% and 76.8% of soft and good fruit were accurately classified respectively (Table 8.1). The FN rate was 12% (Table 8.1), much lower than the 22.6% found before correction (Section 7.3.3).

Table 8.1 Confusion matrix for 2015 validation trial using corrected FF values based on the firmness-speed model described in Feng et al. (2011).

	Predicted		
Actual	Soft	Good	Total
Soft	112 (33.8%)	**219 (67.9%)**	331 (13.6%)
Good	487 (23.2%)	1612 (76.8%)	2099 (86.4%)
Total	599 (24.7%)	1831 (75.3%)	2430

Table 8.2 Reviewed number of soft fruit amongst the three trays (T1 – T3) within a grower line after storage at 0°C for 125 days as a result of pre-storage within grower line segregation (correction based on the firmness-speed model described in Feng et al. (2011)). Green, orange and purple indicate short, medium and long-storing fruit/lines.

GL	n T1	n T2	n T3	GL	Actual total	Predicted total	Actual %	Predicted %
1	1	1	0	14	2	1	2.2%	1.1%
2	2	2	2	18	6	3	6.7%	3.3%
3	0	0	0	15	0	4	0.0%	4.4%
4	1	0	0	24	1	4	1.1%	4.4%
5	0	0	1	16	1	5	1.1%	5.6%
6	1	0	0	6	1	8	1.1%	8.9%
7	5	3	5	12	13	8	14.4%	8.9%
8	17	11	15	10	43	9	47.8%	10.0%
9	1	1	3	11	5	9	5.6%	10.0%
10	2	3	4	5	9	16	10.0%	17.8%
11	2	0	0	13	2	16	2.2%	17.8%
12	4	0	2	26	6	17	6.7%	18.9%
13	1	0	0	4	1	18	1.1%	20.0%
14	0	0	0	21	0	18	0.0%	20.0%
15	6	4	7	23	17	18	18.9%	20.0%
16	2	0	0	22	2	22	2.2%	24.4%
17	8	4	3	17	15	24	16.7%	26.7%
18	5	4	8	27	17	25	18.9%	27.8%
19	13	7	9	2	29	31	32.2%	34.4%
20	12	9	5	1	26	33	28.9%	36.7%
21	0	4	1	19	5	37	5.6%	41.1%
22	4	4	2	20	10	43	11.1%	47.8%
23	12	7	5	25	24	43	26.7%	47.8%
24	7	6	6	8	19	45	21.1%	50.0%
25	5	4	1	3	10	48	11.1%	53.3%
26	8	2	4	9	14	48	15.6%	53.3%
27	17	21	15	7	53	49	58.9%	54.4%
Total	136	97	98		331	602		

For segregation within grower lines, the total number of soft fruit in the last trays (predicted long-storing trays) was 98 out of 810 fruit after correction (Table 8.2). This would mean that: the proportion of soft fruit would be reduced by 11% from 13.6% (without segregation) to 12.1% (with segregation) in the remaining population if fruit from the first and second trays were shipped early. This was not as good compared to the 15.5% reduction in soft fruit obtained without correction of FF values (Section 7.3.3). For segregation between grower lines, the same thresholds (< 10%, 10 – 30% and > 30% predicted fruit) were used to classify 27 grower lines. The number of soft fruit after correction was 73 out of 810 fruit in the predicted long-storing lines (Table 8.2). This would mean that the proportion of soft fruit would be reduced by 33.8% from 13.6% (without segregation) to 9% (with segregation) in the remaining population if short- and medium-storing lines were shipped early. This was slightly better than the 30.7% soft fruit reduction obtained without correction of FF values (Section 7.3.3). This suggests that penetration speed actually affected model performance and hence it should be kept consistent or corrected during new model development.

In the few studies that investigated the use of NIR to segregate storage potential of fruit, in most cases NIR spectral data were used in combination with other means of quality indicators. For instance, Feng (2003) segregated kiwifruit grower lines using Vis-NIR spectra in combination with initial fruit firmness, colour, TSS, DMC and mineral concentrations. This requires extensive laboratory work at the time of harvest which may be impractical on the packing lines when dealing with large volumes of fruit. In Feng et al. (2014), at-harvest NIR spectral data was used in combination with acoustic firmness measurements of fruit during storage, with soft fruit regularly removed from the population to minimise their impact on storability of firmer fruit in the same tray. This would require firmness measurements and replacement of soft fruit during storage and hence may offset any economic benefits gained through reduction of fruit loss as a result of segregation. Conversely, the significance of the current study is that at-harvest spectral data was used as the sole input data for prediction. The initial measurement and segregation is all that is required, meaning the economic impact of the additional labour is minimal.

Currently many packhouses practise ranking of grower lines for storage potential for sequential marketing based on storage behaviour obtained from historical data.

Therefore, a weighted grading system can be designed which combines prediction outcomes from the segregation model developed in the current study and historical industrial data (Fig. 8.3). First, grower lines can be categorised into short, medium and long-storing classes according to historical storage performance prior to the season. The segregation model then ranks the grower lines at harvest based on current season's spectral data and classifies them into the same three groups. A final ranking and/or grouping will be generated based on the percentage value (weight) assigned to each of the two methods. Experiments should be carried out in order to find out the optimal ratio of weightings to be assigned to each of the two segregation methods. Grower lines classified as short-storing should be prioritised for shipping or selling, followed by those classified as medium-storing. The predicted long-storing lines should be kept for later in the season and distributed sequentially to distant markets based on their weighted ranking (first to expire, first out).

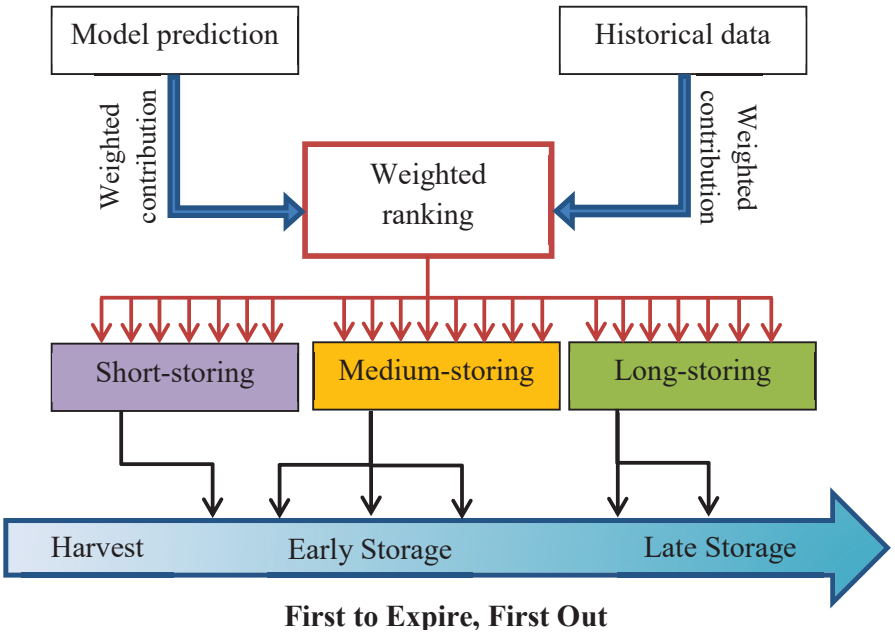

Figure 8.3 Implementation of weighted grading system for segregation grower lines based on storage potential. Fruit are distributed according to "First to Expire, First Out" approach.

8.4.5 Industrial applicability assessment for segregation model

For the industry, implementation of a segregation model into existing sorting line requires justification of financial gain outweighing the cost incurred for installing such as system. An attempt was made to investigate the industrial applicability of the developed segregation model based on the following contributing factors:

1) The associated onshore condition checking and repacking costs

At the point of export, a proportion of the fruit is usually assessed for firmness. The suitability for export is determined by calculating the soft fractile (0.03 fractile), i.e. if the 9th softest fruit of 300 fruit has a FF value above 1 kg_f (9.8 N), the pallet can be exported. If the pallet fails the test it will be off-loaded, put in the coolstore on the wharf and then returned to the packhouse for re-working (Fisher, 2011). This process ensures that fruit quality is controlled at the time of export and that fruit arrives at the destination in suitable condition. However, this process involves intensive labour cost and results in direct fruit loss, hence it contribute to a significant portion of the marginal changes in postharvest costs (Anonymous, 2015d). It is important that both fruit loss and repacking and condition checking costs are reduced.

Segregation between grower line contributed to 30.7% reduction of soft fruit in the classified long-storing population (Section 7.3.3). Considering the 2015/16 season's data where the total sales volume of 'Hayward' is 77.9 million trays (Anonymous, 2016a) and one-third of the population are kept for late season sales with a sales price of ~$5 per tray (Anonymous, 2016a; McBeth, 2016), a quick calculation of the potential benefit of segregation can be made. Assuming the percent fruit loss is 25.1% and 17.4% with and without segregation (Chapter 7), it would seem that a reduction of approx. NZD$10 million per annum in cumulative fruit loss at the end of the season could be achieved (Fig. 8.4). The proportion of repacking/condition check cost would also reduce from currently 12% of the postharvest quality cost ($1.20 per submit tray of exported kiwifruit; Anonymous, 2015a, c) to approx. 8.3% after segregation, assuming that the percent reduction in repacking cost is directly proportional to the reduction in soft fruit (30.7%). This would contribute to an additional cost reduction of NZD$1.2 million per annum (Fig. 8.4).

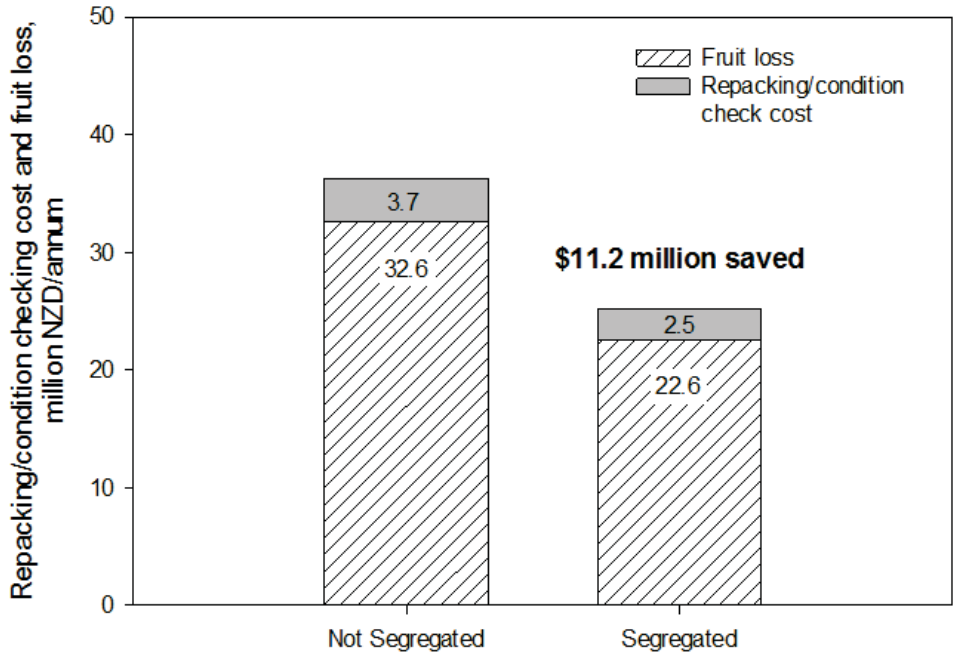

Figure 8.4 Annual costs of cumulative fruit loss and repacking/condition check cost with and without segregation. Values are calculated by assuming: a total sales volume of 77.9 million trays (Anonymous, 2016a); one-third of the population are kept for late season sales with a sales price of ~$5 per tray (Anonymous, 2016a; McBeth, 2016); approximately 25.1% original fruit loss in the later shipment fruit; the postharvest quality cost is $1.20 per submit tray of exported kiwifruit (Anonymous, 2015b, d); and that the percent reduction in repacking cost is directly proportional to the reduction of soft fruit.

The total current repacking, condition check and fruit loss costs are estimated to be NZD$113 million without segregation. This number could have been a slight over-estimation but was considered realistic given that the costs were $81.6 million during the 2007/08 season with a total sales volume of 95 million trays (Anonymous, 2008). The total cost reduction was NZD$11.2 million with segregation. Hence, approximately 10% reduction in the total cost could be achieved. Note that this number only represents the expected reduction for 'Hayward' and does not account for any other commercial cultivars should a similar segregation system be developed and applied. However, this estimation also does not take into consideration the costs incurred with implementing the new segregation system.

2) The total sales volume of kiwifruit

Increasing total kiwifruit sales volume may increase costs due to industry capacity constraints. For instance, condition checking, repacking and fruit loss costs increased from NZD $57.1 million to $81.6 million (43% increase), when sales volume increased by 17% from 81 million trays in 2004/05 season to 95 million trays in 2007/08 (Anonymous, 2008). Although the total sales volume has been affected by the bacterial kiwifruit vine disease, *Pseudomonas syringae pv actinidiae* (Psa), since November 2010 (Anonymous, 2015d), the commercialisation of new Psa-resistant cultivars has stabilised the market and as a result, a recent report by Anonymous (2015c) suggests that the total volume will "continue to recover from the impact of Psa". This is supported by the reported growing number of 117.1 million trays in 2015/16 (Anonymous, 2016a) and a forecast of 129 million trays in 2016/17 (Rotherham, 2016). It is likely that the volume will further increase as the global market of New Zealand kiwifruit expands.

As a result of increase values in production, there are increased risks and reward for managing fruit loss and associated labour costs. Implementation of appropriate segregation systems for not only 'Hayward' but also other commercial cultivars would enable separation of short-storing batches from the population facilitating sequential distribution. This would be useful in prioritising a proportion of the inventory for early shipment, which could alleviate the problem caused by industry capacity constraints. Additionally, increased volumes stimulate the need to store fruit longer in order to cater for higher supply to established markets. Hence a higher percent of fruit will need to be stored longer with larger volume, facilitating an increased value in identifying longer storing fruit. It is important that a well-designed segregation system is in place to facilitate sequential distribution.

3) Constraints for implementation at existing packhouses

Despite the potential cost reduction, additional cost associated with applying spectral sensors onto kiwifruit packing lines should be considered. Currently some packhouses use NIR sensors (Fig. 2.5b) installed on packing lines to sort fruit primarily based on dry matter content. This suggests that there will be costs associated with replacing or modifying current sensors, in order to match the instrumental parameters

required for the purpose of sorting fruit for future storability. The cost would depend on the number of NIR sensors installed and the monthly lease and installation fee (if any) charged by the provider (Tanner et al., 2012). As such the actual cost reduction would be less than that estimated in Fig. 8.4.

In addition, the current segregation method requires model computation after NIR spectral measurements. Hence a proper design to overcome engineering constraint will be required. Potentially computation after initial measurements may slow down the speed of the packing line and would require trained personnel to conduct data analysis on-site, which would contribute to additional costs. In this case, an automated ranking programme can be developed in order to improve applicability of the model.

8.5 Future Opportunities

8.5.1 Time-variable classification (global model)

In this thesis the presented quantitative and qualitative models were developed at fixed points of storage. As a result validation can only be made at time points in accordance with those chosen in previous experiments. An alternative measure would be to develop a global model which incorporates time as an input variable. This potentially widens industrial applicability as prediction can be made at any time during coolstorage once a satisfactory global model has been developed. As a proof of concept, this section attempts to develop such a global model using LogitBoost decision stumps as described in Section 6.4. The objective is to compare the predictive performance of the global model to that of fixed-time models using the same multivariate data analysis technique.

An additional data set from the maturity trial conducted in 2013 was added to the calibration data set described in Chapter 6 (Table 6.1). This experiment is part of a larger trial that studied the effects of storage temperature switches on the storability of kiwifruit (Zhao, 2017). The fruit were sourced from three commercial grower lines located in the Bay of Plenty area of New Zealand. Fruit from each grower line were harvested at three seasonal periods at 2-week intervals commencing 30th April 2013. Fruit were cured for two days during transportation before initial NIR spectral measurements. At day 0 (3 May), a total of 1080 fruit (30 fruit per tray × 4 trays per GL × 3 GLs × 3 maturities) were measured by Vis-NIR spectroscopy. Fruit were then

cooled to 10 °C within 12 hours, followed by 1 week to 0 °C. Single trays from each grower line were measured for FF at each of 12, 16, 19 and 22 weeks after storage. The spectral data and firmness measurements were used in combination with the former four classification data sets (Table 6.1), adding four more time points (84, 112, 133 and 154 days) to the existing ones (75, 100, 125 and 150 days). The same test data set (Section 6.2.1) was used for external validation of the global model.

For calibration, the overall classification accuracy for soft and good fruit were 35% and 92% respectively (data not shown), comparable to those obtained using fixed-time models (17 – 54% and 79 – 97% respectively; Table 6.4). External validation results using the global model were significantly different ($p \leq 0.027$) from those obtained using fixed-time models (Table 8.3). In general the global model showed more promising results. Prediction of soft group using the global model was significantly better at 75 and 100 days ($p \leq 0.001$) but not as good at 150 days ($p < 0.001$), compared to fixed-time models developed using the same classifier. At 125 days the performance was comparable between the two types of models ($p = 0.298$) with the global model having slightly lower TP rate and higher TN rate (Table 8.3). Given this result, it is likely that a global model would provide more benefit by generating more consistent prediction outcomes while keeping a wider range of industrial applicability by combining data sets obtained from various time points.

Table 8.3 Validation results of the global model and fixed-time models to predict kiwifruit storage potential based on at-harvest Vis-NIR spectra data using LogitBoost decision stumps.

Storage time (day)	Validation Accuracy (%)			
	Variable-Time		Fixed-Time	
	Soft	Good	Soft	Good
75	83	66	0	100
100	50	99	0	100
125	34	92	40	81
150	40	86	79	70

8.5.2 Economic NIR sensors

The consumer-scale NIR sensor, SCiO (Consumer Physics Inc., Tel Aviv, Israel) was introduced in Section 2.2.1.2. Beyond the cheap cost, the sensor has high portability enabling measurement anywhere and anytime, and provides the linkage of the data captured to cloud databases and analytics, meaning that rapid diagnostic information is able to be displayed on a regularly available cellular phone. Therefore, this section attempts to assess the performance of SCiO to provide estimation of fruit quality (quantitative) and segregation of fruit groups (qualitative).

Preliminary studies were carried out under supervision during the current study. For spectra acquisition, three scans per fruit were taken from different positions around the equator with the illuminator pointing at the fruit skin. Calibration with a white reference was carried out after approximately every 10 fruit. All spectral measurements were collected with an attached light shield to ensure adequate light seal from background noises. All data analysis was conducted using the SCiOLab online interface, in which limited selections of data pre-processing techniques were applied.

The first experiment consisted of 435 apple fruit from eight commercial cultivars (‘Braeburn’, ‘Eve’, ‘Granny Smith’, ‘Lemonade’, ‘Mahana Red’, ‘Red Delicious’, ‘Rose’, ‘Royal Gala’) and 405 kiwifruit from two commercial cultivars ‘Hayward’ and ‘SunGold’, both sourced from local supermarkets in January, 2016 (Medicott, unpublished work). At the time of purchase fruit were considered to be at various maturity and ripeness stages. Fruit were scanned using the sensor followed by destructive measurements of quality (DMC, TSS and FF). Regression models were developed to provide instant estimation of the measured quality attributes. In addition, classification models were developed for cultivar identification as well as branding discrimination (‘Zespri’ or ‘Southern Green’) for kiwifruit. In general quantitative analysis for both apples and kiwifruit was not successful ($R^2 \approx 0.15 – 0.53$; SDR ≈ 1.2 – 1.5; data not shown). Qualitative analysis of kiwifruit, on the other hand, obtained better results with 82% and 96% classification accuracy for each of the two brands, and 97% and 80% accuracy for each of the two cultivars.

The second experiment included a total of 296 ‘Kakariki’ feijoa fruit collected from a commercial orchard (Shi, unpublished work). Five batches of fruit were

harvested using 'touch-picking' method from the Matamata-based Southern Belle Orchard and at different stages of ripeness. Batches 1, 2 and 3 of feijoa were harvested on 30 March, 4 and 13 April, 2016 respectively, and were assessed two days after each harvest time. Batches 4 and 5 were harvested at the same date as batch 3 but were stored in the Massey postharvest laboratory at 20℃ and then assessed after 1 and 2 weeks of storages respectively to represent different ripening stages. Spectral data collection was carried out using the sensor, followed by fruit quality attributes measured both non-destructively (FF, skin hue°) and destructively (TSS, titratable acidity, internal flesh colour). The data were then used to develop regression models for estimation of quality attributes and a classification model to segregate feijoa by maturity. The sensor quantitatively predicted quality of feijoa with moderate accuracy ($R^2 \approx 0.44 – 0.68$; SDR ≈ 1.3 – 1.6; data not shown). The best quality prediction was obtained from TSS model ($R^2 = 0.60$; RMSE = 1.1 °Brix). The classification model accurately predicted maturity of 44%, 84% and 66% of the unripe, ripe and overripe fruit, respectively. This accuracy was improved to 98%, 91% and 99% respectively when neighbouring groups were included (Table 8.4).

Table 8.4 Prediction accuracy for classification models developed based on NIR spectra collected using SCiO (Consumer Physics Inc., Tel Aviv, Israel) for categorising feijoa (cv. 'Kakariki) maturity (n = 296).

	Actual class		
Predicted	Unripe	Ripe	Overripe
Unripe	44%	7%	0%
Ripe	54%	84%	33%
Overripe	1%	7%	66%

The last experiment consisted of spectral data captured from a total of 2055 kiwifruit from 21 coded commercial cultivars available in NZ and China including 8 green (G), 6 red (R) and 6 yellow varieties (Y), and an additional *A. eriantha* (E) cultivar (Jeffery, unpublished work). Fruit were scanned at various ripening stages in a sensory lab facility located in Shanghai, China. Quality attributes (TSS, FF and skin hue°) of 574 fruit from the same population were also measured. Regression models were developed to predict fruit quality. Again, quantitative analysis was not successful ($R^2 \approx 0.38 – 0.40$; SDR ≈ 1.3; data not shown). A global classification model that

included all of the 21 cultivars was developed to identify cultivar differences, whilst three additional models using only the green, red and yellow cultivars respectively were created. The models were then tested for robustness using 52 additional fruit from 17 cultivars. In calibration, the classification model showed good overall predictive accuracy (≈ 70 – 80%; Table 8.5). In model validation, good repeatability and robustness of the developed classification models were found, with 69.6% of the tested fruit accurately classified using the Global cultivar model, whilst 78.3%, 60.0% and 78.6% of tested fruit from green, red and yellow cultivars correctly identified using the Green, Red and Yellow models respectively (Table 8.5).

Table 8.5 Calibration model for segregation of commercial kiwifruit cultivars (n = 2055) using SCiO™ sensor (Consumer Physics Inc., Tel Aviv, Israel). Green, red, yellow and blue represent green, red, yellow and *A. eriantha* kiwifruit cultivars respectively.

	n	Cultivars	Model used			
			Global	Green	Red	Yellow
Calibration	105	G1	75%	81%		
	30	G2	43%	78%		
	55	G3	44%	69%		
	72	G4	85%	81%		
	71	G5	61%	58%		
	94	G6	89%	88%		
	68	G7	63%	74%		
	25	G8	34%	50%		
	160	R1	78%		79%	
	236	R2	86%		81%	
	263	R3	74%		75%	
	75	R4	51%		35%	
	130	R5	29%		30%	
	99	R6	65%		65%	
	145	Y1	40%			62%
	116	Y2	55%			72%
	45	Y3	58%			78%
	75	Y4	81%			87%
	80	Y5	62%			77%
	75	Y6	93%			93%
	36	E1	57%			
Validation	52		69.6%	78.3%	60.0%	78.6%

Preliminary results suggest that predictive performance of SCiO using the SCiOLab online software was in agreement with the present study. Qualitative classification generated more promising results compared to quantitative estimation which showed no or marginal success. Although the experiments were carried out to perform instant prediction rather than future forecasting, the capability of this sensor to segregate fruit based on cultivar or maturity stages further demonstrated the potential for NIR spectroscopy to be used as a grading/sorting tool rather than a means for quantitative estimation. A rapid and economic NIR sensor such as SCiO molecular sensor would reduce the time and cost spent on construction of calibration model from large data sets, hence enabling wider industrial applicability of this technique. Development of models which are designed to categorise fruit by ripeness to assist with consumer purchase decisions, or ones that detects fruit origin for authentication purposes may have significant commercial implications.

8.5.3 Other kiwifruit cultivars

By far most studies on NIR spectroscopy focus on 'Hayward' and the original gold cultivar, 'Hort16A'. New cultivars have since been developed and introduced to the market. While 'Hayward' continues to have high export volume, the production and export volumes of 'Hort16A' are now almost nil since the outbreak of Psa in 2010. The Psa-resistant cultivar 'Gold3' (Zespri® SunGold) was then widely planted in replacement of most of the 'Hort16A' vines that have been destroyed by the disease (Anonymous, 2016c). This new variety is found to store well and have higher yield and better market acceptability than 'Hort16A' (Fox, 2015). As a result, sale volumes of 'SunGold' continue to grow and are expected to be doubled by 2019/20 (Anonymous, 2016b). Attempts have been made to utilise existing NIR sensors to sort 'SunGold' based on DMC (McGlone and Wohlers, 2016). There would be a need to establish storage performance studies as well and re-evaluate the potential of NIR to predict storability of this new variety.

In addition, pre-commercial trials of the new green cultivar 'G11' (working title 'Zespri® New Green') showed that this variety has the potential of longer storability than 'Hayward' (Knowles, 2016). Therefore it would be useful to study the spectral characteristics of this new cultivar in order to obtain better understanding of how skin properties can be used to indicate storability.

8.5.4 Other non-destructive methods

When the fruit is illuminated by light, a small amount of the light is reflected at the fruit surface by specular reflection depending on the surface properties, and the remaining light penetrates into the fruit where multiple scattering occurs as a result of the change in refractive indices at the interfaces of cellular structures. Some of the scattered light will be absorbed by the chemical bonds found in the tissue, whereas some will scatter back and exit the fruit within 90° of a line normal to the fruit surface, in the form of diffuse reflectance (Williams and Norris, 2001; Lu, 2004; Lu and Peng, 2006). While absorption is determined by the chemical properties of the tissue underneath the surface (e.g. sugar, acid and water), scattering is influenced by the physical or textural properties of the tissue in terms of cellular structures, densities and small interfaces (Nicolaï et al., 2007a). In the current study the NIR sensor measures reflectance which contains information for both absorption and scattering. Given that NIR spectroscopy often performs better in predicting chemical properties of a sample (as observed in Chapter 5), it is possible that devices that explicitly quantify light scattering separately from absorption may have potentials to provide more useful insight for the assessment of fruit properties relating to texture such as firmness.

McGlone et al. (1997) assessed the use of an NIR light scattering device to estimate kiwifruit firmness quantitatively. Although moderate success was obtained (R^2 ~ 0.7) the proposed technique required complex setup procedures and hence was unsuitable for online grading purposes. Similarly, multispectral imaging techniques which enable quantification of backscattered light at a few spectral bands have been used for quantitative prediction of FF in apples (Lu, 2004; Qing et al., 2007; Sun et al., 2015). However, the technique used is too slow to be adapted at online grading speeds. Development of a high speed multispectral imaging system such as one conceptulised in Rowe (2015) with improved accuracy may have the potential to provide on-line prediction of instant and after-storage FF values of kiwifruit.

Previous attempts also used time resolved reflectance spectroscopy which measures light absorption and scattering coefficients based on time of flight distribution of photons (Nicolaï et al., 2007a). In this technique more well-defined, fundamental optical properties of the fruit surface can be obtained and as such, the models are no longer black-box (Zerbini, 2006). The scattering coefficient was found to be related to

pectin composition and textural properties of apples (Vanoli et al., 2010). What is interesting about this technique is the potential to perform qualitative prediction related to macroscopic textural properties given the promising results reported in segregation of textural profiles of kiwifruit (Baranyai and Zude, 2009) and peaches (Attanasio et al., 2015).

The hyperspectral imaging technique can provide spatial and spectral information at contiguous wavelengths over a wide spectral range. It has been applied to provide spatial light scattering images for the prediction of FF of peaches (Lu and Peng, 2006) and apples (Mendoza et al., 2011). The latter also proposed a prototype online system which achieved a scanning speed of 2 seconds per fruit. For industrial purposes a much higher speed would be required. Additionally, the above applications were designed for instant estimation of FF. More studies should look at the ability of this technique to predict future FF values.

Alternatively there are other optical techniques that provide information on surface properties of a sample which may reveal some useful information about textural profiles of the same sample. One of such examples is the fringe projection which generates 3D skin map and supports quantification of surface properties such as surface roughness (Gorthi and Rastogi, 2010; East et al., 2016). On-going studies investigate the skin topography characteristics and surface changes during development of 'SunGold' ('G3') kiwifruit and their relationship with post-storage fruit quality (Lai, unpublished work). In addition, biospeckle laser techniques, which detect biological and physical activity of the surface of the sample over time, have shown potential in predicting quality attributes (Zdunek and Cybulska, 2011) and classifying mealiness (Arefi et al., 2016) of apples.

Other non-destructive methods for firmness measurements should also be considered. For instance, impact and acoustic firmness (Aweta^{TM} Impact & Acoustic Firmness System, Nootdorp, The Netherlands), compression force (TA-XT2i, Stable Micro Systems Ltd., UK) and Kiwifirm (a prototype device developed by Plant & Food Research, New Zealand in conjunction with T.R, Turoni, Italy) were found to have good overall relationships in line with penetrometer measurements (Li et al., 2016). Alternatively, the use of multiple non-destructive sensors ('sensor fusion') was found to provide better predictions and lower errors for measuring FF in apples (Mendoza et al.,

2012) and peaches (Vursavus et al., 2015) and hence should also be considered for kiwifruit. Non-destructive methods may allow an integration of FF and NIR spectral measurements and potentially improve sorting speed and reduce labour cost.

In addition, Guay-Lord et al. (2016) proposed a system for clinical purposes which combined OCT and NIR hyperspectral imaging technique using an optical fibre coupler. This integration enabled the acquisition of sub-surface cellular structures of the sample using OCT, complemented with chemical properties of the measured region obtained using HSI. There is potential for such a system to be adapted to the horticultural industry, for the understanding, estimation and prediction of the internal quality of crops. The information captured by OCT images, NIR spectra and spatial images would provide better pictures of the physiological characteristics of the sample studied and hence may potentially contribute to new and better industrial solutions.

8.6 Thesis Conclusion

The use of OCT as a non-destructive tool to assess internal quality attributes is still in its early development stages. It has potential as a rapid technique to visualise and characterise near surface cellular structures of large parenchyma cells but is also limited by penetration depth. The information captured by the OCT images can be analysed quantitatively using the developed imaging processing protocol. Identification and characterisation of large cells between five commercial cultivars were achieved. Pre-harvest treatment effects on cellular structures within ‘Hayward’ cultivar were not observed, except that low crop load increased maximum cell length possibly due to more vigorous cell expansion during fruit growth. This technique may be used as a screening tool for plant breeding or provide information on postharvest physiological changes over time. Improved resolution may be required in order to widen its applicability.

The post-storage quality attributes of individual ‘Hayward’ kiwifruit can be predicted with marginal success by collecting at-harvest Vis-NIR spectral reflectance and generating blackbox regression models. Overall, the prediction of TSS was superior compared to that of FF. The predictive accuracy of post-storage TSS (R^2 = 0.68 – 0.83; RMSE = 0.66 – 0.86 °Brix; SDR = 1.6 – 2.3) was comparable to previous findings, indicating approximate quantitation was possible. The prediction of post-storage FF was

poor (R^2 = 0.38 – 0.60; RMSE = 3.53 – 4.12 N; SDR = 1.5 – 1.7) but in agreement with previous research on other crops, suggesting poor correlation between at-harvest spectral and post-storage firmness retention properties of kiwifruit. Industrial application of the regression models for TSS would require further reduction of sampling errors and an improvement of variability within the population.

The storage potential of individual fruit can be predicted based on its likelihood to become unacceptable for export (FF < 1 kg_f or 9.8 N) after coolstorage. At-harvest Vis-NIR spectral data and the post-storage FF collected at various time points were required in order to develop blackbox classification models. Using machine learning techniques the models segregated the population into two groups: good (FF ≥ 1 kg_f) and soft (FF < 1 kg_f). Using LogitBoost decision stumps, the true positive and false negative rates for internal cross validation were 54% and 21% respectively for the prediction of storage outcome at 125 days after coolstorage. The classification model enabled ranking and segregation of individual fruit according to their predicted probability belonging to the soft class. In external validation, segregation using the developed classification model prior to storage resulted in significantly different post-storage FF means amongst the segregated trays, with lowest FF found in trays with fruit having highest probability for the soft group. This would contribute to a reduction of soft fruit from 25.1% in the original population to 21.2% if the predicted soft group is sold early in the season, suggesting marginal commercial benefit should this model be applied.

The storage potential of grower lines could also be predicted by ranking these lines based on the predicted proportion of soft fruit using the same classification model. Based on this ranking grower lines were divided into three groups: short-, medium- and long-storing (≥ 30% soft fruit) lines. In external validation, 44% of the lines were accurately classified. The proportion of soft fruit reduced from 25.1% (without segregation) to 17.4% should the segregated short and medium storing lines be shipped earlier in the season, keeping the predicted long storing lines for later sales. Segregation of storability between grower lines showed more promising results compared to segregation of individual fruit. Potentially this could bring meaningful financial benefit to the industry (approx. $11.2M/annum saved) by enabling sequential marketing and subsequently reducing fruit loss and repacking cost and improving total profitability. However, technical capabilities are required within the industry to ensure proper

operation of the equipment and model. Additionally, the cost incurred to implement such a system online should not be overlooked.

Future studies should consider incorporating storage time as an input variable for the model because of promising preliminary results. The knowledge obtained in this thesis can be transferable to other fast-growing new kiwifruit varieties and serve as a reference for future storage related work on these cultivars. Additionally, the quantitative and qualitative models developed in this thesis can be used as guidelines for future model development using rapid and cost-effective small-scale NIR sensors. This would enable a wider range of industrial and consumer applications.

References

Agusti, M., Andreu, I., Juan, M., Almela, V., Zacarias, L., 1998. Effects of ringing branches on fruit size and maturity of peach and nectarine cultivars. J. Horticult. Sci. Biotechnol. 73, 537-540, http://dx.doi.org/10.1080/14620316.1998.11511011

Aires, R., Manfrin, A., Aluísio, S.M., Santos, D., 2004. Which classification algorithm works best with stylistic features of Portuguese in order to classify web texts according to users' needs? Technical Report No. 241. University of São Paulo, São Paulo, pp. 1-9.

Anne-Michelle, N., Mousumi, B., 2007. Machine learning methods for cancer diagnosis and prognostication, In: Khattree, R., Naik, D.N. (Eds.), Computational Methods in Biomedical Research. CRC Press, pp. 77-101.

Anonymous, 2008. Annual report. Zespri Group Ltd., p. 15.

Anonymous, 2012. Horticulture Monitoring 2012 - Bay of Plenty Kiwifruit, https://www.mpi.govt.nz/document-vault/4208 (Accessed 20 March, 2017).

Anonymous, 2013. Technical procedure manual, https://www.ams.usda.gov/sites/default/files/media/TechnicalProceduresManual%5B1%5D.pdf (Accessed 11 March, 2016).

Anonymous, 2015a. 2015 Taste review: Taste committee recommendations for green (Hayward) category, http://www.nzkgi.org.nz/media/24547/taste_committee_hayward_report_to_industry_final_19_nov_15.pdf (Accessed 2 September, 2016).

Anonymous, 2015b. Annual report. Zespri Group Ltd., p. 24.

Anonymous, 2015c. Annual report. Zespri Group Ltd., p. 8.

Anonymous, 2015d. Psa (bacterial kiwifruit vine disease), http://www.biosecurity.govt.nz/pests/kiwifruit-vine-disease (Accessed 14 April, 2016).

Anonymous, 2016a. Annual report. Zespri Group Ltd., p. 1.

Anonymous, 2016b. Annual report. Zespri Group Ltd., p. 6.

Anonymous, 2016c. Breeding for Psa resistance, http://www.plantandfood.co.nz/growingfutures/case-studies/breeding-for-psa-resistance (Accessed 31 October, 2016).

Anonymous, 2016d. Fruit quality, http://www.zespri.com/companyinformation/faqs (Accessed 29 August, 2016).

Antognozzi, E., Boco, M., Famiani, F., Palliotti, A. and Tombesi, A., 1995. Effects of different light intensity on quality and storage life of kiwifruit. ActaHortic. 379, 483-490, http://doi.org/10.17660/ActaHortic.1995.379.60

Arefi, A., Ahmadi Moghaddam, P., Hassanpour, A., Mollazade, K., Modarres Motlagh, A., 2016. Non-destructive identification of mealy apples using biospeckle imaging. Postharvest Biol. Technol. 112, 266-276, http://dx.doi.org/10.1016/j.postharvbio.2015.09.001

Arpaia, M., Boreham, D., Hofshi, R., 2001. Development of a new method for measuring minimum maturity of avocados. California Avocado Society Yearbook 85, 153-178,

Arpaia, M.L., Mitchell, F.G., Kader, A.A., Mayer, G., 1985. Effects of 2% O_2 and varying concentrations of CO_2 with or without C_2H_4 on the storage performance of kiwifruit. J. Am. Soc. Hort. Sci. 110, 200-203,

Assar, P., Eshghi, S., Tafazoli, E., Rahemi, M., Khazaeipoul, Y.G., Monfared, A.S., 2009. Improving fruit quality in 'Hayward' kiwifruit using proper leaf to fruit ratios and girdling. Horticulture, Environment and Biotechnology 50, 481-486,

Attanasio, G., Piagnani, M.C., Chiozzotto, R., Bassi, D., Spinelli, L., Torricelli, A., 2015. A preliminary approach to assess peach fruit texture by time-resolved spectroscopy (TRS). ActaHortic. 1084, 605-614, http://doi.org/10.17660/ActaHortic.2015.1084.82

Autio, W., Greene, D., 1994. Effects of growth retarding treatments on apple tree growth, fruit maturation and fruit abscission. J. Hortic. Sci. 69, 653-664, http://dx.doi.org/10.1080/14620316.1994.11516497

Bally, I.S.E., Johnson, P.R., Kulkarni, V.J., 2000. Mango production in Australia. ActaHortic. 509, 59-68, http://dx.doi.org/10.17660/ActaHortic.2000.509.3

Barandela, R., Sánchez, J.S., García, V., Rangel, E., 2003. Strategies for learning in class imbalance problems. Pattern Recognition 36, 849-851, http://dx.doi.org/10.1016/S0031-3203(02)00257-1

Baranyai, L., Zude, M., 2009. Analysis of laser light propagation in kiwifruit using backscattering imaging and Monte Carlo simulation. Comput. Electron. Agric. 69, 33-39, http://dx.doi.org/10.1016/j.compag.2009.06.011

Bartlett, M.S., Littlewort, G., Lainscsek, C., Fasel, I., Movellan, J., 2004. Machine learning methods for fully automatic recognition of facial expressions and facial actions, Proceedings of the International Conference on Systems, Man and Cybernetics, The Hague, Netherlands, pp. 592-597

Batista, G.E., Prati, R.C., Monard, M.C., 2004. A study of the behavior of several methods for balancing machine learning training data. ACM Sigkdd Explorations Newsletter 6, 20-29, http://dx.doi.org/10.1145/1007730.1007735

Bauchot, A.D., Hallett, I.C., Redgwell, R.J., Lallu, N., 1999. Cell wall properties of kiwifruit affected by low temperature breakdown. Postharvest Biol. Technol. 16, 245-255, http://dx.doi.org/10.1016/S0925-5214(99)00016-2

Beever, D.J., Hopkirk, G., 1990. Fruit development and fruit physiology, In: Warrington, I.J., Weston, G.C. (Eds.), Kiwifruit: science and management. New Zealand Society for Horticultural Science, Auckland, pp. 97-126.

Bellon-Maurel, V., Fernandez-Ahumada, E., Palagos, B., Roger, J.-M., McBratney, A., 2010. Critical review of chemometric indicators commonly used for assessing the quality of the prediction of soil attributes by NIR spectroscopy. TrAC Trends in Analytical Chemistry 29, 1073-1081, http://dx.doi.org/10.1016/j.trac.2010.05.006

Biasi, R., Costa, G., Manson, P.J., 1995. Light influence on kiwifruit (*Actinidia deliciosa*) quality. Acta Horticulturae 379, 245-252, http://doi.org/10.17660/ActaHortic.1995.379.30

Blanco, M., Villarroya, I., 2002. NIR spectroscopy: a rapid-response analytical tool. TrAC Trends in Analytical Chemistry 21, 240-250, http://dx.doi.org/10.1016/S0165-9936(02)00404-1

Bobelyn, E., Serban, A.-S., Nicu, M., Lammertyn, J., Nicolai, B.M., Saeys, W., 2010. Postharvest quality of apple predicted by NIR-spectroscopy: Study of the effect of biological variability on spectra and model performance. Postharvest Biol. Technol. 55, 133-143, http://dx.doi.org/10.1016/j.postharvbio.2009.09.006

Boyd, L.M., 2012. Resource allocation in kiwifruit (*Actinidia chinensis*): a thesis submitted in partial fulfilment of the requirements for the degree of Doctor of Philosophy, Plant Physiol. Massey University, Albany, New Zealand.

Boyd, L.M., Barnett, A.M., 2011. Manipulation of whole-vine carbon allocation using girdling, pruning, and fruit thinning affects fruit numbers and quality in kiwifruit. HortScience 46, 590-595,

Boysworth, M.K., Booksh, K.S., 2007. Aspects of Multivariate Calibration Applied to Near-Infrared Spectroscopy, Handbook of Near-Infrared Analysis, 3rd ed. CRC Press, pp. 207-229.

Breiman, L., 2001. Random forests. Machine Learning 45, 5-32, http://dx.doi.org/10.1023/A:1010933404324

Broom, F.D., Mowat, A.D., Poole, P.R., Miller, S.A., 2000. The influence of canopy management on visible-near infrared spectral properties of kiwifruit berries. ActaHortic. 515, 227-229, http://dx.doi.org/10.17660/ActaHortic.2000.515.29

Burdon, J., Lallu, N., 2011. Kiwifruit (*Actinidia* spp.), In: Yahia, E.M. (Ed.), Postharvest biology and technology of tropical and subtropical fruits. Woodhead Publishing Limited, Cambridge, pp. 326-360.

Burdon, J., Lallu, N., Francis, K., Boldingh, H., 2007. The susceptibility of kiwifruit to low temperature breakdown is associated with pre-harvest temperatures and at-harvest soluble solids content. Postharvest Biol. Technol. 43, 283-290, http://dx.doi.org/10.1016/j.postharvbio.2006.09.011

Burdon, J., McLeod, D., Lallu, N., Gamble, J., Petley, M., Gunson, A., 2004. Consumer evaluation of "Hayward" kiwifruit of different at-harvest dry matter contents. Postharvest Biol. Technol. 34, 245-255, http://dx.doi.org/10.1016/j.postharvbio.2004.04.009

Burdon, J., Pidakala, P., Martin, P., McAtee, P.A., Boldingh, H.L., Hall, A., Schaffer, R.J., 2014a. Postharvest performance of the yellow-fleshed 'Hort16A' kiwifruit in relation to fruit maturation. Postharvest Biol. Technol. 92, 98-106, http://dx.doi.org/10.1016/j.postharvbio.2014.01.004

Burdon, J., Wohlers, M., Pidakala, P., Laurie, T., Punter, M., Billing, D., 2014b. The potential for commonly measured at-harvest fruit characteristics to predict chilling susceptibility of 'Hort16A' kiwifruit. Postharvest Biol. Technol. 94, 41-48, http://dx.doi.org/10.1016/j.postharvbio.2014.03.005

Burdon, J., Wohlers, M., Pidakala, P., Laurie, T., Punter, M., Billing, D., 2014c. The potential for commonly measured at-harvest fruit characteristics to predict chilling susceptibility of 'Hort16A' kiwifruit. Postharvest Biol. Technol. 94, 41-48, https://doi.org/10.1016/j.postharvbio.2014.03.005

Buwalda, J.G., Smith, G.S., 1990. Acquisition and utilization of carbon, mineral nutrients, and water by the kiwifruit vine, In: Janick, J. (Ed.), Horticultural Reviews. Timber Press, Inc., USA, pp. 307-347.

Buxton, K.N., 2005. Preharvest practices affecting postharvest quality of 'Hayward' kiwifruit: a thesis submitted in partial fulfilment of the requirements for the degree of Doctor of Philosophy, Plant Physiology and Horticultural Science. Massey University, Palmerston North, New Zealand.

Cai, W., Li, Y., Shao, X., 2008. A variable selection method based on uninformative variable elimination for multivariate calibration of near-infrared spectra. Chemometrics Intellig. Lab. Syst. 90, 188-194, http://dx.doi.org/10.1016/j.chemolab.2007.10.001

Cai, Y.D., Feng, K.Y., Lu, W.C., Chou, K.C., 2006. Using LogitBoost classifier to predict protein structural classes. J. Theor. Biol. 238, 172-176, http://dx.doi.org/10.1016/j.jtbi.2005.05.034

Cantre, D., East, A., Verboven, P., Trejo Araya, X., Herremans, E., Nicolaï, B.M., Pranamornkith, T., Loh, M., Mowat, A., Heyes, J., 2014. Microstructural characterisation of commercial kiwifruit cultivars using X-ray micro computed tomography. Postharvest Biol. Technol. 92, 79-86, http://dx.doi.org/10.1016/j.postharvbio.2014.01.012

Caruana, R., Niculescu-Mizil, A., 2006. An empirical comparison of supervised learning algorithms, Proceedings of the 23rd International Conference on Machine Learning. ACM, Pittsburgh, Pennsylvania, USA, pp. 161-168.

Celano, G., Minnocci, A., Sebastiani, L., D'Auria, M., Xiloyannis, C., 2009. Changes in the structure of the skin of kiwifruit in relation to water loss. J. Horticult. Sci. Biotechnol. 84, 41-46, http://dx.doi.org/10.1080/14620316.2009.11512477

Chapelle, O., Vapnik, V., Bousquet, O., Mukherjee, S., 2002. Choosing multiple parameters for support vector machines. Machine Learning 46, 131-159, http://dx.doi.org/10.1023/a:1012450327387

Chawla, N.V., Bowyer, K.W., Hall, L.O., Kegelmeyer, W.P., 2002. SMOTE: synthetic minority over-sampling technique. Journal of Artificial Intelligence Research 16, 321-357, http://dx.doi.org/10.1613/jair.953

Chen, P., Tjan, Y., 1998. A real-time impact sensing system for on-line firmness sensing, International Conference of Agricultural Engineery, Oslo, pp. 98-F-006.

Chen, X., Han, W., 2012. Spectroscopic determination of soluble solids content of 'Qinmei' kiwifruit using partial least squares. Afr J Biotechnol 11, 2528-2536, http://dx.doi.org/10.5897/AJB11.3177

Clark, C.J., McGlone, V.A., De Silva, H.N., Manning, M.A., Burdon, J., Mowat, A.D., 2004. Prediction of storage disorders of kiwifruit (*Actinidia chinensis*) based on visible-NIR spectral characteristics at harvest. Postharvest Biol. Technol. 32, 147-158, http://dx.doi.org/10.1016/j.postharvbio.2003.11.004

Clements, J.C., Zvyagin, A.V., Silva, K., Wanner, T., Sampson, D.D., Cowling, W.A., 2004. Optical coherence tomography as a novel tool for non-destructive measurement of the hull thickness of lupin seeds. Plant Breeding 123, 266-270, http://dx.doi.org/10.1111/j.1439-0523.2004.00989.x

Coates, J., 2014. A review of new small-scale technologies for near infrared measurements, http://www.americanpharmaceuticalreview.com/Featured-Articles/163573-A-Review-of-New-Small-Scale-Technologies-for-Near-Infrared-Measurements/ (Accessed 30 March, 2017).

Coombe, B., 1976. The development of fleshy fruits. Annual Review of Plant Physiology 27, 207-228, http://www.annualreviews.org/doi/pdf/10.1146/annurev.pp.27.060176.001231

Costa, G., Andreotti, C., Miserocchi, O., Noferini, M., Smith, G., 1999. Near-infrared (NIR) methods to determine kiwifruit field harvest date and maturity parameters in cool store. ActaHortic. 498, 231-238, http://dx.doi.org/10.17660/ActaHortic.1999.498.26

Costa, G., Grappadelli, L.C., Noferini, M., Fiori, G., 2003a. Use of light reflective mulch to affect yield and fruit quality. ActaHortic. 610, 139-144, http://doi.org/10.17660/ActaHortic.2003.610.17

Costa, G., Noferini, M., Montefiori, M., Brigati, S., 2003b. Non-destructive assessment methods of kiwifruit quality. ActaHortic. 610, 179-189, http://dx.doi.org/10.17660/ActaHortic.2003.610.24

Crisosto, C., Costa, G., 2008. Preharvest factors affecting peach quality, In: Layne, D., Bassi, D. (Eds.), The peach: botany, production and uses. CAB International, UK, pp. 536-549.

Crisosto, C.H., Crisosto, G.M., 2001. Understanding consumer acceptance of early harvested 'Hayward' kiwifruit. Postharvest Biol. Technol. 22, 205-213, http://dx.doi.org/10.1016/S0925-5214(01)00097-7

Crisosto, C.H., Zegbe, J., Hasey, J., Crisosto, G.M., 2011. Is dry matter a reliable quality index for 'Hayward' kiwifruit? ActaHortic. 913, 531-534, http://doi.org/10.17660/ActaHortic.2011.913.71

Crisosto, G., Hasey, J.K., Zegbe, J.A., Crisosto, C.H., 2012a. New quality index based on dry matter and acidity proposed for Hayward kiwifruit. Calif. Agric. 66, http://dx.doi.org/10.3733/ca.v066n02p70

Crisosto, G.M., Hasey, J., Zegbe, J.A., Crisosto, C.H., 2012b. New quality index based on dry matter and acidity proposed for Hayward kiwifruit. Calif. Agric. 66, 70-75, http://doi.org/10.3733/ca.v066n02p70

Currie, M.B., 1997. Source-sink relations in kiwifruit: carbohydrate and hormone effects on fruit growth at the cell, organ and whole plant level: a thesis submitted in partial fulfilment of the requirements for the degree of Doctor of Philosophy, Plant Physiology and Horticultural Science. Massey University, Palmerston North, New Zealand.

Currie, M.B., Jackman, R., Blattmann, P., Max, S., 2007. Reflecting on high dry matter. New Zealand Kiwifruit November/December 2007, 16-21,

Davison, R.M., 1980. Girdling of young kiwifruit vines to increase cropping. Orchardist of New Zealand 53, 5-7,

Davison, R.M., 1990. The physiology of the kiwifruit vine, In: Warrington, I.J., Weston, G.C. (Eds.), Kiwifruit: science and management. New Zealand Society for Horticultural Science, Auckland, pp. 127-154.

Dehzangi, A., Karamizadeh, S., 2011. Solving protein fold prediction problem using fusion of heterogeneous classifiers. Information 14, 3611-3622,

Doud, D.S., Ferree, D.C., 1980. Influence of altered light levels on growth and fruiting of mature delicious apple-trees. J. Am. Soc. Hort. Sci. 105, 325-328,

Drexler, W., Fujimoto, J.G., 2008. State-of-the-art retinal optical coherence tomography. Progress in Retinal and Eye Research 27, 45-88, http://dx.doi.org/10.1016/j.preteyeres.2007.07.005

Dubey, R., Zhou, J., Wang, Y., Thompson, P.M., Ye, J., 2014. Analysis of sampling techniques for imbalanced data: An n= 648 ADNI study. NeuroImage 87, 220-241, http://dx.doi.org/10.1016/j.neuroimage.2013.10.005

East, A.R., Bloomfield, C., Trejo Araya, X., Heyes, J.A., 2016. Evaluation of fringe projection as a method to provide information about horticultural product surfaces. ActaHortic. 1119, 189-196, http://dx.doi.org/10.17660/ActaHortic.2016.1119.26

East, A.R., Jabbar, A., Heyes, J.A., 2013. Approaches to prediction of storage out-turn for units of fresh produce. ActaHortic. 1012, 1303-1309, http://dx.doi.org/10.17660/ActaHortic.2013.1012.175

Eichelberger, R.K., Sheng, V.S., 2013a. Does one-against-all or one-against-one improve the performance of multiclass classifications?, Proceedings of the Twenty-Seventh AAAI Conference on Artificial Intelligence, Washington, USA, pp. 1609-1610.

Eichelberger, R.K., Sheng, V.S., 2013b. An Empirical Study of Reducing Multiclass Classification Methodologies, 9th International Conference on Machine Learning and Data Mining in Pattern Recognition, New York, USA,, pp. 505-519.

Elkan, C., 2001. The foundations of cost-sensitive learning, Proceedings of the 17th International Joint Conference on Artificial Intelligence, Washington, USA, pp. 973-978.

Elrahman, S.M.A., Abraham, A., 2013. A review of class imbalance problem. Journal of Network and Innovative Computing 1, 332-340,

Elvidge, C.D., 1990. Visible and near infrared reflectance characteristics of dry plant materials. Int. J. Remote Sens. 11, 1775-1795, http://dx.doi.org/10.1080/01431169008955129

Ezura, H., Hiwasa-Tanase, K., 2010. Fruit development, In: Pua, E.C., Davey, M.R. (Eds.), Plant developmental biology - biotechnological perspectives. Springer-Verlag, Berlin, Heidelberg, pp. 301-318.

Famiani, F., Baldicchi, A., Farinelli, D., Cruz-Castillo, J.G., Marocchi, F., Mastroleo, M., Moscatello, S., Proietti, S., Battistelli, A., 2012. Yield affects qualitative kiwifruit characteristics and dry matter content may be an indicator of both quality and storability. Scientia Horticulturae 146, 124-130, http://dx.doi.org/10.1016/j.scienta.2012.08.009

Fan, S., Zhang, B., Li, J., Huang, W., Wang, C., 2016. Effect of spectrum measurement position variation on the robustness of NIR spectroscopy models for soluble solids content of apple. Biosys. Eng. 143, 9-19, http://dx.doi.org/10.1016/j.biosystemseng.2015.12.012

Feelders, A., Daniels, H., Holsheimer, M., 2000. Methodological and practical aspects of data mining. Information & Management 37, 271-281, http://dx.doi.org/10.1016/S0378-7206(99)00051-8

Feng, J., 2003. Segregation of 'Hayward' kiwifruit for storage potential: a thesis presented in partial fulfilment of the requirements for the degree of Doctor of Philosophy. Massey University, Palmerston North, New Zealand.

Feng, J., MacKay, B.R., Maguire, K.M., 2001. A procedure for calculating storage life of Hayward kiwifruit. ActaHortic. 566, 455-460, http://dx.doi.org/10.17660/ActaHortic.2001.566.58

Feng, J., McGlone, A., Tanner, D., White, A., Olsson, S., Petley, M., Woolf, l., 2011. Effect of penetration speed on flesh firmness measured on stored kiwifruit. Postharvest Biol. Technol. 61, 29-34, http://dx.doi.org/10.1016/j.postharvbio.2011.01.014

Feng, J., Stanley, J., Othman, M., Woolf, A., Kosasih, M., Olsson, S., Clare, G., Cooper, N., Wang, X., 2013. Segregation of apricots for storage potential using non-destructive technologies. Postharvest Biol. Technol. 86, 17-22, http://dx.doi.org/10.1016/j.postharvbio.2013.06.015

Feng, J., Wohlers, M., Olsson, S., White, A., McGlone, V.A., Seelye, R., Tanner, D., Bollen, F., 2014. Comparison between an acoustic firmness sensor and a near-infrared spectrometer in segregation of kiwifruit for storage potential. ActaHortic. 1119, 279-288, http://doi.org/10.17660/ActaHortic.2016.1119.39

Fercher, A.F., Hitzenberger, C.K., Kamp, G., El-Zaiat, S.Y., 1995. Measurement of intraocular distances by backscattering spectral interferometry. Optics Communications 117, 43-48, http://dx.doi.org/10.1016/0030-4018(95)00119-S

Ferguson, A., Seal, A., 2008. Kiwifruit, In: Hancock, J. (Ed.), Temperate Fruit Crop Breeding. Springer, pp. 235-264.

Ferguson, A.R., 2011. Kiwifruit: Evolution of a crop. ActaHortic. 913, 31-42, http://dx.doi.org/10.17660/ActaHortic.2011.913.1

Ferguson, I., Volz, R., Woolf, A., 1999. Preharvest factors affecting physiological disorders of fruit. Postharvest Biol. Technol. 15, 255-262, http://dx.doi.org/10.1016/S0925-5214(98)00089-1

Fisher, E., 2011. Kiwifruit closely monitored at port, http://www.nzherald.co.nz/bay-of-plenty-times/rural/news/article.cfm?c_id=1503348&objectid=11026062 (Accessed 14 April, 2016).

Ford, H.D., Tatam, R.P., Landahl, S., Terry, L.A., 2012. Investigation of disease in stored onions using optical coherence tomography. ActaHortic. 945, 247-254, http://doi.org/10.17660/ActaHortic.2012.945.33

Fox, A., 2015. Kiwifruit back from the brink, http://www.stuff.co.nz/business/farming/agribusiness/71740134/Kiwifruit-back-from-the-brink (Accessed 31 October, 2016).

Freund, Y., Schapire, R.E., 1996. Experiments with a new boosting algorithm, Proceedings of the 13th International Conference on Machine Learning, Bari, Italy, pp. 148-156.

Friedman, J., Hastie, T., Tibshirani, R., 2000. Additive logistic regression: a statistical view of boosting. The Annals of Statistics 28, 337-407, http://dx.doi.org/10.1214/aos/1016218223

Friedman, J.H., 2006. Recent advances in predictive (machine) learning. Journal of Classification 23, 175-197, http://dx.doi.org/10.1007/s00357-006-0012-4

Fu, X., Ying, Y., Zhou, Y., Xie, L., Xu, H., 2008. Application of NIR spectroscopy for firmness evaluation of peaches. Journal of Zhejiang University Science B 9, 552-557, http://dx.doi.org/10.1631/jzus.B0720018

Fukui, M., Noda, H., Yamada, M., 1980. Properties of the proteolytic enzyme and chemical composition in Chinese gooseberries. Kagawa Agricultural Experiment Station, Japan.

Gardiner, C., Max, S., Currie, M.B., 2005. Zero Leaf Pruning - A new technique for managing 'Hort16A' vigour? New Zealand Kiwifruit Journal July/August, 14-17,

Garrett, G., 2002. Our method explained, US News and World Report: Best Graduate Schools 2003 Edition, Washington, D.C., pp. 34-35.

Ghasemnezhad, M., Ghorbanalipour, R., Shiri, M.A., 2013. Changes in physiological characteristics of kiwifruit harvested at different maturity stages after cold storage. Agric. Conspec. Sci. 78, 41-47,

Goldring, D., Sharon, D., 2012. Low-cost spectrometry system for end-user food analysis. World Intellectual Property Organisation (WIPO).

Gordon Mitchell, F., Mayer, G., Biasi, W., 1992. Effect of harvest maturity on storage performance of 'Hayward' kiwifruit. ActaHortic. 297, 617-625, http://dx.doi.org/10.17660/ActaHortic.1992.297.82

Goren, R., Huberman, M., Goldschmidt, E., 2003. Girdling: physiological and horticultural aspects, In: Janick, J. (Ed.), Horticultural Reviews. John Wiley & Sons, Inc., Oxford, UK, pp. 1-36.

Gorthi, S.S., Rastogi, P., 2010. Fringe projection techniques: Whither we are? Optics and Lasers in Engineering 48, 133-140, http://dx.doi.org/10.1016/j.optlaseng.2009.09.001

Gorunescu, F., 2011. Classification performance evaluation, In: Kacprzyk, J., Jain, L.C. (Eds.), Data mining: concepts, models and techniques, 1st ed. Springer-Verlag, Berlin, pp. 319-331.

Gowen, A.A., Downey, G., Esquerre, C., O'Donnell, C.P., 2011. Preventing over-fitting in PLS calibration models of near-infrared (NIR) spectroscopy data using regression coefficients. J. Chemometrics 25, 375-381, http://dx.doi.org/10.1002/cem.1349

Guay-Lord, R., Attendu, X., Lurie, K.L., Majeau, L., Godbout, N., Bowden, A.K.E., Strupler, M., Boudoux, C., 2016. Combined optical coherence tomography and hyperspectral imaging using a double-clad fiber coupler. Journal of Biomedical Optics 21, 1-6, http://dx.doi.org/10.1117/1.JBO.21.11.116008

Gunn, S.R., 1998. Support vector machines for classification and regression, Technical report. Faculty of Engineering, Science and Mathematics, School of Electronics and Computer Science, University of Southampton.

Hair, J.F., Black, W.C., Babin, B.J., Anderson, R.E., Tatam, R.L., 2006. Multiple Distriminant Analysis and Logistic Regression, In: Hair, J.F., Black, W.C., Babin, B.J., Anderson, R.E., Tatam, R.L. (Eds.), Multivariate Data Analysis. Pearson Prentice Hall, U.S.A., pp. 269-382.

Hall, M., Frank, E., Holmes, G., Pfahringer, B., Reutemann, P., Witten, I.H., 2009. The WEKA data mining software: An update. SIGKDD Explorations 11, 10-18, http://dx.doi.org/10.1145/1656274.1656278

Hallett, I.C., Macrae, E.A., Wegrzyn, T.F., 1992. Changes in kiwifruit cell wall ultrastructure and cell packing during postharvest ripening. Int. J. Plant Sci. 153, 49-60,

Hallett, I.C., Sutherland, P.W., 2005. Structure and development of kiwifruit skins. Int. J. Plant Sci. 166, 693-704, http://dx.doi.org/10.1086/431232

Hallett, I.C., Sutherland, P.W., 2007. Kiwifruit skins: the fruit's natural packaging. ActaHortic. 753, 89-96, http://dx.doi.org/10.17660/ActaHortic.2007.753.8

Hallett, I.C., Sutherland, P.W., Harker, F.R., MacRae, E.A., 2005. Fruit cell walls texture and convenience. Microscopy and Microanalysis 11, 1144-1145, http://dx.doi.org/10.1017/S1431927605504641

Harker, F.R., Carr, B.T., Lenjo, M., MacRae, E.A., Wismer, W.V., Marsh, K.B., Williams, M., White, A., Lund, C.M., Walker, S.B., Gunson, F.A., Pereira, R.B., 2009. Consumer liking for kiwifruit flavour: A meta-analysis of five studies on fruit quality. Food Quality and Preference 20, 30-41, http://dx.doi.org/10.1016/j.foodqual.2008.07.001

Harman, J.E., 1981. Kiwifruit maturity. The Orchardist of New Zealand 54, 126-130,

Harman, J.E., Hopkirk, G., 1982. Kiwifruit testing for maturity, 1st ed. Ministry of Agriculture and Fisheries, Wellington.

Hasey, J.K., 1994. Kiwifruit growing and handling. The Regents of University of California, Division of Agriculture and Natural Resources, USA.

Haughey, S.A., Galvin-King, P., Malechaux, A., Elliott, C.T., 2015. The use of handheld near-infrared reflectance spectroscopy (NIRS) for the proximate analysis of poultry feed and to detect melamine adulteration of soya bean meal. Anal Methods 7, 181-186, http://dx.doi.org/10.1039/C4AY02470B

Hewett, E.W., 2006. An overview of preharvest factors influencing postharvest quality of horticultural products. International Journal of Postharvest Technology and Innovation 1, 4-15, http://dx.doi.org/10.1504/IJPTI.2006.009178

Hopkirk, G., Beever, D.J., Triggs, C.M., 1986. Variation in soluble solids concentration in kiwifruit at harvest. N. Z. J. Agric. Res. 29, 475-484, http://dx.doi.org/10.1080/00288233.1986.10423500

Hopkirk, G., Maindonald, J., White, A., 1996. Comparison of four new devices for measuring kiwifruit firmness. N. Z. J. Crop Hortic. Sci. 24, 273-286, http://dx.doi.org/10.1080/01140671.1996.9513962

Hopping, M., 1976. Structure and development of fruit and seeds in Chinese gooseberry (*Actinidia chinensis* Planch.). N. Z. J. Bot. 14, 63-68, http://dx.doi.org/10.1080/0028825X.1976.10428651

Hu, W., Sun, D.-W., Blasco, J., 2017. Rapid monitoring 1-MCP-induced modulation of sugars accumulation in ripening 'Hayward' kiwifruit by Vis/NIR hyperspectral imaging. Postharvest Biol. Technol. 125, 168-180, http://dx.doi.org/10.1016/j.postharvbio.2016.11.001

Huang, H., 2016. Domestication and Commercialization of *Actinidia*, In: Huang, H. (Ed.), Kiwifruit: the genus *Actinidia*. Academic Press, San Diego, pp. 191-210.

Ignat, T., Lurie, S., Nyasordzi, J., Ostrovsky, V., Egozi, H., Hoffman, A., Friedman, H., Weksler, A., Schmilovitch, Z.e., 2014. Forecast of Apple Internal Quality

Indices at Harvest and During Storage by VIS-NIR Spectroscopy. Food Bioprocess Tech 7, 2951-2961, http://dx.doi.org/10.1007/s11947-014-1297-7

Ivanciuc, O., 2007. Applications of support vector machines in chemistry, In: Lipkowitz, K.B., Cundari, T.R. (Eds.), Reviews in Computational Chemistry. John Wiley & Sons, Inc., Hoboken, New Jersey, pp. 291-400.

Jabbar, A., 2014. Accelerated fruit libraries to predict storage potential of 'hayward' kiwifruit grower lines: A thesis presented in partial fulfilment of the requirements for the Degree of Doctor of Philosophy in Food Technology at Massey University, New Zealand.

Jabbar, A., East, A., 2016. Quantifying the ethylene induced softening and low temperature breakdown of 'Hayward' kiwifruit in storage. Postharvest Biol. Technol. 113, 87-94, http://dx.doi.org/10.1016/j.postharvbio.2015.11.002

Jeffery, P.B., Banks, N.H., 1994. Firmness - temperature coefficient of kiwifruit. N. Z. J. Crop Hortic. Sci. 22, 97-101, http://dx.doi.org/10.1080/01140671.1994.9513811

Jha, S.N., 2010. Near infrared spectroscopy, In: Jha, S.N. (Ed.), Nondestructive evaluation of food quality: theory and practice. Springer-Verlag, Berlin, pp. 141-212.

Jordan, R.B., Seelye, R.J., 2009. Relationship between taste perception, density and soluble solids concentration in kiwifruit (*Actinidia deliciosa*). N. Z. J. Crop Hortic. Sci. 37, 303-317, http://dx.doi.org/10.1080/01140671.2009.9687585

Jordan, R.B., Walton, E.F., Klages, K.U., Seelye, R.J., 2000. Postharvest fruit density as an indicator of dry matter and ripened soluble solids of kiwifruit. Postharvest Biol. Technol. 20, 163-173, http://dx.doi.org/10.1016/S0925-5214(00)00125-3

Juan, M., Mesejo, C., Martínez-Fuentes, A., Reig, C., Agustí, M., 2009. Branch scoring encourages fruit development and climacteric in persimmon. Scientia Horticulturae 122, 497-500, http://dx.doi.org/10.1016/j.scienta.2009.06.003

Jung, J.J., 2009. Trustworthy knowledge diffusion model based on risk discovery on peer-to-peer networks. Expert Systems with Applications 36, 7123-7128, http://dx.doi.org/10.1016/j.eswa.2008.08.048

Kalivas, J.H., Gemperline, P.J., 2006. Calibration, In: Gemperline, P. (Ed.), Practical guide to chemometrics, 2nd ed. CRC Press, pp. 105-166.

Kemper, T., Sommer, S., 2002. Estimate of heavy metal contamination in soils after a mining accident using reflectance spectroscopy. Environ. Sci. Technol. 36, 2742-2747, http://dx.doi.org/10.1021/es015747j

Kenouche, S., Perrier, M., Bertin, N., Larionova, J., Ayadi, A., Zanca, M., Long, J., Bezzi, N., Stein, P.C., Guari, Y., Cieslak, M., Godin, C., Goze-Bac, C., 2014. In vivo quantitative NMR imaging of fruit tissues during growth using Spoiled Gradient Echo sequence. Magn. Reson. Imaging, 1418-1427, http://dx.doi.org/10.1016/j.mri.2014.08.005

Khorshid, M.M., Abou-El-Enien, T.H., Soliman, G.M., 2015. A comparison among support vector machine and other machine learning classification algorithms. IPASJ International Journal of Computer Science 3, 25-35,

Kim, H.O., 1999. The role of ethylene in kiwifruit softening: a thesis presented in partial fulfilment of the requirements for the degree of Doctor of Philosophy in Plant Science. Massey University, Palmerston North, New Zealand.

Kim, J., Mowat, A., Poole, P., Kasabov, N., 2000. Linear and non-linear pattern recognition models for classification of fruit from visible–near infrared spectra. Chemometrics Intellig. Lab. Syst. 51, 201-216, http://dx.doi.org/10.1016/S0169-7439(00)00070-8

Kim, K., Seo, M., Kang, H., Cho, S., Kim, H., Seo, K., 2015. Application of LogitBoost classifier for traceability using SNP chip data. PLoS ONE 10, 1-16, http://dx.doi.org/10.1371/journal.pone.0139685

Knowles, M., 2016. Consumers testing new green Zespri kiwifruit, http://www.fruitnet.com/eurofruit/article/169541/consumers-testing-new-green-zespri-kiwifruit (Accessed 16th February, 2017).

Kojima, T., Fujita, S., Tanaka, M., Sirisomboon, P., 2004. Plant compounds and fruit texture: the case of pear, In: Kilcast, D. (Ed.), Texture in Food, 1st ed. Woodhead Publishing Ltd., Cambridge, England, pp. 259-294.

Kotsiantis, S.B., Kanellopoulos, D., Pintelas, P.E., 2006. Local boosting of decision stumps for regression and classification problems. Journal of Computers 1, 30-37, http://dx.doi.org/10.1.1.90.4420

Kramer, R., Workman, J., Reeves, J.B., 2004. Qualitative analysis, In: Roberts, C.A., Workman Jr, J., Reeves Iii, J.B. (Eds.), Near-Infrared Spectroscopy in Agriculture, 1st ed. American Society of Agronomy, Crop Science Society of America, Soil Science Society of America, Madison, WI, pp. 175-206.

Krishnaraj, Y., Reddy, C.K., 2008. Boosting methods for protein fold recognition: an empirical comparison, International Conference on Bioinformatics and Biomedicine. IEEE, Philadelphia, USA, pp. 393-396.

Kuckenberg, J., Tartachnyk, I., Noga, G., 2008. Evaluation of fluorescence and remission techniques for monitoring changes in peel chlorophyll and internal fruit characteristics in sunlit and shaded sides of apple fruit during shelf-life. Postharvest Biol. Technol. 48, 231-241, http://dx.doi.org/10.1016/j.postharvbio.2007.10.013

Lallu, N., 1997. Low temperature breakdown in kiwifruit. ActaHortic. 444, 579-585, http://doi.org/10.17660/ActaHortic.1997.444.89

Lallu, N., Searle, A.N., Macrae, E.A., 1989. An investigation of ripening and handling strategies for early season kiwifruit (*Actinidia deliciosa* cv Hayward). J. Sci. Food Agric. 47, 387-400, http://dx.doi.org/10.1002/jsfa.2740470402

Lammertyn, J., Nicolaï, B., De Smedt, V., De Baerdemaeker, J., 1997. Non-destructive measurement of pH, soluble solids and firmness of Jonagold apples using NIR-spectroscopy. ActaHortic. 562, 167-173, http://doi.org/10.17660/ActaHortic.2001.562.18

Lammertyn, J., Peirs, A., De Baerdemaeker, J., Nicolaï, B., 2000. Light penetration properties of NIR radiation in fruit with respect to non-destructive quality assessment. Postharvest Biol. Technol. 18, 121-132, http://dx.doi.org/10.1016/S0925-5214(99)00071-X

Landahl, S., Terry, L.A., Ford, H.D., 2012. Investigation of diseased onion bulbs using data processing of optical coherence tomography images. VI International Symposium on Edible Alliaceae 969, 261-269,

Lee, J.S., Kim, S.C., Seong, K.C., Kim, C.H., Um, Y.C., Lee, S.K., 2012. Quality prediction of kiwifruit based on near infrared spectroscopy. Korean J Hortic Sci 30, 709-717, http://dx.doi.org/10.7235/hort.2012.12139

Li, H., Pidakala, P., Billing, D., Burdon, J., 2016. Kiwifruit firmness: Measurement by penetrometer and non-destructive devices. Postharvest Biol. Technol. 120, 127-137, http://dx.doi.org/10.1016/j.postharvbio.2016.06.007

Li, J.Q., Li, X.W., Soejarto, D.D., 2007. *Actinidiaceae*, In: Wu, C.Y., P., R. (Eds.), Flora of China. Science Press, Beijing, pp. 334-360

Liu, W., Hui, G., 2015. Kiwi fruit (*Actinidia chinensis*) quality determination based on surface acoustic wave resonator combined with electronic nose. Bioengineered 6, 53-61, 10.1080/21655979.2014.996430

Liu, Y., Sun, X., Zhou, J., Zhang, H., Yang, C., 2010. Linear and nonlinear multivariate regressions for determination sugar content of intact Gannan navel orange by Vis–NIR diffuse reflectance spectroscopy. Mathematical and Computer Modelling 51, 1438-1443, http://dx.doi.org/10.1016/j.mcm.2009.10.003

Lodge, N., Roberston, G.L., 1990. Processing of kiwifruit, In: Warrington, I.J., Weston, G.C. (Eds.), Kiwifruit: science and management. New Zealand Society for Horticultural Science, Auckland, pp. 461-484.

Loeb, G., Barton, J.K., 2003. Imaging botanical subjects with optical coherence tomography: A feasibility study. Transactions of the American Society of Agricultural Engineers 46, 1751-1757,

López, V., Fernández, A., García, S., Palade, V., Herrera, F., 2013. An insight into classification with imbalanced data: Empirical results and current trends on using data intrinsic characteristics. Information Sciences 250, 113-141, http://dx.doi.org/10.1016/j.ins.2013.07.007

Lu, R., 2001. Predicting firmness and sugar content of sweet cherries using near–infrared diffuse reflectance spectroscopy. Transactions of the American Society of Agricultural Engineers 44, 1265-1271, http://dx.doi.org/10.13031/2013.6421

Lu, R., 2004. Multispectral imaging for predicting firmness and soluble solids content of apple fruit. Postharvest Biol. Technol. 31, 147-157, http://dx.doi.org/10.1016/j.postharvbio.2003.08.006

Lu, R., Guyer, D.E., Beaudry, R.M., 2000. Determination of firmness and sugar content of apples using near-infrared diffuse reflectance. Journal of Texture Studies 31, 615-630, http://dx.doi.org/10.1111/j.1745-4603.2000.tb01024.x

Lu, R., Peng, Y., 2006. Hyperspectral Scattering for assessing Peach Fruit Firmness. Biosys. Eng. 93, 161-171, http://dx.doi.org/10.1016/j.biosystemseng.2005.11.004

MacRae, E., Quick, W.P., Benker, C., Stitt, M., 1992. Carbohydrate metabolism during postharvest ripening in kiwifruit. Planta 188, 314-323, http://dx.doi.org/10.1007/BF00192797

MacRae, E.A., Redgwell, R.J., Wegrzyn, T., 1990. The whens and hows of fruit softening. New Zealand Kiwifruit Journal February, 17,

Magwaza, L.S., Ford, H.D., Cronje, P.J.R., Opara, U.L., Landahl, S., Tatam, R.P., Terry, L.A., 2013. Application of optical coherence tomography to non-destructively characterise rind breakdown disorder of 'Nules Clementine' mandarins. Postharvest Biol. Technol. 84, 16-21, http://dx.doi.org/10.1016/j.postharvbio.2013.03.019

Martinsen, P., Schaare, P., 1998. Measuring soluble solids distribution in kiwifruit using near-infrared imaging spectroscopy. Postharvest Biol. Technol. 14, 271-281, http://dx.doi.org/10.1016/S0925-5214(98)00051-9

Mathur, A., Foody, G., 2008. Multiclass and binary SVM classification: Implications for training and classification users. Geoscience and Remote Sensing Letters 5, 241-245, http://dx.doi.org/10.1109/LGRS.2008.915597

Max, S., Currie, M.B., 2005. Tip squeezing 'Hort16A' shoots to control vegetative growth. New Zealand Kiwifruit Journal September, 22-24,

McBeth, P., 2016. Zespri raises 2016 forecast tray prices, growth seen in 2017, http://www.scoop.co.nz/stories/BU1602/S00756/zespri-raises-2016-forecast-tray-prices-growth-seen-in-2017.htm (Accessed 20th October, 2016).

McCallum, A., Nigam, K., 1998. A comparison of event models for naive bayes text classification, Workshop on Learning for Text Categorization, Madison, USA, pp. 41-48.

McClure, W.F., 2006. Introduction, In: Ozaki, Y., McClure, W.F., Christy, A.A. (Eds.), Near-Infrared Spectroscopy in Food Science and Technology. John Wiley & Sons, Inc., Canada, pp. 1-10.

McClure, W.F., Tsuchikawa, S., Lewis, E.N., Dubois, J., Kidder, L.H., 2006. Instrumentation, In: Ozaki, Y., McClure, W.F., Christy, A.A. (Eds.), Near-Infrared Spectroscopy in Food Science and Technology. John Wiley & Sons, Inc., Canada, pp. 73-132.

McDonald, R.A., Hand, D.J., Eckley, I.A., 2003. An empirical comparison of three boosting algorithms on real data sets with artificial class noise, International Workshop on Multiple Classifier Systems. Springer, pp. 35-44.

McGlone, A., Wohlers, M., 2016. Using NIR sorting for Gold3. New Zealand Kiwifruit Journal March/April, 26-28,

McGlone, V., Abe, H., Kawano, S., 1997. Kiwifruit firmness by near infrared light scattering. Journal of Near Infrared Spectroscopy 5, 83-90, http://dx.doi.org/10.1255/jnirs.102

McGlone, V.A., Clark, C.J., Jordan, R.B., 2007. Comparing density and VNIR methods for predicting quality parameters of yellow-fleshed kiwifruit (*Actinidia chinensis*). Postharvest Biol. Technol. 46, 1-9, http://dx.doi.org/10.1016/j.postharvbio.2007.04.003

McGlone, V.A., Jordan, R.B., Martinsen, P.J., 2002a. Vis/NIR estimation at harvest of pre- and post-storage quality indices for 'Royal Gala' apple. Postharvest Biol. Technol. 25, 135-144, http://dx.doi.org/10.1016/S0925-5214(01)00180-6

McGlone, V.A., Jordan, R.B., Seelye, R., Martinsen, P.J., 2002b. Comparing density and NIR methods for measurement of kiwifruit dry matter and soluble solids content. Postharvest Biol. Technol. 26, 191-198, http://dx.doi.org/10.1016/S0925-5214(02)00014-5

McGlone, V.A., Kawano, S., 1998. Firmness, dry-matter and soluble-solids assessment of postharvest kiwifruit by NIR spectroscopy. Postharvest Biology and Technology 13, 131-141, http://dx.doi.org/10.1016/S0925-5214(98)00007-6

Mebatsion, H.K., Verboven, P., Endalew, A.M., Billen, J., Ho, Q.T., Nicolaï, B., 2009. A novel method for 3-D microstructure modeling of pome fruit tissue using synchrotron radiation tomography images. J. Food Eng. 93, 141-148, http://dx.doi.org/10.1016/j.jfoodeng.2009.01.008

Meglinski, I., Buranachai, C., Terry, L., 2010. Plant photonics: application of optical coherence tomography to monitor defects and rots in onion. Laser Physics Letters 7, 307, http://dx.doi.org/10.1002/lapl.200910141

Mendoza, F., Lu, R., Ariana, D., Cen, H., Bailey, B., 2011. Integrated spectral and image analysis of hyperspectral scattering data for prediction of apple fruit firmness and soluble solids content. Postharvest Biol. Technol. 62, 149-160, http://dx.doi.org/10.1016/j.postharvbio.2011.05.009

Mendoza, F., Lu, R., Cen, H., 2012. Comparison and fusion of four nondestructive sensors for predicting apple fruit firmness and soluble solids content. Postharvest Biol. Technol. 73, 89-98, http://dx.doi.org/10.1016/j.postharvbio.2012.05.012

Mika, A., Treder, W., Buler, Z., Rutkowski, K., 2007. Attempts on improving light relation and apple fruit quality by reflective mulch. ActaHortic. 732, 605-610, http://dx.doi.org/10.17660/ActaHortic.2007.732.90

Miller, C.E., 2001. Chemical principles of near-infrared technology, In: Williams, P.C., Norris, K.H. (Eds.), Near-infrared technology: in the agricultural and food

industries, 2nd ed. American Association of Cereal Chemists, Minnesota, pp. 19-39.

Moghimi, A., Aghkhani, M.H., Sazgarnia, A., Sarmad, M., 2010. Vis/NIR spectroscopy and chemometrics for the prediction of soluble solids content and acidity (pH) of kiwifruit. Biosys. Eng. 106, 295-302, http://dx.doi.org/10.1016/j.biosystemseng.2010.04.002

Mohri, M., Rostamizadeh, A., Talwalkar, A., 2012. Support vector machines, Foundations of machine learning. The MIT Press, Massachusetts, USA, pp. 63-84.

Montanaro, G., Dichio, B., Xiloyannis, C., Celano, G., 2006. Light influences transpiration and calcium accumulation in fruit of kiwifruit plants (*Actinidia deliciosa* var. *deliciosa*). Plant Sci. 170, 520-527, http://dx.doi.org/10.1016/j.plantsci.2005.10.004

Mowat, A.D., Poole, P.R., 1997. Use of visible-near infrared diffuse reflectance spectroscopy to discriminate between kiwifruit with properties altered by preharvest treatments. Journal of Near Infrared Spectroscopy 5, 113-122,

Muskovics, G., Felföldi, J., Kovács, E., Perlaki, R., Kállay, T., 2006. Changes in physical properties during fruit ripening of Hungarian sweet cherry (*Prunus avium* L.) cultivars. Postharvest Biol. Technol. 40, 56-63, http://dx.doi.org/10.1016/j.postharvbio.2005.12.007

Naes, T., Isakson, T., Fearn, T., Davies, T., 2004. A user‐friendly guide to multivariate calibration and classification. J. Chemometrics 17, 571-572, http://dx.doi.org/10.1002/cem.815

Nardozza, S., 2008. Genotypic variation in *Actinidia deliciosa* fruit size and carbohydrate content, Department of Agricultural Sciences. University of Bologna, Bologna, Italy.

Nardozza, S., Hallett, I.C., McCartney, R., Richardson, A.C., MacRae, E.A., Costa, G., Clearwater, M.J., 2011. Is fruit anatomy involved in variation in fruit starch concentration between Actinidia deliciosa genotypes? Funct. Plant Biol. 38, 63-74,

Nguyen, H.-N., Vu, T.-N., Ohn, S.-Y., Park, Y.-M., Han, M.Y., Kim, C.W., 2006. Feature elimination approach based on random forest for cancer diagnosis,

Mexican International Conference on Artificial Intelligence. Springer, pp. 532-542.

Nicolaï, B.M., Beullens, K., Bobelyn, E., Peirs, A., Saeys, W., Theron, K.I., Lammertyn, J., 2007a. Nondestructive measurement of fruit and vegetable quality by means of NIR spectroscopy: A review. Postharvest Biol. Technol. 46, 99-118, http://dx.doi.org/10.1016/j.postharvbio.2007.06.024

Nicolaï, B.M., Theron, K.I., Lammertyn, J., 2007b. Kernel PLS regression on wavelet transformed NIR spectra for prediction of sugar content of apple. Chemometrics Intellig. Lab. Syst. 85, 243-252, http://dx.doi.org/10.1016/j.chemolab.2006.07.001

Osborne, B.G., 2000. Near-infrared spectroscopy in food analysis, In: Meyers, R.A. (Ed.), Encyclopedia of Analytical Chemistry: Applications, Theory and Instrumentation. John Wiley & Sons., Chichester, pp. 1-13.

Osborne, B.G., Fearn, T., 1986. Near infrared spectroscopy in food analysis. Longman Scientific & Technical, Harlow, UK.

Osborne, B.G., Fearn, T., Hindle, P.T., 1993. Practical NIR spectroscopy with applications in food and beverage analysis, 2nd ed. Longman Scientific & Technical, England.

Osborne, S., Künnemeyer, R., Jordan, R., 1999. A low-cost system for the grading of kiwifruit. Journal of Near Infrared Spectroscopy 7, 9-15, http://dx.doi.org/10.1255/jnirs.229

Osborne, S.D., Jordan, R.B., Kunnemeyer, R., 1998. Using near-infrared (NIR) light to estimate the soluble solids and dry matter content of kiwifruit. ActaHortic. 464, 109-114, http://dx.doi.org/10.17660/ActaHortic.1998.464.13

Ozaki, Y., Morita, S., Du, Y., 2006. Spectral Analysis, Near-Infrared Spectroscopy in Food Science and Technology. John Wiley & Sons, Inc., pp. 47-72.

Pachghare, V., Kulkarni, P., 2011. Pattern based network security using decision trees and support vector machine, Proceedings of the 3rd International Conference onElectronics Computer Technology, Kanyakumari, India, pp. 254-257.

Paterson, V.J., Macrae, E.A., Young, H., 1991. Relationships between sensory properties and chemical composition of kiwifruit (*Actinidia deliciosa*). J. Sci. Food Agric. 57, 235-251, http://dx.doi.org/10.1002/jsfa.2740570208

Patterson, K.J., Currie, M.B., 2011. Optimising kiwifruit vine performance for high productivity and superior fruit taste. ActaHortic. 913, 257-268, http://dx.doi.org/10.17660/ActaHortic.2011.913.33

Paz, P., Sánchez, M.-T., Pérez-Marín, D., Guerrero, J.-E., Garrido-Varo, A., 2008. Nondestructive determination of total soluble solid content and firmness in plums using near-infrared reflectance spectroscopy. J. Agric. Food Chem. 56, 2565-2570, http://dx.doi.org/10.1021/jf073369h

Peirs, A., Tirry, J., Verlinden, B., Darius, P., Nicolaï, B.M., 2003. Effect of biological variability on the robustness of NIR models for soluble solids content of apples. Postharvest Biol. Technol. 28, 269-280, http://dx.doi.org/10.1016/S0925-5214(02)00196-5

Peleg, K., 1999. Development of a Commercial Fruit Firmness Sorter. Journal of Agricultural Engineering Research 72, 231-238, https://doi.org/10.1006/jaer.1998.0367

Pérez-Marín, D., Sánchez, M.-T., Paz, P., González-Dugo, V., Soriano, M.-A., 2011. Postharvest shelf-life discrimination of nectarines produced under different irrigation strategies using NIR-spectroscopy. LWT - Food Science and Technology 44, 1405-1414, http://dx.doi.org/10.1016/j.lwt.2011.01.008

Platt, J., 1999. Fast training of support vector machines using sequential minimal optimization, In: Schölkopf, B., Smola, A.J. (Eds.), Advances in Kernel Methods - Support Vector Learning. The MIT Press, Massachusetts, USA, pp. 41-65.

Podoleanu, A.G., 2012. Optical coherence tomography. Journal of Microscopy 247, 209-219,

Pojić, M., Kravić, S., Stojanović, Z., 2015. Analytical methods for determination of moisture and ash in foodstuffs, In: Nollet, L.M.L., Toldra, F. (Eds.), Handbook of Food Analysis, 3rd ed. CRC Press, pp. 275-295.

Qing, Z., Ji, B., Zude, M., 2007. Predicting soluble solid content and firmness in apple fruit by means of laser light backscattering image analysis. J. Food Eng. 82, 58-67, http://dx.doi.org/10.1016/j.jfoodeng.2007.01.016

Quinlan, J.R., 1986. Induction of decision trees. Machine Learning 1, 81-106, http://dx.doi.org/10.1023/a:1022643204877

Ramentol, E., Caballero, Y., Bello, R., Herrera, F., 2012. SMOTE-RSB*: a hybrid preprocessing approach based on oversampling and undersampling for high

imbalanced data-sets using SMOTE and rough sets theory. Knowledge and Information Systems 33, 245-265, http://dx.doi.org/10.1007/s10115-011-0465-6

Redgwell, R., Percy, A., 1992. Cell wall changes during on-vine softening of kiwifruit. N. Z. J. Crop Hortic. Sci. 20, 453-456, http://dx.doi.org/10.1080/01140671.1992.10418064

Reh, C., Irudayaraj, J., 2008. Nondestructive Testing of Food Quality. Blackwell Publishing; IFT Press, Iowa.

Ribeiro, M.T., Singh, S., Guestrin, C., 2016. "Why should i trust you?": Explaining the predictions of any classifier, Proceedings of the 22nd ACM SIGKDD International Conference on Knowledge Discovery and Data Mining. ACM, San Francisco, California, USA, pp. 1135-1144.

Richardson, A.C., Marsh, K.B., Boldingh, H.L., Pickering, A.H., Bulley, S.M., Frearson, N.J., Ferguson, A.R., Thornber, S.E., Bolitho, K.M., Macrae, E.A., 2004. High growing temperatures reduce fruit carbohydrate and vitamin C in kiwifruit. Plant, Cell Environ. 27, 423-435, http://dx.doi.org/10.1111/j.1365-3040.2003.01161.x

Richardson, A.C., McAneney, K., Dawson, T., 1997. Carbohydrate dynamics in kiwifruit. J. Hortic. Sci. 72, 907-917, http://dx.doi.org/10.1080/14620316.1997.11515583

Ridgeway, G., 1999. The state of boosting. Computing Science and Statistics 31, 172-181,

Ritenour, M.A., Crisosto, C.H., Garner, D.T., Cheng, G.W., Zoffoli, J.P., 1999. Temperature, length of cold storage and maturity influence the ripening rate of ethylene-preconditioned kiwifruit. Postharvest Biol. Technol. 15, 107-115, http://dx.doi.org/10.1016/S0925-5214(98)00074-X

Rivera, S.A., Ferreyra, R., Robledo, P., Selles, G., Arpaia, M.L., Saavedra, J., Defilippi, B.G., 2017. Identification of preharvest factors determining postharvest ripening behaviors in 'Hass' avocado under long term storage. Scientia Horticulturae 216, 29-37, http://dx.doi.org/10.1016/j.scienta.2016.12.024

Rizzolo, A., Vanoli, M., Cortellino, G., Spinelli, L., Contini, D., Herremans, E., Bongaers, E., Nemeth, A., Leitner, M., Verboven, P., Nicolaï, B.M., Torricelli, A., 2013. Characterizing the tissue of apple air-dried and osmo-air-dried rings by X-CT and OCT and relationship with ring crispness and fruit maturity at harvest measured by TRS. Innovative Food Science & Emerging Technologies, http://dx.doi.org/10.1016/j.ifset.2013.09.001

Roger, J.-M., Chauchard, F., Bellon-Maurel, V., 2003. EPO–PLS external parameter orthogonalisation of PLS application to temperature-independent measurement of sugar content of intact fruits. Chemometrics Intellig. Lab. Syst. 66, 191-204, http://dx.doi.org/10.1016/S0169-7439(03)00051-0

Rotherham, F., 2016. Zespri cuts forecast 2017 profit, grower returns for Green kiwifruit on increased supply, http://www.nbr.co.nz/article/zespri-cuts-forecast-2017-profit-grower-returns-green-kiwifruit-increased-supply-b-193708 (Accessed 16th February, 2017).

Rowe, P., 2015. Optical techniques for fruit firmness assessment: A thesis submitted in fulfilment of the requirements for the degree of Doctor in Philosophy in Electronic Engineering. University of Waikato, Hamilton, New Zealand.

Saeys, W., Mouazen, A.M., Ramon, H., 2005. Potential for onsite and online analysis of pig manure using visible and near infrared reflectance spectroscopy. Biosys. Eng. 91, 393-402, http://dx.doi.org/10.1016/j.biosystemseng.2005.05.001

Sale, P.R., 1990. Kiwifruit Growing. GP Books, Wellington, New Zealand.

Samarakoon, H.C., 2013. Ethylene flux in postharvest kiwifruit systems: a thesis presented in partial fulfilment of the requirements for the degree of Master of Philosophy. Massey University, Palmerston North, New Zealand.

Savitzky, A., Golay, M.J., 1964. Smoothing and differentiation of data by simplified least squares procedures. Analytical chemistry 36, 1627-1639, http://dx.doi.org/10.1021/ac60214a047

Scarrow, S., 2014. Trunk girdling - a consultant perspective. New Zealand Kiwifruit Journal January/February, 21-22,

Schaare, P.N., Fraser, D.G., 2000. Comparison of reflectance, interactance and transmission modes of visible-near infrared spectroscopy for measuring internal properties of kiwifruit (*Actinidia chinensis*). Postharvest Biol. Technol. 20, 175-184, http://dx.doi.org/10.1016/S0925-5214(00)00130-7

Schröder, R., Atkinson, R.G., 2006. Kiwifruit cell walls: towards an understanding of softening? New Zealand Journal of Forestry Science 36, 112,

Seager, N.G., Hewett, E.W., Warrington, I.J., 1995. Manipulation of carbohydrate concentrations in kiwifruit. N. Z. J. Crop Hortic. Sci. 23, 213-218, http://dx.doi.org/10.1080/01140671.1995.9513889

Sfakiotakis, E., Chlioumis, G., Gerasopoulos, D., 2005. Preharvest chilling reduces low temperature breakdown incidence of kiwifruit. Postharvest Biol. Technol. 38, 169-174, http://dx.doi.org/10.1016/j.postharvbio.2005.06.010

Shepherd, K.D., Walsh, M.G., 2002. Development of reflectance spectral libraries for characterization of soil properties. Soil Sci. Soc. Am. J. 66, http://dx.doi.org/10.2136/sssaj2002.9880

Shewfelt, R.L., 1999. What is quality? Postharvest Biol. Technol. 15, 197-200, http://dx.doi.org/10.1016/S0925-5214(98)00084-2

Sileoni, V., van den Berg, F., Marconi, O., Perretti, G., Fantozzi, P., 2011. Internal and external validation strategies for the evaluation of long-term effects in NIR calibration models. J. Agric. Food Chem. 59, 1541-1547, http://dx.doi.org/10.1021/jf104439x

Smola, A.J., Schölkopf, B., 2004. A tutorial on support vector regression. Statistics and computing 14, 199-222, http://dx.doi.org/10.1023/B:STCO.0000035301.49549.88

Snelgar, W., Blattmann, P., 2012. Trunk girdling Gold3 increases dry matter, but at what risk? New Zealand Kiwifruit Journal September/October, 28-32,

Snelgar, W.P., Hopkirk, G., 1988. Effect of overhead shading on yield and fruit quality of kiwifruit (*Actinidia deliciosa*). J. Hortic. Sci. 63, 731-742, http://dx.doi.org/10.1080/14620316.1988.11515918

Snelgar, W.P., Hopkirk, G., Seelye, R.J., Martin, P.J., Manson, P.J., 1998. Relationship between canopy density and fruit quality of kiwifruit. N. Z. J. Crop Hortic. Sci. 26, 223-232, http://dx.doi.org/10.1080/01140671.1998.9514058

Snelgar, W.P., Thorp, T.G., 1988. Leaf-Area, Final Fruit Weight and Productivity in Kiwifruit. Scientia Horticulturae 36, 241-249, http://dx.doi.org/10.1016/0304-4238(88)90058-1

Snelgar, W.P., Thorp, T.G., Patterson, K.J., 1986. Optimal leaf: Fruit ratios for fruit growth in kiwifruit. ActaHortic. 175, 115-120, http://dx.doi.org/10.17660/ActaHortic.1986.175.17

Stec, M.G.H., Hodgson, J.A., Macrae, E.A., Triggs, C.M., 1989. Role of fruit firmness in the sensory evaluation of kiwifruit (*Actinidia deliciosa* cv Hayward). J. Sci. Food Agric. 47, 417-433, http://dx.doi.org/10.1002/jsfa.2740470404

Sun, D.W., 2009. Infrared spectroscopy for food quality analysis and control, 1st ed. Academic Press, Boston.

Sun, J., Kunnemeyer, R., McGlone, A., Rowe, P., Talele, S., 2015. Development of a multispectral imaging system for apple firmness prediction, 9th International Conference on Sensing Technology, Auckland, New Zealand.

Svetnik, V., Liaw, A., Tong, C., Culberson, J.C., Sheridan, R.P., Feuston, B.P., 2003. Random forest: a classification and regression tool for compound classification and QSAR modeling. Journal of Chemical Information and Computer Sciences 43, 1947-1958,

Swierenga, H., Wülfert, F., De Noord, O., De Weijer, A., Smilde, A., Buydens, L., 2000. Development of robust calibration models in near infra-red spectrometric applications. Anal. Chim. Acta 411, 121-135, http://dx.doi.org/10.1016/S0003-2670(00)00718-2

Tanner, D., Kay, C., Mowat, A.D., 2012. Segregation technologies - Are they ready? New Zealand Kiwifruit Journal July/August, 15-18,

Tavarini, S., Degl'Innocenti, E., Remorini, D., Massai, R., Guidi, L., 2009. Polygalacturonase and β-galactosidase activities in Hayward kiwifruit as affected by light exposure, maturity stage and storage time. Scientia Horticulturae 120, 342-347, http://dx.doi.org/10.1016/j.scienta.2008.11.013

Thorp, T.G., Barnett, A., Blattmann, P., 2011. What are the productivity limits for 'hayward' kiwifruit? ActaHortic. 913, 419, http://dx.doi.org/10.17660/ActaHortic.2011.913.56

Thorp, T.G., Barnett, A.B., Toye, J.D., 2001. Harvesting light in persimmon and kiwifruit orchards with reflective ground covers. ActaHortic. 557, 363-368, https://doi.org/10.17660/ActaHortic.2001.557.48

Tijkens, L.M.M., Veltman, R.H., Heuvelink, E., Simcic, M., 2003. Modelling postharvest quality behaviour as affected by preharvest conditions. ActaHortic. 599, 469-477, http://dx.doi.org/10.17660/ActaHortic.2003.599.59

Tijskens, L.M.M., Konopacki, P., Simcic, M., 2003. Biological variance, burden or benefit? Postharvest Biol. Technol. 27, 15-25, http://dx.doi.org/10.1016/S0925-5214(02)00191-6

Tombesi, A., Antognozzi, E., Palliotti, A., 1993. Influence of light exposure on characteristics and storage life of kiwifruit. N. Z. J. Crop Hortic. Sci. 21, 85-90, http://dx.doi.org/10.1080/01140671.1993.9513750

Vanoli, M., Zerbini, P.E., Rizzolo, A., Spinelli, L., Torricelli, A., 2010. Time-resolved reflectance spectroscopy for the non-destructive detection of inner attributes and

defects of fruit. ActaHortic., 1379-1386, http://dx.doi.org/10.17660/ActaHortic.2010.877.189

Vapnik, V.N., 1995. Methods of pattern recognition, In: Vapnik, V.N. (Ed.), The nature of statistical learning theory, 2nd ed. Springer-Verlag New York, pp. 123-180.

Verboven, P., Nemeth, A., Abera, M.K., Bongaers, E., Daelemans, D., Estrade, P., Herremans, E., Hertog, M., Saeys, W., Vanstreels, E., Verlinden, B., Leitner, M., Nicolaï, B., 2013. Optical coherence tomography visualizes microstructure of apple peel. Postharvest Biol. Technol. 78, 123-132, http://dx.doi.org/10.1016/j.postharvbio.2012.12.020

Vursavus, K.K., Yurtlu, Y.B., Diezma-Iglesias, B., Lleo-Garcia, L., Ruiz-Altisent, M., 2015. Classification of the firmness of peaches by sensor fusion. International Journal of Agricultural and Biological Engineering 8, 104-115, http://dx.doi.org/10.3965/j.ijabe.20150806.1691

Ward, R.L., 2011. Development and applications of a low-field portable NMR system : a thesis presented in partial fulfillment of the requirements for the degree of Doctor of Philosophy in Physics at Massey University, Manawatu, New Zealand.

Wedding, B.B., Wright, C., Grauf, S., White, R.D., Tilse, B., Gadek, P., 2013. Effects of seasonal variability on FT-NIR prediction of dry matter content for whole Hass avocado fruit. Postharvest Biol. Technol. 75, 9-16, http://dx.doi.org/10.1016/j.postharvbio.2012.04.016

Westerhaus, M., Workman, J., Reeves, J.B., Mark, H., 2004. Quantitative Analysis, In: Roberts, C.A., Workman Jr, J., Reeves Iii, J.B. (Eds.), Near-Infrared Spectroscopy in Agriculture. American Society of Agronomy, Crop Science Society of America, Soil Science Society of America, Madison, WI, pp. 133-174.

Wevers, M., Kerckhofs, G., Pyka, G., Herremans, E., Van Ende, A., Hendrickx, R., Verstrynge, E., Mariën, A., Valcke, E., Pareyt, B., 2012. X-ray computed tomography for non-destructive testing, International Conference on Industrial Computed Tomography, Jounieh, Lebanon, pp. 1-29.

White, A., Hallett, I.C., Hunter, D., Marsh, K., Clark, C., Johnston, J., Harker, R., 2016. Linking cell structure and composition to perception of taste in kiwifruit, VIII International Postharvest Symposium, Cartagena, Spain.

Williams, P., Norris, K.H., 2001. Near-infrared technology: in the agricultural and food industries, 2nd ed. American Association of Cereal Chemists, Inc.

Williams, P.C., Norris, K.H., 1987. Near-infrared technology: in the agricultural and food industries, 1st ed. American Association of Cereal Chemists, Inc.

Williams, P.C., Saranwong, S., Kawano, S., Isaksson, T., Segtnan, V.H., 2006. Applications to agricultural and marine products, In: Ozaki, Y., McClure, W.F., Christy, A.A. (Eds.), Near-Infrared Spectroscopy in Food Science and Technology. John Wiley & Sons, Inc., Hoboken, New Jersey, pp. 163-277.

Wilson, D.L., 1972. Asymptotic properties of nearest neighbor rules using edited data. Transactions on Systems, Man and Cybernetics 2, 408-421, http://dx.doi.org/10.1109/TSMC.1972.4309137

Witten, I.H., Frank, E., Hall, M.A., 2011. Data mining: practical machine learning tools and techniques. Morgan Kaufmann Publishers, Burlington, Massachusetts.

Wold, H., 1966. Estimation of principal components and related models by iterative least squares, In: Krishnaiah, P.R. (Ed.), Multivariate Analysis. Academic Press, New York, pp. 391-420.

Wold, H., 1975. Path Models with latent variables: The NIPALS approach, In: Blalock, H.M., Aganbegian, A., Borodkin, F.M., Boudon, R., Capecchi, V. (Eds.), Quantitative sociology: International perspectives on mathematical and statistical modelling. Academic Press, New York, pp. 307-357.

Wold, S., Esbensen, K., Geladi, P., 1987. Principal component analysis. Chemometrics Intellig. Lab. Syst. 2, 37-52,

Wolpert, D.H., Macready, W.G., 1997. No free lunch theorems for optimization. Transactions on Evolutionary Computation 1, 67-82, http://dx.doi.org/10.1109/4235.585893

Woodward, T.J., 2007. Variation in 'Hayward' kiwifruit quality characteristics: a thesis submitted in partial fulfilment of the requirements for the degree of Doctor of Philosophy. The University of Waikato, Hamilton, New Zealand.

Workman, J., Weyer, L., 2007. Practical guide to interpretive near-infrared spectroscopy. CRC Press Inc., Boca Raton, FL, USA.

Wu, J., Roy, J., Stewart, W.F., 2010. Prediction modeling using EHR data: Challenges, strategies, and a comparison of machine learning approaches. Medical Care 48, S106-S113, http://dx.doi.org/10.1097/MLR.0b013e3181de9e17

Yen, S.J., Lee, Y.S., 2009. Cluster-based under-sampling approaches for imbalanced data distributions. Expert Systems with Applications 36, 5718-5727, http://dx.doi.org/10.1016/j.eswa.2008.06.108

Zdunek, A., Cybulska, J., 2011. Relation of biospeckle activity with quality attributes of apples. Sensors 11, 6317-6327, http://dx.doi.org/10.3390/s110606317

Zeaiter, M., Roger, J.M., Bellon-Maurel, V., 2005. Robustness of models developed by multivariate calibration. Part II: The influence of pre-processing methods. TrAC Trends in Analytical Chemistry 24, 437-445, http://dx.doi.org/10.1016/j.trac.2004.11.023

Zerbini, P.E., 2006. Emerging technologies for non-destructive quality evaluation of fruit. Journal of Fruit and Ornamental Plant Research 14, 13-22,

Zhang, G., Fang, B., 2007. LogitBoost classifier for discriminating thermophilic and mesophilic proteins. J. Biotechnol. 127, 417-424, http://dx.doi.org/10.1016/j.jbiotec.2006.07.020

Zhao, M., 2017. Development of mathematical model on 'hayward' kiwifruit softening in supply chain: A Thesis Presented in Partial Fulfilment of the Requirements for the Degree of Doctor of Philosophy in Food Technology at Massey University, New Zealand.

Zou, X., Zhao, J., Povey, M.J., Holmes, M., Mao, H., 2010. Variables selection methods in near-infrared spectroscopy. Anal. Chim. Acta 667, 14-32, http://dx.doi.org/doi:10.1016/j.aca.2010.03.048

Zude, M., Herold, B., Roger, J.-M., Bellon-Maurel, V., Landahl, S., 2006. Non-destructive tests on the prediction of apple fruit flesh firmness and soluble solids content on tree and in shelf life. J. Food Eng. 77, 254-260, http://dx.doi.org/10.1016/j.jfoodeng.2005.06.027

Appendices

Table A.1 Wavelength selection for prediction of post-storage firmness based on at-harvest Vis-NIR spectral data using support vector machines.

Wavelength Selection Technique	75 d			100 d			125 d			150 d		
	R^2	RMSE	SDR	R^2	RMSE	SDR	R^2	RMSE	SDR	R^2	RMSE	SDR
Principal component (PC)	0.40	0.50	**1.23**	0.50	0.48	**1.41**	0.35	0.33	**1.29**	0.50	0.38	**1.40**
Genetic algorithm	0.48	0.41	**1.50**	0.65	0.39	**1.73**	0.47	0.32	**1.30**	0.52	0.37	**1.44**
Sample interval (5 nm)	0.38	0.42	**1.49**	0.60	0.40	**1.67**	0.46	0.27	**1.57**	0.51	0.36	**1.49**
Sample interval (10 nm)	0.44	0.50	**1.23**	0.61	0.43	**1.57**	0.18	0.36	**1.15**	0.50	0.38	**1.39**

Table A.2 Wavelength selection for prediction of post-storage firmness based on at-harvest Vis-NIR spectral data using partial least squares.

Wavelength Selection Technique	75 d			100 d			125 d			150 d		
	R^2	RMSE	SDR	R^2	RMSE	SDR	R^2	RMSE	SDR	R^2	RMSE	SDR
Principal component (PC)	0.41	0.48	**0.28**	0.50	0.48	**1.40**	0.33	0.32	**1.29**	0.44	0.41	**1.31**
Genetic algorithm	0.41	0.43	**1.43**	0.55	0.44	**1.54**	0.39	0.34	**1.23**	0.37	0.42	**1.27**
Sample interval (5 nm)	0.30	0.44	**1.40**	0.50	0.45	**1.48**	0.24	0.31	**1.35**	0.42	0.39	**1.38**
Sample interval (10 nm)	0.48	0.48	**1.29**	0.54	0.47	**1.43**	0.32	0.36	**1.17**	0.46	0.39	**1.35**

Table A.3 Wavelength selection for prediction of post-storage total soluble solids based on at-harvest Vis-NIR spectral data using support vector machines.

Wavelength Selection Technique	75 d			100 d			125 d			150 d		
	R^2	RMSE	SDR	R^2	RMSE	SDR	R^2	RMSE	SDR	R^2	RMSE	SDR
Principal component (PC)	0.41	1.03	**1.37**	0.70	0.94	**1.76**	0.41	1.21	**1.36**	0.70	0.81	**1.87**
Genetic algorithm	0.25	1.32	**0.90**	0.78	0.80	**2.05**	0.37	1.43	**0.98**	0.76	0.77	**1.97**
Sample interval (5 nm)	0.56	1.01	**1.39**	0.77	0.72	**2.29**	0.75	0.76	**2.18**	0.81	0.69	**2.21**
Sample interval (10 nm)	0.68	0.86	**1.64**	0.80	0.74	**2.23**	0.74	0.74	**2.21**	0.83	0.66	**2.32**

Table A.4 Wavelength selection for prediction of post-storage total soluble solids based on at-harvest Vis-NIR spectral data using partial least squares.

Wavelength Selection Technique	75 d			100 d			125 d			150 d		
	R^2	RMSE	SDR	R^2	RMSE	SDR	R^2	RMSE	SDR	R^2	RMSE	SDR
Principal component (PC)	0.41	1.02	**1.38**	0.72	0.88	**1.85**	0.49	1.11	**1.48**	0.61	0.92	**1.65**
Genetic algorithm	0.26	1.27	**1.11**	0.70	0.94	**1.75**	0.41	1.28	**1.29**	0.60	0.98	**1.55**
Sample interval (5 nm)	0.55	1.02	**1.39**	0.57	0.97	**1.70**	0.55	0.98	**1.68**	0.65	0.92	**1.66**
Sample interval (10 nm)	0.70	0.84	**1.68**	0.66	0.96	**1.71**	0.58	0.93	**1.76**	0.60	1.02	**1.50**